PATENT

IN THE UNITED STATES PATENT AND TRADEMARK OFFICE

In re Application of:
  Chada et al.

Serial No.: 10/017,472

Filed: December 7, 2001

For: METHODS OF TREATMENT
     INVOLVING HUMAN MDA-7

Group Art Unit: 1632

Examiner: Li, Qian J.

Atty. Dkt. No.: INGN:097US

DECLARATION OF SUNIL CHADA, Ph.D

I, Sunil Chada, declare:

1.   I am the Director of Research and Development at Introgen Therapeutics. I have been working in the field of gene therapy and cancer biology for at least 15 years. My *curriculum vitae* is attached as Exhibit 1.

2.   I am also one of the inventors named on the application identified above, which concerns the melanoma differentiation associated gene (mda-7) and its encoded protein, MDA-7.

3.   The *mda-7* gene was first identified in human melanoma cell lines as a possible tumor suppressor. Jiang *et al.*, *Oncogene* 11:2477-86 (1995). Subsequent studies confirmed that elevated levels of MDA-7 suppressed cancer cell growth *in vitro* and selectively induced apoptosis in human breast cancer cells and inhibited tumorigenicity in nude

25379990.1

1

mice. Jiang *et al., Proc. Nat'l. Acad. Sci.* **93**:9160-65 (1996); Su *et al., Proc. Nat'l Acad. Sci.* **95**:14400-05 (1998).

4.   I understand that the present application contains claims directed to methods of inhibiting angiogenesis involving administering a nucleic acid expressing the human MDA-7 polypeptide, which have been rejected as lacking enablement.

5.   As described in this application, the first 48 amino acids of the full-length sequence may be cleaved to yield a secreted form of the protein. I have done scientific research on the tumor suppressor gene mda-7 and the MDA-7 protein, both the full-length and truncated versions.

6.   In one study concerning the MDA-7 protein, human melanoma cell lines MeWo and WM35 were treated with increasing concentrations of an MDA-7 protein lacking the first 48 amino acids of the full-length sequence. The cell lines were analyzed in triplicate at 12, 24, 48, 72, and 96 hours after treatment using a trypan blue exclusion assay. This truncated MDA-7 protein induced cell killing in melanoma cells (Exhibit 2), but did not induce killing in lung cancer cells.

7.   In another study, different forms of the MDA-7 protein were evaluated in PC3 human prostate cancer cells and H1299 human non-small cell lung carcinoma cells. The different forms (Exhibit 3) included: a full-length MDA-7, an MDA-7 protein lacking its own secretion signal (cytoplasmic version. lacking first 48 amino acids), an MDA-7 targeted to the nucleus (nuclear version), and an MDA-7 lacking its own secretion signal but containing a signal targeting it to the endoplasmic reticulum (ER version). Cells transfected with either the full-length or ER version of MDA-7 showed growth suppression (Exhibit 4). Furthermore, there were higher levels of apoptosis observed in

cells transfected with the full-length or ER versions, as compared to the cytoplasmic or nuclear versions of MDA-7.

8.   Thus, as discussed in paragraph 6, the truncated version of MDA-7 does indeed induce apoptosis as set forth in the specification of this application. Furthermore, as discussed in paragraph 7, a truncated MDA-7 with a heterologous signal sequence suppresses growth and induces apoptosis.

9.   Moreover, while the specification provides data regarding an Ad-mda7 construct to express MDA-7 in a eukaryotic cell, another study involved formulating a plasmid with an MDA-7 encoding nucleic acid in a liposome composition. The human mda-7 cDNA was placed under the control of the CMV promoter in a plasmid, which was formulated in a DOTAP:cholesterol complex. Nude mice were injected with human non-small cell lung carcinoma cells (A549 cell line) to produce tumors. Tumors were then treated intratumorally with the DOTAP:Chol-*mda-7* complex (50 µg/dose), resulting in the inhibition of tumor growth as compared to tumors in control animals. Similarly, tumors in nude mice from implantation of fibrosarcoma cells (UV223M cells) (syngeneic tumor model) were also inhibited by intratumoral administration of the DOTAP:Chol-*mda-7* complex. Moreover, when the tumor tissue from these animals were evaluated for CD31, they exhibited reduced levels of staining, which is indicative of reduced vascularization.

10.   I hereby declare that all statements made of my own knowledge are true and all statements made on information are believed to be true and further that the statements were made with the knowledge that willful false statements and the like so made are punishable by fine or imprisonment or both under § 1001 of Title 18 of the United States Code, and that such

willful false statements may jeopardize the validity of this application or any patent issued

thereon.

01-29-04
Date

Sunil Chada, Ph.D.
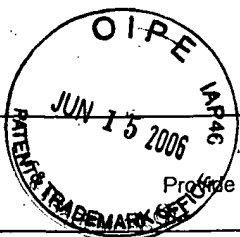
BIOGRAPHICAL SKETCH

Provide the following information for the key personnel in the order listed for Form Page 2.
Follow this format for each person. **DO NOT EXCEED FOUR PAGES.**

NAME	POSITION TITLE
SUNIL CHADA	DIRECTOR OF RESEARCH AND DEVELOPMENT

EDUCATION/TRAINING *(Begin with baccalaureate or other initial professional education, such as nursing, and include postdoctoral training.)*

INSTITUTION AND LOCATION	DEGREE (if applicable)	YEAR(s)	FIELD OF STUDY
Kings College, University of London London, England	B.Sc. (Honors)	1982	Cell & Molecular Biology
University of California at Los Angeles Los Angeles, CA	M.Sc.	1985	Molecular Biology
University of Massachussetts Medical School Worcester, MA	Ph.D.	1988	Molecular Genetics

A.

B. **Positions and Honors.** List in chronological order previous positions, concluding with your present position. List any honors. Include present membership on any Federal Government public advisory committee.

PROFESSIONAL EXPERIENCE

1985-1988	Research Associate, Univ. of Massachusetts Medical School, Worcester MA
1988-1991	Research Scientist I, Dept. of Molecular Virology, Viagene Inc., San Diego CA
1991-1993	Research Scientist II, Dept. of Immunobiology, Viagene Inc., San Diego CA
1993-1995	Senior Scientist, Dept. of Immunobiology, Viagene Inc., San Diego CA
1995-1997	Staff Scientist, Chiron Technologies Inc., San Diego CA
1997-pres	Director of Research and Development, Introgen Therapeutics, Houston TX
2002-pres	Adjunct Faculty, Dept. of Bioimmunotherapy, Division of Cancer Medicine, MD Anderson Cancer Center

Committee Memberships

National Cancer Institute – SBIR/ STTR SRG Reviewer (standing member)
National Cancer Institute – Cancer Chemoprevention (Ad hoc member)
National Cancer Institute – RAID Committee member
Rice University – Advisory Board for NIH and NSF Biotechnology Training Programs
Alliance for Cancer Gene Therapy - Reviewer

C. **Selected peer-reviewed publications (from a total of 68).**

1) Chou C, Gatti RA, Fuller M, Concannon P, Wong A, **Chada S**, Davis R, and Salser W. "Structure and expression of ferritin genes in a human promyelocytic cell line that differentiates in vitro." *Molecular and Cellular Biology* 6:566-573 (1986).

2) Davis RC, Thomason AR, Fuller ML, Slovin JP, Chou CC, **Chada S**, Gatti RA, and Salser W. "mRNA species regulated during the differentiation of HL-60 cells to macrophages and neutrophils." *Developmental Biology* 119:164-174 (1987).

3) **Chada S**, Whitney C, and Newburger, PE. "Control of expression of the human glutathione peroxidase gene by selenium." In: *OxyRadicals in Molecular Biology and Pathology*, eds. Cerutti P, Fridovich I, and McCord J, UCLA Symposia on Molecular and Cellular Biology Vol. 82. Alan R. Liss, New York, pp.273-288 (1988).

4) Holland CA, **Chada S**, Wright J, Whitney C, Harigaya K, Greenberger J, Newburger PE. "Differentiation of Human Hematopoietic Cells Increases Expression of a Gene Transferred by a Retroviral Vector." *J. Leukocyte Biology* 46:221-229 (1989).

5) **Chada S**, Whitney C, and Newburger PE. "Post-transcriptional regulation of glutathione peroxidase gene expression by selenium in the HL-60 human myeloid cell line." *Blood* 74:2535-2541 (1989).

6) **Chada S** and Newburger PE. "Incorporation of selenocysteine at a UGA termination codon in the human glutathione peroxidase gene". In: *Glutathione Centennial; Molecular Perspectives and Clinical Implications*, eds. Taniguchi N, Higashi T, Sakamoto Y, and Meister A. Academic Press, Inc, San Diego pp:145-160 (1989).

7) **Chada S**, LeBeau M, and Newburger PE. "Isolation and chromosomal localization of the human glutathione peroxidase gene." *Genomics* 6:268-271 (1990).

8) Warner JF, Anderson CG, Laube L, Jolly D, Townsend K, **Chada S** and St. Louis D. "Induction of HIV-specific CTL and antibody responses in mice using retroviral vector transduced cells." *AIDS Research and Human Retroviruses* 7:645-655 (1991).

9) Jolly J, **Chada S**, Townsend K, DeJesus C, Chang S, Weinhold K, Anderson CG, Lynn A, Bodner M, Barber J, and Warner J. "CTL cross reactivity between HIV strains." *AIDS Research and Human Retroviruses* 8:1379-1381 (1992).

10) Warner JF, Anderson CG, Laube L, Jolly D, Irwin M and **Chada S**. "Immunotherapy using retroviral vectors" In "*Molecular Basis of Immune Responses*" eds. Nariuchi, H et al. Academic Press, Inc, San Diego. pp.155-165 (1993).

11) **Chada S**, DeJesus C, Townsend K, Lee W, Laube L, Jolly D, Chang S and Warner J. "Cross-reactive lysis of human targets infected with prototypic and clinical HIV-1 strains by murine anti HIV-1 IIIB env specific CTL." *Journal of Virology* 67:3409-3417 (1993)

12) Thor G, Sepulveda H, **Chada S** and Dutton RW. "A monoclonal antibody that distinguishes between a phosphorylated, beta-2 microglobulin associated and a non-phosphorylated, free heavy chain of MHC class I." *Journal of Immunology.*151:1-14 (1993)

13) Sajaddi N, Kamantigue E, Edwards W, Howard T, Jolly D and **Chada S**. "Recombinant retroviral vector delivered intramuscularly localizes to the site of injection in mice." *Human Gene Therapy* 5:693-699 (1994)

14) Irwin M, Laube L, Lee V, Austin M, **Chada S**, Anderson C-G, Townsend K, Jolly D and Warner J. "Direct injection of a recombinant retroviral vector induces HIV specific immune responses in mice and nonhuman primates". *Journal of Virology* 68:5036-5044 (1994)

15) Shen Q, **Chada S**, Whitney C and Newburger PEN. "Regulation of the human cellular glutathione peroxidase gene during monomyelocytic differentiation." *Blood* 84:3902-3908 (1994)

16) Newburger PEN, Malawista S, Dinauer M, Gelbart T, Woodman R, **Chada S**, Shen Q, von Blaricam G, Quie P and Curnutte J. "Chronic Granulomatous Disease and glutathione peroxidase deficiency, revisited" *Blood* 84:3861-3869 (1994)

17) Fouts T R, Tuskan R G, **Chada S**, Hone D and Lewis G K. "Construction and Immunogenicity of *S. typhimurium* Vaccine Vectors that express HIV-1 gp160." *Vaccine* 13: 1797-1705 (1996)

18) T. W. Dubensky, Driver DA, Polo JM, Belli BA, **Chada S**, Brumm D, Banks TA, Mento SJ, Jolly DJ and Chang SM. "Sindbis virus DNA-based expression vectors: utility for *in vitro* and *in vivo* gene transfer." *Journal of Virology* 70: 508-519 (1996)

19) Kamantigue E, Edwards W, **Chada S**, Brumm, D, Austin M, Irwin M, Mento S and Sajjadi N. "Evidence for localization of biologically active recombinant retroviral vector to lymph nodes and the site of injection in mice injected intramuscularly". *Gene Therapy* 3: 128-136 (1996)

20) Song ES, Lee V, Suhr CD, Brumm D, Lynn A, Jolly DJ, Warner JF, **Chada S**. "Mechanisms of retroviral mediated *in* vivo gene transfer and antigen presentation." *Proceedings of the National Academy of Sciences, U S A* 94:1943-1948 (1997)

21) Kline RM and **Chada S**. "Killing The Last Cell: Using The Immune System To Fight Cancer." *MIT Technology Review.* June:48-55 (1997)

22) Nguyen KHY, Boyle DL, McCormack JE, **Chada S** and Firestein G. "Direct synovial gene transfer with retroviral vectors in rat adjuvant arthritis". *Journal of Rheumatology* 25: 1118-1125 (1998)

23) Ishida T, **Chada S**, Stipanov M, Nadaf S, Ciernik FI, Gabrilovich DI and Carbone DP. "Dendritic cells transduced with wild type p53 gene elicit potent anti-tumor immune responses". *Clinical and Experimental Immunology.* 117(2):244-51 (1999)

24) Boyle DL,. Nguyen KHY, Zhaung S, McCormack JE, **Chada S**, and Firestein GS. "Intra-articular IL-4 gene therapy in arthritis: Clinical efficacy and enhanced Th2 activity". *Gene Therapy.* 6:1911-1918 (1999)

25) Russell JS, Lang FF, Huet T, Janicot M, **Chada S**, Wilson DR and Tofilon PJ. "Radiosensitization of human tumor cell lines induced by the adenovirus-mediated expression of an anti-ras single chain antibody fragment". *Cancer Research.* 59(20):5239-44 (1999)

26) Saeki T, Mhashilkar AM, Roth JA,, Branch C, **Chada S** and Ramesh R. "Tumor-suppressive effects by adenovirus-mediated *mda-7* gene transfer in non-small cell lung cancer cell *in vitro*". *Gene Therapy* 7: 2051-2057 (2000)

27) Mhashilkar AM, Schrock RD, Hindi M, Liao J, Sieger K, Kourouma F, Zou-Yang H, Onishi E, Takh O, Vedvick T, Fanger G, Stewart L, Watson GJ, Snary D, Fisher PB, Saeki T, Roth JA, Ramesh R and **Chada S.** "Melanoma-Differentiation Associated Gene (mda-7): A Novel Anti-Tumor Gene for Cancer Gene Therapy". *Molecular Medicine,* 7(4): 271-282 (2001). Cover article.

28) Nikitina EY, Clark JI, Benyen J, **Chada S**, Virmani AK, Carbone DP and Gabrilovich DI. "Generation of Anti-tumor Cytotoxic T Lymphocytes from Peripheral Blood of Cancer Patients using Dendritic cells transduced with Wild Type p53 Gene". *Clinical Cancer Research*, 7:127-135 (2001).

29) Saeki T, Mhashilkar AM, Swanson X, Zou-Yang H, Zumstein L, Sieger K, Branch CD, Roth JA, **Chada S** and Ramesh R. "Inhibition of human lung cancer growth following adenovirus-mediated *mda-7* gene expression *in vivo*". *Oncogene* 21(29): 4558-66 (2002)

30) Ekmekcioglu S, Ellerhorst J, Mhashilkar A, Sahin AA, Read CM, Prieto VG, **Chada S**, and Grimm EA. "Down-Regulation Of Melanoma Differentiation Associated Gene *(mda-7)* Expression In Human Melanomas" *International Journal of Cancer* 94: 54-59 (2001)

31) Huang EY, Madireddi MT, Gopalkrishnan R, Lesczyniecka M, Su ZZ, Lebedeva IV, Kang DC, Jiang H, Lin JJ, Alexandre D, Chen Y, Vozhilla N, Mei MX, Christansen KA, Sivo F, Goldstein N, Mhashilkar A, **Chada S**, Huberman E, Pestka S and Fisher PB. "Genomic Structure, chromosomal localization and expression profile of mda-7, a novel cancer-specific growth suppressing and apoptosis inducing gene". *Oncogene* 20: 7051-7063 (2001)

32) Ellerhorst JA, Prieto VG, Ekmekcioglu S, Broemeling L, Yekell S, **Chada S** and Grimm EA. "Loss of MDA-7 Expression with Progression of Melanoma". *Journal of Clinical Oncology* 20(4):1069-74 (2002)

33) Mohiuddin I, Cao X, Ozarvan MK, Zumstein LA, **Chada S**, Smythe WR. "PTEN Over-expression Engenders Cellular Death In Human Malignant Mesothelioma Cells Via Inhibition of AKT Phosphorylation". *Annals of Surgical Oncology.* 9(3):310-6 (2002)

34) Stewart AL, Mhashilkar AM, Yang X-H, Ekmekcioglu S, Saito Y, Sieger K, Schrock RD, Onishi E, Swanson X, Mumm JB, Zumstein L, Watson G, Snary D, Roth JA, Grimm EA, Ramesh R and **Chada S.** "PI3K blockade by Ad-PTEN Inhibits Invasion and Induces Apoptosis in Radial Growth Phase and Metastatic Melanoma Cells". *Molecular Medicine.* 8:451-462 (2002) Cover article

35) Caudell E, Mumm J, Poindexter N, Ekmekcioglu S, Mhashilkar A, Yang X-H, Sieger K, **Chada S** and Grimm EA. "MDA-7 is a Novel Th1 Cytokine that is Antagonized by IL-10". *Journal of Immunology* 168: 6041-6046 (2002)

36) Nikitina EY, **Chada S**, Muro-Cacho C, Fang B, Zhang R, Roth JA, and Gabrilovich DI. "An effective immunization and cancer treatment with activated dendritic cells transduced with full-length wild-type p53". *Gene Therapy.* 9(5):345-52 (2002)

37) Kawabe S, Nishikawa T, Munshi A, Roth JA, **Chada S** and Meyn R. "Adenovirus Mediated mda-7 Gene Expression Radiosensitizes Non-Small Lung Cancer Cells via p53-independent mechanisms". *Molecular Therapy.* 6(5): 637-644 (2002)

38) Pataer A, Vorburger SA, Barber G, **Chada S**, Mhashilkar A, Zhou-Yang H, Balachandran S, Roth JA, Hunt KK and Swisher SG. "mda-7 induces apoptosis via upregulation of the double-stranded RNA dependent kinase PKR". *Cancer Research* 62:2239-2243 (2002)
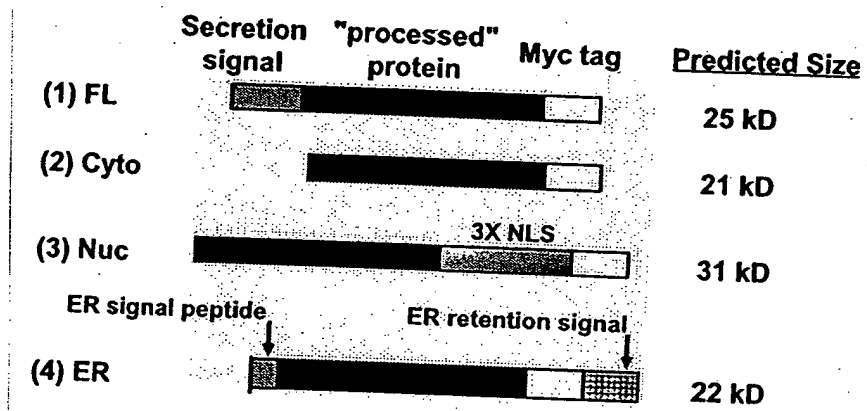
39) Chen J, **Chada S**, Mhashilkar AM and Miano JM. "MDA-7/IL-24 Selectively Inhibits Vascular Smooth Muscle Cell Growth and Migration". *Molecular Therapy.* Aug;8(2):220-9 (2003)

40) Pataer A, **Chada S**, Hunt KK, Roth JA and Swisher SG. "Adenoviral MDA-7 induces apoptosis in lung cancer cells through Mitochondrial Permeability Transition independent Cytochrome C Release". *Journal of Thoracic and Cardiovascular Surgery* 126(6):1328-1325 (2003)

41) Sasaki JI, Ramesh R, **Chada S**, Gomyo Y, Roth JA, and Mukhopadhyay T. "An Anthelminthic Drug to Curb Human Cancer: A Novel Microtubule Inhibitor as a Potential Inducer of Apoptosis in Non-Small Cell Lung Cancer Cells but Not in Normal Cells *In Vitro* and *In Vivo*. *Molecular Cancer Therapeutics.* 1: 1201-1209 (2002)

42) Ekmekcioglu S, Ellerhorst JA, Mumm JB, Zheng M, Broemeling L, Prieto VG, Stewart AL, Mhashilkar AM, **Chada S** and Grimm EA. "Negative Association of Melanoma Differentiation Associated Gene (mda-7) and inducible Nitric Oxide Synthase (iNOS) in Human Melanoma: MDA-7 Regulates iNOS Expression in Melanoma Cells." *Molecular Cancer Therapeutics.* 2(1):9-17 (2003)

43) Ramesh R, Mhashilkar A, Tanaka F, Saito Y, Sieger K, Mumm JB, Stewart A, Branch CD, Boquio A, Doumoutier L, Kotenko S, Roth JA and **Chada S**. " MDA-7/ IL-24 is a novel ligand that regulates angiogenesis via the IL-22 receptor". *Cancer Research.* 63(16):5105-13. (2003)

44) Mhashilkar AM, Stewart A, Sieger K, Ito I, Saito Y, Roth JA, Ramesh R and **Chada S**. "MDA-7 Negatively Regulates the beta-Catenin and PI3K Signaling Pathways in Breast and Lung Tumor Cells". *Molecular Therapy*, 8(2):207-19 (2003)

45) **Chada S**, Mhashilkar A and Gabrilovich D. "Development of vaccines against self antigens: the p53 paradigm". *Current Opinion in Drug Discovery and Development.* Mar;6(2):169-73 (2003)

46) Fisher PB, Gopalkrishnan RV, **Chada S**, Ramesh R, Grimm EA, Rosenfeld MR, Curiel DT and Dent P. "*mda-7/IL-24*, a novel cancer selective apoptosis inducing cytokine gene". *Cancer Biology and Therapy.* 2(4):24-38 (2003)

47) Saito Y, Gopalan B, Mhashilkar AM, Roth JA, **Chada S**, Zumstein L, Ramesh R. Adenovirus-mediated PTEN treatment combined with caffeine produces a synergistic therapeutic effect in colorectal cancer cells. *Cancer Gene Therapy*, 10(11):803-13 (2003).

48) Saito Y, Swanson X, Mhashilkar AM, Oida Y, Schrock R, Branch CD, **Chada S**, Zumstein L, Ramesh R. Adenovirus-mediated transfer of the PTEN gene inhibits human colorectal cancer growth in vitro and in vivo. *Gene Therapy* ;10(23):1961-9 (2003)

49) **Chada S**, Ramesh R, Mhashilkar AM. Cytokine- and chemokine-based gene therapy for cancer *Curr Opin Mol Ther.* 5(5):463-74 (2003). .

50) Sieger KA, Mhashilkar AM, Stewart A, Yang H-Y, Mumm JB, Ramesh R and **Chada S.** "The tumor suppressor activity of MDA-7/IL-24 is mediated by intracellular protein in NSCLC cells". *Molecular Therapy* In Press (2004)

51) **Chada S**, Ekmekcioglu S, Ellerhorst JA, Mumm JB, Sahin A, Hunt KK, Ramesh R, Grimm EA and Mhashilkar AM. MDA-7/IL-24 is a unique cytokine in the IL-10 family". *International Immunopharmacology.* In Press (2004)
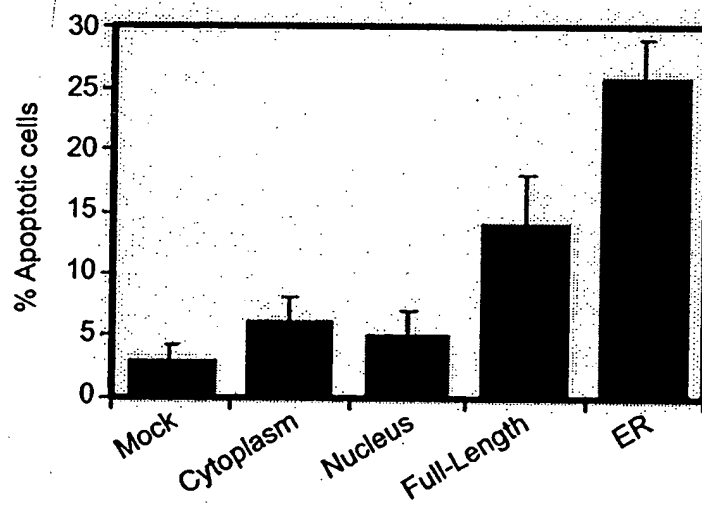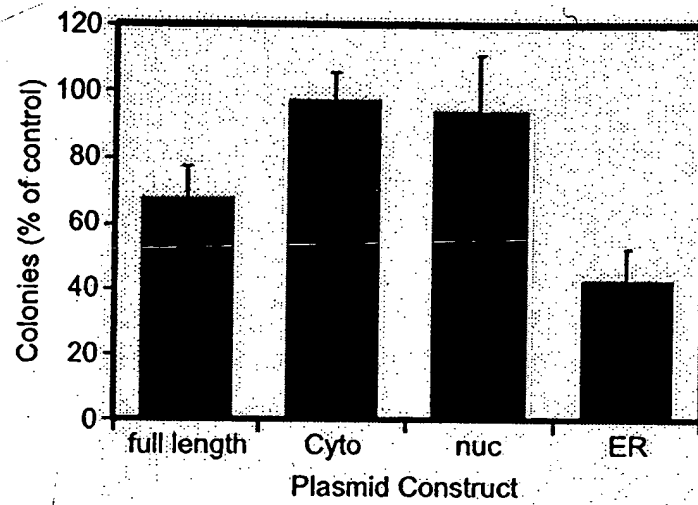
C. Research Support.

GRANTS AWARDED (from a total of 9)

1. Chada S. "Novel Gene Therapeutic for the Treatment of Lung Cancer" SBIR Grant 1R43CA86587-01 (Funded 03/00). Role: PI. Goals: to evaluate Ad-mda7 as a potential therapeutic for NSCLC

2. Meyn R "Tumor cell radiosensitization by gene drugs" STTR Grant. (Funded 08/00). Role: co-PI. Goal: to evaluate radiosensitization by Ad-p16 and Ad-mda7

3. Grimm EA "Novel gene therapy for Melanoma" STTR grant (Funded 06/01). Role: co-PI. Goals: to evaluate Ad--mda7 as a potential therapeutic for melanoma.

4. Chada S "Combination treatment for breast cancer using Ad-mda7 plus Herceptin". SBIR grant (Funded 07/02). Role: PI. Goals: To evaluate synergy between Ad-mda7 and Herceptin in breast cancer

5. Grimm EA "Phase II clinical trial for Melanoma using INGN 241 (Ad-mda7)" STTR grant (Funded 09/03). Role: co-PI

PATENTS and APPLICATIONS 8 issued patents; 17 applications pending

Secretion signal　"processed" protein　Myc tag　Predicted Size

(1) FL　25 kD

(2) Cyto　21 kD

(3) Nuc　3X NLS　31 kD

ER signal peptide　ER retention signal

(4) ER　22 kD

Top chart:

Colonies (% of control)

120
100
80
60
40
20
0

full length   Cyto   nuc   ER

Plasmid Construct

Bottom chart:

30
25
20
15
10
5
0

% Apoptotic cells

Mock   Cytoplasm   Nucleus   Full-Length   ER

A Single Intramuscular Injection of Recombinant Plasmid DNA Induces Protective Immunity and Prevents Japanese Encephalitis in Mice

GWONG-JEN J. CHANG,* ANN R. HUNT, AND BRENT DAVIS

*Division of Vector-Borne Infectious Diseases, Centers for Disease Control and Prevention, Public Health Service,
U.S. Department of Health and Human Services, Fort Collins, Colorado 80522*

Plasmid vectors containing Japanese encephalitis virus (JEV) premembrane (prM) and envelope (E) genes were constructed that expressed prM and E proteins under the control of a cytomegalovirus immediate-early gene promoter. COS-1 cells transformed with this plasmid vector (JE-4B clone) secreted JEV-specific extracellular particles (EPs) into the culture media. Groups of outbred ICR mice were given one or two doses of recombinant plasmid DNA or two doses of the commercial vaccine JEVAX. All mice that received one or two doses of DNA vaccine maintained JEV-specific antibodies 18 months after initial immunization. JEVAX induced 100% seroconversion in 3-week-old mice; however, none of the 3-day-old mice had enzyme-linked immunosorbent assay titers higher than 1:400. Female mice immunized with this DNA vaccine developed plaque reduction neutralization antibody titers of between 1:20 and 1:160 and provided 45 to 100% passive protection to their progeny following intraperitoneal challenge with 5,000 PFU of virulent JEV strain SA14. Seven-week-old adult mice that had received a single dose of JEV DNA vaccine when 3 days of age were completely protected from a 50,000-PFU JEV intraperitoneal challenge. These results demonstrate that a recombinant plasmid DNA which produced JEV EPs in vitro is an effective vaccine.

Japanese encephalitis (JE) is a mosquito-borne viral disease of major public health importance in Asia. More than 35,000 cases and 10,000 deaths are reported annually (52). *Japanese encephalitis virus* (JEV) is a member of the genus *Flavivirus* in the family *Flaviviridae*. More than 70 species in the *Flavivirus* genus have been genetically and serologically classified (29). Other important human pathogenic flaviviruses include yellow fever, dengue type 1 to 4 (DEN1 to DEN4), tick-borne encephalitis (TBE), and St. Louis encephalitis (SLE) viruses. Vaccination has been an effective mechanism for prevention of flavivirus infection in humans and domestic animals. Three JEV vaccines are in widespread production and use (52). These are inactivated virus from infected mouse brain, inactivated virus from primary hamster kidney cells, and a live attenuated SA14-14-2 vaccine. Only inactivated JEV vaccine, JEVAX, produced in mouse brain is distributed commercially and available internationally (52). Inactivated, mouse brain-derived whole virus vaccine is costly to prepare and carries the risk of allergic reaction to murine encephalitogenic basic proteins or gelatin stabilizer (45; M. M. Andersen, and T. Ronne, Letter, Lancet 337:1044, 1991). Since 1989, an unusual number of systemic reactions characterized by generalized urticaria and/or angioedema following JEVAX immunization have been reported from Australia, Canada, and Denmark (36). A major problem associated with use of the inactivated mouse brain vaccine is the failure to stimulate long-term immunity (39). Multiple immunization is recommended to provide adequate protection (28, 39). The attenuated JEV vaccine, SA14-14-2, is undergoing clinical trials (31). However, because of regulatory issues this vaccine has not found wide acceptance outside the People's Republic of China (11).

Several experimental recombinant virus, attenuated virus, and subunit JEV vaccines have been reported. Recombinant baculovirus vector that contained the JEV envelope (E) protein gene has been used to infect insect cells and produce E protein that has been studied as a biosynthetic immunogen (33). Recombinant vaccinia viruses expressing the JEV genes extending from premembrane (prM) to NS2B proteins have been the most promising candidate vaccines. These candidate vaccines produced extracellular virus-like particles (EPs) in infected cell culture that induced high titers of neutralizing and hemagglutination-inhibiting antibodies and protective immunity in mice (19–21, 47, 54). Recombinant vaccinia viruses expressing the same JEV genes based on the attenuated vaccinia virus strain, NYVAC-JEV, or canarypox, ALVAC-JEV, were tested in phase I human trials (18). In this trial, only 1 in 10 ALVAC-JEV recipients developed detectable viral neutralizing antibody, and vaccinia virus-preimmune recipients had a significantly lower humoral immune response.

Inoculation of animals with purified plasmid vectors (DNA) by the intramuscular (i.m.) or intradermal route leads to expression of the recombinant vector-encoded protein in transfected cells, resulting in stimulation of a protein-specific immune response. Plasmid DNA vaccines provide an alternative to attenuated, inactivated, or virus-vectored subunit vaccines. Flavivirus DNA vaccines for Murray Valley encephalitis, DEN2, JE, SLE, and TBE (Central European encephalitis and Russian spring summer encephalitis) viruses have been developed and tested in the mouse model (4, 17, 24, 30, 38, 49). All of these plasmid DNA constructs contained similar transcriptional regulatory elements and a flavivirus gene cassette. Vaccination of mice with these plasmid DNA vaccines induced a virus-specific antibody response, as detected by enzyme-linked immunosorbent assay (ELISA). However, production of neutralizing antibody leading to 100% protection of vaccinated animals from virus challenge was observed only after multiple immunizations or delivery of DNA to the epidermis by particle

* Corresponding author. Mailing address: P.O. Box 2087, Division of Vector-Borne Infectious Diseases, CDC, Foothill Campus, Fort Collins, CO 80522-2087. Phone: (970) 221-6497. Fax: (970) 221-6476. E-mail: gxc7@cdc.gov.
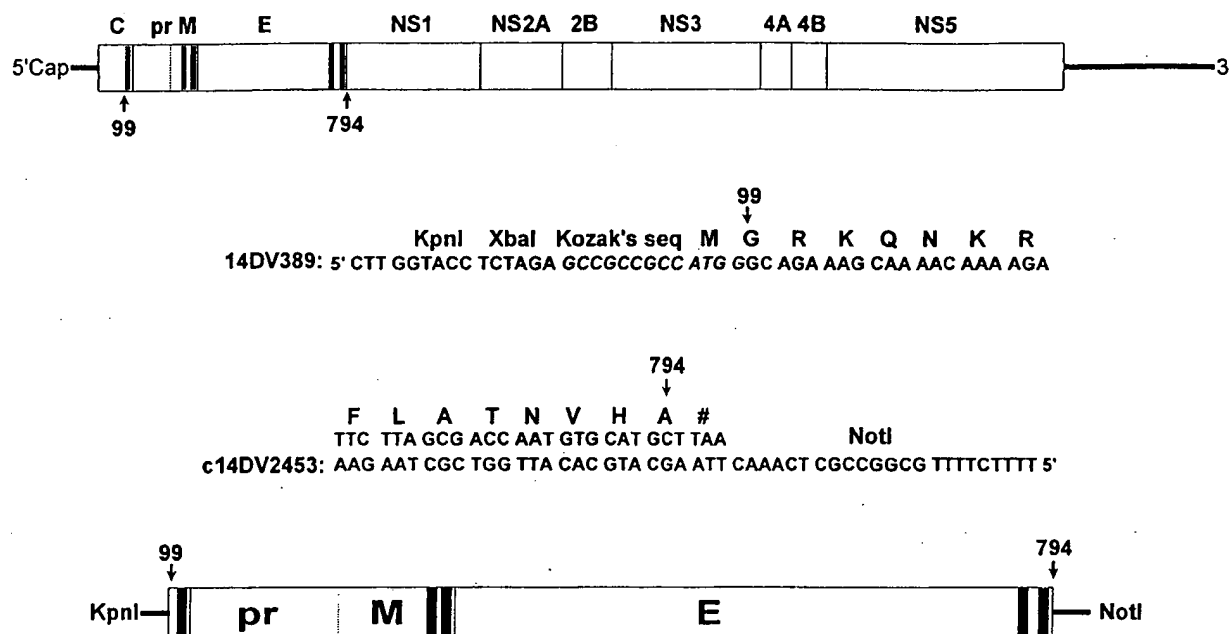
FIG. 1. Map of the JEV genomic structure (top) and the DNA sequence of oligonucleotides used in RT-PCR to construct the transcription unit for the expression of prM-E protein coding regions (bottom). Potential transmembrane helices of viral polyprotein are indicated by blackened areas.

bombardment (4, 24, 49). In this study, we constructed a JEV prM and E gene cassette that incorporates an extended signal peptide sequence at the NH$_2$ terminus of the prM gene and Kozak's sequence, an optimal translation enhancing element surrounding the AUG site. JEV protein expression was characterized using six different recombinant vectors containing the same insert. The humoral immune response and protection from virulent JEV challenge following immunization with the recombinant plasmid DNAs were compared to findings for the human vaccine, JEVAX, licensed by the U.S. Food and Drug Administration, in outbred ICR mice.

MATERIALS AND METHODS

Cell culture and virus strain. COS-1, COS-7, and SV-T2 cells (1650-CRL, 1651-CRL, and 163.1-CCL; American Type Culture Collection) were grown at 37°C in Dulbecco's modified Eagle medium (Gibco Laboratories, Grand Island, N.Y.) supplemented with 10% heat-inactivated fetal bovine serum (HyClone Laboratories, Inc., Logan, Utah), 1 mM sodium pyruvate, 0.1 mM nonessential amino acids, 7.5% NaHCO$_3$ (30 ml/liter), penicillin (100 U/ml), streptomycin (100 µg/ml). COS-1 and COS-7 cells were derived from simian virus 40 (SV40) transformed CV1 cells which have an African green monkey kidney cell origin. SV-T2 cells were derived from SV40-transformed mouse fibroblasts. Vero cells were grown under the same conditions except that 5% fetal calf serum without nonessential amino acid was used. C6/36 cells (13) were grown at 28°C in the same medium used for the COS-1 cells. The SA14 strain of JEV, propagated by intracranial inoculation into suckling mouse brain, was used for animal challenges and plaque reduction neutralization tests (PRNT). The SA14 virus used in ELISA and Western blot experiments was propagated in C6/36 cells and purified by ultracentrifugation on 30% glycerol–45% potassium tartrate gradients (37).

Construction of plasmids expressing JEV prM and E gene proteins. Genomic RNA was extracted from 150 µl of SA14 mouse brain JEV by using a QIAamp viral RNA kit (Qiagen, Santa Clarita, Calif.). RNA was adsorbed on a silica membrane, eluted in 80 µl of diethyl pyrocarbonate (Sigma Chemical Co., St. Louis, Mo.)-treated water, and used as a template for amplification of JEV prM and E genes. Primer sequences were obtained from the published data (35). A single cDNA fragment containing genomic nucleotides (nt) 389 to 2478 was amplified by reverse transcriptase-mediated PCR (RT-PCR). Restriction enzyme sites for *Kpn*I and *Xba*I and Kozak's sequence for an optimal translation initiation (25, 26) were engineered at the 5' terminus of the cDNA by amplimer 14DV389. An in-frame translation termination codon, followed by a *Not*I restriction site, was introduced at the 3' terminus of the cDNA by amplimer

c14DV2453 (Fig. 1). A single-tube RT-PCR was performed using a Titan RT-PCR Kit (Roche Molecular Biochemical, Indianapolis, Ind.). The RT-PCR product was purified using a QIAquick PCR purification kit (Qiagen), and the DNA was eluted with 50 µl of 1 mM Tris-HCl (pH 7.5).

All vector constructions and analyses were carried out using standard techniques (46). RT-PCR-amplified cDNA was digested with enzymes *Kpn*I and *Not*I and inserted into the *Kpn*I-*Not*I site of eukaryotic expression plasmid vector pCDNA3 (Invitrogen, Carlsbad, Calif.). Electroportion-competent *Escherichia coli* XL1-Blue cells (Stratagene, La Jolla, Calif.) were transformed by electroporation (Gene Pulser; Bio-Rad Laboratories, Hercules, Calif.) and plated on Luria broth (LB) agar plates that contained carbenicillin (100 µg/ml; Sigma). Clones were picked and inoculated into 3 ml of LB containing carbenicillin (100 µg/ml). Plasmid DNA was extracted from a 14-h LB culture by using a QIAprep Spin Miniprep kit (Qiagen). Automated DNA sequencing was performed as recommended on an ABI Prism 377 DNA sequencer (Perkin-Elmer/Applied Biosystems, Foster City, Calif.). Both strands of the cDNA were sequenced and compared to the published SA14 virus sequence (35).

The pCDNA3 fragment from nt 1289 to nt 3455, which contained the fl-encoded eukaryotic origin of replication (ori), SV40 ori, neomycin coding region, and SV40 poly(A) elements, was deleted by *Pvu*II digestion and then self-ligated to generate plasmid pCBamp. The pCIBamp vector, which contained a chimeric intron insertion at the *Nco*I-*Kpn*I site of the pCB vector, was constructed by excising the intron sequence from pCI (Promega, Madison, Wis.) by digestion with *Nco*I and *Kpn*I. The resulting 566-bp fragment was cloned into *Nco*I-*Kpn*I-digested pCBamp to replace its 289-bp fragment. Figure 2 shows a schematic drawing of plasmids pCDNA3, pCBamp, and pCIBamp.

The DNA fragment containing the JEV coding region in the recombinant plasmid pCDJE2-7, derived from the pCDNA3 vector, was excised by *Not*I and *Kpn*I or *Xba*I digestion and cloned into the *Kpn*I-*Not*I sites of pCB, pCIB, pCEP4 (Invitrogen), and pREP4 (Invitrogen) and into the *Spe*I-*Not*I site of the pRc/RSV (Invitrogen) expression vector to create pCBJE1-14, pCIBJES14, pCEJE, pREJE, and pRCJE, respectively. Both strands of the cDNA from each plasmid vector were sequenced, and recombinant clones with a correct nucleotide sequence were identified. Plasmid DNA for in vitro transformation or mouse immunization was purified by anion-exchange chromatography using an Endo-Free Plasmid Maxi kit (Qiagen).

IFA. Expression of JEV-specific gene products by the various recombinant expression plasmids was evaluated by indirect immunofluorescence antibody assay (IFA) in the transient expression system using COS-1, COS-7, and SV-T2 cells. For transformation, cells were grown to 75% confluence in 150-cm^2 culture flasks, trypsinized, and resuspended in 4°C phosphate-buffered saline (PBS) to a final density of 1 × 10^7 to 2 × 10^7 cells/ml. Five hundred microliters of cell suspension was then electroporated with 10 µg of plasmid DNA, using a Bio-Rad Gene Pulser II set at 250 V and 960 µF. Cells were diluted with 25 ml of fresh medium after electroporation and seeded into one 75-cm^2 flask. Forty-eight hours after transformation, the medium was removed, and the cells were

TATA box   KpnI   BamHI   EcoRI   EcoRV   NotI

TATATAA...(92nt)...*GGTACC*GAGCTC*GGATCC*ACTAGTAACGGCCGCCAGTGTGCTG*GAATTC*TGCA*GATATC*CATCACACTG*GCGGCCGC*...BHG-poly(A)
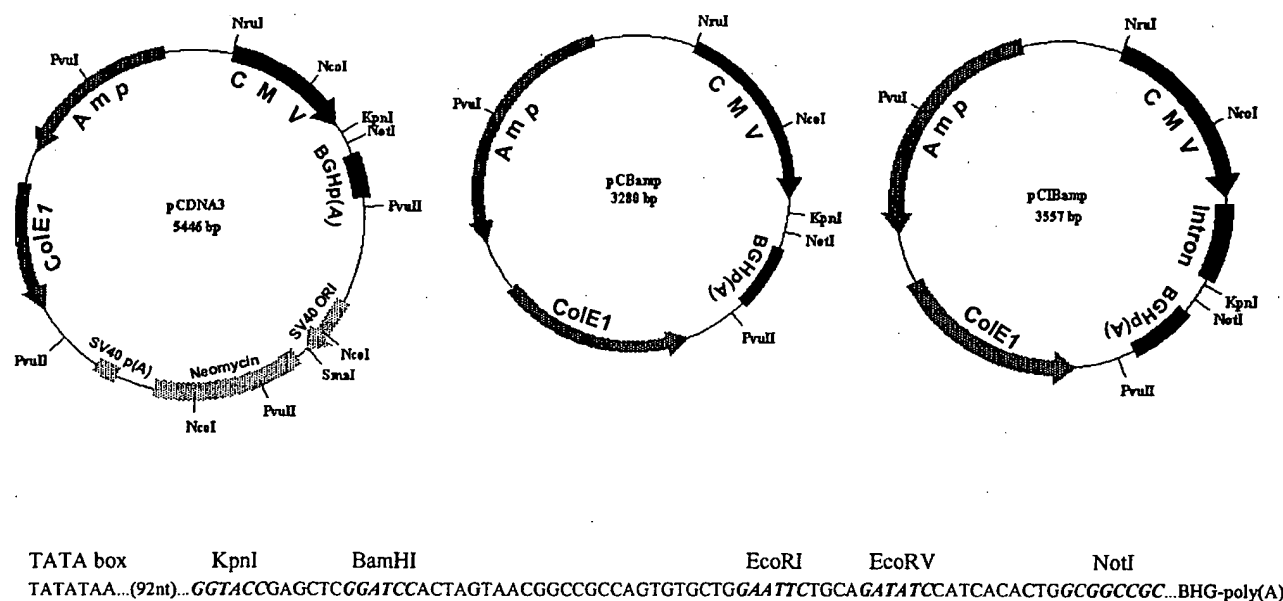
FIG. 2. Schematic representations of plasmid vectors pCDNA3, pCBamp, and pCIBamp. These plasmids include the CMV promoter/enhancer element, BGH poly(A) signal and transcription termination sequence [BHGp(A)], ampicillin resistance gene (Amp), and ColE1 ori for selection and maintenance in *E. coli*. The fl ori for single-stranded rescue in *E. coli* cells, SV40 ori, neomycin coding region, and SV40 poly(A) [SV40 p(A)] sequences were deleted from pCDNA3 to generate pCBamp. An intron sequence was inserted in the *Nco*I-*Kpn*I site of pCBamp to generate pCIBamp. The multiple cloning site for the insertion of JEV genes, located between the TATA box of the CMV promoter/enhancer and BHG poly(A) site, is shown.

trysinized and resuspended in 5 ml of PBS with 3% normal goat serum. Ten-microliter aliquots of the cell suspension were then spotted onto slides, air dried, and fixed with acetone at 4°C for 10 min. Immunofluorescent mapping of the E protein-specific epitopes was performed using a panel of murine monoclonal antibodies (MAbs) (15, 42, 55) and JEV-specific hyperimmune mouse ascitic fluid (HIAF). All antibodies were tested at 1:400 dilution in PBS.

Selection of an in vitro-transformed stable cell line constitutively expressing JEV-specific gene products. COS-1 cells transformed with 10 μg of pCDJE2-7 DNA by electroporation were incubated in nonselective culture medium for 24 h and then treated with neomycin (G418; 0.5 mg/ml; Sigma). G418-resistant colonies, which became visible after 2 to 3 weeks, were cloned by limited dilution in G418-containing medium. Expression of the JEV proteins was determined by IFA using JEV HIAF. One IFA-positive (JE-4B) and one IFA-negative (JE-5A) clone were selected for further analysis and maintained in medium containing 200 μg of G418 per ml. These stably transformed cells secreted antigen in the form of EPs (A. Hunt and G. J. Chang, unpublished data).

Antigen capture ELISA for detection of E protein secreted into culture fluid. The antigen capture ELISA, a modification of the procedure described by Guirakhoo et al. (8), was used to detect E protein from transiently transformed cells or JE-4B culture fluid. Flavivirus group-reactive MAb 4G2 was used to capture the JEV antigens (7). The 4G2-captured antigen was detected using horseradish peroxidase-conjugated MAb 6B6C-1 by incubation for 1 h at 37°C. Enzyme activity on the solid phase was detected with 3,3′,5,5′-tetramethylbenzidine ELISA substrate (Life Technologies, Grand Island, N.Y.); the reaction was stopped with the addition of 2 M H_2SO_4, and the optical density was measured at 450 nm.

Mouse experiments. Three-day-old mixed-sex or 3-week-old female ICR outbred mice were vaccinated i.m. with 50 or 100 μg of plasmid DNA at a concentration of 1 μg/μl in PBS or subcutaneously (s.c.) with 1/10 or 1/5 of the adult human dose of JEVAX (manufactured by the Research Foundation for Microbial Disease of Osaka University and distributed by Connaught Laboratories, Swiftwater, Pa.). The chloramphenicol acetyltransferase (CAT) protein expression plasmid pCDNA3/CAT (Invitrogen) was used as the vaccination control. Selected groups of mice were boosted 3 weeks later with an additional dose of plasmid vaccine or JEVAX. Mice were bled from the retro-orbital sinus; serum samples were evaluated for JEV antibody by ELISA and Western blotting using purified JEV and by PRNT.

Mice vaccinated at 3 days of age were challenged intraperitoneally (i.p.) 7 weeks postvaccination with JEV strain SA14 (50,000 PFU/100 μl) and observed for 3 weeks. To evaluate passive protection by maternal antibody, pups were obtained from mating of nonimmunized males with immunized females 9 weeks following their vaccination with plasmid DNA at 3 weeks of age. Pups were challenged by the i.p. route 3 to 15 days after birth with SA14 virus (5,000 PFU/100 μl) and observed daily for 3 weeks. Postchallenge serum was collected from survivors and tested for reactivity with JEV antigens by ELISA and Western blotting.

Serological tests. Postvaccination and postchallenge serum samples were tested for the ability to bind to purified JEV by ELISA, neutralize JEV infectivity by PRNT, or recognize JEV proteins by Western blotting (12, 41, 48). The PRNT assay was performed by incubating ~200 PFU of SA14 virus in 100 μl of Dulbecco's modified Eagle medium containing 5% bovine serum albumin and 20 mM HEPES buffer (pH 8.0) with serial twofold dilutions of serum specimens, started at 1:10, in 100 μl of the same buffer in 96-well trays at 4°C overnight. Serum specimens were heat inactivated at 56°C for 30 min before use. Duplicate 100-μl aliquots were assayed for infective virus by plaque formation on Vero cell monolayers. The percent plaque reduction was calculated relative to virus controls without serum. Titers were expressed as the reciprocal of serum dilutions yielding a 90% reduction in plaque number ($PRNT_{90}$).

RESULTS

Effect of the promoter and poly(A) signal on the efficiency of JEV prM and E protein expression. Four eukaryotic cell expression plasmids that contained the JEV coding region extending from genomic nt 390 to nt 2478 were constructed. This region of the genome encoded the prM and E genes. The Kozak sequence for the eukaryotic translation initiation site (underlined) of −9 to +4, GCCGCCGCC<u>ATGG</u>, at the 5′ terminus (2, 25, 26, 27) and the in-frame translation termination sequence at the 3′ terminus of cDNA were incorporated directly into cDNA by RT-PCR using viral RNA as a template. Transcription of the JEV genes in plasmid pCDJE2-7 was controlled by the human cytomegalovirus (CMV) early IA gene promoter/enhancer. The resulting mRNA is terminated and stabilized by a bovine growth hormone (BGH) transcription terminator and a poly(A) signal, respectively. The transcriptional control elements in pREJE were replaced by the Rous sarcoma virus (RSV) long terminal repeat promoter and SV40 poly(A). The pCEJE and pRCJE plasmids contain CMV plus SV40 poly(A) and RSV plus BGH poly(A), respectively (Table 1).

To determine the influence of the promoter and poly(A) elements on JEV prM and E protein expression, recombinant plasmids pCDJE2-7, pCEJE, pRCJE, and pREJE were ini-

TABLE 1. Transient expression of JEV prM and E proteins by various recombinant plasmids in two transformed cell lines

Name	Promoter	Intron	Poly(A)	Ori	Recombinant plasmid	IFA intensity/% positive[a]	
						COS-1	COS-7
pCDNA3	CMV	No	BGH	SV40	pCDJE2-7	3+/40	3+/35
pCBamp	CMV	No	BGH	No	pCBJE1-14	3+/45	ND
pCIBamp	CMV	Yes	BGH	No	pCIBJES14	3+/39	ND
pCEP4	CMV	No	SV40	OriP	pCEJE	2+/4	2+/3
pREP4	RSV	No	SV40	OriP	pREJE	1+/3	1+/2
pRc/RSV	RSV	No	BGH	SV40	pRCJE	1+/3	1+/3
pCDNA3	CMV	No	BGH	SV40	pCDNA3/CAT	−	−

[a] Various cell lines were transformed with pCDNA3/CAT (negative control), pCDJE2-7, pCBJE1-14, pCIBJES14, pCEJE, pREJE, or pRCJE. Cells were trypsinized 48 h later and tested by IFA with JEV HIAF. Data are presented as the intensity (scale of 1+ to 4+) and percentage of IFA-positive cells. pCDNA3/CAT-transformed cells were used as the negative control. ND, not determined. −, negative.

tially tested for the ability to express JEV prM and E proteins following transformation of various mammalian cells. COS-1, COS-7, and SV-T2 cells were transiently transformed with equal amounts of pCDJE2-7, pCEJE, pRCJE, or pREJE plasmid DNA. The SV-T2 cell line was excluded from further testing after preliminary results showed that less than 1% of pCDJE2-7-transformed SV-T2 cells were expressing JEV antigen.

JEV antigens were expressed in COS-1 and COS-7 cells transformed by all four recombinant plasmids, thus confirming that the CMV or RSV promoter and BGH or SV40 poly(A) elements were functionally active. However, the percentage of transformed cells and the level of JEV antigens expressed, as determined by the number of IFA-positive cells and IFA intensity, respectively, differed significantly (Table 1). A significantly higher percentage of pCDJE2-7-transformed COS-1 cells expressed JEV proteins with greater IFA intensity at a level equal to that observed with JEV-infected cells. Cells transformed with the pCEJE, pREJE, or pRCJE vector, on the other hand, showed a lower percentage of antigen-expressing cells as well as a lower IFA intensity. Vectors containing the CMV promoter and BGH poly(A) were selected for further analysis (Fig. 2).

To determine whether the enhanced expression of JEV proteins by the pCDJE2-7 vector was influenced by the SV40 ori, we constructed the pCBJE1-14 vector in which a 2,166-bp fragment containing the f1 ori, SV40 ori, neomycin coding region, and SV40 poly(A) elements was deleted. A chimeric intron was then inserted into pCBJE1-14 to generate pCIBJES14. Plasmid pCIBJES14 was used to determine whether the expression of JEV proteins could be enhanced by an intron sequence. Following transformation, both pCBJE1-14 and pCIBJES14 vectors resulted in cells expressing levels of JEV proteins similar to that observed with the pCDJE2-7 vector (Table 1). These results indicated that expression of the JEV proteins was influenced only by the transcriptional regulatory elements encoded in the recombinant plasmid. Neither the SV40 ori nor the intron sequence enhanced JEV protein expression in the cells used.

Epitope mapping of E protein expressed by a stably transformed cell line constitutively expressing JEV-specific gene products. Authenticity of the JEV E protein expressed by the JE-4B clone was demonstrated by epitope mapping by IFA using a panel of JEV E-specific murine MAbs. JEV HIAF and one irrelevant mouse ascitic fluid were used as positive and negative antibody controls, respectively. Four JEV-specific, six flavivirus subgroup-specific, and two flavivirus group-reactive MAbs reacted similarly with the 4B clone and with JEV-infected COS-1 cells (Table 2).

Detection of JEV E protein secreted by the JE-4B COS-1 cell line. An antigen capture ELISA, employing flavivirus group-reactive, anti-E MAbs 4G2 and 6B6C-1, was used to detect JEV E proteins that were secreted into the culture fluid by the COS-1 cell clone JE-4B. Antigen could be detected in the culture fluid the first day following seeding of the cells with maximum ELISA titers that ranged from 1:16 to 1:32.

Comparison of immune responses in mice vaccinated with pCDJE2-7 genetic vaccine and JEVAX. Plasmid pCDJE2-7 was used as a nucleic acid vaccine to induce an antibody response in mice by immunizing groups of five 3-week-old female ICR outbred mice. Mice were bled at 3, 6, 9, 23, 40, and 60 weeks after immunization, and antibody titers were determined by ELISA or by PRNT. As expected, sera from animals in the pCDNA3/CAT control group did not contain JEV antibody. All animals immunized with pCDJE2-7 and JEVAX seroconverted by 3 weeks after the first vaccination (Table 3). The antibody titers were similar irrespective of the number of doses

TABLE 2. Epitope mapping of E protein expressed by JE-4B, a pCDJE2-7 stably transformed clone of COS-1 cells, with JEV-reactive antibodies[a]

MAb or antiserum	Biological activity of MAb		IFA intensity of cells	
	Specificity	Biological function	JEV infected	4B
MAbs				
MC3	JEV specific		2+	2+
2F2	JEV specific	HI, N	4+	4+
112	JEV specific		4+	4+
503	JEV specific	N	4+	3+
109	Subgroup	HI	2+	1+
N.04	Subgroup	HI, N	3+	4+
201	Subgroup		1+	1+
203	Subgroup		4+	3+
204	Subgroup		2+	2+
301	Subgroup	HI	2+	2+
504	Flavivirus		4+	4+
6B6C-1	Flavivirus		2+	2+
3B4C-4	VEE		−	−
HIAF				
Anti-JEV			4+	3+
Anti-WEE			−	−
PBS			−	−

[a] VEE, Venezuelan equine encephalomyelitis virus; WEE, Western equine encephalomyelitis virus. −, negative.

TABLE 3. Persistence of the immune response in mice (five per group) immunized with pCDJE2-7 or JEVAX

Inoculation[a]	ELISA titer ($\log_{10}$)						PRNT$_{90}$ titer		
	3[b]	6	9	23	40	60[c]	3	6	9
pCDJE2-7									
1 dose	2.6–3.2	3.8–5.0	3.8–4.4	>3.2	>3.2	2.4, 2.4, 3.8, 4.4	<20	20	40–160
2 doses	2.6–3.8	4.4	3.8–4.4	>3.2	>3.2	2.6, 3.8, 3.8	<20	20–40	40–160
JEVAX, 2 doses	2.6–3.8	4.4–5.0	3.8–5.6	>3.2	>3.2	<2, <2, <2, 4.4	<20	20–40	20–160
pCDNA3/CAT, 2 doses	<100	<100	<100	ND[d]	ND	ND	<20	<20	<20

[a] Three-week-old mice were inoculated i.m. with one or two 100-μg doses of plasmid DNA or twice s.c. with one-fifth of the human dose of JEVAX.
[b] Weeks postimmunization.
[c] Individual serum titers.
[d] ND, not determined.

of pCDJE2-7 or JEVAX given. Mouse serum samples collected 9 weeks after immunization were also tested by Western blotting using purified JEV. Serum specimens from DNA-vaccinated mice, which had reactivity similar to that of JEV HIAF, detected E and prM proteins (Fig. 3). However, mouse serum from JEVAX-immunized mice reacted only with E protein. Comparable ELISA antibody titers were maintained in DNA-vaccinated groups for up to 60 weeks, at which time the experiment was terminated. Only one of four mice in the JEVAX group remained JEV antibody positive at 60 weeks postinoculation. These results demonstrated that one dose of JEV-specific nucleic acid vaccine was more effective in maintaining JEV antibody levels in mice than the commercially available vaccine JEVAX.

Comparison of various nucleic acid vaccine constructs and JEVAX for ability to induce JEV-reactive antibody in different age groups of mice. Similar amounts of JEV protein were expressed by COS-1 cells transformed by either pCDJE2-7, pCBJE1-14, or pCIBJES14. JEV antibody induction by these nucleic acid constructs was compared to results for JEVAX in two different age groups of mice. Three-day-old mixed-sex or 3-week-old female ICR outbred mice, 10 per group, were vac-

cinated i.m. with 50 or 100 μg of plasmid DNA or s.c. with 1/10 or 1/5 of the adult human dose of JEVAX, respectively. Serum specimens were collected at 7 weeks after immunization and tested at 1:400 or 1:1,600 by ELISA. Ninety to 100% of all 3-week-old mice that received pCBJE1-14, pCDJE2-7, pCIBJES14, or JEVAX had antibody titers of ≥1:1,600. However, a significant difference in antibody response was observed in 3-day-old groups that received various vaccines. None of the 3-day-old JEVAX-vaccinated mice had antibody titers higher than 1:400. All 3-day-old mice vaccinated with pCBJE1-14 had antibody titers higher than 1:1,600. Seroconversion of 100% was observed at 1:400 in 3-day-old mice that received pCDJE2-7 or pCIBJES14, but only 60% of both mouse groups were positive at 1:1,600. pCBJE1-14 was the most effective of three DNA constructs tested. The minimum dose of this DNA construct capable of providing 100% seroconversion (1:400 by ELISA) by i.m. immunization in 3-week-old mice was determined to be 25 μg (data not shown).

Protective immunity conferred by the nucleic acid vaccine. Mice immunized at 3 days of age were challenged by the i.p. route at 7 weeks postvaccination with the SA14 strain of JEV (50,000 PFU/100 μl) and observed for 3 weeks. One hundred percent of the animals that received various nucleic acid vaccine constructs were protected. In contrast, only 40 and 30% of mice that received JEVAX and pCDNA3/CAT, respectively, survived virus challenge (Fig. 4). These results suggested that the DNA vaccine could be effective as a neonatal vaccine. In contrast, JEVAX was not as effective in neonatal animals.
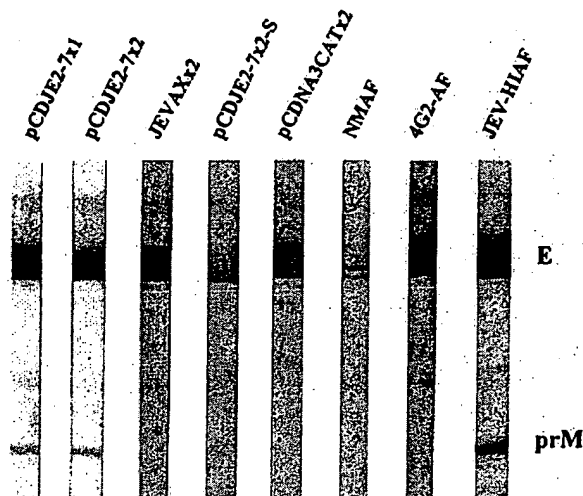

FIG. 3. JEV-specific reactivity of prechallenge and postchallenge serum samples obtained from mice immunized with DNA vaccine or JEVAX. Serum specimens collected from the mice used in the experiments represented in Tables 3 and 4 were randomly selected and tested at 1:1,000 dilution by Western blot analysis using purified JEV as the antigen. pCDJE2-7x2-S was the serum from one of the mice challenged at 4 days of age (Table 4). NMAF, 4G2-AF, and JEV HIAF were the mouse ascitic fluids included as normal mouse, E-specific, and JEV hyperimmune controls, respectively.
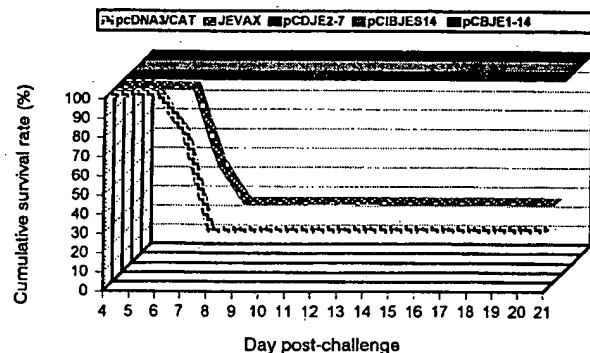

Day post-challenge

FIG. 4. Postchallenge survival rates of mice (10 per group) that were immunized with pCDJE2-7, pCBJE1-14, pCIBJES14, pcDNA3/CAT, or JEVAX at 3 days of age and challenged i.p. with 50,000 PFU of JEV (SA14) 7 weeks postimmunization. A P value of 0.003 was obtained by Fisher's exact test when the survival rate of the JEV DNA-immunized groups was compared with that of the pcDNA3/CAT or JEVAX group.

TABLE 4. Ability of maternal antibody from JEV nucleic acid-vaccinated female mice to protect their pups from fatal JE

Vaccinated mother[a]		JEV-challenged pups			
Vaccine	PRNT$_{90}$	Age (days)	No. of survivors/ total in litter	Avg survival time (days)	ELISA[b]
1 × pCDJE2-7	40	4	0/11	5.27	
2 × pCDJE2-7	80	4	12/12	NA[c]	12/12
2 × JEVAX	20	3	0/16	4.75	
2 × pCDNA3/CAT	<10	5	0/14	4.00	
1 × pCDJE2-7	20	15	5/11	10.0	5/5
2 × pCDJE2-7	40	14	8/12	13.75	7/8
2 × JEVAX	80	13	5/5	NA	5/5
2 × pCDNA3/CAT	<10	14	0/14	6.14	

[a] Mice were inoculated i.m. with one or two 100-μg doses of pCDJE2-7 DNA or twice s.c. with one-fifth of the adult human dose of JEVAX. Serum samples were collected 9 weeks postvaccination for PRNT testing prior to mating with nonimmune male.

[b] Number of JEV ELISA antibody-positive animals (titer ≥ 1:400)/number of survivors. Serum specimens were collected for testing 12 weeks after challenge.

[c] NA, not applicable.

Passive protection of neonatal mice correlated with the maternal antibody titer. Female 3-week-old ICR mice were vaccinated with one or two doses of pCDJE2-7 plasmid DNA (100 μg/100 μl) or twice with one-fifth of the adult human dose of JEVAX. For evaluation of passive protection by maternal antibody, pups were obtained from matings of experimental females with nonimmunized male mice. Pups were challenged by the i.p. route at 3 to 5 or 13 to 15 days after birth with SA14 virus (5,000 PFU/100 μl). Survival rates and average survival time correlated with the maternal neutralizing antibody titers (Table 4). One hundred percent of pups nursed by mothers with a PRNT of 1:80 survived viral infection regardless of the type of vaccine received by the mothers. None of the pups from mothers which received pCDNA3/CAT plasmid DNA survived (Table 4). Partial protection (45% [5 of 11 pups] to 67% [8 of 12 pups]) was observed in older pups that were nursed by the mothers which had serum PRNT titers of 1:20 and 1:40, respectively. However, none of the 3-day-old pups survived virus challenge when the mothers had a serum PRNT titer of 1:20 or 1:40. Maternally transferred antibody can only be detected in the circulation of the young mouse up to 40 days after birth. An appreciable level of maternally derived antibody is maintained in the circulation of the young mouse 24 days or more postpartum (1). JEV ELISA antibody detected in the serum of 97% (29 of 30) of the postchallenge pups at 12 weeks after virus challenge was unlikely to be residual maternally transferred antibody. The presence of JEV antibody in the surviving pups challenged at 3 to 4 or 13 to 15 days of age strongly suggested that maternal antibody did not provide sterilizing immunity to the pups. It also indicated that 3- to 4- or 13- to 15-day-old mice could mount an immune reaction to a live-virus challenge. Partial protection in older pups could be explained by the opportunity to accumulate a large quantity of passive antibody due to the length of nursing time before challenge. One randomly selected postchallenge serum sample also reacted with prM and E proteins by Western blotting (Fig. 3).

DISCUSSION

The flavivirus virion contains a capsid protein (C), a membrane protein (M), and an E protein. The prM MAbs, exhibiting weak or undetectable neutralizing activity in vitro, can provide passive protection following DEN2 virus challenge (16). However, the E protein plays a dominant role in generating neutralizing antibodies and providing protective immunity in the host. Passive transfer of JEV E-specific neutralizing MAbs has been shown to protect recipients from JEV-induced fatal encephalitis (3, 16, 32, 55). Antigenic and structural analysis using various panels of MAbs has shown that most of the E protein epitopes that elicit virus-neutralizing antibodies are conformationally dependent (9, 40). Coexpression of both proteins as type I transmembrane proteins is essential to maintain proper E conformation and prevent the E protein from undergoing irreversible, low-pH-catalyzed conformational changes (8–10, 19, 50). A 2-kb genomic region, from the internal signal peptide at the carboxyl terminus of C to the transmembrane domain at the carboxyl terminus of the E gene, is essential for expressing authentic proteins. These authentic prM and E proteins are able to self-assemble into virus-like particles in cells infected by either recombinant vaccinia virus or alphavirus vector or in cells transformed by recombinant plasmid DNA (4, 19, 22, 48; Hunt and Chang, unpublished data).

A gene cassette including the elements listed above was amplified from SA14 virus by RT-PCR in the present study. Optimal sequence composition surrounding the translation initiation site (−9 to +4) was incorporated into the 14DV398 amplifying primer (2, 26, 27) (Fig. 1). Recombinant plasmids containing the CMV early gene promoter/enhancer and the BHG poly(A) terminator as transcription regulatory elements expressed JEV proteins with the highest efficiency in three different cell lines. Protein expression and the serological response of mice immunized with DNA vaccine were not influenced by the presence or absence of the SV40 ori or an intron sequence in recombinant plasmids. Virus-specific proteins, secreted into culture medium, could be detected by antigen capture ELISA as early as 48 h after plasmid transformation (data not shown). The authenticity of the E protein produced by the pCDJE2-7 stably transformed cell line, JE-4B, was demonstrated by MAb epitope mapping.

Vaccine potential and characteristics of various eukaryotic plasmids that express flavivirus prM and E proteins are summarized in Tables 5 and 6. All constructs listed had the same transcriptional control elements and similar viral gene cassettes. DEN2 plasmid, which contains prM and 91% of E, is the only exception (Table 6). The JEV DNA vaccine reported in this study is the only construct that stimulated complete protective immunity in mice by a single dose of vaccine given by the i.m. route (Table 5). Sequences surrounding the translation initiation site and the composition of the signal peptide preceding the prM protein are the two major differences among the constructs that may contribute to increasing the vaccine potential of our construct (Table 6). Conserved features of the sequences which flank vertebrate translation initiation sites include a strong preference for purine at the −3 position; a higher frequency of G at positions −9, −6, −3, and +4; and a preference for A or C at positions −5, −4, −2, and −1 (2). Instead of the sequence used in previous publications, the sequence used in our construct was −9 · GCCGCCGCC ATGG, which fits the general criteria listed above. Although less than 1% of eukaryotic mRNA sequences exhibit this sequence, the experimental data have suggested that this sequence provides exceptionally high levels of translation potential (2, 26).

Signal peptides determine translocation and orientation of inserted protein, hence the topology of prM and E. Signal peptide differences in our plasmid construct may account for the efficient translocation and correct topology, thus increasing prM and E secretion. A machine-learning program using neu-

TABLE 5. Vaccine potential of various eukaryotic plasmids that express flavivirus prM and E proteins[a]

Virus	In vitro secretion of EPs	Immunization			Protection from virus challenge	Reference
		Dosage	Route/method	Neutralizing antibody[b]		
JE	Yes	25–100 μg × 1	i.m./needle	Yes (1:20–1:160$_{90\%}$)	100%	This report
	ND	100 μg × 2	i.m./needle	No	Partial	30
	ND	10–100 μg × 2	i.m. or i.d./needle	Yes (1:10–1:20$_{90\%}$)	100%	24
MVE	Yes	100 μg × 4	i.m./needle	ND	Partial	4
	Yes	1–2 μg × 2–4	i.d./gene gun	Yes (80–320$_{50\%}$)	100%	4
SLE	ND	100 μg × 2	i.m./needle	No	Partial	38
CEE	ND	1 μg × 1–2	i.d./gene gun	Yes (1:100–1:1,600$_{80\%}$)	100%	49
RSSE	ND	1 μg × 1–2	i.d./gene gun	ND	100%	49
DEN2	ND	200 μg × 3	i.d./needle	Yes (1:10–1:320$_{50\%}$)	None	17

[a] MVE, Murray Valley encephalitis; CEE, Central European encephalitis; RSSE, Russian spring-summer encephalitis; i.d., intradermal; ND, not done.
[b] Plaque reduction neutralization titer followed by percentage reduction endpoint used in the test.

ral networks trained on eukaryotes (SignalP-NN at http://www.cbs.dtu.dk/services/) was applied to test the efficiency of the prM signal peptide sequence in the different plasmid constructs (34) (Table 6). The most probable location and orientation of transmembrane helices in the prM-E protein were then determined by a hidden Markov model-trained computer program (6 [TMHMM at http://www.cbs.dtu.dk/services/]). SignalP-NN searches correctly predicted the signal peptidase cleavage site of all constructs. However, a considerable difference in cleavage potential (C score, between 0.578 and 1.000) was observed (Table 6). Cleavage potential differences may be influenced by the amino acid composition and length of the h region in various constructs (44).

The TMHMM program correctly predicted five transmembrane helices encoded in the prM-E protein. Significant difference in the probable orientation of the first transmembrane helix was observed in three JEV constructs (Fig. 5). In our pCDJE2-7 construct, the first 12 amino acids of the n region form a short loop in the cytoplasmic side that causes the following h region (transmembrane helix) to be inserted in a tail orientation. Secretion of JEV protein could be detected by antigen capture ELISA in pCDJE2-7 transient expression studies in which less than 5% of the cells were positive by IFA (data not shown). Thus, there is a high probability that prM and E proteins expressed by pCDJE2-7 would be expressed in the correct orientation, as type I transmembrane proteins (Fig. 5A). There is also a high probability that the prM protein of pcDNA3JEME could be expressed as a type II membrane protein with its transmembrane h region inserted in a head orientation because of the absence of positively charged amino acids in its n region (Fig. 5B). Efficient protein synthesis in

conjunction with correct topology of expressed prM and E (Fig. 5A) would most likely enhance EP formation and secretion in transformed cells.

Another characteristic that could explain the excellent vaccine potential of our JEV construct is its ability to produce EPs which have a virus-like polymeric structure that enhances antigenic stability and provides a high-density presentation to antigen-presenting cells, such as macrophages, dendritic cells, and Langerhans cells (5). When DNA is given by the i.m. route, the majority of antigen is expressed by non-antigen-presenting muscle cells. The efficacy of a DNA vaccine is therefore dependent on transfection of antigen-presenting cells or to reprocessing of antigen derived from other cells. Muscle cells transfected by our construct could conceivably synthesize and secrete EPs, which are highly immunogenic and have been shown to elicit good cellular and humoral responses (22, 23).

Genetic JEV vaccine that induced a completely protective immunity in neonatal mice and a maternally transferable protective immunity in young adult mice by a single i.m. immunization was demonstrated in this study. Additional studies are planned to address the effectiveness of a DNA vaccine in overcoming the potential influence of maternally transferred flavivirus antibodies on the induction of JEV antibody in neonatal mice.

Immunization of pigs is a theoretical means of interrupting transmission and amplification of JEV and thereby preventing human infections (43). The JEV DNA vaccine could also be used as a veterinary vaccine in pregnant sows to prevent JEV-induced stillbirth and abortion (51, 53). Maternally transferred antibody could also interrupt piglets as the JEV-amplifying host and thus reduce human infection.

TABLE 6. Characteristics of various eukaryotic plasmids expressing flavivirus prM and E proteins

Virus[a]	Plasmid	Sequence surrounding translation initiation site	Amino acids preceding prM protein[b]	SP potential (C score)[c]	Reference
JE	pCDJE2-7	−9•GCCGCCGCCATGG•+4	MGRKQNKRGGNEGSIMWLASLAVVIACAGA /MKL	Yes (0.921)	This report
	pJME	−9•GGCTCAATCATGG•+4	MWLASLAVVIACAGA /MKL	Yes (0.578)	30
	pCDNA3JEME	−9•GAATTCACCATGG•+4	MNEGSIMWLASLAVVIACAGA /MKL	Yes (0.921)	24
MVE	pCDNA3.prM-E	−9•TGATTTCAAATGT•+4	MSKKRGGSETSVLMVIFMLIGFAAA /LKL	Yes (0.819)	4
SLE	pSLE1	?	?LDTINRRPSKKRGGTRSLLGLAALIGLASS /LQL	Yes (0.709)	38
DEN2	p1012D2ME	?	?AGMIIMLIPTVMA /FHL	Yes (0.646)	17
TBE	SV-PE$_{wt}$	−9•GCGGCCGCCATGG•+4	MVGLQKRGKRRSATDWMSWLLVITLLGMTLA /ATV	Yes (1.000)	48
RSSE	pWRG7077	−9•GTAGACAGGATGG•+4	MGWLLVVVLLGVTLA /ATV	Yes (0.762)	50
CEE	pWRG7077	−9•ACGGACAGGATGG•+4	MSWLLVITLLGMTIA /ATV	Yes (0.609)	50

[a] Abbreviations are as given in Table 5, footnote a.
[b] Single amino acid code. Positively charged amino acid is indicated by bold letter. Signal peptidase cleavage site is indicated by /.
[c] Cleavage potential of signal peptide (SP) predicted by SignalP-NN at http://www.cbs.dtu.dk/services (34).
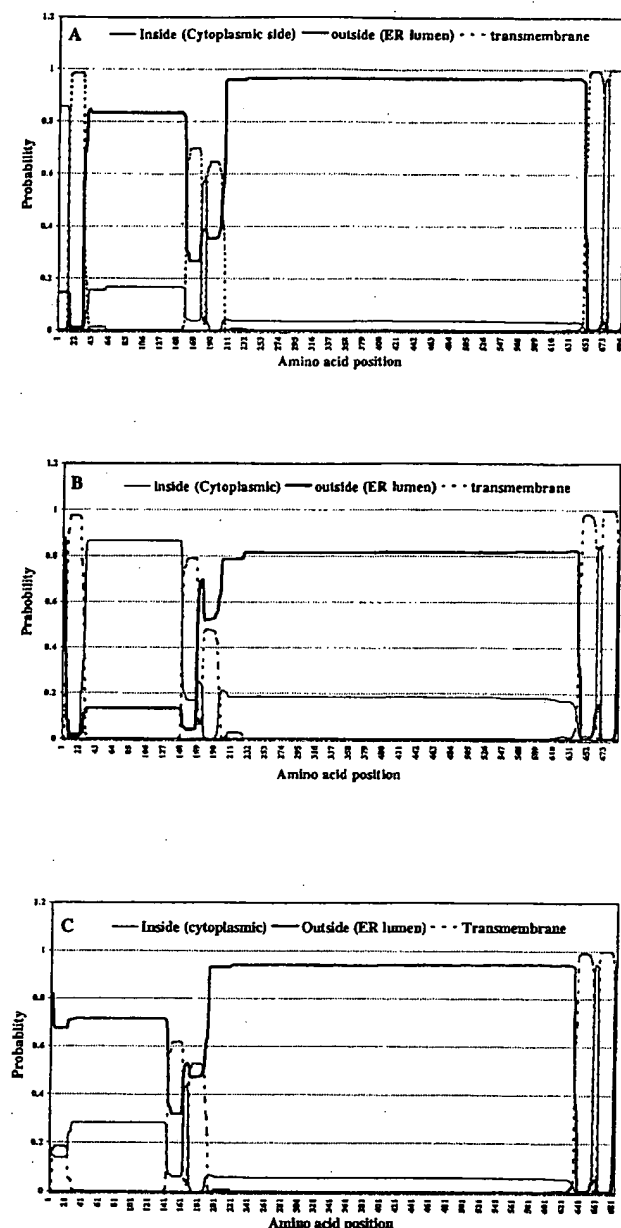
FIG. 5. Graphic representation, generated by the TMHMM program, indicating probable orientations of five transmembrane helices in the prM-E protein expressed by pCDJE2-7 (A), pcDNA3JEME (B), and pJME (C). ER, endoplasmic reticulum.

ACKNOWLEDGMENTS

REFERENCES

1. Appleby, P., and D. Catty. 1983. Transmission of immunoglobulin to foetal and neonatal mice. J. Reprod. Immunol. 5:203–213.
2. Cavener, D. R., and S. C. Ray. 1991. Eukaryotic start and stop translation sites. Nucleic Acids Res. 19:3185–3192.
3. Cecilia, D., D. A. Gadkari, N. Kedarnath, and S. N. Ghosh. 1988. Epitope mapping of Japanese encephalitis virus envelope protein using monoclonal antibodies against an Indian strain. J. Gen. Virol. 69:2741–2747.
4. Colombage, G., R. Hall, M. Pavy, and M. Lobigs. 1998. DNA-based and

5. Condon, C., S. C. Watkins, C. M. Celluzzi, K. Thompson, and L. D. Falo, Jr. 1996. DNA-based immunization by in vivo transfection of dendritic cells. Nat. Med. 2:1122–1128.
6. Erik, L. L., S. G. von Heijne, and A. Krogh. 1998. A hidden Markov model for predicting transmembrane helices in protein sequences, p. 175–182. In J. Glasgow, T. Littlejohn, F. Major, R. Lathrop, D. Sankoff, and C. Sensen (ed.), Proceedings of the Sixth International Conference on Intelligent Systems for Molecular Biology. AAAI Press, Menlo Park, Calif.
7. Gentry, M. K., E. A. Henchal, J. M. McCown, W. E. Brandt, and J. M. Dalrymple. 1982. Identification of distinct antigenic determinants on dengue-2 virus using monoclonal antibodies. Am. J. Trop. Med. Hyg. 31:548–555.
8. Guirakhoo, F., R. A. Bolin, and J. T. Roehrig. 1992. The Murray Valley encephalitis virus prM protein confers acid resistance to virus particles and alters the expression of epitopes within the R2 domain of E glycoprotein. Virology 191:921–931.
9. Heinz, F. X., R. Berger, W. Tuma, and C. Kunz. 1983. A topological and functional model of epitopes on the structural glycoprotein of tick-borne encephalitis virus defined by monoclonal antibodies. Virology 126:525–537.
10. Heinz, F. X., K. Stiasny, G. Puschner-Auer, H. Holzmann, S. L. Allison, C. W. Mandl, and C. Kunz. 1994. Structural changes and functional control of the tick-borne encephalitis virus glycoprotein E by the heterodimeric association with protein prM. Virology 198:109–117.
11. Hennessy, S., Z. Liu, T. F. Tsai, B. L. Strom, C. M. Wan, H. L. Liu, T. X. Wu, H. J. Yu, Q. M. Liu, N. Karabatsos, W. B. Bilker, and S. B. Halstead. 1996. Effectiveness of live-attenuated Japanese encephalitis vaccine (SA14-14-2): a case-control study. Lancet 347:1583–1586.
12. Hunt, A. R., and C. H. Calisher. 1979. Relationships of bunyamwera group viruses by neutralization. Am. J. Trop. Med. Hyg. 28:740–749.
13. Igarashi, A. 1978. Isolation of a Singh's Aedes albopictus cell clone sensitive to dengue and Chikungunya viruses. J. Gen. Virol. 40:531–544.
14. Kaufman, B. M., P. L. Summers, D. R. Dubois, W. H. Cohen, M. K. Gentry, R. L. Timchak, D. S. Burke, and K. H. Eckels. 1989. Monoclonal antibodies for dengue virus prM glycoprotein protect mice against lethal dengue infection. Am. J. Trop. Med. Hyg. 41:576–580.
15. Kimura-Kuroda, J., and K. Yasui. 1983. Topographical analysis of antigenic determinants on envelope glycoprotein V3 (E) of Japanese encephalitis virus, using monoclonal antibodies. J. Virol. 45:124–132.
16. Kimura-Kuroda, J., and K. Yasui. 1988. Protection of mice against Japanese encephalitis virus by passive administration with monoclonal antibodies. J. Immunol. 141:3606–3610.
17. Kochel, T., S. J. Wu, K. Raviprakash, P. Hobart, S. Hoffman, K. Porter, and C. Hayes. 1997. Inoculation of plasmids expressing the dengue-2 envelope gene elicit neutralizing antibodies in mice. Vaccine 15:547–552.
18. Konishi, E., I. Kurane, P. W. Mason, R. E. Shope, N. Kanesa-Thasan, J. J. Smucny, C. H. Hoke, Jr., and F. A. Ennis. 1998. Induction of Japanese encephalitis virus-specific cytotoxic T lymphocytes in humans by poxvirus-based JE vaccine candidates. Vaccine 16:842–849.
19. Konishi, E., and P. W. Mason. 1993. Proper maturation of the Japanese encephalitis virus envelope glycoprotein requires cosynthesis with the pre-membrane protein. J. Virol. 67:1672–1675.
20. Konishi, E., S. Pincus, B. A. Fonseca, R. E. Shope, E. Paoletti, and P. W. Mason. 1991. Comparison of protective immunity elicited by recombinant vaccinia viruses that synthesize E or NS1 of Japanese encephalitis virus. Virology 185:401–410.
21. Konishi, E., S. Pincus, E. Paoletti, W. W. Laegreid, R. E. Shope, and P. W. Mason. 1992. A highly attenuated host range-restricted vaccinia virus strain, NYVAC, encoding the prM, E, and NS1 genes of Japanese encephalitis virus prevents JEV viremia in swine. Virology 190:454–458.
22. Konishi, E., S. Pincus, E. Paoletti, R. E. Shope, T. Burrage, and P. W. Mason. 1992. Mice immunized with a subviral particle containing the Japanese encephalitis virus prM/M and E proteins are protected from lethal JEV infection. Virology 188:714–720.
23. Konishi, E., K. S. Win, I. Kurane, P. W. Mason, R. E. Shope, and F. A. Ennis. 1997. Particulate vaccine candidate for Japanese encephalitis induces long-lasting virus-specific memory T lymphocytes in mice. Vaccine 15:281–286.
24. Konishi, E., M. Yamaoka, Khin-Sane-Win, I. Kurane, and P. W. Mason. 1998. Induction of protective immunity against Japanese encephalitis in mice by immunization with a plasmid encoding Japanese encephalitis virus pre-membrane and envelope genes. J. Virol. 72:4925–4930.
25. Kozak, M. 1984. Compilation and analysis of sequences upstream from the translational start site in eukaryotic mRNAs. Nucleic Acids Res. 12:857–872.
26. Kozak, M. 1987. At least six nucleotides preceding the AUG initiator codon enhance translation in mammalian cells. J. Mol. Biol. 196:947–950.
27. Kozak, M. 1997. Recognition of AUG and alternative initiator codons is augmented by G in position +4 but is not generally affected by the nucleotides in positions +5 and +6. EMBO J. 16:2482–2492.
28. Ku, C. C., C. C. King, C. Y. Lin, H. C. Hsu, L. Y. Chen, Y. Y. Yueh, and G. J. Chang. 1994. Homologous and heterologous neutralization antibody re-

alphavirus-vectored immunisation with prM and E proteins elicits long-lived and protective immunity against the flavivirus, Murray Valley encephalitis virus. Virology 250:151–163.

sponses after immunization with Japanese encephalitis vaccine among Taiwan children. J. Med. Virol. 44:122–131.

29. Kuno, G., G. J. Chang, K. R. Tsuchiya, N. Karabatsos, and C. B. Cropp. 1998. Phylogeny of the genus *Flavivirus*. J. Virol. 72:73–83.

30. Lin, Y. L., L. K. Chen, C. L. Liao, C. T. Yeh, S. H. Ma, J. L. Chen, Y. L. Huang, S. S. Chen, and H. Y. Chiang. 1998. DNA immunization with Japanese encephalitis virus nonstructural protein NS1 elicits protective immunity in mice. J. Virol. 72:191–200.

31. Liu, Z. L., S. Hennessy, B. L. Strom, T. F. Tsai, C. M. Wan, S. C. Tang, C. F. Xiang, W. B. Bilker, X. P. Pan, Y. J. Yao, Z. W. Xu, and S. B. Halstead. 1997. Short-term safety of live attenuated Japanese encephalitis vaccine (SA14-14-2): results of a randomized trial with 26,239 subjects. J. Infect. Dis. 176:1366–1369.

32. Mason, P. W., J. M. Dalrymple, M. K. Gentry, J. M. McCown, C. H. Hoke, D. S. Burke, M. J. Fournier, and T. L. Mason. 1989. Molecular characterization of a neutralizing domain of the Japanese encephalitis virus structural glycoprotein. J. Gen. Virol. 70:2037–2049.

33. McCown, J., M. Cochran, R. Putnak, R. Feighny, J. Burrous, E. Henchal, and C. Hoke. 1990. Protection of mice against lethal Japanese encephalitis with a recombinant baculovirus vaccine. Am. J. Trop. Med. Hyg. 42:491–499.

34. Nielsen, H., J. Engelbrecht, S. Brunak, and G. von Heijne. 1997. A neural network method for identification of prokaryotic and eukaryotic signal peptides and prediction of their cleavage sites. Int. J. Neural Syst. 8:581–599.

35. Nitayaphan, S., J. A. Grant, G. J. Chang, and D. W. Trent. 1990. Nucleotide sequence of the virulent SA-14 strain of Japanese encephalitis virus and its attenuated vaccine derivative, SA-14-14-2. Virology 177:541–552.

36. Nothdurft, H. D., T. Jelinek, A. Marschang, H. Maiwald, A. Kapaun, and T. Loscher. 1996. Adverse reactions to Japanese encephalitis vaccine in travellers. J. Infect. 32:119–122.

37. Obijeski, J. F., D. H. Bishop, E. L. Palmer, and F. A. Murphy. 1976. Segmented genome and nucleocapsid of La Crosse virus. J. Virol. 20:664–675.

38. Phillpotts, R. J., K. Venugopal, and T. Brooks. 1996. Immunisation with DNA polynucleotides protects mice against lethal challenge with St. Louis encephalitis virus. Arch. Virol. 141:743–749.

39. Poland, J. D., C. B. Cropp, R. B. Craven, and T. P. Monath. 1990. Evaluation of the potency and safety of inactivated Japanese encephalitis vaccine in US inhabitants. J. Infect. Dis. 161:878–882.

40. Roehrig, J. T., R. A. Bolin, and R. G. Kelly. 1998. Monoclonal antibody mapping of the envelope glycoprotein of the dengue 2 virus, Jamaica. Virology 246:317–328.

41. Roehrig, J. T., A. R. Hunt, A. J. Johnson, and R. A. Hawkes. 1989. Synthetic peptides derived from the deduced amino acid sequence of the E-glycoprotein of Murray Valley encephalitis virus elicit antiviral antibody. Virology 171:49–60.

42. Roehrig, J. T., J. H. Mathews, and D. W. Trent. 1983. Identification of epitopes on the E glycoprotein of Saint Louis encephalitis virus using monoclonal antibodies. Virology 128:118–126.

43. Rosen, L. 1986. The natural history of Japanese encephalitis virus. Annu. Rev. Microbiol. 40:395–414.

44. Sakaguchi, M., R. Tomiyoshi, T. Kuroiwa, K. Mihara, and T. Omura. 1992. Functions of signal and signal-anchor sequences are determined by the balance between the hydrophobic segment and the N-terminal charge. Proc. Natl. Acad. Sci. USA 89:16–19.

45. Sakaguchi, M., M. Yoshida, W. Kuroda, O. Harayama, Y. Matsunaga, and S. Inouye. 1997. Systemic immediate-type reactions to gelatin included in Japanese encephalitis vaccines. Vaccine 15:121–122.

46. Sambrook, J., E. F. Fritsch, and T. Maniatis. 1989. Molecular cloning: a laboratory manual, 2nd ed. Cold Spring Harbor Laboratory Press, Cold Spring Harbor, N.Y.

47. Sato, T., C. Takamura, A. Yasuda, M. Miyamoto, K. Kamogawa, and K. Yasui. 1993. High-level expression of the Japanese encephalitis virus E protein by recombinant vaccinia virus and enhancement of its extracellular release by the NS3 gene product. Virology 192:483–490.

48. Schalich, J., S. L. Allison, K. Stiasny, C. W. Mandl, C. Kunz, and F. X. Heinz. 1996. Recombinant subviral particles from tick-borne encephalitis virus are fusogenic and provide a model system for studying flavivirus envelope glycoprotein functions. J. Virol. 70:4549–4557.

49. Schmaljohn, C., L. Vanderzanden, M. Bray, D. Custer, B. Meyer, D. Li, C. Rossi, D. Fuller, J. Fuller, J. Haynes, and J. Huggins. 1997. Naked DNA vaccines expressing the prM and E genes of Russian spring summer encephalitis virus and Central European encephalitis virus protect mice from homologous and heterologous challenge. J. Virol. 71:9563–9569.

50. Stocks, C. E., and M. Lobigs. 1998. Signal peptidase cleavage at the flavivirus C-prM junction: dependence on the viral NS2B-3 protease for efficient processing requires determinants in C, the signal peptide, and prM. J. Virol. 72:2141–2149.

51. Takashima, I., T. Watanabe, N. Ouchi, and N. Hashimoto. 1988. Ecological studies of Japanese encephalitis virus in Hokkaido: interepidemic outbreaks of swine abortion and evidence for the virus to overwinter locally. Am. J. Trop. Med. Hyg. 38:420–427.

52. Tsai, T. F., G. J. Chang, and Y. X. Yu. 1999. Japanese encephalitis vaccines, p. 672–710. *In* A. P. Stanley and W. A. Orenstein (ed.), Vaccines, 3rd ed. W. B. Saunders, Philadelphia, Pa.

53. Ueba, N., T. Kimura, S. Nakajima, T. Kurimura, and T. Kitaura. 1978. Field experiments on live attenuated Japanese encephalitis virus vaccine for swine. Biken J. 21:95–103.

54. Yasuda, A., J. Kimura-Kuroda, M. Ogimoto, M. Miyamoto, T. Sata, T. Sato, C. Takamura, T. Kurata, A. Kojima, and K. Yasui. 1990. Induction of protective immunity in animals vaccinated with recombinant vaccinia viruses that express PreM and E glycoproteins of Japanese encephalitis virus. J. Virol. 64:2788–2795.

55. Zhang, M. J., M. J. Wang, S. Z. Jiang, and W. Y. Ma. 1989. Passive protection of mice, goats, and monkeys against Japanese encephalitis with monoclonal antibodies. J. Med. Virol. 29:133–138.

Sex Differences in Seoul Virus Infection Are Not Related to Adult Sex Steroid Concentrations in Norway Rats

SABRA L. KLEIN, BRIAN H. BIRD, AND GREGORY E. GLASS*

Department of Molecular Microbiology and Immunology, The Johns Hopkins School
of Hygiene and Public Health, Baltimore, Maryland 21205-2179

Field studies of hantavirus infection in rodents report that a higher percentage of infected individuals are males than females. To determine whether males were more susceptible to hantavirus infection than females, adult male and female Long Evans rats (*Rattus norvegicus*) were inoculated with doses of Seoul virus ranging from 10^{-4} to 10^6 PFU. The 50% infective doses (ID_{50}) were not significantly different for male and female rats ($10^{0.05}$ and $10^{0.8}$ PFU, respectively). To determine whether sex differences in response to infection were related to circulating sex steroid hormones, sex steroid concentrations were manipulated and antibody responses and virus shedding were assessed following inoculation with the ID_{90}. Regardless of hormone treatment, males had higher anti-Seoul virus immunoglobulin G (IgG) and IgG2a (i.e., Th1) responses than females and IgG1 (i.e., Th2) responses similar to those of females. Males also shed virus in saliva and feces longer than females. Manipulation of sex steroids in adulthood did not alter immune responses or virus shedding, suggesting that sex steroids may organize adult responses to hantavirus earlier during ontogeny.

Hantaviruses are negative-sense RNA viruses (family *Bunyaviridae*) encompassing over 20 different viruses that are each carried by a different host species, with rodents serving as the primary reservoirs (18). Field surveys of several rodent species, including brush mice, deer mice, harvest mice, bank voles, and cotton rats, indicate that males are more commonly infected than females (4, 8, 11, 19, 20, 27). Because these studies used serology to determine hantavirus infection, sex differences in infection could reflect either a lack of infection or the absence of sustained antibody production in females. Experimental inoculation of female rodents with hantavirus, however, illustrates that females produce long-lasting, detectable antibody (22). Alternatively, sex differences in hantavirus prevalence may reflect differences in endocrine-immune interactions (15). The extent to which sex steroids affect immune responses against hantavirus infection has not been examined.

In contrast to other rodent species, sex differences in hantavirus prevalence have not been reported consistently among natural populations of Norway rats. Among adult rats, however, males (90%) tend to be infected with Seoul virus more often than females (75%) (7, 10). Seoul virus is hypothesized to be transmitted via wounding, and adult male rats are more likely to be wounded than either females or juvenile males (10). Thus, sex differences in hantavirus prevalence may reflect complex interactions between behavior and physiology. The first goal of this study was to control for sex differences in exposure and determine whether males were more susceptible to hantavirus infection than females. At 70 to 80 days of age, 5 to 10 male and 5 to 10 female Long Evans rats (*Rattus norvegicus*) were inoculated with either 10^{-4}, 10^{-3}, 10^{-2}, 10^2, 10^4, or 10^6 PFU of Seoul virus (strain SR-11) suspended in 0.2 ml of Eagle minimum essential medium (with Earle's salts; Meditach Cellgro, Va.). Seoul virus was obtained from the U.S. Army Medical Research Institute of Infectious Diseases (Ft. Detrick, Md.), where the virus was isolated from neonatal rat brains and

passaged four times in Vero E6 cells. Blood samples were obtained from each animal prior to infection and then 10, 20, 30, and 40 days postinoculation under anesthesia with methoxyflurane vapors (Metofane; Schering Plough, Union, N.J.).

Plasma was used to detect anti-Seoul virus immunoglobulin G (IgG) using an enzyme-linked immunosorbent assay in which microtiter plates were coated overnight at 4°C with gamma-irradiated Vero E6 cells infected with Seoul virus or gamma-irradiated uninfected Vero E6 cells diluted 1:500 in carbonate buffer. Thawed plasma samples, as well as positive control samples (i.e., pooled plasma from rats previously determined to have anti-Seoul virus IgG) and negative control samples (i.e., pooled plasma from Seoul virus-naive rats), were diluted 1:100 in phosphate-buffered saline (PBS)–Tween (PBS-T) with 2% fetal bovine serum and added in duplicate to antigen-coated wells containing either infected or uninfected Vero E6 cells. The plates were sealed, incubated at 37°C for 1 h, and washed with PBS-T, and secondary antibody (Kirkegaard and Perry Laboratories, Gaithersburg, Md.; alkaline phosphatase-conjugated anti-rat IgG [heavy plus light chains], horseradish peroxidase-conjugated anti-rat IgG1, or horseradish peroxidase-conjugated anti-rat IgG2a diluted 1:400 in PBS with 2% fetal bovine serum) was added. The plates were resealed, incubated for 1 h at 37°C, and washed with PBS-T, and substrate buffer (0.5 mg of *p*-nitrophenyl phosphate per ml diluted in diethanolamine substrate buffer for alkaline phosphatase reactions or tetramethylbenzidine for horseradish peroxidase reactions) was added to each well. Plates were protected from light during the enzyme-substrate reaction, which was terminated after 30 to 45 min by adding 1.5 M NaOH to each well for alkaline phosphatase reactions or 2 N H_2SO_4 to each well for horseradish peroxidase reactions. The optical density (OD) was measured at 405 nm for alkaline phosphatase reactions and 450 nm for horseradish peroxidase reactions, and the average OD for each set of uninfected Vero E6 duplicates was subtracted from the average OD for each set of infected Vero E6 duplicates. Samples were considered positive if the average adjusted OD was ≥0.100. To minimize intra- and interplate variability, the average adjusted OD for each sample

* Corresponding author. Mailing address: Department of Molecular Microbiology and Immunology, Johns Hopkins School of Hygiene and Public Health, 615 N. Wolfe St., Baltimore, MD 21205-2179. Phone: (410) 955-3708. Fax: (410) 955-0105. E-mail: ggurrigl@jhsph.edu.
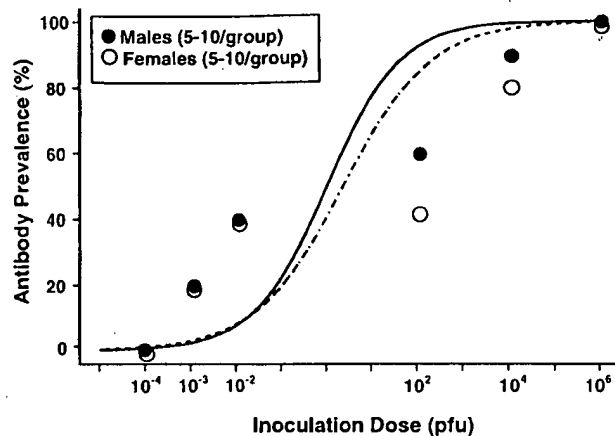
FIG. 1. Antibody prevalence among intact male and female rats inoculated with either 10^{-4}, 10^{-3}, 10^{-2}, 10^2, 10^4, or 10^6 PFU of Seoul virus. Data are presented as percentages of individuals producing detectable antibody (i.e., adjusted average OD $\geq$ 0.100) against Seoul virus by day 40 postinoculation, with the fitted logistic regression curves for both males (solid line) and females (dashed line) included. Equal percentages of males and females seroconverted in response to each dose of Seoul virus ($P > 0.05$ in each case).

was expressed as a percentage of its plate-positive control OD for statistical analyses (9).

Antibody prevalence (i.e., the number of animals with detectable anti-Seoul virus IgG) by day 40 postinoculation was compared between males and females using chi-square analyses. Antibody prevalence was assessed 40 days after inoculation because previous studies illustrate that hantavirus-specific antibody is detectable 15 to 30 days postinoculation (7, 14, 22). Antibody prevalence did not differ between males and females at any of the six doses of Seoul virus ($P > 0.05$). Logistic regression was used to compare the infective-dose (ID) curves and estimate the 50% ID (ID_{50}). The ID_{50} did not differ significantly between males (mean $\pm$ standard deviation, 1.1 $\pm$ 2.0 PFU) and females (7.6 $\pm$ 2.0 PFU) (Fig. 1).

Although the prevalence of males and females that became infected did not differ, studies of other viral infections suggest that patterns of immune responses differ between the sexes and are mediated by sex steroid hormones (1, 15, 29). Thus, males and females may differ because testosterone suppresses and estradiol enhances several aspects of immune function (1, 15, 17, 24, 26, 29). The second aim of this study was to examine whether adult sex steroid hormone concentrations influence immune responses and virus shedding following hantavirus infection. Immunologically, patterns of helper T (Th) cell responses (i.e., Th1 or Th2) differ between males and females, with males exhibiting elevated Th1 responses (i.e., elevated gamma interferon, interleukin-2 [IL-2], and IgG2a levels) and females exhibiting increased Th2 responses (i.e., higher IL-4, IL-5, IL-6, and IL-10 levels) (5, 12, 13). Treatment of males with estradiol and females with testosterone prior to infection with pathogens, such as coxsackievirus, reverses the Th responses, suggesting that hormones can modify immune responses to virus infection (12, 13). To determine whether adult sex steroid hormone concentrations influence immune responses and virus shedding following hantavirus infection, at 70 to 80 days of age 20 male and 20 female rats were bilaterally gonadectomized under ketamine (80 mg/kg of body mass)–xylazine (6 mg/kg) anesthesia (Phoenix Pharmaceutical, St. Joseph, Mo.) and given 2 weeks to recover from surgery. After recovery, 10 castrated males were each subcutaneously implanted with a 30-mm Silastic capsule (inside diameter [i.d.] =

1.47 mm, outside diameter [o.d.] = 1.96 mm) containing 20 mm of testosterone propionate (Sigma, St. Louis, Mo.). The remaining 10 castrated males, as well as 10 intact males, were each implanted with an empty capsule of equal length. Ten ovariectomized females were each subcutaneously implanted with a 15-mm Silastic capsule (i.d. = 1.47 mm, o.d. = 1.96 mm) containing 10 mm of estradiol benzoate (Sigma). The remaining 10 ovariectomized females and 9 intact females were each implanted with an empty Silastic capsule of equal length. Silastic capsule length was based on previous reports that these hormone doses (i.e., the length of the Silastic capsule) are sufficient to maintain physiological testosterone and estradiol concentrations in male and female rats, respectively (25). At the time the Silastic capsules were implanted, all animals received an intraperitoneal inoculation of 10^4 PFU of Seoul virus (strain SR-11) suspended in 0.2 ml of Eagle minimum essential medium (i.e., the ID_{90} from the first experiment). Blood, saliva, and fecal samples were then obtained from each animal on days 0, 10, 15, 20, 30, and 40 postinoculation under anesthesia with methoxyflurane vapors. Saliva samples were collected from anesthetized rats after injecting them intraperitoneally with 2.5 mg of pilocarpine HCl (Sigma) per kg of body mass suspended in 0.9% sterile saline (6). After samples were collected on day 40 postinoculation, animals were killed and seminal vesicles were removed from the males and weighed as an index of long-term testosterone concentrations. All procedures described in this paper were approved by the Johns Hopkins Animal Care and Use Committee (protocol number RA98H536) and the Johns Hopkins Office of Health, Safety, and Environment (registration number A9902030102).

Relative seminal vesicle weights (i.e., corrected for body mass) were higher among intact males (0.282 $\pm$ 0.13 g) and castrated males treated with testosterone (0.326 $\pm$ 0.12 g) than among castrated males (0.095 $\pm$ 0.06 g) [$F(2, 29) = 12.75, P < 0.05$]. Plasma testosterone concentrations in males and estradiol concentrations in females were assayed by radioimmunoassay using the manufacturer's protocols (ICN Biochemicals, Inc., Carson, Calif.). Testosterone concentrations were higher for intact males and castrated males treated with testosterone than for castrated male rats; castrated males treated with testosterone also had higher testosterone concentrations than intact males on days 10, 15, 20, and 30, but not on day 40, postinoculation [$F(10, 179) = 19.30, P < 0.05$] (Table 1). Plasma estradiol concentrations were higher for intact females and ovariectomized females treated with estradiol than for ovariectomized females 10, 15, 20, 30, and 40 days postinoculation; ovariectomized females treated with estradiol also had higher estradiol concentrations than intact females on days 10, 15, 20, 30, and 40 postinoculation [$F(10, 173) = 10.29, P < 0.05$] (Table 1).

Manipulation of testosterone concentrations in males and estradiol concentrations in females did not affect production of antibody against Seoul virus ($P > 0.05$). Overall, males had higher anti-Seoul virus IgG responses than females on days 20, 30, and 40 postinoculation, regardless of hormone treatment [$F(5, 353) = 18.72, P < 0.05$] (Table 2). Male rats also had higher anti-Seoul virus IgG2a responses than females on days 30 and 40 postinoculation despite hormone manipulation [$F(5, 353) = 7.81, P < 0.05$] (Fig. 2A). In contrast, females tended to show higher IgG1 responses than males on days 30 and 40 postinoculation, though this did not reach statistical significance ($P > 0.05$) (Fig. 2B).

Viral RNA was identified using nested reverse transcription-PCR (RT-PCR), and the presence of virus in saliva and feces was used to determine whether virus was shed. Viral RNA was isolated using a guanidine isothiocyanate procedure (3). For

TABLE 1. Sex steroid hormone concentrations[a]

Hormone and group	Hormone concn (mean ± SE) on day postinoculation[b]					
	0	10	15	20	30	40
Testosterone						
Intact males	0.69 ± 0.17*	0.84 ± 0.17*	1.13 ± 0.36*	0.92 ± 0.25*	0.77 ± 0.19*	0.70 ± 0.13*
Castrated males	0.00 ± 0.00	0.00 ± 0.00	0.00 ± 0.00	0.00 ± 0.00	0.00 ± 0.00	0.00 ± 0.00
T-treated males	0.00 ± 0.00	8.24 ± 0.74*†	6.28 ± 0.91*†	6.62 ± 1.18*†	2.73 ± 0.42*†	0.71 ± 0.28*
Estradiol						
Intact females	25.8 ± 6.81*	27.0 ± 5.57*	20.8 ± 8.39*	25.9 ± 7.78*	38.2 ± 10.1*	55.2 ± 10.2*
Ovx females	0.00 ± 0.00	0.00 ± 0.00	0.00 ± 0.00	0.00 ± 0.00	0.00 ± 0.00	0.00 ± 0.00
E$_2$-treated females	0.00 ± 0.00	166.6 ± 20.6*†	123.1 ± 21.9*†	87.5 ± 8.9*†	162.3 ± 18.8*†	109.7 ± 19.3*†

[a] Sex steroid hormone concentrations in males and females that either were intact, gonadectomized (i.e., males were castrated and females were ovariectomized [Ovx]), or gonadectomized with sex steroids replaced (i.e., gonadectomized males received testosterone [T]-filled capsules and gonadectomized females received estradiol [E$_2$]-filled capsules).

[b] Testosterone levels are in nanograms per milliliter, and estradiol levels are in picograms per milliliter. An asterisk indicates that intact and hormone-treated animals had higher hormone concentrations than their gonadectomized counterparts on the corresponding day, based on an analysis of variance ($P < 0.05$). A dagger indicates that hormone-treated animals had higher sex steroid concentrations than their intact counterparts on the corresponding day, based on an analysis of variance ($P < 0.05$).

RNA isolation from saliva, samples were collected from each rat and added to Trizol LS reagent (Life Technologies, Rockville, Md.) at a 3:1 ratio, with RNase-free glycogen (10 μg) added as a carrier. For RNA isolation from feces, approximately 100 mg of feces was homogenized in Tris-EDTA buffer (pH 8.0) and centrifuged at 12,000 × g for 10 min at 4°C; supernatants were collected, incubated with proteinase K (50 μg/ml; Life Technologies) and 0.5% sodium dodecyl sulfate at 50°C for 30 min to digest proteins, and then added to Trizol LS at a 3:1 ratio. To separate, precipitate, and resuspend viral RNA, the manufacturer's protocol was used (Trizol LS; Life Technologies).

For RT-PCR, a 280-bp nucleotide sequence of the SR-11 small (S) genome was amplified using two 20-bp primers, HTN-S4 (5' GATAGGTGTCCACCAACATG 3') and HTN-S6 (5' AGCTCTGGATCCATGTCATC 3'), that amplified positions 979 through 1259 (3). The DNA fragment obtained from the RT-PCR was further amplified using primers HTN-S3 (5' GCCTTCTTTTCTATACTTCAGG 3') and HTN-S5 (5' CCAGGCAACCATAAACATAAC 3'), designed to amplify a 176-bp nucleotide sequence (positions 1031 through 1207). First-strand cDNA was prepared using the GeneAmp RNA PCR kit protocol (Perkin-Elmer, Branchburg, N.J.), incubated in a DNA thermocycler (Techne Genius) at 42°C for 15 min, 99°C for 5 min, and 5°C for 5 min, and then held at 4°C. The reaction mixture contained 5 mM MgCl$_2$, 1 mM deoxynucleoside triphosphates, 1 U of RNase inhibitor, and 2.5 U of murine leukemia virus reverse transcriptase. The positive control was SR-11 RNA isolated

from virus stock, and the negative control was diethyl pyrocarbonate water that was included in the cDNA syntheses and primary and secondary amplifications.

The 280-bp sequence was amplified in a 100-μl reaction mixture containing 20 μl of the cDNA, 0.3 μM HTN-S6 primer, and 2.5 U of polymerase (AmpliTaq; Perkin-Elmer). Reactions were amplified for one cycle at 94°C for 3 min and 40 cycles of 94°C for 30 s, 55°C for 45 s, and 72°C for 60 s, followed by 10 min at 72°C. The nested 176-bp sequence was amplified in a 100-μl reaction mixture containing 2 μl of the product of the first DNA amplification, 20 μM HTN-S3 primer, 20 μM HTN-S5 primer, 10 mM MgCl$_2$, 1 mM deoxynucleoside triphosphates, and 2.5 U of polymerase. Nested-PCR products were amplified using the same cycle series as was used for the primary amplification. The PCR products were electrophoresed on a 4% gel (3% NuSieve plus 1% SeaKem; FMC Bioproducts, Rockland, Maine), stained with ethidium bromide, and examined for bands of the appropriate size. Randomly selected positive PCR products from saliva and fecal samples from males and females, as well as positive and negative control products, were purified using QIAquick (Qiagen, Valencia, Calif.) and sequenced.

Virus shedding in saliva and feces was not altered by hormone manipulation ($P > 0.05$) (Table 3). Overall, more males shed virus in saliva than females 10 days ($\chi^2 = 3.82, df = 1, P = 0.051$) and 30 days ($\chi^2 = 8.19, df = 1, P < 0.05$) after inoculation with Seoul virus (Table 3). The prevalence of Seoul virus in feces also differed between males and females on day 30 postinoculation; more males shed virus in feces than females

TABLE 2. Plasma anti-Seoul virus IgG responses[a]

Group	Anti-Seoul virus IgG response (mean ± SE) on day postinoculation[b]					
	0	10	15	20	30	40
Intact males	0.8 ± 0.6	4.9 ± 3.0	84.0 ± 22.0	106.0 ± 19.0*	332.0 ± 47.0*	342.1 ± 56.0*
Castrated males	1.0 ± 0.7	1.0 ± 1.0	82.0 ± 21.0	106.0 ± 27.0*	280.0 ± 71.0*	387.3 ± 84.0*
T-treated males	1.0 ± 0.7	2.0 ± 0.9	33.0 ± 10.0	108.0 ± 14.0*	314.0 ± 41.0*	426.7 ± 43.0*
Intact females	3.0 ± 1.0	9.0 ± 4.0	36.0 ± 10.0	60.0 ± 14.0	189.0 ± 55.0	219.6 ± 63.0
Ovx females	2.0 ± 0.8	4.0 ± 2.0	7.0 ± 3.0	54.0 ± 16.0	187.0 ± 56.0	209.2 ± 53.0
E$_2$-treated females	3.0 ± 1.0	8.0 ± 2.0	19.0 ± 6.0	39.0 ± 8.0	178.0 ± 42.0	209.1 ± 39.0

[a] Plasma anti-Seoul virus IgG responses in males and females that either were intact, gonadectomized (i.e., males were castrated and females were ovariectomized [Ovx]), or gonadectomized with sex steroids replaced (i.e., gonadectomized males received testosterone [T]-filled capsules and gonadectomized females received estradiol [E$_2$]-filled capsules).

[b] Data are presented as IgG units, in which the mean OD of each test sample was divided by the OD of the positive control sample run on the same microtiter plate. An asterisk indicates that males had higher IgG responses than females, regardless of hormone manipulation, based on an analysis of variance ($P < 0.05$).
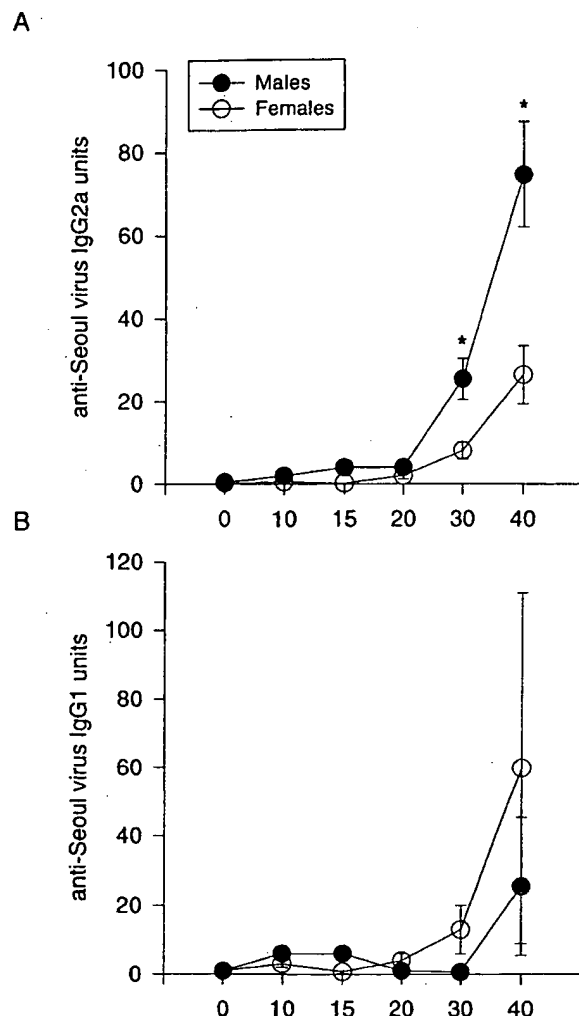
A

B

FIG. 2. (A) Plasma anti-Seoul virus IgG2a responses (mean ± standard error) in male and female rats. (B) Plasma anti-Seoul virus IgG1 responses (mean ± standard error) in male and female rats. Blood samples were collected 0, 10, 15, 20, 30, and 40 days following inoculation with Seoul virus. For calculation of IgG2a or IgG1 units, the mean OD of each test sample was divided by the OD of the positive control sample run on the same microtiter plate. Because neither gonadectomy nor hormone replacement had an effect on antibody production, responses from the different treatments groups were collapsed and graphed together. An asterisk indicates that males had higher IgG2a responses than females ($P < 0.05$).

($\chi^2 = 6.88$, $df = 1$, $P < 0.05$) (Table 3). In general, males shed virus in saliva and feces more consistently than females, regardless of hormone manipulation (Table 3). The PCR product obtained from saliva and feces of males and females was sequenced and verified as Seoul virus DNA.

Sex differences in the prevalence of hantavirus infection have been observed in several natural rodent populations, including deer mice, brush mice, harvest mice, bank voles, and cotton rats (4, 8, 11, 19, 20, 27). In each case, males are infected more often than females. Field studies of Norway rats suggest that sex differences in hantavirus prevalence reflect sex differences in behaviors, like aggression, that increase the likelihood of males being infected (10). High circulating testosterone concentrations increase the probability of engaging in aggressive encounters in several vertebrate species (21). In addition to modulating aggression, sex steroid hormones can

affect immune responses against infection. Studies of viral infections, such as coxsackievirus, suggest that sex differences in both the prevalence and intensity of infection are due to differences in endocrine-immune interactions (12, 13).

Despite the known effects of sex steroids on infection, in the present study, manipulation of adult sex steroids had no effect on immune responses or virus shedding following exposure to Seoul virus. Specifically, males had higher antibody responses and shed virus longer than females, regardless of adult hormone manipulation. Sex steroid hormones affect physiology and behavior at two distinct times during ontogeny (2, 16, 23). During perinatal development, sex steroids cause sex differences in the differentiation or organization of central and peripheral structures. In adulthood, exposure to sex steroids serves to activate preexisting hormonal circuits. The data from the present study may suggest that sex steroid hormones are not involved in hantavirus infection. Alternatively, these data may illustrate that manipulation of activational sex steroids does not alter responses to infection because the hormonal circuitry was organized earlier during development. If sex steroids organize adult responses to infection, then manipulation of neonatal sex steroids should alter adult responses to hantavirus infection.

Regardless of hormone manipulation, males had higher anti-Seoul virus IgG2a responses than females. Recent data from our laboratory indicate that following Seoul virus inoculation, males have elevated IL-2 and gamma interferon concentrations and females have elevated IL-4 responses (S. L. Klein and G. E. Glass, unpublished data). Taken together, these data suggest that males may have higher Th1 responses to hantavirus infection than females. Studies of other viral infections in rodents suggest that females typically have higher Th2 re-

TABLE 3. Virus shedding[a]

Sample and group	No. of virus-shedding rats/total on day postinoculation[b]				
	10	15	20	30	40
Saliva samples					
Intact males	6/11	7/10	6/11	6/11	6/11
Castrated males	4/9	4/9	6/9	5/9	8/9
T-treated males	9/10	7/10	4/10	6/10	7/10
Total males	19/30*	18/29	16/30	17/30*	21/30
Intact females	3/9	6/9	5/9	2/9	2/9
Ovx females	4/10	7/10	2/10	2/10	6/10
E$_2$-treated females	3/10	10/10	3/10	1/10	6/10
Total females	10/29	23/29	11/29	5/29	14/29
Fecal samples					
Intact males	5/11	4/11	4/11	5/11	1/11
Castrated males	6/9	5/9	7/9	4/8	1/9
T-treated males	4/10	6/10	7/10	7/9	1/10
Total males	15/30	15/30	18/30	16/29*	3/30
Intact females	7/9	4/9	4/9	1/8	0/9
Ovx females	9/10	4/10	6/10	2/10	2/10
E$_2$-treated females	6/9	5/10	8/10	2/10	1/10
Total females	22/28	13/29	18/29	5/28	3/29

[a] Virus shedding in saliva and feces from males and females that either were intact, gonadectomized (i.e., males were castrated and females were ovariectomized [Ovx]), or gonadectomized with sex steroids replaced (i.e., gonadectomized males received testosterone [T]-filled capsules and gonadectomized females received estradiol [E$_2$]-filled capsules).

[b] An asterisk indicates that more males shed virus than females on the respective day postinoculation, based on chi-square analyses ($P < 0.05$).

sponses than males and that this is due, in part, to the effects of estrogens on cytokine production (12). In the present study, females tended to produce higher IgG1 responses than males. In contrast to estrogens, androgens promote differentiation of $CD4^+$ T cells to a Th1 phenotype (12). In the present study, however, castrated and intact males had similar IgG2a responses, suggesting that increased Th1 responses are not contingent on the direct effects of androgens.

High antibody responses in males may indicate that males have more efficient immune responses against infection than females. This outcome seems unlikely given the rapid increase and long duration of virus shedding in males compared to females. Alternatively, males may have higher antibody responses than females because virus replication is increased in males. Higher Th1 responses are associated with increased susceptibility to infections caused by coxsackievirus and Sindbis virus in mice (12, 28). Although quantitative analyses were not conducted, males shed Seoul virus longer than females, suggesting that higher Th1 responses among males may be a consequence of increased virus replication.

In summary, although males and females are equally susceptible to infection with Seoul virus, males shed virus longer and produce higher Th1 responses against Seoul virus than females. Increased virus shedding among males may explain why males are more likely to acquire Seoul virus infection following aggressive encounters among natural populations of Norway rats (10). In the present study, manipulation of adult sex steroid hormones did not alter immune responses or virus shedding following inoculation with Seoul virus. Although sex steroid hormones may not mediate sex differences in response to hantavirus infection, sex differences in infection among adults may be altered by sex steroids earlier during development. Alternatively, sex differences in infection may reflect other neuroendocrine changes, such as differences in glucocorticoids, that may affect responses to Seoul virus infection.

REFERENCES

1. Alexander, J., and W. H. Stimson. 1988. Sex hormones and the course of parasitic infection. Parasitol. Today 4:189–193.
2. Arnold, A. P., and S. M. Breedlove. 1985. Organizational and activational effects of sex steroids on brain and behavior: a reanalysis. Horm. Behav. 19:469–498.
3. Arthur, R. R., R. S. Lofts, J. Gomez, G. E. Glass, J. W. LeDuc, and J. E. Childs. 1992. Grouping of hantaviruses by small (S) genome segment polymerase chain reaction and amplification of viral RNA from wild-caught rats. Am. J. Trop. Med. Hyg. 47:210–224.
4. Bernshtein, A. D., N. S. Apekina, T. V. Mikhailova, Y. A. Myasnikov, L. A. Khlyap, Y. S. Korotkov, and I. N. Gavrilovskaya. 1999. Dynamics of Puumala hantavirus infection in naturally infected bank voles (Clethrionomys glareolus). Arch. Virol. 144:2415–2428.
5. Bijlsma, J. W. J., M. Cutolo, A. T. Masi, and I. C. Chikanza. 1999. The neuroendocrine immune basis of rheumatic diseases. Trends Immunol. 20: 298–301.
6. Bodner, L., and B. J. Baum. 1985. Characteristics of stimulated parotid gland secretion in the aging rat. Mech. Ageing Dev. 31:337–342.
7. Childs, J. E., G. W. Korch, G. E. Glass, J. W. LeDuc, and K. V. Shah. 1987. Epizootiology of hantavirus infections in Baltimore: isolation of a virus from Norway rats, and characteristics of infected rat populations. Am. J. Epidemiol. 126:55–68.
8. Childs, J. E., T. G. Ksiazek, C. F. Spiropoulou, J. W. Krebs, S. Morzunov, G. O. Maupin, K. L. Gage, P. E. Rollin, J. Sarisky, R. E. Enscore, J. K. Frey, C. J. Peters, and S. T. Nichol. 1994. Serologic and genetic identification of Peromyscus maniculatus as the primary reservoir for a new hantavirus in the southwest United States. J. Infect. Dis. 169:1271–1280.
9. de Savigny, D., and A. Voller. 1980. The communication of ELISA data from laboratory to clinician. J. Immunoass. 1:105–128.
10. Glass, G. E., J. E. Childs, G. W. Korch, and J. W. LeDuc. 1988. Association of intraspecific wounding with hantaviral infection in wild rats (Rattus norvegicus). Epidemiol. Infect. 101:459–472.
11. Glass, G. E., W. Livingstone, J. N. Mills, W. G. Hlady, J. B. Fine, W. Biggler, T. Coke, D. Frazier, S. Atherley, P. E. Rollin, T. G. Ksiazek, C. J. Peters, and J. E. Childs. 1998. Black Creek Canal virus infection in Sigmodon hispidus in southern Florida. Am. J. Trop. Med. Hyg. 59:699–703.
12. Huber, S. A., J. Kupperman, and M. K. Newell. 1999. Hormonal regulation of $CD4^+$ T-cell responses in coxsackievirus B3-induced myocarditis in mice. J. Virol. 73:4689–4695.
13. Huber, S. A., and B. Pfaeffle. 1994. Differential Th_1 and Th_2 cell responses in male and female BALB/c mice infected with coxsackievirus group B type 3. J. Virol. 68:5126–5132.
14. Hutchinson, K. L., P. E. Rollin, W.-J. Shieh, S. Zaki, P. W. Greer, and C. J. Peters. 2000. Transmission of Black Creek Canal virus between cotton rats. J. Med. Virol. 60:70–76.
15. Klein, S. L. The effects of hormones on sex differences in infection: from genes to behavior. Neurosci. Biobehav. Rev., in press.
16. Konstadoulakis, M. M., K. N. Syrigos, C. N. Baxevanis, E. I. Syrigou, M. Papamichail, P. Peveretos, M. Anapliotou, and B. C. Golematis. 1995. Effect of testosterone administration, pre- and postnatally, on the immune system of rats. Horm. Metab. Res. 27:275–278.
17. Mankau, S. K., and R. Hamilton. 1972. The effect of sex and sex hormones on the infection of rats by Trichinella spiralis. Can. J. Zool. 50:597–602.
18. Mertz, G. J., B. L. Hjelle, and R. T. Bryan. 1997. Hantavirus infection. Adv. Intern. Med. 42:369–421.
19. Mills, J. N., J. M. Johnson, T. G. Ksiazek, B. A. Ellis, P. E. Rollin, T. L. Yates, M. O. Mann, M. R. Johnson, M. L. Campbell, J. Miyashiro, M. Patrick, M. Zyzak, D. Lavender, M. G. Novak, K. Schmidt, C. J. Peters, and J. E. Childs. 1998. A survey of hantavirus antibody in small-mammal populations in selected United States national parks. Am. J. Trop. Med. Hyg. 58:525–532.
20. Mills, J. N., T. G. Ksiazek, B. A. Ellis, P. E. Rollin, S. T. Nichol, T. L. Yates, W. L. Gannon, C. E. Levy, D. M. Engelthaler, T. Davis, D. T. Tanda, J. W. Frampton, C. R. Nichols, C. J. Peters, and J. E. Childs. 1997. Patterns of association with host and habitat: antibody reactive with Sin Nombre virus in small mammals in the major biotic communities of the southwestern United States. Am. J. Trop. Med. Hyg. 56:273–284.
21. Nelson, R. J. 2000. An introduction to behavioral endocrinology, 2nd ed. Sinauer Associates, Inc., Sunderland, Mass.
22. Nuzum, E. O., C. A. Rossi, E. H. Stephenson, and J. W. LeDuc. 1988. Aerosol transmission of Hantaan and related viruses to laboratory rats. Am. J. Trop. Med. Hyg. 38:636–640.
23. Pheonix, C. H., R. W. Goy, A. A. Gerall, and W. C. Young. 1959. Organizing action of prenatally administered testosterone propionate on the tissues mediating mating behavior in the female guinea pig. Endocrinology 65:369–382.
24. Rajan, T. V., F. K. Nelson, L. D. Shultz, K. L. Shultz, W. G. Beamer, J. Yates, and D. L. Greiner. 1994. Influence of gonadal steroids on susceptibility to Brugia malayi in scid mice. Acta Trop. 56:307–314.
25. Smith, E. R., D. A. Damassa, and J. M. Davidson. 1977. Hormone administration: peripheral and intracranial implants, p. 259–279. In R. D. Myers (ed.), Methods in psychobiology. Academic Press, New York, N.Y.
26. Tiuria, R., Y. Horii, S. Tateyama, K. Tsuchiya, and Y. Nawa. 1994. The Indian soft-furred rat, Millardia meltada, a new host for Nippostrongylus brasiliensis, showing androgen-dependent sex difference in intestinal mucosal defence. Int. J. Parasitol. 24:1055–1057.
27. Weigler, B. J., T. G. Ksiazek, J. G. Vandenbergh, M. Levin, and W. T. Sullivan. 1996. Serological evidence for zoonotic hantaviruses in North Carolina rodents. J. Wildl. Dis. 32:354–357.
28. Wesselingh, S. L., B. Levine, R. J. Fox, S. Choi, and D. E. Griffin. 1994. Intracerebral cytokine mRNA expression during fatal and nonfatal alphavirus encephalitis suggests a predominant type 2 T cell response. J. Immunol. 152:1289–1297.
29. Zuk, M., and K. A. McKean. 1996. Sex differences in parasite infections: patterns and processes. Int. J. Parasitol. 26:1009–1024.

Repeated Intravesical Instillations of an Adenoviral Vector in Patients With Locally Advanced Bladder Cancer: A Phase I Study of p53 Gene Therapy

By Lance C. Pagliaro, Afsaneh Keyhani, Dallas Williams, Denise Woods, Baoshun Liu, Paul Perrotte, Joel W. Slaton, James A. Merritt, H. Barton Grossman, and Colin P. Dinney

Purpose: We investigated the feasibility, safety, and biologic activity of adenovirus-mediated p53 gene transfer in patients with locally advanced bladder cancer.

Patients and Methods: Patients with measurable, locally advanced transitional-cell carcinoma of the bladder who were not candidates for cystectomy were eligible. On a 28-day cycle, intravesical instillations of INGN 201 (Ad5CMV-p53) were administered on days 1 and 4 at three dose levels (10^{10} particles to 10^{12} particles) or on either 4 or 8 consecutive days at a single dose level (10^{12} particles).

Results: Thirteen patients received a total of 22 courses without dose-limiting toxicity. Specific transgene expression was detected by reverse transcriptase polymerase chain reaction in bladder biopsy tissue from two of seven assessable patients. There were no changes in p53, $p21^{waf1/cip1}$, or bax

protein levels in bladder epithelium evident from immunohistochemical analysis of 11 assessable patients. Outpatient administration of multiple courses was feasible and well tolerated. A patient with advanced superficial bladder cancer showed evidence of tumor response.

Conclusion: Intravesical instillation of Ad5CMV-p53 is safe, feasible, and biologically active when administered in multiple doses to patients with bladder cancer. Observations from this study indicate that this treatment has an antitumor effect in superficial transitional-cell carcinoma. Improvements in the efficiency of gene transfer and the levels of gene expression are required to develop more effective gene therapy for bladder cancer.

J Clin Oncol 21:2247-2253. © 2003 by American Society of Clinical Oncology.

A PPROXIMATELY 80% of patients with bladder cancer are diagnosed with tumors confined to the bladder.[1] Endoscopic surgery is the standard treatment for superficial bladder cancer, but the majority of patients remain at risk for tumor recurrence or progression because of minimal residual disease and a urothelial field defect. The intravesical administration of bacille Calmette-Guérin (BCG) or other therapeutic agents as adjuvant therapy is effective and changes the natural history of the disease.[2] Unfortunately, 20% to 30% of patients still suffer recurrences despite BCG immunotherapy, and radical cystectomy is often necessary for continued local control and to prevent life-threatening progression and metastasis.

Therapeutic gene transfer is a new strategy for modifying the urothelium.[3] In previous work, we used a mouse model to show that the luciferase reporter gene was highly expressed in bladder tissue after intravesical administration of an adenoviral vector, and in contrast to intravenous injection, there was nearly complete absence of transfection in other organs.[4] Intravesical administration has potential advantages over intratumoral injection, which is the method commonly used for vector-mediated gene transfer in other tumor types.[3,5,6] In a recently reported study, Kuball et al[7] looked for evidence of adenovirus-mediated wild-type p53 gene transfer in the cystectomy specimens of patients who received either intratumoral injection (7.5×10^{11} particles in 1 mL) or intravesical instillation (7.5×10^{11} to 7.5×10^{13} particles) of the vector preoperatively. They detected expression of the vector transgene in bladder tissue by reverse transcriptase polymerase chain reaction (RT-PCR) in seven of eight assessable patients after an intravesical instillation and in none of those who had received an intratumoral injection, though the sample size was small (three patients).

In the case of adenovirus-mediated gene therapy, some of the obstacles to achieving transfection of tumor cells include the difficulties in reaching a tissue target and the low transduction efficiency of the vector.[8] The safety and convenience of intravesical administration offers an opportunity to overcome these problems, however, through repetitive dosing in the treatment of patients with bladder cancer. There have been no clinical studies to determine the safety, long-term effects, or biologic activity of multiple-dosing schedules or long-term intravesical treatment with an adenoviral vector for patients with bladder cancer. Intravesical gene therapy has potential future applications as a bladder-sparing intervention and for controlling minimal residual disease.[3] Therefore, the feasibility of repetitive dosing with an adenoviral vector and long-term effects on the urothelium in vivo are important end points.

The p53 gene is frequently mutated in bladder cancer and is known to govern processes critical to cell proliferation and survival.[9] Preclinical data indicate that adenovirus-mediated

delivery of the wild-type *p53* gene to human bladder cancer cell lines results in growth inhibition and apoptosis, including lines with and without *p53* mutations.[10,11] Furthermore, animal studies and phase I data from a single study indicate that adenovirus-mediated *p53* expression is cytotoxic to bladder cancer cells but not to normal urothelium.[7,12]

To further investigate the safety, feasibility, and biologic activity of adenovirus-mediated wild-type *p53* gene transfer in patients with bladder cancer, we conducted a phase I, dose-escalation study of INGN 201 (Ad5CMV-*p53*) administered intravesically to patients with measurable, mucosal lesions of the urinary bladder, who were not eligible for cystectomy. In this study, we also assessed the feasibility of endoscopic tissue sampling for monitoring the biologic effects of investigational therapy.

PATIENTS AND METHODS

Patient Eligibility

Adult patients with pathologically documented transitional-cell carcinoma (TCC) of the bladder were eligible for the study if they had refused or were not candidates for a cystectomy after failure of the primary therapy. The eligibility criteria were Zubrod performance status of 2 or lower; at least one bidimensionally measurable lesion in the bladder; at least one prior cisplatin-based cytotoxic treatment, unless contraindicated, for patients with muscle invasion or at least one prior course of BCG treatment for patients without muscle invasion; expected survival more than 12 weeks; urine viral culture negative for adenovirus; negative serology for human immunodeficiency virus type 1; no prior gene therapy; and written, informed consent. Patients with National Cancer Institute (NCI) grade 3 urinary incontinence, pregnant or lactating females, or patients with persistent toxicity of grade 3 or worse from prior chemotherapy were not eligible.

Study Design

This was a single-center, phase I, dose-escalation study of INGN 201 (Ad5CMV-*p53*) intravesical instillation. The study vector was supplied by the NCI Cancer Therapy Evaluation Program under a Cooperative Research and Development Agreement with Introgen Therapeutics, Inc (Houston, TX). Three patients were treated at each dose level, and dose escalation was permitted if no NCI grade 3 or worse toxicity was observed in each cohort. The protocol was approved by The University of Texas M.D. Anderson Cancer Center Institutional Review Board, NCI Cancer Therapy Evaluation Program, and the Recombinant DNA Advisory Committee of the National Institutes of Health Office of Biotechnology Activities. Informed consent was obtained from all participants.

Treatment Plan

The replication-defective adenoviral vector Ad5CMV-*p53* contains the cytomegalovirus (CMV) promotor, wild-type human *p53* cDNA, and an SV40 polyadenylation signal in a minigene cassette inserted into the E1-deleted region of modified adenovirus-5.[13] Individual doses were 10^{10}, 10^{11}, or 10^{12} viral particles (total dose per instillation), and the first group of patients was to be treated on days 1 and 4 at each of these dose levels (Table 1). The second group of patients was to be treated on consecutive days (days 1 through 4) at 10^{12} viral particles or the maximum-tolerated dose (MTD) defined in the first group. The third group of patients was to be treated on days 1 through 4 and days 8 through 11 at 10^{12} viral particles unless a lower MTD was defined in the second group. The vector was suspended in phosphate-buffered saline, which was kept on ice until the time of administration, and a volume of 50 mL was used for each instillation with a dwell time of 20 minutes.

Table 1. Dose Levels

Patient Group	Cohort Size (no. of patients)	Viral Particles per Instillation	Schedule
Group 1, dose level			
1	3	10^{10}	Days 1 and 4
2	3	10^{11}	Days 1 and 4
3	3	10^{12}	Days 1 and 4
Group 2	3	10^{12}	Days 1-4
Group 3	Up to 6	10^{12}	Days 1-4, 8-11

For the first dose, patients were placed under general or spinal anesthesia, and under sterile conditions, a cystoscopy and bimanual palpation were performed. All measurable intravesical lesions were photographed, and perpendicular dimensions were recorded. Pretreatment transurethral biopsies were obtained from tumor or normal urothelium from up to four locations, which were mapped for future identification. A cystogram was performed, and if ureteral reflux was observed, the ureters were cannulated and occluded with Fogarty catheters before the intravesical administration of Ad5CMV-*p53*. After day 1, the subsequent intravesical instillations were performed through a Foley catheter without anesthesia in the outpatient setting, except in the first group when the treatment coincided with a follow-up cystoscopy on day 4. All treatments were performed in a negative-pressure environment with biosafety precautions. Patients who were free of progression at day 28 were offered additional treatment up to a maximum of six courses.

Clinical Monitoring

Patients were monitored for adverse effects for a minimum of 12 months. A follow-up cystoscopy was performed on day 4, 8, or 15 for patients in groups 1, 2, and 3, respectively, and on day 28 for all patients. Patients were seen for tumor assessment every month, including cystoscopy every 3 months, until there was evidence of progression or a cystectomy was performed. Patients who underwent cystectomy and were clinically disease-free were evaluated radiographically every 6 months thereafter. Hematology, serum chemistry (including electrolytes, ALT, AST, lactate dehydrogenase, total bilirubin, urea nitrogen, and creatinine), and urinalysis were performed before treatment and during follow-up visits. Urine was collected for cytology before treatment and on day 28.

Analysis of Bladder Biopsy Tissue

Tissue samples were either formalin-fixed or flash-frozen at the time of resection. For RT-PCR, RNA was extracted from thawed, homogenized, DNase-digested tissue. After reverse transcription, PCR was performed using primers specific to the Ad5CMV-*p53* vector or to glyceraldehyde phosphate dehydrogenase (*GAPDH*). The bladder cancer cell line 5637 was transfected in vitro and used as a positive control. The vector-*p53* transcript contains viral sequences from the CMV promotor, which serve to distinguish it from endogenous *p53* mRNA.[5,6] For RT-PCR detection of vector-*p53* gene expression, primers were constructed to bridge the viral and human transcribed sequences (Table 2; Fig 1). Only samples with a positive *GAPDH* reaction were considered assessable by RT-PCR. PCR products were resolved on 1% agarose gels and visualized by ethidium bromide staining.

Table 2. Primers for RT-PCR

Vector-p53	
Forward	5'-GGTGCATTGGAACGCGGATT-3'
Reverse	5'-GGGGACAGAACGTTGTTTTC-3'
GAPDH	
Forward	5'-TGAAGGTCGGAGTCAACGGATTTGGT-3'
Reverse	5'-CATGTGGGCCATGAGGTCCACCAC-3'

Abbreviations: RT-PCR, reverse transcriptase polymerase chain reaction; GAPDH, glyceraldehyde phosphate dehydrogenase gene.
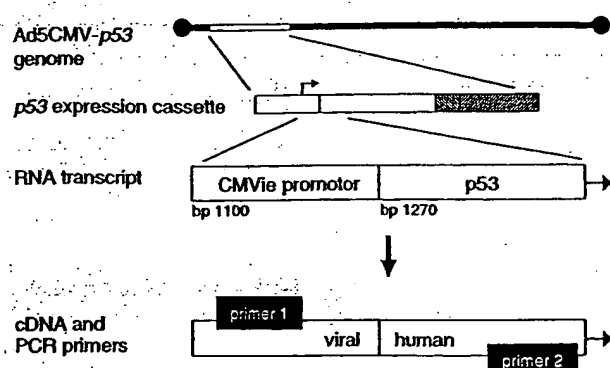
Fig 1. Primers for reverse transcriptase polymerase chain reaction (PCR) of vector-p53 are designed to bridge the viral and human sequences, as shown. Abbreviations: bp, base pair; CMV, cytomegalovirus.

Immunohistochemistry was performed on paraffin sections using monoclonal antibodies to human p53 (DO7 antibody; Dako, Carpinteria, CA), p21$^{waf1/cip1}$ (Oncogene Research; Boston, MA), and bax proteins (Zymed, San Francisco, CA). For detection and visualization, we used a horseradish peroxidase–conjugated secondary antibody, diaminobenzidine substrate, and hematoxylin counterstain. For the detection of apoptotic cells, terminal deoxynucleotidyl transferase–mediated deoxyuridine triphosphate-biotin nick end-labeling (TUNEL) was performed on paraffin sections using a commercially available kit (FragEL, Oncogene Research).

Statistical Methods

Three patients were to be treated at each dose level, with up to six patients at the final dose level. Toxicity was graded according to NCI common toxicity criteria (version 1.0). Toxicity not included in the toxicity scale was scored as grade 3 if hospitalization was required and grade 4 if toxicity was regarded as life-threatening. Overall survival was defined as the interval between the first treatment and death or last follow-up visit. Time to progression was defined as the interval between first treatment and appearance of a new metastasis, increased size of an established metastasis, increased size of an established bladder tumor, new hydronephrosis, or any progression in tumor stage (eg, from superficial to muscle-invasive). Positive urine cytology and recurrences of superficial TCC were not considered progression. Response was not an end point of the study, but any changes in

tumor dimension, radiographic appearance, or cystoscopic appearance of an index lesion were noted.

RESULTS

Patient Characteristics

From December 1998 to June 2001, a total of 14 patients were registered, 13 of whom met eligibility criteria (Table 3). One patient was registered and subsequently found ineligible because of a positive urine adenoviral culture and lack of measurable disease on cystoscopy, and he was not treated with Ad5CMV-p53. All other patients had histologically confirmed TCC of the bladder. Nine patients were treated in the first group, three in the second group, and one in the third group, at which point we terminated the trial early because we had not observed significant toxicity and did not expect to reach the MTD. Of the patients treated, 10 had previously documented muscle-invasive bladder cancer, and three had extensive superficial disease that had recurred after BCG immunotherapy. Three patients who were treated with Ad5CMV-p53 subsequently underwent radical cystectomy for local control of residual TCC (patients 2, 11, and 14). Pretreatment tissue samples were obtained from all patients, and all but one patient had sufficient residual tumor for a second biopsy. Thus, tumor samples were successfully obtained from 12 patients, at all dose levels, before and after treatment with Ad5CMV-p53.

Toxicity

The MTD was not reached because none of the patients experienced dose-limiting toxicity. The most common toxicity was bladder spasm (NCI grade 1) which was observed in three patients at the higher dose levels (Table 4). One patient was observed to have superficial ulcerations of the bladder mucosa that were asymptomatic (NCI grade 1) on day 4 after the first dose of 10^{12} viral particles (Fig 2A to 2C). The cystoscopic appearance was improved on day 28, and this patient went on to

Table 3. Patient Characteristics and Transgene Expression

| Patient and Treatment | | | | | | Tumor Stage | | | Cytology | | Vector-p53 Expression | |
Patient No.	Age (years)	Sex	Dose (viral particles)	Schedule (day no.)	No. Courses	Highest Pretreatment	Day 1	Day 28	Day 1	Day 28	Tissue (day no.)	RT-PCR
1	73	Male	10^{10}	1 and 4	2	T1	T1	T1	+		4	+
2	79	Male	10^{10}	1 and 4	4	T3b	T2	T2			4	ND
3	73	Female	10^{10}	1 and 4	1	T2	T2	T0	+		ND	ND
5	74	Female	10^{11}	1 and 4	1	T2	T2	T2	+	+	4	+
6	75	Female	10^{11}	1 and 4	1	T2	T2	T2	+	+	4	ND
7	88	Male	10^{11}	1 and 4	2	T3b	T3b	T3b	–	+	4	–
8	72	Male	10^{12}	1 and 4	1	T1	T1	T1	+	+	4	ND
9	74	Male	10^{12}	1 and 4	1	T2	T2	T2	+	+	4	ND
10	85	Male	10^{12}	1 and 4	5	T2	T1	Ta	–	–	4	+
11	61	Female	10^{12}	1-4	1	T3b	T3b	T3b	NA	NA	8	+
12	70	Male	10^{12}	1-4	1	T1	T1	T2	–	+	8	ND
13	46	Male	10^{12}	1-4	1	T2	CIS	CIS/adeno	+	+	8	–
14	67	Male	10^{12}	1-4,8-11	1	T2	T2	T3b	–	–	16	–

NOTE. Patient 4 was not eligible.
Abbreviations: CIS, carcinoma in-situ; CIS/adeno, flat lesion with mixed CIS (transitional cell) and adenocarcinoma histology; cytology, presence or absence of malignant cells in urine; tissue, posttreatment biopsy (day obtained); RT-PCR, results of reverse transcriptase polymerase chain reaction using primers specific for vector-p53 transcript; NA, not applicable because of defunctionalized bladder; ND, not done because of insufficient tissue (patient 3) or RNA (all others) recovered from sample.

Table 4. - Adverse Events

Patient Group	n	Toxicity (NCI-CTC Grade)	No. of Patients
Group 1, dose level			
1	3	None	—
2	3	Edema/azotemia (grade 2)	1
2	3	Bladder spasm (grade 1)	1
		Urothelial ulceration (grade 1)*	1
		Hypothyroidism (grade 1)*	1
		Pneumonia (grade 3)*	1
Group 2	3	Bladder spasm (grade 1)	2
Group 3	1	None	—

Abbreviation: NCI-CTC, National Cancer Institute common toxicity criteria.
*Observed in patient 10 during different courses.

receive a total of five courses without local complications. One patient was hospitalized twice with edema and azotemia (NCI grade 2), which were related to pre-existing cardiac disease, chronic renal failure, and poor nutritional status. This patient died 47 days after the start of treatment or 44 days after the second and last dose, but the death did not seem to be related to treatment with Ad5CMV-p53.

Urine was collected for cytologic analysis from 12 patients on days 1 and 28 (Table 3). All of the patients with positive pretreatment cytology remained positive at day 28. Granulocytes indicating an acute inflammatory reaction were observed in the urine samples from patients 12 and 14 on day 28, and from patient 10 after two courses. These patients received 10^{12} viral particles per instillation and each had received at least four instillations before the detection of inflammatory cells. There were no other significant laboratory abnormalities detected on follow-up evaluations while patients were enrolled on the study.

Detection of p53 Transgene

Tissue samples were obtained and flash-frozen in liquid nitrogen before and after treatment from 12 patients. Of these,
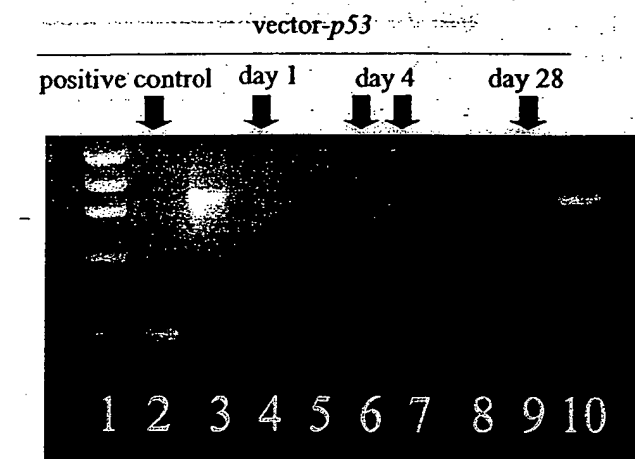

Fig 3. Reverse transcriptase polymerase chain reaction detection of vector-p53 in tissue samples from patient 10. Glyceraldehyde phosphate dehydrogenase (GAPDH) detection day 28 is shown in lane 10, with positive control in lane 3. Size markers, lane 1; negative controls, lanes 5 and 8.

seven were assessable for detection of vector-p53 expression by RT-PCR. The assessable posttreatment biopsies were obtained on day 4 (four patients), day 8 (two patients), or day 16 (one patient). We found vector-specific p53 expression in posttreatment bladder biopsies from two assessable patients who had received 10^{12} viral particles per dose (Table 3; Fig 3). Transgene expression was detected in both tumor tissue and in random biopsies of normal-appearing mucosa.

Immunohistochemistry and TUNEL

The follow-up biopsy from one patient did not contain sufficient viable tumor for accurate immunohistochemical analysis. Therefore, 11 patients were assessable for changes in p53, p21$^{waf1/cip1}$, and bax proteins by immunostaining. The pretreat-
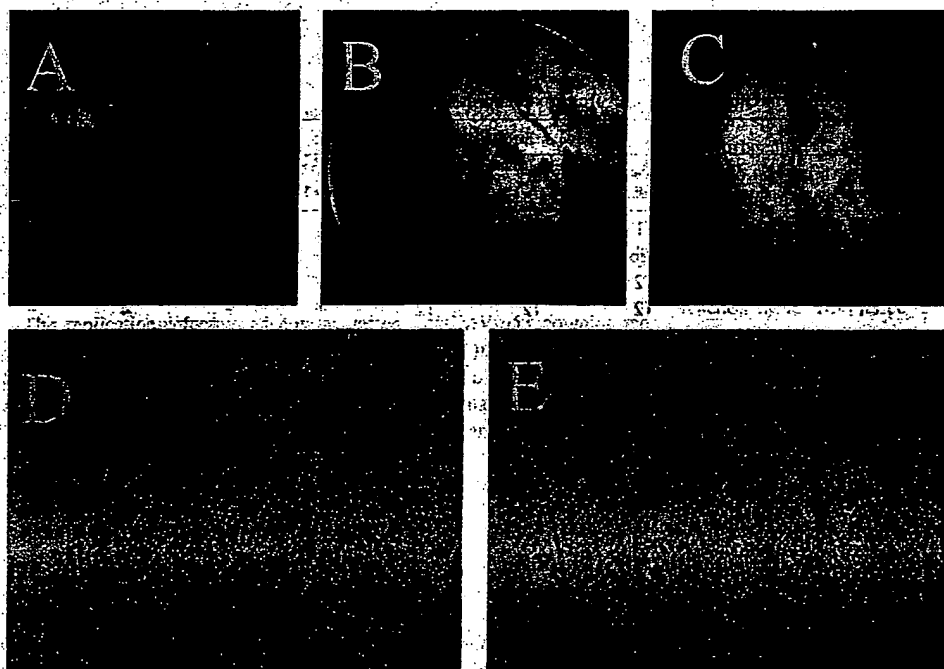

Fig 2. Patient 10, cystoscopic appearance day 1 (A) showing multiple superficial tumors; day 4 (B) showing superficial mucosal ulceration; day 28 (C) showing improvement; and p53 immunostain day 1 (D) and day 4 (E).

ment tissue samples from 10 patients showed overexpression of p53, which was consistent with a pre-existing p53 mutation (Fig 2D and 2E). Comparison with follow-up tissue samples obtained on days 4, 8, 16, or 28 did not reveal significant increases in p53 expression at any dose level. There were no detectable changes in $p21^{waf1/cip1}$ or bax in any of the patients studied. TUNEL staining revealed high background levels of positive staining in the pretreatment tumor biopsies; thus, the assay was inadequate for assessment of an apoptotic response in this setting.

Long-Term Follow Up

Eleven of the 13 eligible patients have died. Two are alive at 15 and 44 months follow-up, respectively. Eleven patients have progressed, and the median time to progression was 2 months.

Patient 2 had muscle-invasive disease (T3b) previously treated with methotrexate, vinblastine, doxorubicin, and cisplatin chemotherapy. He received four courses at the lowest dose level (10^{10} viral particles), during which time there was stable, residual muscle-invasive TCC on bladder biopsy. There was no tumor progression, and a radical cystectomy was performed at 10 months. He remained disease-free at 44 months' follow-up.

Patient 10 had a history of muscle-invasive TCC resected transurethrally, was not a candidate for cystectomy, and had only superficial (Ta/T1) lesions visible on day 1 (Fig 2A). Index lesions were reduced in size on days 4 and 28, after which the residual tumor tissue was resected entirely. He received a total of five courses, with 10^{12} viral particles on days 1 and 4 of each course; during this time, he had a single recurrence of noninvasive TCC (Ta) that was resected. A second superficial recurrence was transurethrally resected at 12 months, during the follow-up period after treatment had been stopped. The patient died of a cerebral hemorrhage at 15 months. He did not experience progression after treatment with AdSCMV-p53, and he was not known to have any residual or recurrent disease at the time of death.

Patient 14, the only patient treated at the highest dose level, demonstrated stable disease on day 16 (the cystoscopy was performed 1 day later than planned) and tumor progression on day 28. He tolerated eight installations of AdSCMV-p53 10^{12} viral particles without any toxicity. He subsequently underwent radical cystectomy for local control and was alive with metastatic disease at 15 months of follow-up.

DISCUSSION

Our results demonstrate that daily outpatient administration of AdSCMV-p53 intravesical instillation is feasible, safe, and well tolerated. Acute NCI grade 1 toxicities, including bladder spasm and superficial mucosal ulceration, were acceptable and provided further evidence of biologic activity from the treatment. The observation of acute inflammation on urine cytology obtained during long-term follow-up of three patients at the higher dose levels was an unexpected finding. Transduction of the vector-p53 gene into bladder tissue was confirmed by vector-specific RT-PCR analysis in two of seven assessable patients after as few as one dose, but in no patient did we see any significant change in the results of immunohistochemical staining for p53, $p21^{waf1/cip1}$,

or bax. This analysis was confounded, in part, by abnormally high p53 staining in 11 of 12 assessable patients. Accumulation of immunoreactive p53 occurs in approximately 50% of TCC primary tumors and is usually related to the presence of mutations of the p53 gene and prolonged half-life of the abnormal gene product.[14] The high frequency of increased p53 staining in this study was most likely a consequence of our patient selection, which targeted patients with advanced, treatment-refractory disease. We cannot exclude the possibility of p53 protein induction that was obscured by the high background.

The utility of endoscopic tissue sampling for the evaluation of biologic end points was also examined in this study. We successfully obtained bladder biopsies before and after treatment from 12 of 13 eligible patients, of which 11 were adequate for immunohistochemistry and seven contained RNA of sufficient quality for RT-PCR. We found that endoscopic retrieval of small tissue samples is an effective method for RT-PCR detection of therapeutic gene transduction, and that it can be accomplished in the course of routine cystoscopy with minimal additional discomfort to the patient and at multiple time points. Biopsies of normal-appearing mucosa were frequently found to be histologically abnormal, reflecting the well-described field effect that characterizes urothelial malignancy.[15] In another recently published study, Kuball et al[7] collected cystectomy specimens from 12 patients who received preoperative p53 gene therapy, of which 11 were assessable by RT-PCR and seven were positive for vector-p53 transgene expression. They also were unable to detect differences in immunostaining for p53, $p21^{waf1/cip1}$, and bax or for the TUNEL assay, despite having access to unlimited tissue.

Response was not an end point of the study, but all patients had measurable disease and were evaluated for evidence of antitumor activity. Eleven patients experienced progression within 3 months of starting treatment; nine patients had local progression, whereas two had progression of distant metastases. Patient 2 was treated at the lowest dose level of 10^{10} viral particles per dose and had stable TCC (grade 2) invading the muscularis propria throughout four courses of treatment. A radical cystectomy was performed at 10 months, and the patient was alive and disease-free at 44 months. This clinical course is unusual for muscle-invasive TCC that persists after neoadjuvant chemotherapy,[16] as had occurred in this patient. Our data do not indicate that there is significant p53 transduction at this small dose; however, and it is likely that the favorable outcome reflected an indolent growth pattern rather than a treatment effect. Patient 10, conversely, received a 100-fold higher dose of 10^{12} viral particles (days 1 and 4) and showed noticeable improvement in multiple superficial TCC tumors (grade 2 to 3). In addition, mucosal ulceration was noted on days 4 and 28, indicating a cytopathic effect of the treatment. Vector-specific p53 expression was detected by RT-PCR analysis of multiple biopsies obtained on day 4, and was negative on day 28 (Fig 3). On the basis of these observations, we suspect that there was an antitumor effect with AdSCMV-p53 given at 10^{12} viral particles on days 1 and 4.

Possible mechanisms of antitumor effect include p53 gene expression as well as a nonspecific inflammatory (or BCG-like) effect of the adenoviral vector. Patient 10 had histologically confirmed muscle-invasive TCC on a transurethral resection performed 5 months before study entry, so was not previously treated with BCG. We detected acute inflammation on the follow-up urine cytology, providing evidence of a cellular immune response. In light of the known sensitivity of superficial TCC to an inflammatory response,[17] and considering the low level of vector-p53 expression observed, we favor the hypothesis that a BCG-like effect occurred in this patient.

Several factors can limit the efficiency of adenovirus-mediated gene transfer and may have contributed to the low levels of transduction observed in this study. In the specific case of the bladder mucosa, a protective glycosaminoglycan (GAG) layer forms a physiologic barrier to infection and could interfere with adenoviral gene transfer. In a rodent model of experimentally induced bladder tumors, however, the GAG layer was not present in tumor-bearing areas and seemed to block transfection of only the normal urothelium.[18] Other factors that may interfere with adenoviral gene transfer are uneven distribution of the vector, which has been observed after intratumoral injection in animal models and results in focal rather than diffuse expression of the transgene;[19] a neutralizing antibody response to the adenovirus; low levels of coxsackie and adenovirus receptor (CAR) expression on the surfaces of target cells, limiting the adhesion and internalization of viral particles;[20,21] and the genetic milieu of a particular cell, which may be more or less permissive for expression of the transgene after the vector has been internalized.[22]

There is considerable interest in developing agents that enhance adenoviral gene transfer across the urothelial GAG layer.[7] Connor et al[23] purified the polyamide Syn-3 for this purpose, but

its effect in rats indicated interaction with CAR and increased adenoviral attachment, rather than GAG disruption alone, as the mechanism. Intravesical Syn-3 pretreatment also enabled efficient adenoviral gene transfer to human TCC cells growing superficially within the bladders of athymic nude mice, despite their relatively low CAR expression.[24] The CAR protein has been shown to facilitate intracellular adhesion in bladder cancer cell lines, indicating that its loss may not be a random event,[21] and that the CAR status must be considered in the design of more effective bladder cancer gene therapy.

In conclusion, we have demonstrated that repeated daily administration of intravesical Ad5CMV-p53 is a feasible and well-tolerated method for therapeutic p53 gene transfer in patients with bladder cancer. RT-PCR analysis of tissue samples confirmed that bladder cancer cells were successfully transfected, but we found, as have other investigators,[7] that there was not a detectable change in the immunostaining characteristics of bladder tissue after intravesical gene therapy. Clinical benefit was observed in a patient receiving long-term treatment with Ad5CMV-p53, although a nonspecific inflammatory response seems to have occurred rather than a p53-mediated antitumor effect. Recognition of this nonspecific mechanism will be important in future clinical trials of intravesical adenoviral gene therapy for bladder cancer, particularly because superficial bladder cancer and carcinoma-in-situ are logical targets for intravesical gene therapy.[3,9] Future work must address the need for more efficient gene delivery systems[25] and stronger transgene expression in the target tissue.

ACKNOWLEDGMENT

REFERENCES

1. Grossman HB: Surgical staging and surgery for superficial bladder cancer, in Raghavan D, Scher HI, Leibel S, et al (eds): Principles and Practice of Genitourinary Oncology. Philadelphia, PA, Lippincott-Raven, 1997, pp 269-272

2. Herr HW, Lamm DL, Denis L: Management of superficial bladder cancer, in Raghavan D, Scher HI, Leibel S, et al (eds): Principles and Practice of Genitourinary Oncology. Philadelphia, PA, Lippincott-Raven, 1997, pp 273-280

3. Pagliaro LC: Gene therapy for bladder cancer. World J Urol 18:148-151, 2000

4. Wood M, Perrotte P, Onishi R, et al: Biodistribution of an adenoviral vector carrying the luciferase reporter gene following intravesical or intravenous administration in a mouse. Cancer Gene Ther 6:367-372, 1999

5. Clayman GL, El-Naggar AK, Lippman SM, et al: Adenovirus-mediated p53 gene transfer in patients with advanced recurrent head and neck squamous cell carcinoma. J Clin Oncol 16:2221-2232, 1998

6. Swisher SG, Roth JA, Nemunaitis J, et al: Adenovirus-mediated p53 gene transfer in advanced non-small-cell lung cancer. J Natl Cancer Inst 91:763-771, 1999

7. Kuball J, Wen SF, Leissner J, et al: Successful adenovirus-mediated wild-type p53 gene transfer in patients with bladder cancer by intravesical vector instillation. J Clin Oncol 20:957-965, 2002

8. Morris BD, Drazan KE, Csete ME, et al: Adenoviral-mediated gene transfer to bladder in vivo. J Urol 152:506-509, 1994

9. Slaton JW, Benedict WF, Dinney CPN: p53 in bladder cancer: Mechanism of action, prognostic value, and target for therapy. Urology 57:852-859, 2001

10. Pagliaro LC, Keyhani A, Liu B, et al: Adenoviral P53 gene transfer in human bladder cancer cell lines: Cytotoxicity and synergy with cisplatin. Urol Oncol, In press

11. Miyake H, Hara I, Hara S, et al: Synergistic chemosensitization and inhibition of tumor growth and metastasis by adenovirus-mediated p53 gene transfer in human bladder cancer model. Urology 56:332-336, 2000

12. Perrotte P, Wood M, Slaton JW, et al: Biosafety of in vivo adenovirus-p53 intravesical administration in mice. Urology 56:155-159, 2000

13. Zhang WW, Fang X, Mazur W, et al: High-efficiency gene transfer and high-level expression of wild-type p53 in human lung cancer cells mediated by recombinant adenovirus. Cancer Gene Ther 1:5-13, 1994

14. Esrig D, Elmajian D, Groshen S, et al: Accumulation of nuclear p53 and tumor progression in bladder cancer. N Engl J Med 331:1259-1264, 1994

15. Ayala AG, Ro JY: Premalignant lesions of the urothelium and transitional cell tumors, in Young RH (ed): Pathology of the Urinary Bladder. New York, NY, Churchill Livingstone, 1989, pp 65-101

16. Millikan R, Dinney C, Swanson D, et al: Integrated therapy for locally advanced bladder cancer: Final report of a randomized trial of cystectomy plus adjuvant M-VAC versus cystectomy with both preoperative and postoperative M-VAC. J Clin Oncol 19:4005-4013, 2001

17. Ratliff TL: Role of the immune response in BCG for bladder cancer. Eur Urol 21:17-21, 1992 (suppl 2)

18. Shimizu H, Akasaka S, Suzuki S, et al: Preferential gene transfer to BBN-induced rat bladder tumor by simple instillation of adenoviral vector. Urology 57:579-584, 2001

19. Oakley R, Phillips E, Hooper R, et al: A preclinical model of minimal residual cancer in the muscle highlights challenges associated with adenovirus-mediated p53 gene transfer. Clin Cancer Res 8:1984-1994, 2002

20. Li Y, Pong RC, Bergelson JM, et al: Loss of adenoviral receptor expression in human bladder cancer cells: A potential impact on the efficacy of gene therapy. Cancer Res 59:325-330, 1999

21. Okegawa T, Pong RC, Li Y, et al: The mechanism of the growth-inhibitory effect of coxsackie and adenovirus receptor (CAR) on human bladder cancer: A functional analysis of CAR protein structure. Cancer Res 61:6592-6600, 2001

22. Nemunaitis J, Swisher SG, Timmons T, et al: Adenovirus-mediated p53 gene transfer in sequence with cisplatin to tumors of patients with non-small-cell lung cancer. J Clin Oncol 18:609-622, 2000

23. Connor RJ, Engler H, Machemer T, et al: Identification of polyamides that enhance adenovirus-mediated gene expression in the urothelium. Gene Ther 8:41-48, 2001

24. Yamashita M, Rosser CJ, Zhou JH, et al: Syn3 provides high levels of intravesical adenoviral-mediated gene transfer for gene therapy of genetically altered urothelium and superficial bladder cancer. Cancer Gene Ther 9:687-691, 2002

25. Haviv YS, Blackwell JL, Kanerva A, et al: Adenoviral gene therapy for renal cancer requires retargeting to alternative cellular receptors. Cancer Res 62:4273-4281, 2002

Phase I Trial of Adenovirus-Mediated p53 Gene Therapy for Recurrent Glioma: Biological and Clinical Results

By Frederick F. Lang, Janet M. Bruner, Gregory N. Fuller, Kenneth Aldape, Michael D. Prados, Susan Chang, Mitchel S. Berger, Michael W. McDermott, Sandeep M. Kunwar, Larry R. Junck, William Chandler, James A. Zwiebel, Richard S. Kaplan, and W.K. Alfred Yung

Purpose: Advances in brain tumor biology indicate that transfer of p53 is an alternative therapy for human gliomas. Consequently, we undertook a phase I clinical trial of p53 gene therapy using an adenovirus vector (Ad-p53, INGN 201).

Materials and Methods: To obtain molecular information regarding the transfer and distribution of exogenous p53 into gliomas after intratumoral injection and to determine the toxicity of intracerebrally injected Ad-p53, patients underwent a two-stage approach. In stage 1, Ad-p53 was stereotactically injected intratumorally via an implanted catheter. In stage 2, the tumor-catheter was resected en bloc, and the postresection cavity was treated with Ad-p53. This protocol provided intact Ad-p53-treated biologic specimens that could be analyzed for molecular end points, and because the resection cavity itself was injected with Ad-p53, patients could be observed for clinical toxicity.

Results: Of fifteen patients enrolled, twelve underwent both treatment stages. In all patients, exogenous p53 protein was detected within the nuclei of astrocytic tumor cells. Exogenous p53 transactivated $p21^{CIP/WAF}$ and induced apoptosis. However, transfected cells resided on average within 5 mm of the injection site. Clinical toxicity was minimal and a maximum-tolerated dose was not reached. Although anti-adenovirus type 5 (Ad5) titers increased in most patients, there was no evidence of systemic viral dissemination.

Conclusion: Intratumoral injection of Ad-p53 allowed for exogenous transfer of the p53 gene and expression of functional p53 protein. However, at the dose and schedule evaluated, transduced cells were only found within a short distance of the injection site. Although toxicity was minimal, widespread distribution of this agent remains a significant goal.

J Clin Oncol 21:2508-2518. © *2003 by American Society of Clinical Oncology.*

T HE TREATMENT of malignant glioma remains a major therapeutic challenge. In patients with glioblastoma multiforme (GBM), the most common adult glioma, the median survival duration is 1 year, and only 15% of patients survive for 2 years after diagnosis despite the use of maximal conventional therapy.[1,2] However, recent advances in the fundamental understanding of brain tumor biology have indicated that transfer of the tumor suppressor p53 using a gene therapy strategy is an alternative approach to brain tumor treatment.[3-10]

Transfection of p53 is a rational therapeutic strategy for human gliomas because p53 is frequently inactivated in astrocytic tumors either through mutation of the p53 gene,[11-15] overexpression of murine double minute 2 (mdm-2; the primary negative regulator of p53), inactivation of $p14^{ARF}$ (an inhibitor of mdm-2),[16,17] or interference with p53 posttranslational modifications (eg, phosphorylation).[18] Furthermore, studies using a variety of approaches have shown that inactivation of p53 is a critical event in the formation and progression of gliomas.[15,19-24] Lastly, wild-type p53 is a primary mediator of cell cycle arrest and apoptosis, parameters intimately involved in tumor growth and response to treatment.[25] Transfer of p53 would be expected to restore or enhance these critical functions.

Mercer et al[3] initially demonstrated that plasmid-mediated transfection of the p53 gene is capable of suppressing cell growth in gliomas. Kock et al[4] and Gomez-Manzano et al[5,6] were among the first to demonstrate that delivering the p53 gene using an adenovirus vector (Ad-p53) results in dramatic apoptosis in glioma cell lines. In animal models, intratumoral injections of Ad-p53 have been shown to inhibit the subcutaneous growth of gliomas and to extend the survival of rodents harboring intracranially implanted gliomas.[4,9,26] Moreover, Ad-p53 has been shown to restore the sensitivity of gliomas to radiotherapy and chemotherapy.[8,18,27]

Ad-p53 (INGN 201; ADVEXIN, Introgen Therapeutics, Inc, Houston, TX) is a type 5 replication-incompetent adenovirus in

which the E1 region has been replaced with the cDNA of the wild-type *p53* gene driven by the cytomegalovirus promoter.[28,29] In addition to its anticancer effects in gliomas, Ad-*p53* has been shown to be effective against a variety of other tumor types, including lung,[30] colon,[31] head and neck,[32] ovarian,[33] and breast cancers.[34] Ad-*p53* (INGN 201) has also been shown to produce minimal toxicity after direct intratumoral injection during phase I clinical trials of patients with lung[30,35,36] or head and neck cancer.[32,37,38]

Despite the promising preclinical results in brain tumors and the encouraging clinical results in other tumor types, the clinical potential of Ad-*p53* (INGN 201) in the treatment of human gliomas has not yet been demonstrated. Consequently, we undertook a phase I trial of Ad-*p53* in the treatment of patients with recurrent malignant gliomas. The purpose of this trial was not only to determine the clinical toxicity of Ad-*p53* but also to obtain molecular information regarding the expression and distribution of the p53 protein after intratumoral treatment of human gliomas with Ad-*p53*. To meet both of these objectives we used a two-stage surgical protocol, unique to brain tumor trials, which allowed treated patients to be observed for toxicity and provided brain tumor specimens that could be analyzed for the molecular effects of Ad-*p53*. We report here that intratumoral injection of Ad-*p53* into gliomas was associated with minimal toxicity and resulted in transfer of the *p53* gene and expression of a functionally active p53 protein. However, with the bolus injection method used in this trial, the distribution of Ad-*p53* was limited to a short distance from the injection site.

MATERIALS AND METHODS

Institutional Review

The institutional review boards of all participating institutions approved this study.

Objectives

The objectives of this trial were to determine the molecular effects of injecting Ad-*p53* into human primary brain tumors (gliomas) by analyzing the expression, function, and distribution of exogenous p53 protein, and to determine the maximum-tolerated dose and toxicity (including viral dissemination) associated with intracranial injection of Ad-*p53*.

Study Design

This was a phase I dose escalation study with a biologic component. To meet the molecular and clinical objectives, we used a two-stage surgical approach (Fig 1). In stage 1, we obtained a stereotactic biopsy to confirm the presence of a recurrent tumor. We then replaced the biopsy needle with a silastic ventricular catheter (Codman & Shurtleff, Inc, Raynham, MA) using stereotactic techniques and injected the designated dose of Ad-*p53* into the tumor as a single bolus via the catheter; the injections (1 mL of Ad-*p53*) were given in a 10-minute period at 0.1 mL/min. We left the catheter in place to mark the injection site, cut the catheter flush with the skull, secured it to the dura, and closed the incision. In stage 2, patients underwent an open craniotomy 3 days after stage 1 (when p53 expression was expected to be maximal), during which we performed an en bloc tumor resection by circumferentially dissecting the tumor using computer-assisted stereotactic techniques and taking care not to dislodge the catheter. After resection, a grid of 1-cm squares was laid within the surgical cavity, and a free-hand method was used to inject the appropriate dose of Ad-*p53* in the designated volume (see Ad-*p53* Dose) into the center of each grid square with a 20-gauge
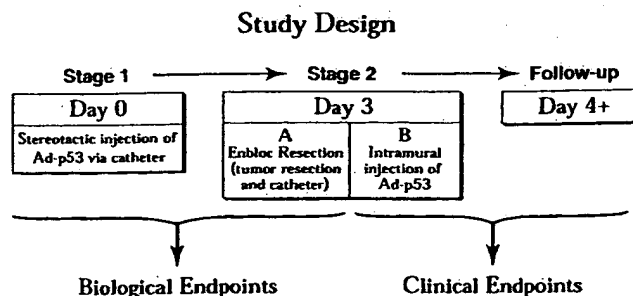
Study Design

Fig 1. Outline of two-stage surgical design.

blunt-tip Dandy needle inserted 1 to 2 cm into the brain parenchyma. The volume injected into each grid square was calculated by dividing the total injected volume (on the basis of tumor size, see Ad-*p53* Dose) by the number of injection sites (typically, 0.1 mL of the Ad-*p53* solution in each square). This two-stage approach provided an intact biologic specimen that had received Ad-*p53* treatment, and because the resection cavity itself was injected with Ad-*p53*, patients could be observed for evidence of clinical toxicity.

Eligibility Criteria

Patients $\geq$ 18 years old with a Karnofsky performance score $\geq$ 70 and with surgically accessible, histologically confirmed recurrent malignant glioma were enrolled in this study. Patients were required to have recovered from the toxic effects of prior therapy, and had to have adequate bone marrow (granulocyte count $>$ 1,500/μL and platelet count $>$ 100,000/μL), liver (ALT and alkaline phosphatase levels $<$ two times institutional norms), and renal functions (creatinine $<$ 1.5 mg/dL). Patients were excluded if they received radiotherapy during the 4 weeks before study entry, had an active uncontrolled infection, had evidence of bleeding diathesis, or were taking anticoagulants. Males and females were recruited with no sex preference, and there were no exclusions on the basis of race. Women who were pregnant, at risk for pregnancy, or breast-feeding were excluded. All of the patients were able to read and understand the informed consent form, and all signed it indicating that they were aware of the investigational nature of the study.

Adenoviral Vector Construct and Testing

The two lots of Ad-*p53* (INGN 201, ADVEXIN) used in this study were supplied by Introgen Therapeutics, Inc (Houston, TX), and were free of detectable adventitious viruses, bacteria, *Mycoplasma*, fungi, and endotoxins. The level of replication-competent adenovirus in these lots was less than 1 in 3 $\times$ 10^9 plaque-forming units. The wild-type sequence of the *p53* cDNA in the vector was confirmed via dideoxy DNA sequencing.[28,29]

Ad-p53 Dose

The dose of Ad-*p53* was increased from 3 $\times$ 10^{10} to 3 $\times$ 10^{12} viral particles in four dose levels (levels 1 to IV; Table 1). All of the patients received the same total amount of Ad-*p53* in surgical stages 1 and 2. In stage 1, the injection volume was 1 mL regardless of the tumor size, whereas in stage 2, the injection volume depended on the size of the tumor (for tumors 2 to 3 cm in greatest diameter, the injection volume was 3 mL; for tumors $>$ 3 cm but $<$ 6 cm in diameter, the volume was 5 mL).

Stereotactic Biopsy Specimens

Specimens obtained at the time of stereotactic biopsy as frozen sections were analyzed using hematoxylin and eosin staining for the presence of recurrent glioma. Formalin-fixed specimens were analyzed for baseline *p53* expression using immunohistochemical detection with antibody PAb1801 (Oncogene Science, Cambridge, MA) via an avidin-biotin-peroxidase complex method as described previously.[14,39] Frozen specimens were analyzed for *p53* gene mutation using direct DNA sequencing to detect mutations in exons 5 to 8.

Table 1. Patient Population

Patient No.	Dose Level	Dose (vp)	Age (years)	Sex	Preoperative KPS Score	Dx	Stages Completed	Duration Dx to Rx (months)	Prior Rx	Tumor Location	Preoperative Tumor Volume (mL)	Institution
1	I	3×10^{10}	42	F	90	GM	1, 2	11	RT, PCV	L temporal	5.56	MDA
2	I	3×10^{10}	44	M	90	AA	1, 2	7	RT, BCNU + cisplatin	L temporal-parietal	43.05	MDA
3	I	3×10^{10}	56	F	90	GM	1, 2	7	RT, BCNU, TG, TMZ + CRA	L frontal	38.51	MDA
4	II	3×10^{11}	55	F	90	GM	1, 2	7	RT, BCNU + TMZ, SxRx	R frontal-parietal	ND	UCSF
5	II	3×10^{11}	44	F	90	GM	1, 2	10	RT, TMZ + CRA	L occipital	8.89	MDA
6	II	3×10^{11}	52	M	90	GM	1, 2	5	RT, SxRx	R frontal	ND	UCSF
7	III	1×10^{12}	77	F	80	GM	1, 2	11	RT, TMZ	R parietal-occipital	18.51	MDA
8	III	1×10^{12}	42	M	90	GM	1, 2	6	RT, BCNU + TG	L frontal	16.32	MDA
9	III	1×10^{12}	47	M	80	GM	1, 2	3	RT	L temporal-parietal	39.98	MDA
10	III	1×10^{12}	24	M	90	GM	2	21	RT, TMZ	R frontal	6.76	MDA
11	III	1×10^{12}	47	F	90	AG	2	8	RT/Hydrea, PCV, CCNU, TMZ/Marimastat	R frontal	7.67	MDA
12	III	1×10^{12}	48	M	90	GM	2	8	RT, FU, Carboplatin, TMZ/Thalidomide, TMZ/CRA	L parietal	29.84	MDA
13	IV	3×10^{12}	66	F	80	GM	1, 2	4	RT	R frontal	60.70	UCSF
14	IV	3×10^{12}	51	M	70	GM	1, 2	7	RT, BCNU + TG	R parietal	59.62	MDA
15	IV	3×10^{12}	35	M	90	GM	1, 2	8	RT	R parietal-occipital	ND	U Mich

Abbreviations: vp, viral particles; KPS, Karnofsky performance scale; M, male; F, female; Dx, diagnosis; Rx, treatment; GM, glioblastoma multiforme; RT, radiotherapy; FU, fluorouracil; PCV, procarbazine; CCNU, vincristine; MDA, M.D. Anderson; UCSF, University of California San Francisco; U Mich, University of Michigan; AA, anaplastic astrocytoma; AG, anaplastic mixed glioma; TMZ, temozolomide; BCNU, bis-chloronitrosourea; CRA, cis-retinoic acid; TG, thioguanine; SxRx, stereotactic radiosurgery; L, left; R, right.

Surgical Specimens

Postresection specimens with the catheter in place were fixed in formalin immediately after resection and blocked perpendicular to the catheter. Serial sections (10 μm) were evaluated for tumor content and the position of the catheter using hematoxylin and eosin staining. Adjacent sections were evaluated for p53 expression by immunohistochemistry using antibody PAb1801 as described previously.[14,39] Specimens were analyzed for the pattern of p53 immunopositivity around the catheter site, the presence of nuclear or cytoplasmic staining, and the intensity of staining near the catheter relative to areas distant from it. The distribution of p53 was quantified by measuring the maximum distance of p53 immunostaining from the catheter site in four orthogonal directions under low magnification and using the maximal result.

Sections immediately adjacent to those stained for p53 (10-μm separation) were analyzed by immunohistochemistry for the expression of $p21^{CIP/WAF}$, a p53-inducible gene, using an anti-p21$^{CIP/WAF}$ monoclonal (Ab-3) antibody (Oncogene Science) as described previously.[40] Adjacent sections were used in this analysis to determine whether the pattern of p21 staining overlapped the pattern of p53 staining.

To more definitively determine whether individual p53-positive cells also expressed high levels of p21$^{CIP/WAF}$, sequential double immunostaining for p53 and p21 was performed on the same section in two patient samples. Briefly, sections were first exposed to anti-p21$^{CIP/WAF}$ monoclonal antibody, followed by secondary antibody (chromogen was diaminobenzidine) and then placed in 70% alcohol and rinsed with phosphate-buffered saline. The section was then exposed to anti-p53 antibody PAb1801 followed by secondary antibody (chromogen was aminoethyl carbazole). The diaminobenzidine produces a brown stain, whereas the aminoethyl carbazole produces a red stain.

To detect apoptotic cells, adjacent sections were also analyzed by terminal deoxynucleotidyl transferase–mediated deoxyuridine triphosphate-biotin nick end-labeling (TUNEL) using the DeadEnd Colorimetric TUNEL System (Promega, Madison, WI), according to the manufacturer's instructions. The degree and distribution of apoptotic cells were analyzed relative to p53 immunostaining.

Clinical Patient Evaluation

Clinical evaluations (including a medical history, general physical exam, neurologic exam, and Karnofsky performance score determination) were

performed at baseline (ie, within 1 week of the first Ad-p53 injection), daily after the stereotactic injection of Ad-p53, daily while the patient was in the hospital after craniotomy, and at on-study follow-up visits (ie, every 2 weeks for 6 weeks; then every 4 weeks for 8 weeks; then every 8 weeks, beginning with the first postoperative visit).

All patients underwent laboratory testing at baseline, at 24 hours after craniotomy, and on each on-study follow-up visit. Laboratory evaluations included hematology testing (complete blood count, differential, platelet count, prothrombin time, partial thromboplastin time), biochemistry (levels of standard electrolytes, calcium, magnesium, phosphate, blood urea nitrogen, creatinine, glucose, ALT, AST, total protein, albumin, alkaline phosphatase, bilirubin, total cholesterol, triglycerides, creatine phosphokinase, lactate dehydrogenase, and uric acid), and measurement of anticonvulsant levels.

All patients underwent multiplanar magnetic resonance imaging (MRI) both with and without gadolinium contrast enhancement within 2 weeks of study entry to assess the location and size of the tumors. Noncontrast computed tomography was performed within 12 hours of catheter placement to assess the catheter position. Postresection MRI was performed within 48 hours of surgery (to assess the extent of resection), 4 weeks later, and then every 8 weeks after craniotomy during follow-up.

Samples of plasma, sputum, urine, and stool were obtained for vector dissemination assays (see Cytopathic Effect Assay), and serum was collected for antiadenoviral-type 5 antibody assays (see Adenovirus Antibody Assay) at baseline and 24 hours after stereotactic injection of Ad-p53. After injection of Ad-p53 into the wall of the resection cavity (ie, after craniotomy), this sampling was repeated within 24 hours, after 2 weeks, and monthly.

Toxicity and Response Evaluation

Careful patient monitoring was applied throughout the study. Adverse events were determined according to the National Cancer Institute (NCI) common toxicity criteria, recorded on NCI Adverse Event Forms, and reported according to NCI guidelines. Because our protocol involved technical procedures (eg, placement of an intratumoral catheter, tumor resection, needle injection into a postresection cavity), as well as testing of a new agent (Ad-p53), we determined the relationship of the adverse event to the procedure and to the agent.

Because the major thrust of this study was to evaluate toxicity at each dose of Ad-p53, we made an attempt to evaluate its efficacy on the basis of clinical

Table 2. Biological Analysis

| Patient No. | Dose Level | Pretreatment Biopsy | | Postinjection Specimen | | | | | p21 IHC | TUNEL |
| | | | | p53 IHC | | | | | | |
		p53 IHC	p53 Mutational Status*	Nuclear Staining	Cytoplasmic Staining	Hyperplastic Vessels	Maximum Distance (mm)		Nuclear	
1	I	Rare	ND	+	–	–	4.0		+	ND
2	I	+	Wt	+	–	–	5.5		+	+
3	I	–	Wt	+	–	–	5.0		ND	ND
4	II	ND	ND	+	–	–	4.5		+	ND
5	II	–	Wt	+	+	–	5.0		+	+
6	II	ND	ND	NA	NA	NA	NA		NA	ND
7	III	–	Wt	+	–	–	5.0		+	ND
8	III	–	Wt	+	+	–	6.0		–	+
9	III	–	Wt	+	+	–	5.0		+	+
13	IV	ND	ND	NA	NA	NA	NA		NA	ND
14	IV	–	Wt	+	–	–	1.0†		+	ND
15	IV	ND	ND	+	+	Rare	8.0		ND	ND

Abbreviations: IHC, immunohistochemistry; ND, not done; Wt, wild-type; NA, not assessable; TUNEL, terminal deoxynucleotidyl transferase-mediated deoxyuridine triphosphate-biotin nick end-labeling.

*Patients 10, 11, and 12 (Table 1) were also analyzed for p53 mutation using the pretreatment biopsy specimen. Mutations were identified in patient 10 (codon 234 [Tyr/stop] and codon 157 [Val/Phe]) and patient 11 (codon 248 [Arg/Gln]).

†Intracystic injection.

criteria. Because all of the patients underwent complete resection of the gadolinium-enhancing tumor mass, the primary outcome statistic was time to tumor progression as measured from the time of Ad-p53 injection into the wall of the resection cavity. Tumor recurrence was defined as the occurrence of a new region of MRI contrast enhancement that increases by 25% on sequential scans.

Adenovirus Antibody Assay

Serum samples were tested for the presence of antiadenoviral-type 5 immunoglobulin G by Virolab Inc (Berkeley, CA) using an indirect immunofluorescence assay to indicate the patient's humoral immune response to the vector as previously described.[36]

Cytopathic Effect (CPE) Assay

To semiquantitatively detect the amount of vector contained in biologic fluid, a CPE assay was performed. This assay also can detect replication-competent adenoviruses. CPE assays were performed using the cell lines IT293 and A549, as previously described.[30,32,36] Supernatants obtained from positive CPE assays were tested for adenovirus type 5 (Ad5) hexon protein using a commercially available enzyme-linked immunosorbent assay kit (Adenoclone EIA; Meridian Diagnostics, Cincinnati, OH) to confirm the presence of an adenovirus in the bioassay.

Statistical Methods

Descriptive data analysis was applied as the primary statistical analysis tool. The progression-free survival (PFS) rate and overall survival (OS) rate were calculated from the time of surgical resection using the Kaplan-Meier method. For histologic evaluations, the χ^2 method was used to determine the significant differences between dose levels.

RESULTS

Patients and Treatment

Fifteen patients received treatment in this study. Twelve patients completed both surgical stages of the protocol, whereas three patients completed stage 2 only (Table 1). The patients' demographics, treatment dose and dose level, tumor type, prior treatments, and tumor features are listed in Table 1.

Molecular Analyses of Pretreatment Biopsies and Posttreatment Tumor Specimens

Posttreatment specimens that preserved the tumor architecture relative to the injection site were obtained in 10 of the 12 patients who completed both stages of the protocol. These 10 patients formed the basis of the molecular analyses (Table 2). The posttreatment formalin-fixed specimens were cut perpendicular to the catheter, and serial histologic sections in which the site of the Ad-p53 injection could be determined were analyzed (Figs 2 and 3). For comparison, pretreatment biopsy specimens were analyzed from eight of these 10 patients (Table 2). Mutational analysis revealed that all analyzed patients in this cohort had wild-type p53 alleles (Table 2).

To assess the expression and distribution of exogenous p53, we performed immunohistochemical staining using an antibody specific to wild-type p53 (PAb-1801). Pretreatment biopsies were negative for p53 immunostaining in six specimens and demonstrated low levels or rare staining in two specimens (Table 2). In contrast, in all 10 assessable posttreatment patients, delivery of Ad-p53 resulted in robust p53 immunoreactivity in an inhomogeneous pattern around the catheter site (Table 2; Figs 2D and 3A). In areas of immunopositivity, 95% to 100% of the cells were intensely stained. Analysis of the sections at higher magnification revealed that p53 expression occurred within the nucleus of tumor cells, as would be expected of a transcription factor such as p53 (Fig 2E). However, we also observed cytoplasmic p53 expression in four specimens (Table 2; Fig 3B).

To more quantitatively determine the depth of spread of the vector, we measured the maximum distance from the injection site (defined by the catheter position) at which positive immunoreactivity was detectable in representative sections from each specimen (Table 2). The mean maximal distance was only 4.9 ± 1.7 mm (range 1 to 8 mm). Thus, with the injection technique
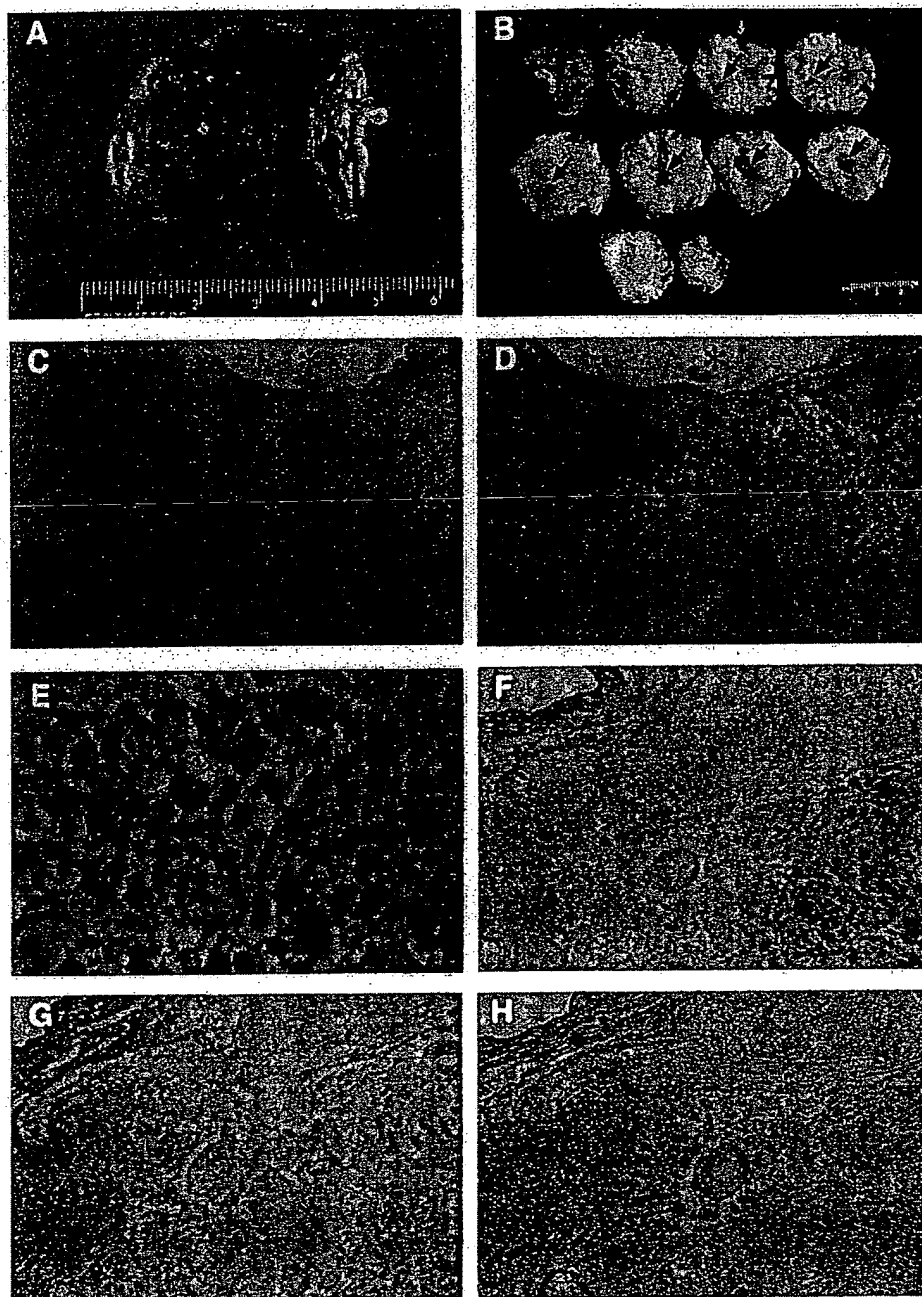
Fig 2. Biologic analysis of tumor specimen (patient 2). (A) Posttreatment surgical specimen that was resected en bloc. Catheter marks the injection site. (B) Specimen from A after fixation, and cutting perpendicular to the catheter. Arrows mark the catheter track. (C) Section from A stained with hematoxylin and eosin demonstrating classic glioblastoma multiforme. (*) Position of the catheter (40×). (D) Section adjacent to C after staining using antibody to p53. Staining (dark cells) is evident around the catheter (40×). (E) High-power view of D showing p53 immunostaining within the nuclei of tumor cells (200×). (F to H) Serial adjacent sections of specimen analyzed by immunohistochemistry for (F) p53, (G) p21$^{CIP/WAF}$, and (H) by terminal deoxynucleotidyl transferase-mediated deoxyuridine triphosphate-biotin nick end-labeling (TUNEL). (F) p53-positive cells (100×) are evident in the right corner of the field and the injection site is in the left upper corner. (G) The area of p21$^{CIP/WAF}$ staining (100×) correlates with the area of p53 staining. (H) TUNEL staining (100×) is most prominent adjacent to catheter where p53 staining is minimal.

used in this study, we found that p53-transduced cells reside within only a short distance from the injection site. In addition, the mean maximal distance (± SD) was 4.8 ± 0.8 mm for dose level I, 4.8 ± 0.4 mm for level II, 5.3 ± 0.6 mm for level III, and 4.5 ± 4.9 mm for level IV. Thus, there was no significant increase in the extent of distribution with increasing dose of Ad-p53 (P = .3, χ^2 test), although there were a small number of specimens in each group.

In an effort to determine whether exogenous p53 was functional, we assayed specimens for increases in p21$^{CIP/WAF}$, a known p53-inducible protein, by immunostaining with a p21-specific antibody. Analyses of sections adjacent to the p53-

immunostained sections revealed that in seven of eight tested specimens, the distribution of p21 immunostaining was similar to that of exogenous p53, indicating that exogenous p53 was capable of inducing p21 (Figs 2F and 2G). In addition, in two patient cases, simultaneous immunostaining for expression of p53 and p21 was performed sequentially using different colored chromogens. As shown in Fig 3B, individual p53-positive cells also expressed high levels of p21. Taken together, these data support the notion that the exogenously delivered p53 was capable of transactivating p21 and was thus functionally active.

To determine whether Ad-p53 was capable of inducing apoptosis, in situ TUNEL staining was undertaken. All four
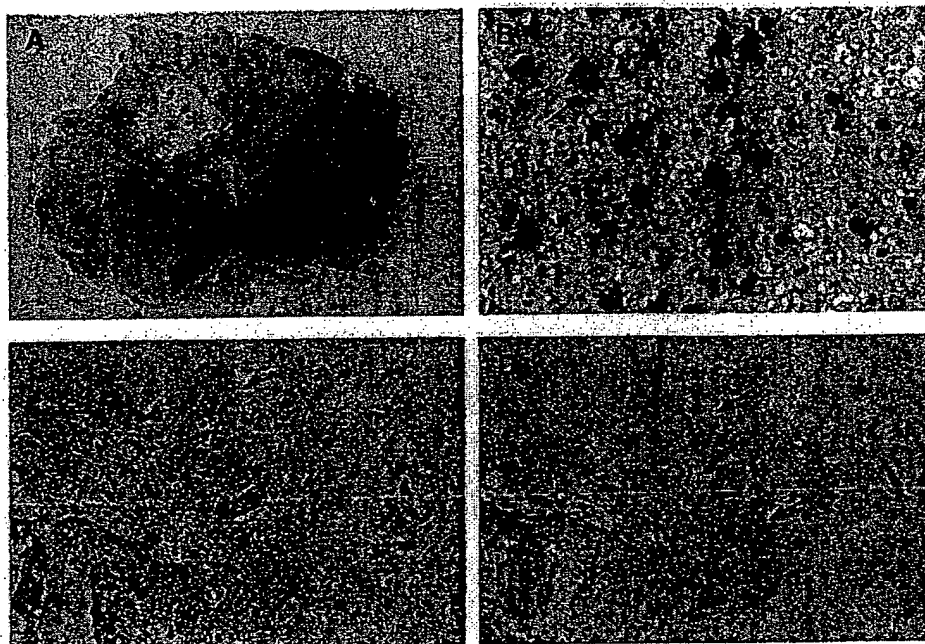
Fig 3. Biologic analysis of tumor specimen (patient 5). (A) Entire specimen after immunostaining for p53 protein. The position of the catheter is evident (*). p53 immunostaining is evident within 5 mm of the catheter. (B) Sequential immunostaining for p21^{CIP/WAF} (brown chromogen), and p53 (red chromogen) (200×). Cytoplasmic p53 immunostaining (red) allows p53-positive cells to be identified. Although the nuclei of some cells stain only for p53 (red nuclei, arrow), the majority of nuclei stain black (arrow head), indicating colocalization of p53 and p21^{CIP/WAF}. (C and D) Photomicrographs of adjacent serial sections demonstrating (C) pattern of p53 (100×) and (D) terminal deoxynucleotidyl transferase-mediated deoxyuridine triphosphate-biotin nick end-labeling (TUNEL) staining (100×). p53-positive cells are close to the injection site (*). Although rare TUNEL-positive cells (arrows in D) are located among the p53-positive cells, the majority of cells are not undergoing apoptosis.

specimens analyzed demonstrated positive staining concentrated only around the injection site (Figs 2H and 3D). Apoptotic cells were only rarely seen away from the catheter. Analysis of adjacent sections demonstrated that zones of TUNEL-positive cells were associated with zones of positive p53 immunostaining; however, TUNEL-positive cells were not the same cells as those that were p53-positive, which is an expected finding given that TUNEL positivity is indicative of an end-stage cellular state in which the integrity of most proteins (including p53) is disrupted. Most commonly, the p53-positive cells were farther away from the catheter site than the TUNEL-positive cells (Figs 2F and 2H). In areas where p53 positive cells were close to the catheter (Fig 3C), the number of p53-positive cells exceeded the number of apoptotic cells (Fig 3D), indicating that at least at 72 hours postinjection a subset of Ad-p53-infected cells were not undergoing apoptosis.

Clinical Studies: Adverse Events

We assessed clinical toxicity in all 15 patients after treatment with Ad-p53 (INGN 201). There was one adverse event (a grade 3 hemiparesis [patient 5] cause by a hematoma) related to the injection of Ad-p53 into the tumor. Nonsurgical adverse events possibly, probably, or definitely related to Ad-p53 treatment, regardless of grade, are listed in Table 3. The most common adverse events potentially attributable to Ad-p53 were headache (53% of the patients), fatigue (40%), and fever (27%).

Neurologic events potentially related to Ad-p53 occurred in two patients at dose level III (a grade 3 aphasia and a grade 2 aphasia). Because of the occurrence of the grade 3 toxicity, we evaluated three additional patients at this level (Table 1). None of these patients had significant neurologic toxicity, although one patient (patient 10) had an asymptomatic hematoma that was observed on MRI scans taken 3 months after treatment and was

temporally related to trauma. Three patients were then treated at level IV with no significant toxicity. Thus, a maximum-tolerated dose was not defined in this study, and additional escalation was not undertaken because of difficulties with manufacturing and storing the agent at higher concentrations.

Table 3. Nonsurgical Adverse Events

Adverse Event	Grade	Relationship to Treatment Possible (no. of events)	Relationship to Treatment Probable/Definite (no. of events)	Total
CNS hemorrhage	3	1	0	1
Confusion	2	1	0	1
Fatigue	1	5	0	5
	2	1	1	2
Fever without neutropenia	1	3	1	4
Granulocytopenia	1	1	0	1
Headache	1	7	1	8
	2	2	0	2
	3	1	0	1
Leukopenia	1	2	0	2
Motor dysfunction	2	1	0	1
Nausea alone	1	2	0	2
Pyramidal tract dysfunction	2	1	0	1
Seizure	2	2	0	2
	4	1	0	1
Speech impairment	1	1	0	1
	2	3	0	3
	3	2	0	2
Viral-like syndrome	2	0	1	1
Vomiting	1	3	0	3
	2	1	0	1
Total		41	4	45

NOTE. Results are reported as independent events. More than one event may have occurred per patient or the same event may have occurred more than once in a given patient.
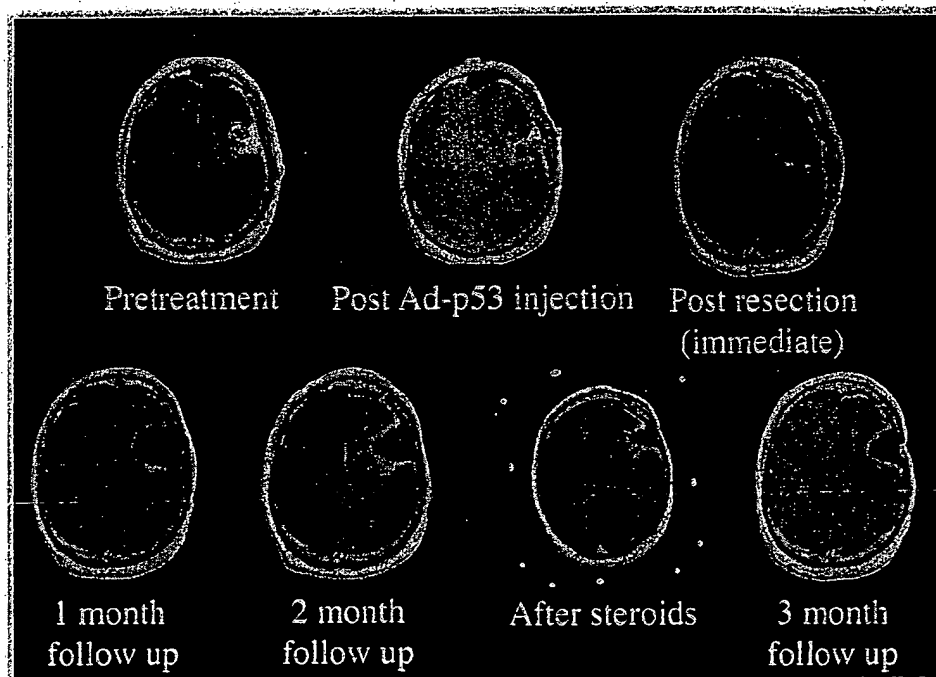
Fig 4. Serial T1-weighted postgadolinium magnetic resonance images (MRIs) of patient 8. Initial MRI demonstrates lesion in left frontal lobe. The catheter is evident on the poststereotactic-injection image. Postresection image shows a clean resection cavity. The one-month scan is stable, but the 2-month scan shows evidence of pericavity enhancing spikes; the patient had worsening speech. Treatment with corticosteroids (1 week) reduced the enhancement and improved the symptoms. By 3 months, the spike-like enhancement resolved.

It should be noted that three seizures were reported in two patients. However, these events occurred many months after treatment with Ad-p53 and were associated with tumor recurrence. Because of the common occurrence of seizures in this disease, we concluded that these events were not dose limiting.

Radiographic Evaluation

Serial MRI studies showed that the majority of the patients had a spike-like pattern of contrast enhancement on 1-month follow-up scans that we attributed to the multiple injections of Ad-p53 into the wall of the resection cavity and that typically resolved within 2 to 3 months. However, for many patients, we later found nonspecific enhancing patterns around the surgical cavity; it was difficult to determine whether these patterns represented inflammation or recurrent tumor. The results from patient 8 were particularly informative because the onset of his neurological symptom (aphasia, as described) at 2 months posttreatment correlated with an increase in contrast enhancement around his resection cavity (Fig 4). At the same time as the patient's symptoms improved with the administration of corticosteroids, the amount of enhancement on his MRI scans also decreased. Thus, these changes seemed to indicate inflammatory effects of the Ad-p53 treatment rather than tumor recurrence. Contrast enhancement on MRIs representative of a true recurrence at 7.5 months did not respond to corticosteroid administration.

Immune Response to Adenovirus Type 5

To determine whether any systemic immune responses occurred after intracranial injection of Ad-p53 (INGN 201), we measured the titers of antiadenoviral type 5 immunoglobulin G antibodies both before Ad-p53 treatment and at fixed intervals after treatment. Ten

(83%) of 12 assessable patients showed an antibody response (defined as > two-fold increase in antibody titer). Antibody titers increased 1 to 2 weeks after craniotomy, were maximal at 1 to 2 months, and decreased at 5 to 6 months (Table 4).

Adenovirus Vector Dissemination

To determine whether intracranial injection of Ad-p53 (INGN 201) resulted in widespread systemic dissemination of the vector, we performed CPE assays at fixed intervals after treatment. We did not detect replication-deficient virus in patients' plasma, urine, sputum, or rectal samples at any of the time points. There was no evidence for conversion of Ad-p53 to a replication-competent form.

Clinical Outcome

Although the number of patients in this phase I trial was limited, we obtained information about the outcome of treating the resection cavity using Ad-p53 (Table 5). Because all of the patients had essentially undergone gross total resection of their tumors, we could not determine response to Ad-p53. However, the median PFS duration in these patients was 13 weeks, and the median OS duration was 43 weeks (Fig 5). Notably, one patient is still alive more than 3 years after treatment without evidence of recurrence; this patient has received no other treatment. Moreover, of the remaining 14 patients, four experienced no recurrence more than 6 months after treatment and two of these patients survived for more than 1 year.

DISCUSSION

This phase I trial demonstrated that injection of Ad-p53 (INGN 201) into malignant brain tumors is safe and results in transfer of p53 gene to astrocytic tumor cells, leading to the

Table 4. Serum Anti-Ad5 Antibody Titers

Patient No.	Preoperative	Postbiopsy	Postcraniotomy							
			24 Hours	2 Weeks	1 Month	2 Months	3 Months	4 Months	5 Months	6 Months
1	128	256	256	—	—	1,024	—	—	—	—
2	128	128	128	—	512	512	—	128	—	—
3	512	512	—	1,024	1,024	1,024	—	—	—	—
4	512	512	512	—	512	512	—	—	—	—
5	128	—	—	1,024	—	4,096	—	—	—	—
6	256	256	512	—	2,048	—	—	—	—	—
7	64	64	32	—	64	—	—	—	—	—
8	512	512	—	2,048	8,192	4,096	2,048	1,024	512	—
9	512	256	—	2,048	2,048	2,048	—	1,024	1,024	512
10	128	128	128	4,096	2,048	1,024	—	—	—	—
11	512	512	512	2,048	—	2,048	2,048	—	—	—

NOTE. Values are reported as the inverse of the titer.

Abbreviation: Ad5, adenovirus type 5.

expression of functionally active p53 protein that is capable of transducing other genes (eg, $p21^{WAF/CIP}$) and inducing apoptosis in a subset of cells. Surgical specimens that preserved the anatomic integrity of the tissue showed limited distribution of Ad-p53 with the injection technique employed in this study.

We showed that the two-stage surgical design used in this study is feasible for brain tumor patients. For new biologic agents, there has been an increasing desire to incorporate molecular analysis of tumor specimens into phase I trials.[41,42] However, for brain tumors, in which tissue accessibility is a major problem and the potential for repeat biopsy is limited, such trials are particularly challenging.[43] The incorporation of pretreatment biopsy and posttreatment craniotomy for tissue acquisition that was undertaken in this trial provided valuable biologic information that would otherwise not have been obtained if more standard phase I designs were followed. Importantly, the biologic evaluation did not interfere with the long-term clinical evaluation. However, the difficulties associated with obtaining adequate tissue in brain tumor patients limited our assessment of the biologic effects of Ad-p53 to only one time point after Ad-p53 delivery (3 days). Moreover, including cases of catheter implantation without Ad-p53 injection (as a negative control)

Table 5. Outcome of Patients Treated with Ad-p53

Dose Level	Patient No.	Recurrence (weeks)	Survival (weeks)
I	1	26	D, 43
I	2	13	D, 50
I	3	35	D, 52
II	4	9	D, 72
II	5	—	A, 179
II	6	18	D, 25
III	7	9	D, 13
III	8	30	D, 44
III	9	35	D, 79
III	10	12	D, 40
III	11	2	D, 19
III	12	17	A, 68
IV	13	5	D, 13
IV	14	12	D, 33
IV	15	4	D, 42

Abbreviations: D, dead; A, alive.

may have been beneficial, but was not possible because of the complexity of the approach. Nevertheless, the design of this trial may be used as a model for future brain tumor studies.

The biologic analyses demonstrate robust p53 immunostaining within tumor cells, indicating expression of the p53 transgene. However, it must be recognized that the antibody used in this study could not distinguish between exogenous and endogenous p53. We interpreted the p53 immunostaining seen in the specimens to be from exogenously delivered p53 rather than endogenous p53 protein because in all but two patients, pretreatment biopsies did not demonstrate endogenous p53 immunoreactivity (consistent with wild-type p53 allele studies; Table 2); the intensity of the staining in all posttreatment specimens was significantly more robust than that typically seen for endogenous p53 protein; and even in patients having p53-positive immunoreactivity in the preoperative biopsy analysis, the intensity of the staining around the catheter was clearly distinguishable from the low level of endogenous p53 staining more distant from the catheter (ie, each patient had his or her own internal control for endogenous p53 staining). Nevertheless, the possibility remains that the observed increase in p53 immunostaining adjacent to the catheter could have been the result of overexpression of endogenous p53 in response to nonspecific adenovirus infection, as reported by McPake et al,[44] who analyzed adenoviral-induced changes of p53 in neuroblastoma and human fibroblast cell lines grown in vitro. However, observations similar to those of these investigators have not been made in glioma cell lines.[5,6,18] In addition, studies in non–small-cell lung cancer and head and neck cancer using the polymerase chain reaction with vector-specific primers for adenovirus and p53 sequences have confirmed the presence of exogenous p53 transgenes in treated specimens.[30,32,35,38] Thus, it is reasonable to conclude that the robust staining seen in our specimens arose from the exogenously delivered p53.

Although other clinical trials of head and neck[32,38] and lung cancer[30,35] have demonstrated p53 expression after intratumoral injection of Ad-p53 (INGN 201), to our knowledge, no other study has determined the spatial distribution of p53 relative to the injection site. We analyzed this parameter because preclinical
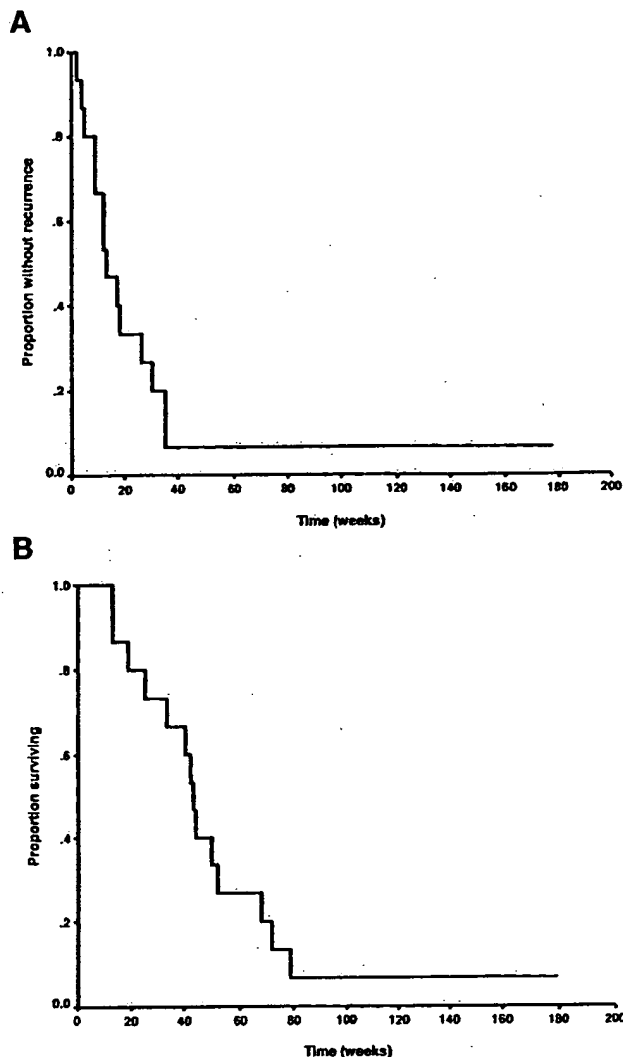
A

B

Fig 5. Kaplan-Meier plots showing (A) progression-free survival and (B) overall survival rates.

studies indicated that adenoviral vectors are capable of extensive distribution throughout tumor-bearing rat brains.[45] In addition, widespread delivery is particularly important in brain tumors, where tumor control requires transduction of unresectable tumor cells that infiltrate normal parenchyma several centimeters away from the solid tumor mass.[46,47] Previous trials relied on molecular techniques that precluded anatomic analyses (eg, polymerase chain reaction) and therefore could not define spatial relationships. In contrast, by leaving the injection catheter in place and analyzing intact specimens with immunohistochemistry, we were able to demonstrate that with the bolus injection method used in this trial, the distribution of Ad-p53 in brain tumors was quite limited, reaching a zone of less than 1 cm around the injection site. Nevertheless, it seems that injection of Ad-p53 resulted in more widespread transgene expression than did instillation of producer cells, which was used in an earlier trial of herpes simplex virus–thymidine kinase (TK) gene therapy, in which only a few cells expressed the TK transgene.[48] Thus,

direct injection of adenovirus vectors may be more advantageous than the use of producer cells. Furthermore, although the narrow distribution could be overcome by multiple injections (as we did in the postresection stage of this trial), this technique is not ideal for brain tumors because of the potential for traumatic injury. The results in this trial provide useful baseline data for evaluating future methods aimed at improving the distribution of Ad-p53.

Our data indicate that the exogenously expressed p53 protein was functional. First, we showed that p53 expression correlated with p21$^{CIP/WAF}$ expression (Figs 2 and 3). Although previous clinical studies have also demonstrated increased p21$^{CIP/WAF}$ in tumors that were treated with Ad-p53 because the posttreatment biopsy specimens were random samples of the tumor mass, a direct relationship between p53 and p21$^{CIP/WAF}$ expression was not demonstrated in these studies.[35,38] In our study, zones of p53 staining around the injection site also demonstrated p21$^{CIP/WAF}$ staining when adjacent posttreatment sections were analyzed. Moreover, when sections were stained for both proteins, individual cells expressing exogenous p53 and p21$^{CIP/WAF}$ were evident. Thus, this correlation between p53 and p21$^{CIP/WAF}$ expression indicates that the exogenous p53 is capable of carrying out its expected function as a transcription factor.

The second piece of evidence indicating that p53 was functional was the correlation between zones of apoptotic (TUNEL-positive) cells and the area of tissue exposed to Ad-p53. Specifically, TUNEL-positive cells were essentially confined to the limited region around the catheter site where p53 expression was also high. Because the process of apoptosis results in degradation of cellular components, it was not surprising that p53-positive cells were not themselves TUNEL-positive. Instead, p53-positive cells were typically adjacent to regions of TUNEL-positive cells. It was of interest that the p53-positive cells were usually farther away from the catheter than were the TUNEL-positive cells. Although this observation may be related to nonspecific cell death from catheter manipulations, it may also relate to the timing of apoptosis induction relative to Ad-p53 exposure. In other words, as the Ad-p53 diffused from the site of injection, cells nearer the injection would have been exposed to Ad-p53 first and were thus more likely to have undergone apoptosis at the time of tissue sampling than were the more distant cells, which were still expressing p53; biopsies taken later than 72 hours after injection may have revealed more extensive apoptosis and less p53 staining. It was also of interest that some cells adjacent to the catheter site were p53-positive but TUNEL-negative. Although these cells should have had enough time to undergo apoptosis, it seemed that they were less sensitive to the apoptotic effects of Ad-p53. Indeed, in vitro studies have shown that glioma cells lines that do not harbor a mutation in their p53 gene are often less sensitive than mutant p53 gliomas to Ad-p53–mediated apoptosis,[5,8,18] although wild-type p53 gliomas do undergo cell cycle arrest via p21$^{WAF/CIP}$ induction. Because most of the tumors in this study had normal p53 alleles (Table 2), it is possible that the limited amount of apoptosis observed in these specimens was a predictable consequence of their wild-type p53 gene status. Nevertheless, permanent G$_1$-

arrest may be an effective mechanism for inducing the anticancer effect of Ad-p53 in situ.

The Ad-p53–associated toxicities identified in this study are similar to those reported in other cancer-related Ad-p53 (INGN 201) trials,[30,32,35-38] and we interpret the occurrence of fever, fatigue, and headache in our study to be most consistent with a transient inflammatory response to the adenoviral vector. Previous trials in which p53 was injected into head and neck tumors that could be directly visualized demonstrated inflammatory changes at the injection site.[32,37,38] Although the location within the intracranial compartment precluded direct observation of an inflammatory response, the pericavitary enhancement seen on MRI scans after Ad-p53 injection and its attenuation by administration of corticosteroids are indirect evidence of a local inflammatory response. Supporting this conclusion was the finding of a systemic increase in anti-Ad5 antibody titers in all but two of the patients within 2 months of Ad-p53 injection; similar increases in anti-Ad5 antibody have been reported in previous Ad-p53 trials.[32,36,37] Lastly, MRI changes and an inflammatory response to Ad-p53 were also observed in animal studies. Smith et al[49] reported studies of rats and monkeys in which injection of an adenoviral vector, albeit one containing the TK gene rather than p53, resulted in dose-dependent occurrence of fever; MRI of the animals showed increased enhancement around the injection tract, and histologic analysis of their brains demonstrated local astrogliosis that worsened as the dose increased. In preclinical studies from our laboratory,[9] injection of Ad-p53 into Wistar rats resulted in local astrogliosis, which was most prominent on day 7 and had resolved by day 14. Thus, the potential of an immune response, although transient, may be an important component of the efficacy and toxicity of Ad-p53.

In previous clinical studies, injection of Ad-p53 (INGN 201) into head and neck and non–small-cell lung cancer tumors resulted in dose-dependent shedding of the adenovirus in the urine and saliva or sputum.[32,35] In contrast, using the same CPE assay, which can detect as few as 10 particle-forming units/mL, we were unable to identify any viral shedding in the urine or sputum both immediately and up to 2 months after Ad-p53

injection. We also did not detect the adenovirus in the plasma. However, our initial measurements were performed 24 hours after Ad-p53 injection, whereas previous trials detected the adenovirus within 30 minutes of treatment, and these titers became undetectable by 90 minutes. Thus, it is possible that in our study, some Ad-p53 was released into the plasma but was not detected because of our sampling schedule. Nevertheless, shedding of a virus after intracranial injection seems to be significantly less likely than that after injection into systemic tumors.

Although it was not intended to determine efficacy, the results of our trial indicate that Ad-p53 (INGN 201) warrants additional study as an anticancer agent (Table 5). Most notably, one patient in our study with a GBM is still alive and without evidence of recurrence nearly 3.5 years after Ad-p53 treatment. Furthermore, at each dose level (except level IV), patients experienced extended disease-free intervals. The poor results in patients at level IV may reflect difficulties in maintaining viable viral particles when the product is stored at such a high titer. Nevertheless, the outcomes of patients treated with Ad-p53 compared favorably with those of GBM patients who have similar clinical attributes treated in other clinical trials. Most notably, Wong et al[50] compiled the results of 225 patients with GBM treated at The University of Texas M. D. Anderson Cancer Center (Houston, TX) in phase II trials and found that the median PFS and OS were approximately 9 weeks and 25 weeks, respectively. In comparison, after Ad-p53 treatment, the median PFS was 13 weeks and the median OS was 43 weeks. In addition, although tumor cells containing a mutant p53 allele are typically more sensitive to the apoptotic effects of Ad-p53, the majority of patients in our study had tumors containing cells with wild-type p53, which are often less sensitive to Ad-p53–mediated apoptosis. Inclusion of patients with tumors composed of cells containing mutant p53 alleles may have resulted in a longer PFS. Alternatively, because preclinical data indicate that combining Ad-p53 with DNA-damaging agents (such as radiation or chemotherapy) may be more efficacious than Ad-p53 alone,[8,18] future trials should incorporate these modalities into the design.

REFERENCES

1. Walker AE, Robins M, Weinfeld FD: Epidemiology of brain tumors: The national survey of intracranial neoplasms. Neurology 35:219-226, 1985

2. CBTRUS: Statistical Report: Primary Brain Tumors in the United States, 1995-1999. Central Brain Tumor Registry of the United States, Chicago, IL, 2002

3. Mercer WE, Shields MT, Amin M, et al: Negative growth regulation in a glioblastoma tumor cell line that conditionally expresses human wild-type p53. Proc Natl Acad Sci U S A 87:6166-6170, 1990

4. Kock H, Harris MP, Anderson SC, et al: Adenovirus-mediated p53 gene transfer suppresses growth of human glioblastoma cells in vitro and in vivo. Int J Cancer 67:808-815, 1996

5. Gomez-Manzano C, Fueyo J, Kyritsis AP, et al: Adenovirus-mediated transfer of the p53 gene produces rapid and generalized death of human glioma cells via apoptosis. Cancer Res 56:694-699, 1996

6. Gomez-Manzano C, Fueyo J, Kyritsis AP, et al: Characterization of p53 and p21 functional interactions in glioma cells en route to apoptosis. J Natl Cancer Inst 89:1036-1044, 1997

7. Fulci G, Ishii N, Van Meir EG: p53 and brain tumors: From gene mutations to gene therapy. Brain Pathol 8:599-613, 1998

8. Lang FF, Yung WKA, Raju U, et al: Enhancement of radiosensitivity of wild-type p53 human glioma cells by adenovirus-mediated delivery of the p53 gene. J Neurosurg 89:125-132, 1998

9. Lang FF, Yung WKA, Sawaya R, et al: Adenovirus-mediated p53 gene therapy for human gliomas. Neurosurgery 45:1093-1104, 1999

10. Roth JA, Swisher SG, Meyn RE: p53 tumor suppressor gene therapy for cancer. Oncology (Huntingt) 13:148-154, 1999

11. Nigro JM, Baker SJ, Preisinger AC, et al: Mutations in the *p53* gene occur in diverse human tumour types. Nature 342:705-708, 1989

12. Frankel RH, Bayona W, Koslow M, et al: p53 mutations in human malignant gliomas: Comparison of loss of heterozygosity with mutation frequency. Cancer Res 52:1427-1433, 1992

13. Louis DN, Rubio MP, Correa KM, et al: Molecular genetics of pediatric brain stem gliomas: Application of PCR techniques to small and archival brain tumor specimens. J Neuropathol Exp Neurol 52:507-515, 1993

14. Lang FF, Miller DC, Pisharody S, et al: High frequency of p53 protein accumulation without *p53* gene mutation in human juvenile pilocytic, low grade and anaplastic astrocytomas. Oncogene 9:949-954, 1994

15. Bogler O, Huang H-JS, Kleihues P, et al: The *p53* gene and its role in human brain tumors. Glia 15:308-327, 1995

16. Kamijo T, Weber JD, Zambetti G, et al: Functional and physical interactions of the *ARF* tumor suppressor with *p53* and *Mdm2*. Proc Natl Acad Sci U S A 95:8292-8297, 1998

17. Pomerantz J, Schreiber-Agus N, Liegeois NJ, et al: The *Ink4a* tumor suppressor gene product, *p19Arf*, interacts with *MDM2* and neutralizes *MDM2*'s inhibition of *p53*. Cell 92:713-723, 1998

18. Shono T, Tofilon PJ, Schaefer TS, et al: Apoptosis induced by adenovirus-mediated *p53* gene transfer in human glioma correlates with site-specific phosphorylation. Cancer Res 62:1069-1076, 2002

19. Lang FF, Miller DC, Koslow M, et al: Pathways leading to glioblastoma multiforme: A molecular analysis of genetic alterations in 65 astrocytic tumors. J Neurosurg 81:427-436, 1994

20. Pollack IF, Finkelstein SD, Woods J, et al: Expression of *p53* and prognosis in children with malignant gliomas. N Engl J Med 346:420-427, 2002

21. Kyritsis AP, Bondy ML, Xiao M, et al: Germline *p53* gene mutations in subsets of glioma patients. J Natl Cancer Inst 86:344-349, 1994

22. Malkin, D: p53 and the Li-Fraumeni syndrome. Biochim Biophys Acta 1198:197-213, 1994

23. Lubbe J, von Ammon K, Watanabe K, et al: Familial brain tumour syndrome associated with a *p53* germline deletion of codon 236. Brain Pathol 5:15-23, 1995

24. Kleihues P, Schauble B, zur Hausen A, et al: Tumors associated with *p53* germline mutations: A synopsis of 91 families. Am J Pathol 150:1-13, 1997

25. Prives C, Hall PA: The *p53* pathway. J Pathol 187:112-126, 1999

26. Li H, Alonso-Vanegas M, Colicos MA, et al: Intracerebral adenovirus-mediated *p53* tumor suppressor gene therapy for experimental human glioma. Clin Cancer Res 5:637-642, 1999

27. Badie B, Kramar MH, Lau R, et al: Adenovirus-mediated *p53* gene delivery potentiates the radiation-induced growth inhibition of experimental brain tumors. J Neurooncol 37:217-222, 1998

28. Zhang WW, Fang X, Branch CD, et al: Generation and identification of recombinant adenovirus by liposome-mediated transfection and PCR analysis. Biotechniques 15:868-872, 1993

29. Zhang WW, Alemany R, Wang J, et al: Safety evaluation of Ad5CMV-p53 in vitro and in vivo. Hum Gene Ther 6:155-164, 1995

30. Swisher SG, Roth JA, Nemunaitis J, et al: Adenovirus-mediated *p53* gene transfer in advanced non-small-cell lung cancer. J Natl Cancer Inst 91:763-771, 1999

31. Spitz FR, Nguyen D, Skibber JM, et al: Adenoviral-mediated wild-type *p53* gene expression sensitizes colorectal cancer cells to ionizing radiation. Clin Cancer Res 2:1665-1671, 1996

32. Clayman GL, el-Naggar AK, Lippman SM, et al: Adenovirus-mediated *p53* gene transfer in patients with advanced recurrent head and neck squamous cell carcinoma. J Clin Oncol 16:2221-2232, 1998

33. Modesitt SC, Ramirez P, Zu Z, et al: In vitro and in vivo adenovirus-mediated *p53* and *p16* tumor suppressor therapy in ovarian cancer. Clin Cancer Res 7:1765-1772, 2001

34. Parker LP, Wolf JK, Price JE: Adenoviral-mediated gene therapy with Ad5CMVp53 and Ad5CMVp21 in combination with standard therapies in human breast cancer cell lines. Ann Clin Lab Sci 30:395-405, 2000

35. Roth JA, Swisher SG, Merritt JA, et al: Gene therapy for non-small cell lung cancer: A preliminary report of a phase I trial of adenoviral *p53* gene replacement. Semin Oncol 25:33-37, 1998

36. Nemunaitis J, Swisher SG, Timmons T, et al: Adenovirus-mediated *p53* gene transfer in sequence with cisplatin to tumors of patients with non-small-cell lung cancer. J Clin Oncol 18:609-622, 2000

37. Merritt JA, Roth JA, Logothetis CJ: Clinical evaluation of adenoviral-mediated *p53* gene transfer: Review of INGN 201 studies. Semin Oncol 28:105-114, 2001

38. Clayman GL, Frank DK, Bruso PA, et al: Adenovirus-mediated wild-type *p53* gene transfer as a surgical adjuvant in advanced head and neck cancers. Clin Cancer Res 5:1715-1722, 1999

39. Bruner JM, Connelly JH, Saya H: p53 protein immunostaining in routinely processed paraffin-embedded sections. Mod Pathol 6:189-194, 1993

40. Ruan S, Fuller G, Levin V, et al: Detection of p21WAF1/Cip1 in brain metastases. J Neurooncol 37:223-228, 1998

41. Eisenhauer EA: Phase I and II trials of novel anti-cancer agents: Endpoints, efficacy and existentialism—The Michel Clavel Lecture, held at the 10th NCI-EORTC Conference on New Drugs in Cancer Therapy, Amsterdam, 16-19 June 1998. Ann Oncol 9:1047-1052, 1998

42. Gelmon KA, Eisenhauer EA, Harris AL, et al: Anticancer agents targeting signaling molecules and cancer cell environment: Challenges for drug development? J Natl Cancer Inst 91:1281-1287, 1999

43. Lang FF, Gilbert MR, Puduvalli VK, et al: Toward better early-phase brain tumor clinical trials: A reappraisal of current methods and proposals for future strategies. Neuro-oncol 4:268-277, 2002

44. McPake CR, Shetty S, Kitchingman GR, et al: Wild-type p53 induction mediated by replication-deficient adenoviral vectors. Cancer Res 59:4247-4251, 1999

45. Parr MJ, Manome Y, Tanaka T, et al: Tumor-selective transgene expression in vivo mediated by an E2F-responsive adenoviral vector. Nat Med 3:1145-1149, 1997

46. Kelly PJ, Daumas-Duport C, Scheithauer BW, et al: Stereotactic histologic correlations of computed tomography- and magnetic resonance imaging-defined abnormalities in patients with glial neoplasms. Mayo Clin Proc 62:450-459, 1987

47. Kelly PJ, Daumas-Duport C, Kispert DB, et al: Imaging-based stereotaxic serial biopsies in untreated intracranial glial neoplasms. J Neurosurg 66:865-874, 1987

48. Ram Z, Culver KW, Oshiro EM, et al: Therapy of malignant brain tumors by intratumoral implantation of retroviral vector-producing cells. Nat Med 3:1354-1361, 1997

49. Smith JG, Raper SE, Wheeldon EB, et al: Intracranial administration of adenovirus expressing HSV-TK in combination with ganciclovir produces a dose-dependent, self-limiting inflammatory response. Hum Gene Ther 8:943-954, 1997

50. Wong ET, Hess KR, Gleason MJ, et al: Outcomes and prognostic factors in recurrent glioma patients enrolled onto phase II clinical trials. J Clin Oncol 17:2572-2578, 1999

Adenovirus-mediated Wild-Type *p53* Gene Transfer as a Surgical Adjuvant in Advanced Head and Neck Cancers[1]

Gary L. Clayman,[2] Douglas K. Frank,
Patricia A. Bruso, and Helmuth Goepfert

Department of Head and Neck Surgery, The University of Texas
M. D. Anderson Cancer Center, Houston, Texas 77030

ABSTRACT

A high incidence of locoregional failure contributes to the poor overall survival rate of around 50% for patients with squamous cell carcinoma of the head and neck (SCCHN). *In vitro* and *in vivo* preclinical work with adenovirus-mediated wild-type *p53* gene transfer using the recombinant *p53* adenovirus (Ad-*p53*) has shown its promise as a novel intervention strategy for SCCHN. These data have translated into Phase I and Phase II studies of Ad-*p53* gene transfer in patients with advanced, locoregionally recurrent SCCHN. The safety and overall patient tolerance of Ad-*p53* has been demonstrated. Of 15 resectable but historically noncurable patients in the surgical arm of a Phase I study, 4 patients (27%) remain free of disease, with a median follow-up time of 18.25 months. Surgical and gene transfer-related morbidities were minimal. These results provide preliminary support for the use of Ad-*p53* gene transfer as a surgical adjuvant in patients with advanced SCCHN. The implications of our findings for the management of SCCHN in general are discussed.

INTRODUCTION

The treatment of advanced primary human SCCHN[3] in the upper aerodigestive tract remains a major therapeutic challenge, despite advances in surgical and radiotherapeutic techniques. Locoregionally recurrent disease, which has a particularly dismal prognosis and few meaningful treatment options, remains the principal cause of death among patients with advanced SCCHN (1, 2). In addition, it has been shown that detection of clonal specific *p53* mutations at tumor margins in SCCHN is a predictor of local recurrence (3, 4). These molecular pathological advances suggest that despite adjuvant radiotherapy, residual disease (microscopic as well as histologically normal but genotypically abnormal) is a major problem in the treatment of patients with SCCHN. Our interest in developing new treatment strategies for SCCHN is generated by the humbling overall survival rate of approximately 50%, which has not changed over the last several decades (5).

Mutation of the *p53* tumor suppressor gene is one of the most common genetic alterations in human malignancy (6). Approximately 60% of human tumors are thought to possess mutation at the *p53* locus. Transient overexpression of the wild-type *p53* gene in various malignancies has been considered a potential molecular intervention strategy (7–12). This strategy is based on the role that wild-type *p53* plays as a tumor suppressor gene and an inducer of cell cycle arrest and apoptosis (6, 13–16). Our laboratory has focused on the potential of wild-type *p53* gene transfer as a strategy for the selective induction of apoptosis in SCCHN. The recombinant adenovirus Ad-*p53* has been used as the gene delivery tool in all of our preclinical studies (7–9). The tropism of the adenovirus for tissues of the upper aerodigestive tract, the ability to produce the adenovirus in high titers, and the efficiency of adenovirus-mediated gene transfer have made this vector an attractive tool for transient gene delivery.

In our preclinical studies with Ad-*p53*, transduction of wild-type *p53* into several different SCCHN cell lines induced apoptosis without adversely affecting normal cells (7, 8). We have also shown that Ad-*p53* reduces the growth of established tumors in xenograft models of SCCHN (8). Additionally, we have demonstrated that in a nude mouse xenograft model of microscopic residual disease, Ad-*p53* can prevent the establishment of tumors from subcutaneously deposited SCCHN cell lines in a dose-dependent fashion (7).

In our recently completed Phase I clinical trial of Ad-*p53* gene transfer in patients with advanced locoregionally recurrent SCCHN who were unsuccessfully treated with conventional therapy including radiotherapy, two treatment arms were established. Our previous report (17) demonstrated the feasibility and tolerance of Ad-*p53* administered to patients with nonresectable disease and to patients who could be surgically treated but were historically deemed incurable; tissue vector biodistribution was evaluated in this publication as well. In this current focused analysis with longer patient follow-up (median follow-up, 18.25 months), we report the potential antitumor activity and complications of Ad-*p53* in a surgical adjuvant setting (the surgical treatment arm), based on our Phase I experience.

MATERIALS AND METHODS

Study Subjects. Of the 33 total patients entered into the Phase I study, 15 patients with advanced locoregionally recur-

Table 1   Demographics of surgical treatment arm study participants

Patient no.	Age (yr)	Sex	p53 genotype	Index tumor site	Prior treatments related to index tumor	Recurrent tumor site
1	31	F	Mutant	Tongue, floor of mouth	1. laser exc. L. tongue[a] 2. XRT to oral cavity 3. L. hemiglossectomy, mandibulectomy, MRND 4. 1 cycle CDDP & 5FU	Left face and neck
2	58	M	Mutant	Supraglottic larynx	1. supraglottic laryngectomy 2. completion laryngectomy, bilateral MRND 3. XRT to bilateral necks	Submental and submaxillary area
3	72	M	WT	Unknown primary	1. L. MRND 2. XRT to L. neck and supraclavicular region (5400 cGY)	Left neck
4	46	M	Mutant	Tongue base	1. L. RND and R. cervical node biopsy 2. XRT to L. and R. necks and tongue base (6600 cGy)	Tongue base
5	58	M	Mutant	Larynx	1. wide field laryngectomy 2. XRT to larynx (6300 cGy)	Hypopharynx
6	48	M	Mutant	Tongue base	1. XRT to tongue base, chemotherapy	Right superior larynx
7	76	F	Mutant	Supraglottic larynx	1. XRT to larynx, retropharyngeal and subdigastric nodes	Left supraclavicular area
8	53	M	WT	Unknown primary	1. R. RND 2. XRT to R. neck (5400 cGy) 3. XRT to submentum (4600 cGy) 4. 2 cycles cisplatin	Right submentum
9	56	M	Mutant	Larynx	1. verticle hemilaryngectomy 2. XRT to anterior neck and larynx (5500 cGy) 3. total laryngectomy	Neopharynx and peristomal region
10	49	F	NE	Left oral tongue	1. wide local exc. L. tongue 2. XRT to L. supraclavicular area (5040 cGy), L. neck (5600 cGy), and tongue and floor of mouth (3600 cGy)	Tongue
11	68	M	Mutant	Left tonsil	1. XRT to L. tonsil, L. upper neck, L. supraclavicular fossa (7000 cGy)	Left tonsil
12	37	M	Mutant	Left oral tongue	1. hemiglossectomy 2. re-excision L. tongue 3. XRT to tongue (6400 cGy) 4. L. MND	Left tongue base
13	34	F	NE	Floor of mouth and submentum	1. wide local exc. tongue and floor of mouth, L. MRND 2. 2 cycles of Taxol, ifosphamide, cisplatin 3. XRT and 2 cycles of 5FU and cisplatin	Left tongue and floor of mouth
14	56	M	Mutant	Right hypopharynx	1. 2 cycles of 5FU and cisplatin 2. partial laryngopharyngectomy, R. RND 3. XRT to R. neck (6300 cGy)	Right hypopharynx
15	73	F	Mutant	Left buccal mucosa	1. exc. L. buccal lesion 2. exc. L. retromolar trigone 3. L. hemimandibulectomy, L. MRND 4. XRT to L. cheek, face, and neck (4500 cGy) 5. XRT boost (900 cGy) to L. cheek	Left buccal mucosa

[a] L., left; R., right; exc., excision; XRT, radiation therapy; CDDP, cis-diamminedichloroplatinum; 5FU, 5-fluorouracil; MRND, modified radical neck dissection; RND, radical neck dissection; WT, wild-type; NE, could not be evaluated. Recurrent tumor site refers to the recurrent lesion that was treated in this Phase I trial.

rent or refractory SCCHN were placed into the surgical treatment arm. These 15 patients are the subjects of this report. For this report, we also examined biopsy samples of tumor margin and untreated adjacent normal tissues from a representative nonsurgical patient for evidence of apoptosis as well as expression of the wild-type p53 and p21^{Waf1} gene products.

Patients typically had multiple treatments for either refractory or locoregionally recurrent disease before study entry (Ta-

ble 1). All patients had previously received radiotherapy at some point during their treatment. Entry into the surgical treatment arm required only that the tumor could be resected to microscopic residual disease (without resection of the internal carotid artery), but resection offered little or no opportunity for cure as determined by the Multidisciplinary Head and Neck Oncology Treatment Planning Committee at The University of Texas M. D. Anderson Cancer Center. There were 10 males and 5 females, with a mean patient age of 54.3 years. Tumor p53 genotype was analyzed (by direct sequencing) for each patient, although a mutant genotype was not a prerequisite for study entry. Patients were required to practice contraception while in the study, and women of child-bearing age had to have negative pregnancy tests. A detailed description of the 15 subjects can be found in Table 1. The study was reviewed and approved by the Institutional Surveillance Committee of The University of Texas M. D. Anderson Cancer Center, the NIH Recombinant DNA Advisory Committee, and the Food and Drug Administration. Informed consent was obtained from all patients before study entry, with emphasis placed upon the investigational nature of the study and the absence of therapeutic intent.

Recombinant Adenovirus. The recombinant adenovirus Ad-p53 was used to directly introduce the wild-type p53 gene into all subjects. Preparation of the recombinant adenovirus was described previously (18). Ad-p53, also designated as INGN201, is a replication-defective adenovirus serotype 5 vector with a cytomegalovirus-promoted p53 cDNA insert replacing the E1 region of the vector. Ad-p53 is a BL-2 agent and was handled with the appropriate level of biological containment. Ad-p53 was produced by Magenta, Inc. (now MA Biosciences, Rockville, MD) and Introgen Therapeutics (Houston, TX) and stored at $-80°C$ at concentrations of 2×10^{10} to 3×10^{10} pfu/ml in PBS supplemented with 10% glycerol. Ad-p53 was thawed and diluted in PBS at $4°C$ within 2 h of use.

Administration of Ad-p53. All Ad-p53 was administered on an inpatient basis under strict aseptic conditions. Ad-p53 was delivered to sites of disease recurrence only. There were three Ad-p53 intervention approaches/patient: (a) preoperative; (b) intraoperative; and (c) postoperative.

Ad-p53 was given in escalating doses to determine a maximum tolerated dose for this treatment strategy. The Ad-p53 dose did not vary throughout each patient's treatment (Table 2). Doses started at 1×10^6 pfu and were increased in log increments until 1×10^9 pfu was reached and then increased in one-half log increments until 1×10^{11} pfu was reached.

The preoperative Ad-p53 administration consisted of direct tumor injections given three times weekly for 2 consecutive weeks (six treatments overall). The preoperative injection volumes were based on the estimated volume of the injected mass and the number of injection sites. Ad-p53 was administered using 27-gauge needles and 3–10-ml syringes, depending on the volume injected. Ad-p53 was injected directly into tumors by inserting the needle to the tumor depth and injecting upon withdrawal. Ad-p53 was diluted in a volume of PBS concordant with the number of tumor injections to be performed. Generally, we injected about 0.5 ml of vector solution at 1-cm (surface area) tumor increments. Thus, a very large tumor required the appropriate amount of vector to be diluted in a larger volume of PBS. Tumor maps were generated depicting the injection sites

so that these areas could be reinjected. A typical tumor map for a recurrent oral tongue lesion is shown in Fig. 1.

Seventy-two h after the last Ad-p53 intratumoral injection, patients had their surgery. At the time of surgery, after total gross tumor removal and just before closure, another dose of Ad-p53 (diluted to 10 ml in PBS) was delivered by injection to the surgical sites where microscopic residual disease was presumed to be present, including mucosal margins of the resected neoplasms (Fig. 2). A small amount of this dose was saved and administered liberally (a vector wash) to the tumor bed via a syringe and left in contact for 60 min before wound closure.

Seventy-two h after surgery, the patients received the final Ad-p53 administration (again diluted to 10 ml in PBS) via retrograde instillation through wound catheters that had been placed intraoperatively in the areas of presumed microscopic residual disease. Clamps were used to prevent efflux of the Ad-p53 for 1 h. The drains were removed 24–48 h after the postoperative instillation.

Statistical Analysis of Patient Outcome. Kaplan-Meier disease-specific survival and disease-free intervals were analyzed for all 15 patients entered into the surgical arm of the study. The time of study entry was the day of the first preoperative Ad-p53 administration. All patients were macroscopically free of disease after surgical resection.

Patient Monitoring. Because the treatment of patients with Ad-p53 was within the context of a Phase 1 clinical trial, diligent patient monitoring for the detection of untoward and toxic effects was obligatory. Surgical complications as well as potential Ad-p53-related toxic effects were recorded. Vital signs were recorded, performance status was evaluated, and chest X-rays and hematology and blood chemistry testing were performed daily. Patients were closely monitored for 2 h after each Ad-p53 administration.

Detection of Wild-Type p53 and p21^Waf1 Gene Product Expression and Apoptosis. Biopsy samples taken from the tumor margins of a representative nonsurgical patient were analyzed 48 h after Ad-p53 delivery (10^6 pfu) to the tumor. This immunohistochemical analysis examined the expression of the wild-type p53 gene product and the gene product of the downstream p53-transactivated gene p21^Waf1 (19) via an avidin-biotin-peroxidase complex method (20). The DO-1 anti-p53 mouse monoclonal antibody (Santa Cruz Biotechnology, Santa Cruz, CA) and the anti-p21^Waf1 mouse monoclonal antibody (Oncogene, Uniondale, NY) were used for all p53 and p21^Waf1 immunohistochemical studies, respectively. Standard H&E staining as well as TdT end-labeling to detect apoptotic cells were performed on similarly prepared tumor margin biopsy samples 48 h after Ad-p53 delivery to the tumor. TdT end-labeling was performed with the ApoTag Plus kit (Oncor, Gaithersburg, MD) according to the manufacturer's instructions. All of the these studies were matched with biopsy samples taken from adjacent uninjected grossly normal tissues of the same patient 48 h after Ad-p53 delivery to the tumor.

RESULTS

Patient Outcome. The Kaplan-Meier disease-specific survival curve for the patients enrolled in the surgical arm of the

Table 2 Ad-*p53* and surgical treatment and related complications of surgical treatment arm study participants

Patient no.	Ad-*p53* dose per treatment 1 × 10^x pfu	Adenovirus complications	Surgical treatment of recurrence	Surgical complications	Current disease status
1	6	Headache with first preoperative injection	Left maxillectomy and mandibulectomy, bilateral NDs,[a] total laryngectomy, partial pharyngectomy, latisimus free flap and bilateral pectoralis flap reconstruction	Postoperative fever with positive blood cultures for *Staphylococcus*	DOD
2	6	Erythema at preoperative injection site	Total glossectomy, total pharyngectomy, bilateral NDs, resection anterior neck skin, right pectoralis flap reconstruction	Intraoperative bradycardia and atrial flutter, electrolyte imbalance	DOD
3	7	None	Left extended RND, left pectoralis flap reconstruction	None	NED
4	7	Pain with preoperative injections	Total laryngectomy, total glossectomy, right MRND, marginal mandibulectomy, left verticle rectus myocutaneous flap reconstruction	None	DOD
5	8	None	Total pharyngectomy, cervical esophagectomy, completion thyroidectomy, bilateral MRND, mediastinal nodal dissection, free jejunum reconstruction	Anemia, electrolyte imbalance, confusion, fever, mild respiratory insufficiency, acute renal insufficiency	NED
6	8	None	Total laryngectomy, right MRND, left RND, partial pharyngectomy, subtotal thyroidectomy, total glossectomy, free rectus flap and pectoralis flap reconstruction	Anemia, electrolyte imbalance, acute renal insufficiency	DOD
7	9	Tenderness at preoperative injection site	Left extended RND, pectoralis flap reconstruction	Anemia, electrolyte imbalance, aspiration pneumonia	DOC
8	9.5	Fever during early preoperative injections, pain with preoperative injections	Right ND	None	DOD
9	10.5	Sore throat, increased dysphagia, sinus congestion, and headache during preoperative injections	Total pharyngectomy, total thyroidectomy, bilateral MRND, free jejunum reconstruction	Anemia, electrolyte imbalance, ascites, hypothyroidism, pneumatosis intestinalis	DOD
10	10.5	Fever, sore throat, headache, and increased odynaphagia and dysphagia during preoperative injections	Partial glossectomy, hemimandibulectomy, left MRND, free fibula osseocutaneous flap reconstruction	Anemia, electrolyte imbalance, hypertension, pneumonia, delayed cervical wound healing	DOD
11	10.5	Fever during preoperative injections, and pain associated with injections	Left partial pharyngectomy, left partial mandibulectomy, left RND, right verticle rectus free flap reconstruction	Anemia, electrolyte imbalance, pleural effusion, pneumonia and respiratory failure, hypertension, cellulitis left neck	DOC
12	11	Pain after preoperative injections, throat swelling after first preoperative injection	Total glossectomy, total laryngectomy, partial pharyngectomy, partial mandibulectomy, bilateral ND, free transverse rectus abdominis flap reconstruction	Anemia, electrolyte imbalance and hypovolemia, fever	DOD

Phase 1 Ad-*p53* clinical trial is shown in Fig. 3. Median survival was 12.4 months. Currently, four patients are alive with no evidence of disease (at 29.1, 23.8, 11.5, and 12.7 months). One patient is alive with disease (at 13.1 months), and eight patients have died of disease. Two patients died of unrelated causes (at 13.4 and 4.8 months). The current disease status of each study participant is shown in Table 2.

The median disease-free interval was 3.9 months for the nine patients enrolled in the surgical treatment arm whose disease recurred. The four patients without evidence of disease (disease free at 29.1, 23.8, 11.5, and 12.7 months) and the two patients who were without evidence of disease at the time of death (at 13.4 and 4.8 months) were not included in this calculation.

Table 2 Continued

Patient no.	Ad-p53 dose per treatment 1 × 10^x pfu	Adenovirus complications	Surgical treatment of recurrence	Surgical complications	Current disease status
13	11	Fever after first two preoperative injections, erythema and induration at preoperative injection sites, headaches postinjection	Total glossectomy, total laryngectomy, partial mandibulectomy, bilateral ND, free rectus flap reconstruction	Anemia, electrolyte imbalance, breakdown of flap reconstruction	NED
14	11	Fever and headache following preoperative injections	Total laryngopharyngectomy, left MRND, free jejunum reconstruction	Electrolyte imbalance, respiratory failure, hypothyroidism and hypoparathyroidism	NED
15	11	Fever after first preoperative injection, erythema and induration at preoperative injection site	Resection left buccal mucosa, partial maxillectomy, partial mandibulectomy, infratemporal fossa resection, left MRND, free flap reconstruction	Electrolyte imbalance, flap hematoma, agitation and confusion	AWD

a ND, neck dissection; AWD, alive with disease; DOC, died of other causes; DOD, died of disease; NED, no evidence of disease; RND, radical neck dissection; MRND, modified radical neck dissection.

Surgical Complications. Despite the extensive prior treatments and often tremendous tumor burdens, surgical complications in the context of Ad-p53 administration were relatively minor among the 15 study subjects, considering the extent of resection in most cases. There was one instance of delayed wound healing (patient 10) and one instance of flap breakdown (patient 13) requiring operative revision. There were no fistulas or wound infections. A detailed list of the surgical procedures for each patient, along with related complications, is provided in Table 2. The most common complications were electrolyte imbalance (usually consisting of transient hypokalemia or hypomagnesemia due to prolonged anesthesia; 11 of 15 patients), anemia (8 of 15 patients), pneumonia (3 of 15 patients), acute renal insufficiency (2 of 15 patients), and transient hypothyroidism (2 of 15 patients). All complications resolved with appropriate fluid or pharmacological intervention or both.

Ad-p53-related Complications. The dose of Ad-p53 that was administered to each patient is indicated in Table 2, along with a detailed list of treatment-related sequelae. All Ad-p53-related complications occurred during the preoperative administrations and were mild. All patients were able to tolerate the full course of Ad-p53 interventions (preoperative, intraoperative, and postoperative). As can be seen in Table 2, Ad-p53-related complications were more frequent at the higher viral doses ($\geq 1 \times 10^9$ pfu). Fever after Ad-p53 administration was the most common finding, occurring in six patients. Fever was not observed in patients who received less than 1×10^9 pfu/dose and was only transiently observed after the first injection or the first and second injections during preoperative administration. Fevers ranged from 38.1°C in patient 11 to 39.4°C in patient 10. Pain at the site of injection was also a frequent finding, occurring in five patients. This sequela was believed to be related to the cold temperature of the injected Ad-p53 solution. In patients 9, 10, 12, and 13, mild, transient, flu-like symptoms were observed early in their preoperative Ad-p53 administration courses.

Gene Product Expression and Induction of Apoptosis. Dark green positive immunohistochemical stainings for the wild-type p53 gene product (Fig. 4D) and the p21^Waf1 gene product (Fig. 4F) were demonstrated at the tumor margins of an Ad-p53-treated tumor from a representative nonsurgical patient. Matched samples from adjacent untreated normal tissue (Fig. 4, C and E) stained negatively. Only mild suprabasal detection of endogenous p53 was detected in the untreated tissue (Fig. 4C). It should be noted that the wild-type p53 gene product was detected despite the presence of a rigorous immune infiltrate (and systemic anti-adenovirus antibody titer; data not shown) seen on a posttreatment H&E-stained section from the tumor margin (Fig. 4B). Fig. 3H shows the brown-stained apoptotic tumor cells in the submucosa (by TdT end-labeling assay) present in a biopsy sample of the tumor margin after Ad-p53 injection, relative to the matched biopsy of adjacent untreated normal tissue (Fig. 4G).

DISCUSSION

Because of its propensity for locoregional recurrence and poor survival, SCCHN remains a devastating disease, despite treatment advances (1, 2, 5). A major factor leading to locoregional recurrence of SCCHN is microscopic residual disease after definitive surgery, radiotherapy, chemotherapy, or any combination of the three. Even histologically "normal" tissue at the margins of tumor resection can harbor molecular characteristics that portend disease recurrence (3, 4).

The situation of patients with locoregionally advanced SCCHN who have unsuccessfully undergone other therapies, including radiotherapy, is particularly problematic. Additional chemotherapy does not seem to offer a significant survival advantage to these patients (21), and they have few viable treatment options, even when tumors are surgically resectable. Thus, we selected this population of patients for our Phase 1 clinical trial of Ad-p53 gene therapy. The known role of p53 as a tumor suppressor gene and an inducer of cell cycle arrest and apoptosis in mammalian cells (6, 13–16), as well as our encouraging preclinical *in vitro* and *in vivo* animal findings with Ad-p53 in SCCHN (7–9), made this an attractive treatment strategy.

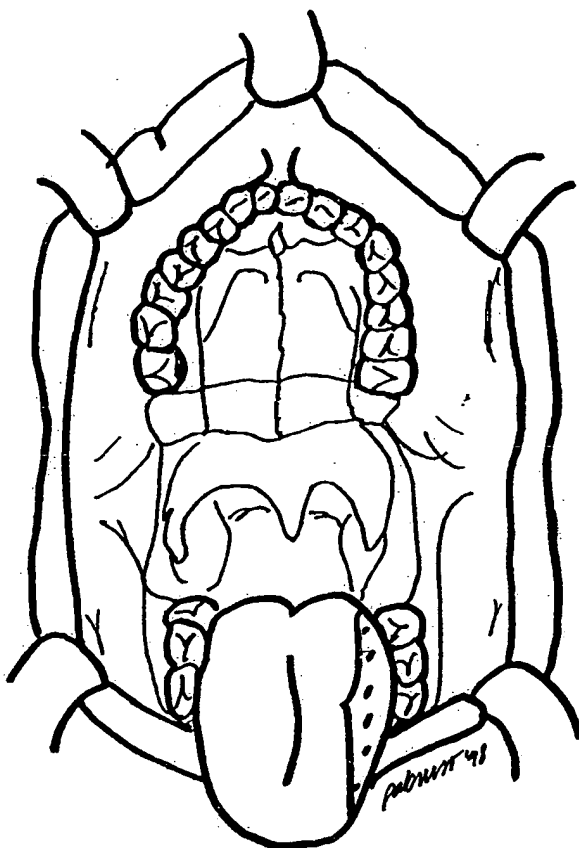As indicated earlier, the Phase 1 study of patients with

Fig. 1 Example of a typical tumor map for a left tongue carcinoma. Note the incremental markings along left tongue lesion indicating sites where Ad-*p53* is injected.

Fig. 2 Intraoperative delivery of Ad-*p53* to the tumor bed. Ad-*p53* is being injected into the tumor margins before a vector wash of the tumor bed.

advanced locoregionally recurrent SCCHN revealed that Ad-*p53* gene transfer is safe and well tolerated (17). Furthermore, in the current analysis, apoptosis and expression of the wild-type p53 and p21^{Waf1} (a downstream p53-transactivated gene) gene products were demonstrated in tumor margin biopsy samples taken from a representative nonsurgical patient after Ad-*p53* delivery. The findings with regard to median survival in the surgical arm of the study (Ad-*p53* delivered as an adjuvant to surgical therapy) prompted the current report, although our sample size was small, and thus the results should not be overinterpreted. The median survival for these patients (12.4 months) was about 60% longer than that found in chemotherapy trials for similar patients (21). Furthermore, the median disease-free interval of 3.9 months among those patients whose disease recurred suggests that this trial was not preselecting a favorable patient population. The observations made with regard to potential antitumor activity among patients with resectable tumors is encouraging as we proceed with the international Phase II evaluation of Ad-*p53* gene transfer in patients with SCCHN. Recurrence rates and mortality are higher in patients with molecular evidence of residual disease (as determined by PCR-based assay of *p53* mutation) at tumor margins (1, 2). Thus, the use of Ad-*p53* as an adjuvant modality in surgical wound beds may lower those rates.
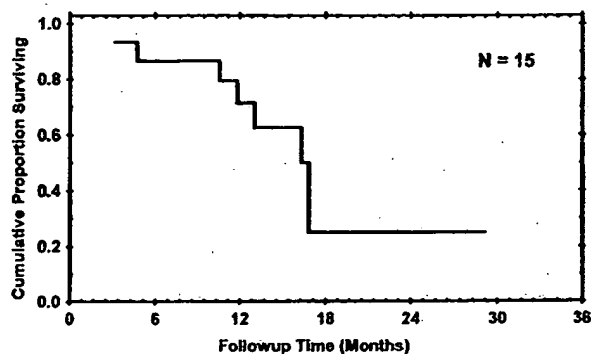

Fig. 3 Kaplan-Meier survival curve for patients in the surgical treatment arm.

There are several implications of our findings. Given the low toxicity of Ad-*p53*, this agent may be applied as an adjuvant therapy after primary definitive treatment of advanced lesions (or early lesions), as indicated above. Furthermore, Ad-*p53* gene transfer may be efficacious in dysplastic lesions because *p53* mutations have been found in head and neck premalignancies

Fig. 4 Immunohistochemical, H&E, and TdT end-labeling analyses of biopsies taken from the tumor margins of a representative nonsurgical patient 48 h after Ad-*p53* delivery to the tumor. In tumor margin biopsy samples, immunohistochemical staining for expression of the wild-type p53 gene product (*D*) and p21^{Waf1} gene product (*F*) is shown 48 h after Ad-*p53* delivery to the tumor. *C* (immunostained for expression of the wild-type p53 gene product) and *E* (immunostained for expression of the p21^{Waf1} gene product) show matched biopsy samples taken from untreated normal tissues 48 h after Ad-*p53* delivery to the tumor. In tumor margin biopsy samples, H&E staining (*B*) and TdT end-labeling (*H*) are shown 48 h after Ad-*p53* delivery to the tumor. *A* (stained with H&E) and *G* (end-labeled with TdT) show matched biopsy samples taken from untreated normal tissues 48 h after Ad-*p53* delivery to the tumor.
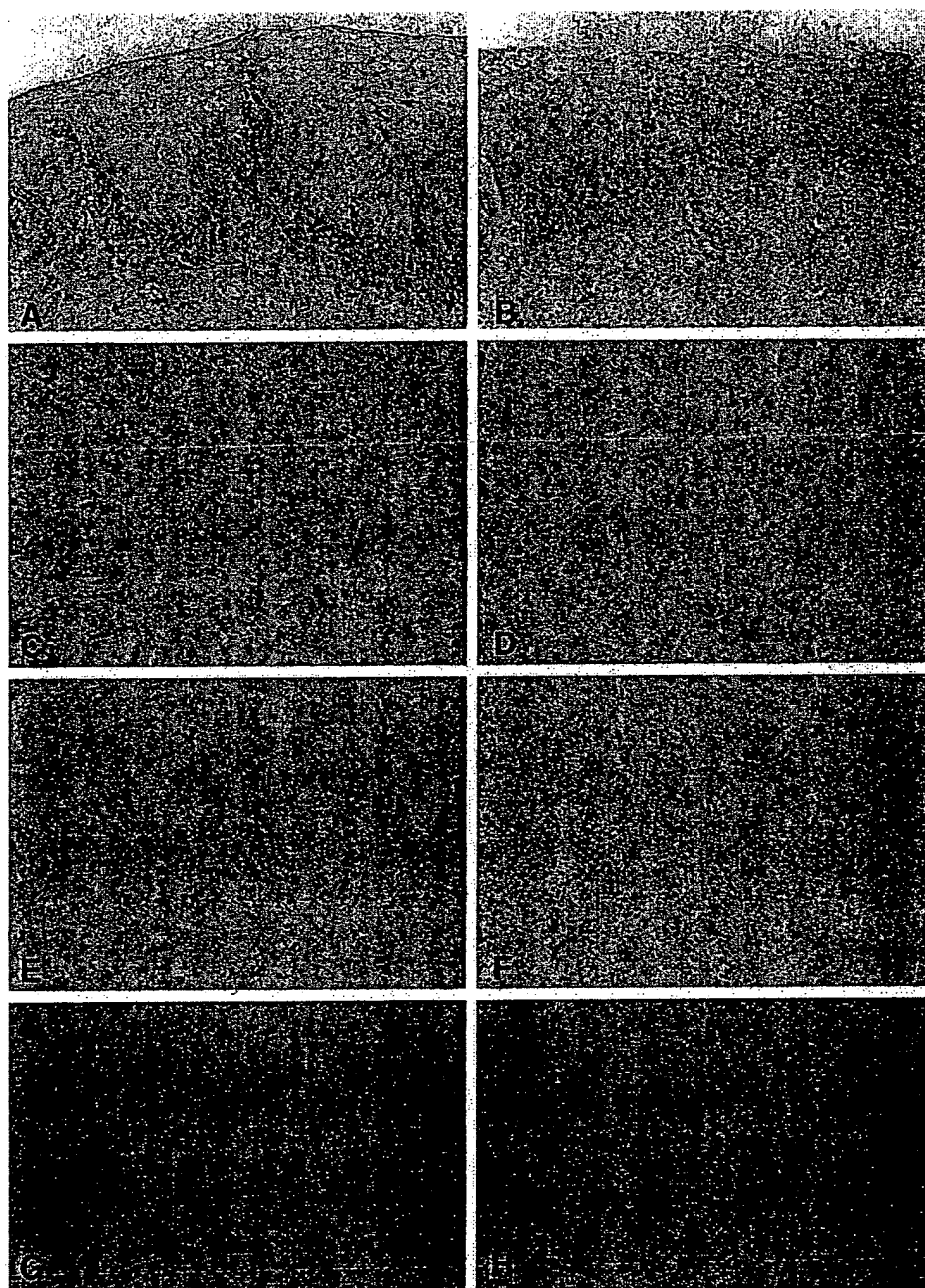
(22). Finally, Ad-*p53* gene therapy may be applied in combination with radiotherapy or chemotherapy because enhanced antitumor activity has been seen in such combination treatment models in preclinical studies (23, 24).

ACKNOWLEDGMENTS

REFERENCES

1. Day, G. L., Blot, R. E., Shore, R. E., McLaughlin, J. K., Austin, D. F., Greenberg, R. S., Liff, J. M., Preston-Martin, S., Sarkar, S., and Schoenberg, J. B. Second cancers following oral and pharyngeal cancers: role of tobacco and alcohol. J. Natl. Cancer Inst., *86:* 131–137, 1994.

2. Vokes, E. E., Weichselbaum, R. R., Lippman, S. M., and Hong, W. K. Head and neck cancer. N. Engl. J. Med., *328:* 184–194, 1993.

3. Brennan, J. A., Mao, L., Hruban, R. H., Boyle, J. O., Eby, Y. J., Koch, W. M., Goodman, S. N., and Sidransky, D. Molecular assessment of histopathologic staging in squamous cell carcinoma of the head and neck. N. Engl. J. Med., *332:* 429–435, 1995.

4. Koch, W. M., Brennan, J. A., Zahurak, M., Goodman, S. N., Westra, W. H., Schwab, D., Yoo, G. H., Lee, D. J., Forastiere, A. A., and Sidransky, D. p53 mutations and locoregional treatment failure in head

and neck squamous cell carcinoma. J. Natl. Cancer Inst., *88:* 1580–1586, 1996.

5. American Cancer Society. American Cancer Society Facts and Figures. Washington, DC: American Cancer Society, 1993.

6. Levine, A. J., Momand, J., and Finlay, C. A. The p53 tumor suppressor gene. Nature (Lond.), *351:* 453–456, 1991.

7. Clayman, G. L., El-Naggar, A. K., Roth, J. A., Zhang, W. W., Goepfert, H., Taylor, D. L., and Liu, T. J. *In vivo* molecular therapy with p53 adenovirus for microscopic residual head and neck squamous carcinoma. Cancer Res., *55:* 1–6, 1995.

8. Liu, T. J., El-Naggar, A. K., McDonnell, T. J., Steck, K. D., Wang, M., Taylor, D. L., and Clayman, G. L. Apoptosis induction mediated by wild-type p53 adenoviral gene transfer in squamous cell carcinoma of the head and neck. Cancer Res., *55:* 3117–3122, 1995.

9. Liu, T. J., Zhang, W. W., Taylor, D. L., Roth, J. A., Goepfert, H., and Clayman, G. L. Growth suppression of human head and neck cancer cells by the introduction of a wild-type *p53* gene via a recombinant adenovirus. Cancer Res., *54:* 3662–3667, 1994.

10. Fujiwara, T., Grimm, E. A., Mukhopadhyay, T., Cai, D. W., Owen-Schaub, L. B., and Roth, J. A. A retroviral wild-type p53 expression vector penetrates human lung spheroids and inhibits growth by inducing apoptosis. Cancer Res., *53:* 4129–4133, 1993.

11. Mercer, W. E., Shields, M. T., Amin, M., Sauve, G. J., Appella, E., Romano, J. W., and Ullrich, S. J. Negative growth regulation in a glioblastoma cell line that conditionally expresses human wild-type p53. Proc. Natl. Acad. Sci. USA, *87:* 6166–6170, 1990.

12. Shaw, P., Bovey, R., Tardy, S., Sahli, R., Sordat, B., and Costa, J. Induction of apoptosis by wild-type p53 in a human colon tumor-derived cell line. Proc. Natl. Acad. Sci. USA, *89:* 4495–4499, 1992.

13. Martinez, J., Georgoff, I., Martinez, J., and Levine, A. J. Cellular localization and cell cycle regulation by a temperature-sensitive p53 protein. Genes Dev., *5:* 151–159, 1991.

14. Diller, L., Kassel, J., Nelson, C. E., Gryka, M. A., Litwak, G., Gebhardt, M., Bressac, B., Ozturk, M., Baker, S. J., Vogelstein, B., and Friend, S. H. p53 functions as a cell cycle control protein in osteosarcomas. Mol. Cell. Biol., *10:* 5772–5781, 1990.

15. Baker, S. J., Markowitz, S., Fearon, E. R., Willson, J. K., and Vogelstein, B. Suppression of human colorectal carcinoma cell growth by wild-type p53. Science (Washington DC), *249:* 912–915, 1990.

16. Yonish-Rouach, E., Resnitzky, D., Lotem, J., Sachs, L., Kimchi, A., and Oren, M. Wild-type p53 induces apoptosis of myeloid leukaemic cells that is inhibited by interleukin-6. Nature (Lond.), *352:* 345–347, 1991.

17. Clayman, G. L., El-Naggar, A. K., Lippman, S. M., Henderson, Y. C., Frederick, M., Merritt, J. A., Zumstein, L. A., Timmons, T. M., Liu, T. J., Ginsberg, L., Roth, J. A., Hong, W. K., Bruso, P., and Goepfert, H. Adenovirus-mediated *p53* gene transfer in patients with advanced recurrent head and neck squamous cell carcinoma. J. Clin. Oncol., *16:* 2221–2232, 1998.

18. Zhang, W. W., Fang, X., Branch, C. D., Mazur, W., French, B. A., and Roth, J. A. Generation and identification of recombinant adenovirus by liposome-mediated transfection and PCR analysis. Biotechniques, *15:* 869–872, 1993.

19. El-Deiry, W. S., Tokino, T., Velculescu, V. E., Levy, D. B., Parsons, R., Trent, J. M., Lin, D., Mercer, W. E., Kinzler, K. W., and Vogelstein, B. WAF1, a potential mediator of p53 tumor suppression. Cell, *75:* 817–825, 1993.

20. Hsu, S. M., Raine, L., and Fanger, H. Use of avidin-biotin-peroxidase complex (ABC) in immunoperoxidase techniques: comparison between ABC and unlabeled antibody (PAP) procedures. J. Histochem. Cytochem., *29:* 577–580, 1981.

21. Schornagel, J. H., Verweij, J., de Mulder, P. H., Cognetti, F., Vermorken, J. B., Cappelaere, P., Armand, J. P., Wildiers, J., de Graeff, A., Clavel, M., Sahmoud, T., Kirkpatrick, A., and Lefebvre, J. L. Randomized Phase III trial of edatrexate *versus* methotrexate in patients with metastatic and/or recurrent squamous cell carcinoma of the head and neck: a European Organization for Research and Treatment of Cancer Head and Neck Cancer Cooperative Group study. J. Clin. Oncol., *13:* 1649–1655, 1995.

22. Boyle, J. O., Hakim, J., Koch, W., van der Riet, P., Hruban, R. H., Roa, R. A., Correo, R., Eby, Y. J., Ruppert, J. M., and Sidransky, D. The incidence of p53 mutation increases with progression of head and neck cancer. Cancer Res., *53:* 4477–4480, 1993.

23. Fujiwara, T., Grimm, E. A., Mukhopadhyay, T., Zhang, W. W., Owen-Schaub, L. B., and Roth, J. A. Induction of chemosensitivity in human lung cancer cells *in vivo* by adenovirus-mediated transfer of the wild-type *p53* gene. Cancer Res., *54:* 2287–2291, 1994.

24. Pirollo, K. F., Hao, Z., Rait, A., Jang, Y. J., Fee, W. E., Ryan, P., Chiang, Y., and Cheng, E. H. p53-mediated sensitization of squamous cell carcinoma of the head and neck to radiotherapy. Oncogene, *14:* 1735–1746, 1997.

Featured Article

Evidence That Transfer of Functional p53 Protein Results in Increased Apoptosis in Prostate Cancer

Louis L. Pisters,[1] Curtis A. Pettaway,[1]
Patricia Troncoso,[3] Timothy J. McDonnell,[2]
L. Clifton Stephens,[4] Christopher G. Wood,[1]
Kim-Anh Do,[5] Shawn M. Brisbay,[2]
Xuemei Wang,[5] Elizabeth A. Hossan,[6]
Robert B. Evans,[1] Cindy Soto,[3]
Marc G. Jacobson,[7] Karen Parker,[9]
James A. Merritt,[9] Mitchell S. Steiner,[8] and
Christopher J. Logothetis[6]

Departments of [1]Urology, [2]Molecular Pathology, [3]Pathology, [4]Veterinary Medicine and Surgery, [5]Biostatistics, [6]Genitourinary Medical Oncology, and [7]Diagnostic Radiology, The University of Texas M. D. Anderson Cancer Center, Houston, Texas; [8]University of Tennessee Department of Urology, Memphis, Tennessee; and [9]Introgen Therapeutics, Inc., Houston, Texas

ABSTRACT

Purpose: INGN 201 (Ad-p53) is a replication-defective adenoviral vector that encodes a wild-type *p53* gene driven by the cytomegalovirus promoter. INGN 201 has been shown to have antitumoral activity against human prostate cancer cell lines. This study was undertaken to determine the safety of INGN 201 in patients with locally advanced prostate cancer, to assess transgene expression, and to evaluate antitumoral activity.

Experimental Design: Our study included patients with clinical stage T3, T1c-T2a with Gleason score 8–10 disease, or T2a-T2b with Gleason score 7 disease and a prostate-specific antigen level >10 ng/mL. INGN 201 was administered by intraprostatic injection under ultrasonographic guidance. One course of INGN 201 was defined as three separate INGN 201 administrations 2 weeks apart. Biopsies at baseline and 24 h after the first administration were assessed for p53 protein by immunohistochemical staining and for apoptosis by terminal deoxynucleotidyl transferase-mediated nick end labeling assay.

Results: A total of 38 courses of INGN 201 gene therapy were administered to 30 patients, of whom 26 underwent radical prostatectomy. There were no grade 3 or 4 adverse events related to INGN 201 administration. Of the 11 patients with negative baseline immunostaining for p53 protein, 10 had positive p53 immunostaining after the first administration of INGN 201, and 8 had an increase in apoptotic cells by terminal deoxynucleotidyl transferase-mediated nick end labeling staining. All 26 of the patients who underwent radical prostatectomy had significant residual viable prostate cancer, and 12 have experienced biochemical failure (median follow-up, 42 months).

Conclusion: Intraprostatic INGN 201 gene therapy is safe and can reliably result in p53 protein production and apoptosis.

INTRODUCTION

Approximately 10% of patients diagnosed with prostate cancer have locally advanced disease and are at high risk of disease progression despite local therapy with radical prostatectomy or radiation therapy. These patients can be accurately identified based on their clinical stage, tumor grade, and initial prostate-specific antigen (PSA) level, but the optimal treatment for this group remains controversial. Because external beam radiation therapy and radical prostatectomy used alone have significant limitations in their ability to eradicate locally advanced prostate cancer, interest has shifted toward the use of multimodality therapy. In the development of multimodality approaches involving radical prostatectomy, to date, there has been no evidence of any improvement in biochemical outcome for patients treated with hormonal therapy plus surgery when compared with surgery alone. Because standard therapies have poor results, we believe that patients with locally advanced prostate cancer are excellent candidates for experimental therapies including gene therapy.

The *p53* gene has been extensively studied and is known to play a critical role in cell cycle regulation and control of apoptosis (1). The p53 protein is a multifunctional protein that can act as a transcriptional activator or repressor, is induced by DNA damage, and interacts with proteins involved in DNA replication and repair (2). The *p53* gene appears to have an important role in sensing and repairing DNA damage, inhibiting the cell cycle to allow DNA repair, and inducing apoptosis to eliminate severely damaged cells (2). Alterations in the *p53* gene play an important role in the progression of human prostate cancer (3). Overexpression of the p53 protein has been shown to be an independent predictor of disease-free and overall survival after surgery (4, 5) or radiation therapy (6, 7) in patients with prostate cancer. Most studies have reported a low frequency (4–20%) of *p53* alterations in primary prostate tumors (8, 9). In contrast, when samples of metastatic tumors are included, particularly samples of bone metastases, the frequency of *p53* alterations increases to 50–79% (10–12). Both Navone *et al.* (13) and Stapleton *et al.* (3) have demonstrated clonal expansion of *p53* mutations from the primary tumor to metastases in paired sam-

ples of primary cancers and metastases from the same patients. Taken together, these results suggest that foci of *p53* mutants in the primary tumor may have a selective advantage and a higher metastatic potential.

An adenoviral vector system was selected for gene therapy because of its ability to infect many cell types, including quiescent and dividing cells, without integration into the host genome, because of its high-level transient expression and capacity to be produced at high titers, and because of the reported safety of adenoviral vaccines (14). INGN 201 (Ad-p53) is a replication-impaired adenoviral vector that encodes a wild-type *p53* gene driven by the cytomegalovirus promoter. Preclinical studies with INGN 201 have shown that *p53* transduction can induce apoptosis and decrease cell proliferation in a number of cancer cell lines without adversely affecting normal cells (15–17). Importantly, *p53* gene therapy is active against cancer cells expressing wild-type or mutated *p53* (18, 19). INGN 201 reduces tumor growth in xenograft models of prostate cancer and other malignancies (20–24). In model systems, INGN 201 has also been shown to enhance the antitumoral activity of chemotherapy and radiation therapy (24–26).

This study was undertaken to determine the safety of INGN 201 in patients with locally advanced prostate cancer, to evaluate transgene expression, and to assess antitumoral activity. The feasibility of direct intraprostatic injections of INGN 201 was investigated in patients with locally advanced prostate cancer in a neoadjuvant setting before radical prostatectomy.

PATIENTS AND METHODS

Protocol Approval. The protocol used in our study was approved by the Biosafety Committees and the Surveillance Committees/Institutional Review Boards of the participating institutions, the Recombinant DNA Advisory Committee of the NIH, and the United States Food and Drug Administration. Written informed consent was obtained from all of the patients stating that they were aware of the investigational nature of this study, in keeping with institutional policies.

Gene Transfer Vector. INGN 201 (Adyexin) was supplied by Introgen Therapeutics, Inc. (Houston, TX) in frozen aliquots containing 1×10^{12} viral particles per ml in PBS containing 10% glycerol. Construction and generation of the vector was reported previously (27).

Eligibility Criteria and Treatment Protocol. The study was limited to patients with histologically confirmed prostate adenocarcinoma and no clinical evidence of metastasis (negative bone scan and computed tomography of the pelvis). Patients were eligible for inclusion in the study if their cancers were clinically staged as T3, T1c-T2a with Gleason score 8–10 disease, or T2a-b with Gleason score 7 disease and a PSA level >10 ng/ml. Patients with these inclusion criteria are unlikely to be cured with surgery alone. Patients were required to have a surgically resectable prostate and a 10-year life expectancy. No prior therapy for prostate cancer was allowed. Because INGN 201 has been shown to have antitumoral activity in cancer cells expressing wild-type *p53*, study participants were not required to have evidence of p53 protein overexpression in pretreatment tumor biopsy samples.

All of the patients had measurable lesions on baseline transrectal ultrasonography (TRUS) or magnetic resonance imaging (MRI) before treatment, and underwent repeat TRUS and MRI after each course of INGN 201 gene therapy. Lesions seen on TRUS or MRI were only considered positive if they corresponded to a region of the prostate shown to have cancer on biopsy. One course of INGN 201 therapy was defined as three separate INGN 201 administrations 2 weeks apart. Patients who demonstrated a clinical response to INGN 201 ($\geq 25\%$ reduction in volume of visible lesions on TRUS or MRI) after one course were treated with additional courses of INGN 201. We estimated tumor volumes by calculating the product of the perpendicular diameters of the indicator lesion seen on TRUS or MRI. Patients could receive up to three courses of INGN 201 before radical prostatectomy. Each administration of INGN 201 consisted of injecting 3 ml of INGN 201 divided equally among five to six transperineal percutaneous injection sites. The INGN 201 administrations were performed under transrectal ultrasonographic guidance with the patient under monitored sedation. At each injection site, the needle was inserted to the base of the prostate, and INGN 201 was injected as the needle was withdrawn toward the apex of the prostate. The goal was to encompass the entire prostate with INGN 201. All of the patients underwent prostate biopsies 1 day after the first administration of INGN 201 to assess gene transfer. The doses of INGN 201 were escalated between patient groups from 3×10^{10} viral particles to 3×10^{12} viral particles, with escalations in one half or one log increments. Between 3 and 18 patients were assigned to each dose level. All 30 of the patients in the study received INGN 201, and 26 of 30 patients underwent radical prostatectomy 2 weeks after the final course of INGN 201. The toxic effects of therapy were evaluated according to National Cancer Institute toxicity criteria (28).

Patients were followed postoperatively at 3-month intervals with serial PSA determinations. No additional therapy was given until evidence of biochemical failure, defined as any detectable PSA level after radical prostatectomy or as two serial rises in PSA level in a patient who did not undergo radical prostatectomy.

Tissue Samples for Analysis of Gene Expression and Apoptosis. Patients were selected for inclusion in immunohistochemical analyses and terminal deoxynucleotidyl transferase-mediated nick end labeling (TUNEL) assays by review of biopsy samples obtained before treatment and 24 h after the first administration of INGN 201. If sufficient tumor cells were appreciated in the same geographical area in both sets of samples from a patient, the samples were earmarked for analysis.

Immunohistochemistry. To determine p53 protein status, tissue sections were immunostained using p53 antibody D07 (Dako) as the primary antibody. Tissue preparation has been described previously (12). A biotinylated Universal Secondary Antibody (Dako) was applied followed by horseradish peroxidase-labeled streptavidin (Dako; K0690). Events were visualized using 3,3'-diaminobenzidine substrate (Dako; K3466). A specimen was scored as positive if at least 5% of the tumor cells showed nuclear staining.

TUNEL Assay for DNA Fragmentation. To assess apoptosis, tissue sections for TUNEL analysis were processed as described previously (29). The apoptotic index was determined by scoring the TUNEL-positive tumor cells and expressing the

Table 1 Clinical characteristics of 30 patients with prostate cancer

Characteristic	No. of patients
Age	
Median (yrs)	62.9
Range (yrs)	52–74
Clinical T stage	
T1c	0
T2a	17
T2b	2
T3a	6
T3b	5
Gleason score	
6	1
7	16
8	9
9	3
10	1
Pretherapy serum prostate-specific antigen level	
0–4.0 ng/ml	2
4.1–10.0 ng/ml	10
10.1–20.0 ng/ml	9
>20.0 ng/ml	9

value as a percentage of 500 tumor cells in the tissue section. The immunohistochemistry and TUNEL sections were each coded and read by a single observer who had no knowledge of the patients, biopsy sequence, or clinical status.

RESULTS

Patient and Tumor Characteristics. Thirty patients were enrolled in the study, and their clinical characteristics are summarized in Table 1. A total of 38 courses (114 separate administrations) of INGN 201 gene therapy were administered to these 30 patients (1 course in 23 patients, 2 courses in 6

patients, and 3 courses in 1 patient). The median follow-up was 19 months. Twenty-six patients underwent a radical prostatectomy after the final course of INGN 201; in 3 patients, the planned radical prostatectomy was aborted because of intraoperative findings of nodal metastasis, and 1 patient withdrew consent before surgery.

Assessment of Gene Transfer and Apoptosis. Prostate samples of 19 patients were suitable for immunohistochemical analysis and TUNEL assay (Table 2). Positive immunostaining for p53 in the untreated samples presumably reflects cells with mutant p53, whereas negative samples are assumed to express wild-type p53. Of the 11 patients with negative baseline immunostaining for the p53 protein, 10 had positive p53 immunostaining after the first administration of INGN 201, and 8 had an increase in TUNEL staining. In total, 16 of the 19 patients had positive immunostaining for the p53 protein 24 h after the first administration of INGN 201, and 12 patients had increased TUNEL staining. Representative samples are shown in Fig. 1. The mean pretreatment apoptotic index was 0.39 with a SD of 0.25. The mean post-treatment apoptotic index was 1.18 with a SD of 1.25. A one-sided Wilcoxon signed-rank test showed that the post-treatment apoptotic index was significantly higher than the baseline apoptotic index ($P = 0.002$; Fig. 2).

Clinical Results. Serum PSA measurements before and after INGN 201 administration were available in 28 patients. There was no significant change between the baseline and post-INGN 201 gene therapy serum PSA ($P = 0.65$, Wilcoxon rank-sum test). The pathological findings in the 29 patients who underwent pelvic lymph node dissection and 26 patients who underwent radical prostatectomy are summarized in Table 3. All 26 of the patients who underwent radical prostatectomy had significant residual viable prostate cancer. We observed a moderate to intense inflammatory cell infiltrate in 14 of the radical

Table 2 Assessment of gene transfer and apoptosis in biopsy samples before and after first treatment with INGN 201

		Pretherapy			p53 Immunostaining		Apoptotic Index	
Patient	Clinical stage	Gleason score	Serum PSA[a] ng/ml	Viral dose VP	Baseline	Post-treatment	Baseline	Post-treatment
5	T2a	7	11.9	1×10^{11}	−	+	0.2	1.4[b]
8	T3a	7	4.4	3×10^{11}	+	−	0.4	0.4
9	T2a	7	17.7	3×10^{11}	−	+	0.2	0.6[b]
11	T3b	8	63.8	1×10^{12}	−	+	0.2	0.4
14	T3b	7	4.2	3×10^{12}	−	+	0.4	0.8[b]
16	T2a	8	22.5	3×10^{12}	−	−	0.0	0.0
17	T2a	7	45.7	3×10^{12}	−	+	0.4	3.6[b]
18	T2b	7	21.8	3×10^{12}	+	−	0.6	0.6
19	T2a	10	6.2	3×10^{12}	−	+	0.4	1.6[b]
20	T3a	9	4.2	3×10^{12}	−	±	0.2	2.8[b]
21	T2a	9	13.0	3×10^{12}	+	+	0.8	0.4
22	T3a	7	4.4	3×10^{11}	+	−	0.4	0.4
23	T3b	7	15.5	3×10^{12}	+	+	0.4	0.8[b]
24	T3a	7	17.9	3×10^{12}	−	+	1.0	0.6
25	T3b	8	3.2	3×10^{12}	+	+	0.4	0.8[b]
26	T2a	8	5.7	3×10^{12}	+	+	0.4	1.2[b]
27	T3b	9	7.7	3×10^{12}	−	+	0.2	0.2
28	T2a	7	22.4	3×10^{12}	+	+	0.4	0.4
29								
30	T2a	8	5.7	3×10^{12}	+	+	0.6	1.2[b]

[a] PSA, prostate-specific antigen; VP, viral particles; [b] Posttreatment apoptotic index above 95% confidence interval of pretreatment apoptotic index.
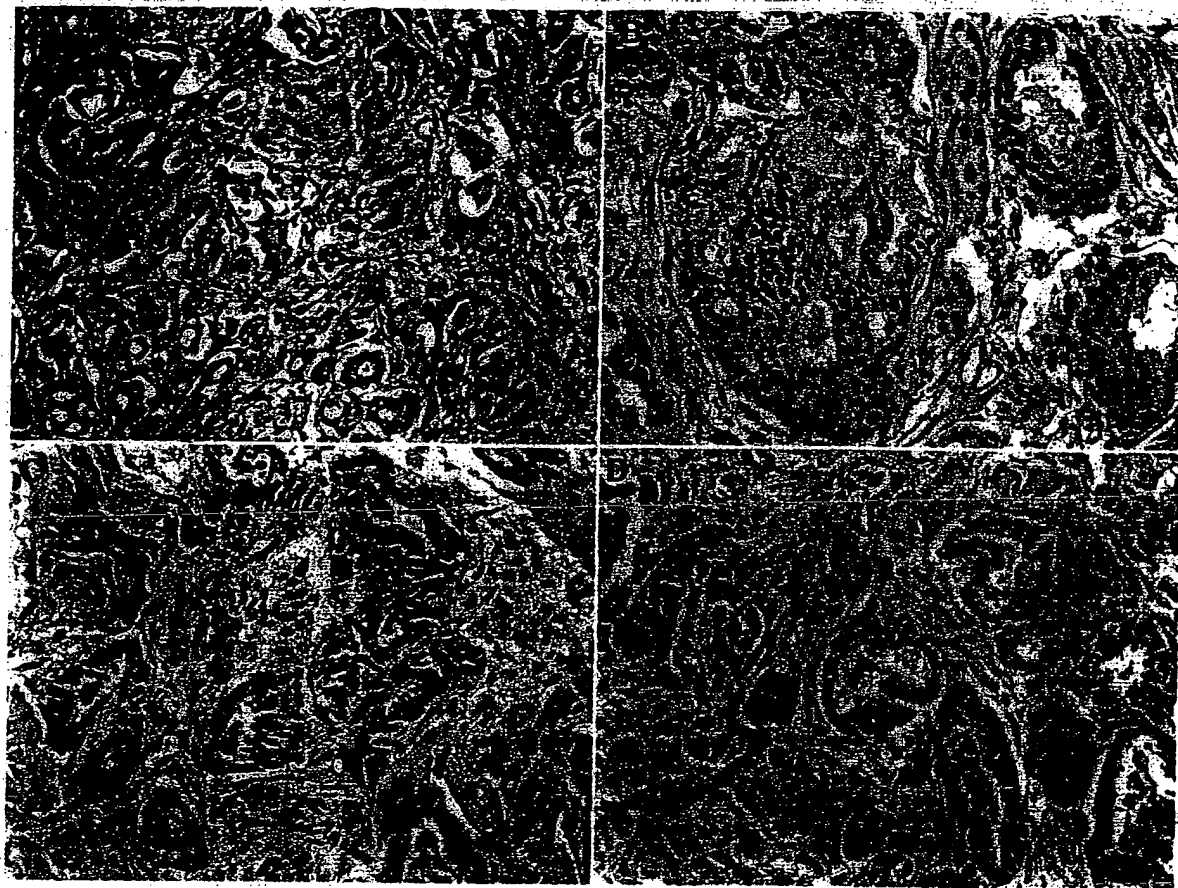
Fig. 1 Immunohistochemical staining for p53 protein and terminal deoxynucleotidyl transferase-mediated nick end labeling (TUNEL) staining for apoptotic cells before and 24 h after first administration of INGN 201. A, negative baseline p53 immunostaining. B, positive immunostaining for p53 protein after INGN 201 administration. C, baseline TUNEL assay. D, TUNEL assay showing increased apoptosis after INGN 201 administration.

prostatectomy specimens, consistent with other reports of immune-mediated responses after adenovirus treatment (30). There was no clear relationship between the degree or extent of inflammation and the viral dose or number of courses of gene therapy. Of the 26 patients who underwent radical prostatectomy, 12 have experienced biochemical failure with a median follow-up of 42 months. The biochemical disease-free survival for the 26 patients undergoing radical prostatectomy is shown in Fig. 3. Of the 4 patients who did not undergo radical prostatectomy, 1 has had a rising PSA level, and the other 3 were lost to follow-up.

Adverse Events. All 30 of the patients who underwent INGN 201 gene therapy were evaluable for adverse events (Table 4). There were no treatment-related or disease-related deaths during the study period. Fever, headache, chills, and perineal pain at the injection site were the most common adverse events of INGN 201 administration. The fever was generally self-limiting and easily treated with acetaminophen. No grade 3 or 4 adverse events were noted.

The 26 patients who underwent radical prostatectomy did not experience any unusual surgical complications. No patient developed a wound infection, seroma, or lymphocele. One patient (4%) had a rectal injury that was closed primarily without sequelae, 1 patient (4%) had a transient urine leak postoperatively, and 5 patients (19%) had long-term stress urinary incontinence requiring pad use.

DISCUSSION

There is mounting evidence of the importance of the *p53* gene in the progression of human prostate cancer. On the basis of preclinical evidence of the antitumor activity of INGN 201 in human prostate cancer models containing wild-type or mutated *p53*, we opted to evaluate this treatment in a neoadjuvant setting before radical prostatectomy in patients with locally advanced prostate cancer.

One important finding of our study was that multiple doses of INGN 201 could be safely administered by intraprostatic injection. Our study was a dose-escalation study, and because of the lack of serious adverse events, we were able to rapidly increase to the highest dose level allowed by our protocol, 3 × 10^{12} viral particles. No grade 3 or 4 adverse events related to INGN 201 administration were seen. The most common grade 1 and 2 adverse events were fever, headache, chills, and perineal pain at the injection site; the fever was treated with acetaminophen and resolved within 24–48 h in most cases. Similarly,

Fig. 2 Actual baseline and post-treatment apoptotic indices in 19 patients undergoing INGN 201 gene therapy. $P = 0.002$, Wilcoxon signed rank test.
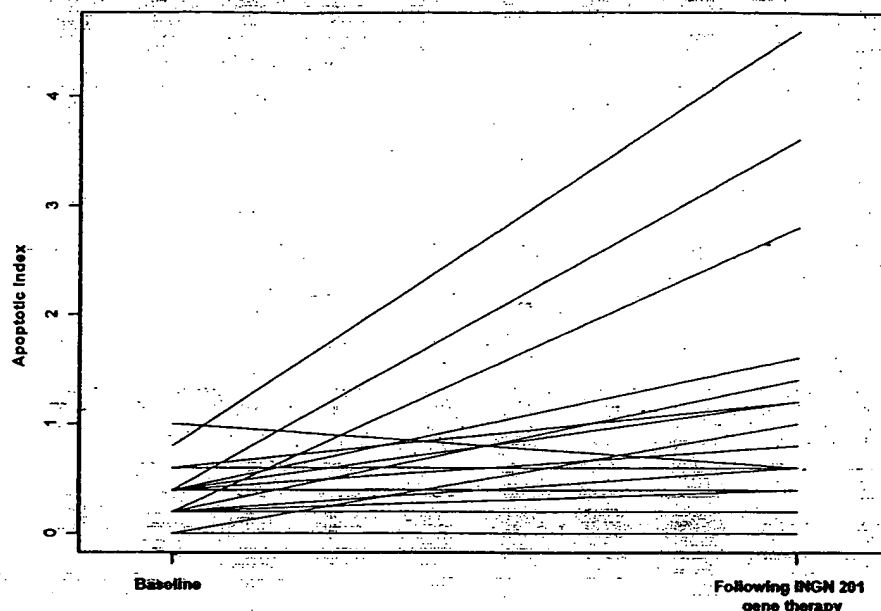
pain at the injection site and fever were the most common adverse events reported by Clayman *et al.* (31) and Swisher *et al.* (32) with INGN 201 injection into head and neck cancers and lung cancers, respectively. Due to the lack of serious adverse events, most of our patients were treated on an outpatient basis. The minimal adverse effects of INGN 201 may allow it to be used in combination with conventional treatments such as radiation therapy or hormonal therapy.

In our study, we evaluated p53 gene expression and the desired biological effect of apoptosis by comparing p53 immunostaining and TUNEL results in prostate needle biopsies before and 24 h after INGN 201 administration. Prostate biopsy tissue is sparse, and we attempted to reduce the potential influence of sampling error by limiting our analysis to samples of histologically similar tumor obtained from the same location of the prostate. Despite these efforts, sampling error remains a potential limitation of our report. The clearest evidence for successful INGN 201 gene expression was seen among the 11 patients with negative baseline immunostaining for the p53 protein. Ten of these patients had positive p53 immunostaining after the first administration of INGN 201, and 8 had an increase in TUNEL staining of cancer cells. We opted to perform biopsies 24 h after the first INGN 201 administration to make the procedure con-

Table 3 Pathologic findings for 29 patients who underwent pelvic lymph node dissection and 26 patients who underwent radical prostatectomy

Pathologic finding	No. of patients	%
Organ-confined	9/26	35
Extraprostatic extension	16/26	62
Seminal vesicle invasion	11/26	42
Bladder neck and/or rectal invasion	0/26	0
Positive lymph nodes	13/29	45
Positive surgical margin	5/26	19

venient for patients and to retrieve tissue samples at a time when gene expression should be high. Data in preclinical models, including *in vivo* models, indicate that apoptosis is induced 24 h after administration of INGN 201 at a level far beyond that seen with a control adenoviral vector (23, 24). Detection of gene expression *in vivo* after completion of INGN 201 gene therapy may be difficult because successful transfer and expression of wild-type *p53* in a tumor may result in rapid apoptosis and cell death. One limitation of our study is that we did not use an empty control vector; therefore, we cannot exclude that the viral infection *per se* or the injection procedure itself, was responsible for this increased apoptosis. We believe that our TUNEL assay findings indicate that proapoptotic pathways are present in locally advanced prostate cancer and are a therapeutically exploitable target.

Our study is, to our knowledge, the first to involve targeted gene therapy to an organ followed by surgical extirpation. Radical prostatectomy in our patients was performed 2 weeks after the last administration of INGN 201, at a time when gene expression is known to be reduced and pathological evidence of antitumoral activity should be optimally detectable. All of the patients had significant residual areas of viable carcinoma, and no areas of widespread cell destruction were noted. Thus, INGN 201 gene therapy alone is insufficient to eradicate locally advanced prostate cancer (at least by this schedule of administration), and this therapy may have greater antitumoral activity when used in combination with other proapoptotic treatments, such as systemic chemotherapy, hormonal therapy, or radiation therapy. Preclinical studies suggest synergistic activity between INGN 201 and systemic chemotherapy (25), and INGN 201 and radiation therapy (24, 26) *in vitro*. In the study by Cowen *et al.* (24), prostate tumor growth *in vivo* was inhibited supra-additively when $p53^{null}$ and $p53^{wild-type}$ tumors were treated with INGN 201 and 5 Gy radiation.
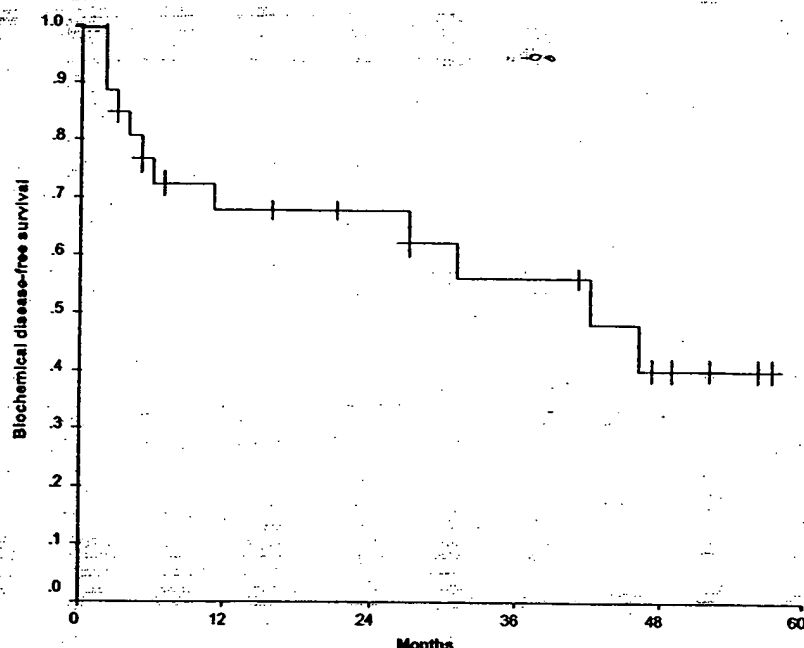
Fig. 3 Biochemical disease-free survival for 26 patients undergoing radical prostatectomy after INGN 201 gene therapy. Biochemical failure was defined as any detectable prostate-specific antigen level after radical prostatectomy. Downward ticks represent censored patients.

The biochemical disease-free survival of patients treated with INGN 201 and radical prostatectomy is similar to the biochemical disease-free survival of similar staged locally advanced patients treated with systemic chemotherapy followed by radical prostatectomy (33). It is conceivable that the biochemical results of patients treated with INGN 201 in a preoperative setting might improve if INGN 201 was used in combination with other proapoptotic stimuli such as hormonal therapy or systemic chemotherapy.

The main treatments for prostate cancer, surgery, radiation therapy, and hormonal therapy, have been around for well over 50 years, and there is a desperate need for new therapeutic strategies. Prostate-targeted gene therapy offers hope, with a variety of biological mechanisms that might be exploited. In our study, we demonstrated that INGN 201 can be safely administered by intraprostatic injection and that intraprostatic injection of INGN 201 reliably results in p53 protein production and apoptosis. Our findings indicate that the molecular pathways for apoptosis are present in locally advanced prostate cancer and can be therapeutically exploited using gene therapy. Furthermore, INGN 201 activity may be enhanced, to fully exploit proapoptotic pathways,

when combined with radiation therapy, hormonal therapy, or systemic chemotherapy.

REFERENCES

1. Kastan MB, Canman CE, Leonard CJ. p53, cell cycle control and apoptosis: implications for cancer. Cancer Metastasis Rev 1995; 14:3–15.

2. Hansen R, Oren M. p53: from inductive signal to cellular effect. Curr Opin Genet Dev 1997;7:46–51.

3. Stapleton AM, Timme TL, Gousse AE, et al. Primary human prostate cancer cells harboring p53 mutations are clonally expanded in metastases. Clin Cancer Res 1997;3:1389–97.

4. Bauer JJ, Sesterhenn IA, Mostofi FK, McLeod DG, Srivastava S, Moul JW. Elevated levels of apoptosis regulator proteins p53 and bcl-2 are independent prognostic biomarkers in surgically treated clinically localized prostate cancer. J Urol 1996;156:1511–6.

5. Theodorescu D, Broder SR, Boyd JC, Mills SE, Frierson HF Jr. p53, bcl-2 and retinoblastoma proteins as long-term prognostic markers in localized carcinoma of the prostate. J Urol 1997;158:131–7.

6. Scherr DS, Vaughan ED Jr, Wei J, et al. bcl-2 and p53 expression in clinically localized prostate cancer predicts response to external beam radiotherapy. J Urol 1999;162:12–6.

7. Grignon DJ, Caplan R, Sarkar FH, et al. p53 status and prognosis of locally advanced prostatic adenocarcinoma: a study based on RTOG 8610. J Natl Cancer Inst 1997;89:158–65.

8. Hall MC, Navone NM, Troncoso P, et al. Frequency and characterization of p53 mutations in clinically localized prostate cancer. Urology 1995;45:470–5.

9. Visakorpi T, Kallioniemi OP, Keikkinen A, Koivula T, Isola J. Small subgroup of aggressive, highly proliferative prostatic carcinomas defined by p53 accumulation. J Natl Cancer Inst 1992;84:883–7.

10. Heidenberg HB, Sesterhenn IA, Gaddipati JP, et al. Alteration of the tumor suppressor gene p53 in a high fraction of hormone refractory prostate cancer. J Urol 1995;154:414–21.

11. Navone NM, Troncoso P, Pisters LL, et al. p53 protein accumulation and gene mutation in the progression of human prostate carcinoma. J Natl Cancer Inst 1993;85:1657–69.

Table 4 Total number of adverse events in 30 patients after 38 courses of intraprostatic INGN 201 administration.

Event	Grade 1	Grade 2	Grade 3	Grade 4	Total
Perineal pain	10	5	0	0	15
Fever	40	4	0	0	44
Chills	14	2	0	0	16
Headache	15	3	0	0	18
Hematospermia	4	0	0	0	4
Hematuria	3	1	0	0	4
Scrotal edema	0	2	0	0	2

12. McDonnell TJ, Navone NM, Troncoso P, et al. Expression of bcl-2 oncoprotein and p53 protein accumulation in bone marrow metastases of androgen-independent prostate cancer. J Urol 1997;157:569–74.

13. Navone NM, Labate ME, Troncoso P, et al. p53 mutations in prostate cancer bone metastases suggest that selected p53 mutants in the primary site define foci with metastatic potential. J Urol 1999;161:304–8.

14. Horwitz MS. Adenoviruses. In: Fields BN, Knipe DM, Howley PM, and Chanock RM, editors. Fields Virology, 3rd Edition. Philadelphia, PA: Lippincott-Raven, 1996. p. 2146–71.

15. Chen PL, Chen YM, Bookstein R, Lee WH. Genetic mechanisms of tumor suppression by the human p53 gene. Science 1990;250:1576–80.

16. Yonish-Rouach E, Resnitzky D, Lotem J, Sachs L, Kimchi A, Oren M. Wild-type p53 induces apoptosis of myeloid leukemic cells that is inhibited by interleukin-6. Nature 1991;352:345–7.

17. Liu TJ, Zhang WW, Taylor DL, Roth JA, Goepfert H, Clayman GL. Growth suppression of human head and neck cancer cells by the introduction of a wild-type p53 gene via a recombinant adenovirus. Cancer Res 1994;54:3662–7.

18. Schumacher G, Bruckheimer EM, Beham AW, et al. Molecular determinants of cell death induction following adenoviral-mediated gene transfer of wild-type p53 in prostate cancer cells. Int J Cancer 2001;91:159–66.

19. Yang C, Cirielli C, Capogrossi MC, Passaniti A. Adenovirus-mediated wild-type p53 expression induces apoptosis and suppresses tumorigenesis of prostatic tumor cells. Cancer Res 1995;55:4210–3.

20. Ko SC, Gotoh A, Thalmann GN, et al. Molecular therapy with recombinant p53 adenovirus in an androgen-independent, metastatic human prostate cancer model. Hum Gene Ther 1996;7:1683–91.

21. Eastman JA, Hall SJ, Sehgal I, et al. In vivo gene therapy with p53 or p21 adenovirus for prostate cancer. Cancer Res 1995;55:5151–5.

22. Nielsen LL, Dell J, Maxwell E, Armstrong L, Maneval D, Catino JJ. Efficacy of p53 adenovirus-mediated gene therapy against human breast cancer xenografts. Cancer Gene Ther 1997;4:129–38.

23. Spitz FR, Nguyen D, Skibber JM, Cusack J, Roth JA, Christiano RJ. In vivo adenovirus-mediated p53 tumor suppressor gene therapy for colorectal cancer. Anticancer Res 1996;16:3415–22.

24. Cowen D, Salem N, Ashoori F, et al. Prostate cancer radiosensitization in vivo with adenovirus-mediated p53 gene therapy. Clin Can Res 2000;6:4402–8.

25. Fujiwara T, Grimm EA, Mukhopadhyay T, Zhang WW, Owen-Schaub LB, Roth JA. Induction of chemosensitivity in human lung cancer cells in vivo by adenovirus-mediated transfer of the wild-type p53 gene. Cancer Res 1994;54:2287–91.

26. Spitz FR, Nguyen D, Skibber JM, Meyn RE, Christiano RJ, Roth JA. Adenoviral-mediated wild-type p53 gene expression sensitizes colorectal cancer cells to ionizing radiation. Clin Cancer Res 1996;2:1665–71.

27. Zhang WW, Fang X, Branch CD, Mazur W, French BA, Roth JA. Generation and identification of recombinant adenovirus by liposome-mediated transfection and PCR analysis. Biotechniques 1993;15:868–72.

28. Ajani JA, Welch SR, Raber MN, Fields WS, Krakoff IH. Comprehensive criteria for assessing therapy-induced toxicity. Cancer Invest 1990;8:147–59.

29. Buckheimer EM, Brisbay S, Johnson DJ, Gingrich J, Greenberg N, McDonnell TJ. Bcl-2 accelerates multistep prostate carcinogenesis in vivo. Oncogene 2000;19:5251–8.

30. Dai Y, Schwarz EM, Gu D, Zhang W, Sarvetnick N, Verma IM. Cellular and humoral immune responses to adenoviral vectors containing factor IX gene: tolerization of factor IX and vector antigens allows for long-term expression. Proc Natl Acad Sci USA 1995;92:1401–5.

31. Clayman GL, El-Nagger AK, Lippman SM, et al. Adenovirus-mediated p53 gene transfer in patients with advanced recurrent head and neck squamous cell carcinoma. J Clin Oncol 1998;16:2221–32.

32. Swisher SG, Roth JA, Nemunaitis J, et al. Adenovirus-mediated p53 gene transfer in advanced non-small-cell lung cancer. J Natl Cancer Inst 1999;91:763–71.

33. Pettaway CA, Pisters LL, Troncoso P, et al. Neoadjuvant chemotherapy and hormonal therapy followed by radical prostatectomy: feasibility and preliminary results. J Clin Oncol 2000;18:1050–7.

A phase I study of Adp53 (INGN 201; ADVEXIN) for patients with platinum- and paclitaxel-resistant epithelial ovarian cancer

Judith K. Wolf,[a,*] Diane C. Bodurka,[a] Jacalyn B. Gano,[a] Michael Deavers,[b] Lois Ramondetta,[a] Pedro T. Ramirez,[a] Charles Levenback,[a] and David M. Gershenson[a]

[a] The Department of Gynecologic Oncology, The University of Texas M. D. Anderson Cancer Center, Houston, TX 77030, USA
[b] The Department of Pathology, The University of Texas M. D. Anderson Cancer Center, Houston, TX 77030, USA

Abstract

Purpose. Adenoviral p53 (Adp53) is a replication-deficient adenovirus containing human p53 cDNA. This phase I study was designed as a toxicity study of multiple dosing of Adp53 administered by intraperitoneal (IP) delivery to patients with ovarian cancer.

Experimental Design. Eligibility criteria included patients with platinum- and paclitaxel-resistant metastatic epithelial ovarian cancer; a Zubrod performance status of 0, 1, or 2; and adequate bone marrow, liver, and renal function. Patients underwent laparoscopy, washings, biopsies, and placement of an IP catheter within 10 days of Adp53 administration. Adp53 was given daily for 5 days every 3 weeks at one of the following four dose levels: 3×10^{10}, 3×10^{11}, 1×10^{12}, or 3×10^{12} viral particles (vp).

Results. Seventeen patients were enrolled in the trial. Fifteen (88%) patients are evaluable for toxicity. The mean age of the study group was 51 years (range 32–67). All but one patient received two or more chemotherapy regimens before study entry. No dose-limiting toxicities (DLT) were observed. Grade 3 toxicities included fatigue (six patients), fever (two patients), chills (one patient), abdominal pain (three patients), nausea (two patients), and sinus congestion (one patient). One patient had Grade 3 edema and headache. There were no hematologic toxicities. Eleven patients (65%) are evaluable for response. Two of 17 patients (12%) had a mixed response. Four patients (24%) had stable disease for up to four courses. Five patients (29%) had progressive disease after one to two courses.

Conclusions. Multiple dosing of IP Adp53 was well tolerated in this group of heavily pretreated patients; however, the dosing schedule and the amount cannot be concluded from this study. With a negative randomized trial of ovarian cancer in front-line treatment that included an adenovirus p53 plus chemotherapy, we feel that further refinement of gene therapy is required before additional trials are undertaken.

Overview summary. Ovarian cancer is the most lethal of the gynecologic malignancies. It also tends to recur and progress within the abdominal cavity. Because of this, regional intraperitoneal therapy for ovarian cancer is attractive.

Mutation and/or deletion of the p53 gene are common in advanced ovarian cancer. In this study, we have tested the safety and practicality of using an adenovirus-mediated delivery of the p53 gene to patients with chemo-refractory ovarian cancer via an intraperitoneal catheter.

Fifteen patients were treated. Common toxicities were abdominal pain, fever, and chills. Several patients also had catheter infections. One patient had prolonged decrease in CA125 and stable disease.

The best mechanism of delivery of gene therapy for patients is unclear, however, no severe toxicities were found using an adenovirus-mediated p53 gene in this group heavily pretreated patients with recurrent ovarian cancer.

Introduction

Ovarian cancer is the leading cause of gynecologic cancer deaths in the United States, with approximately 25,400 new cases and 14,300 deaths predicted for 2003 [1]. Seventy-five to 80% of patients present with advanced-stage disease, wherein the survival rate is only 15% to 20%. Patients who undergo an optimal tumor-reductive surgery at pre-

* Corresponding author. Department of Gynecologic Oncology, The University of Texas M. D. Anderson Cancer Center, 1515 Holcombe Boulevard., Box 440, Houston, TX 77030. Fax: +1-713-792-7586.
E-mail address: jwolf@mdanderson.org (J.K. Wolf).

sentation have an increased disease-free interval, but most eventually die of disease [2]. Approximately 70% to 80% of patients with advanced-stage disease respond to initial treatment with platinum-based chemotherapy [3]. Unfortunately, the majority of patients will relapse or their tumors will progress within 2 years of treatment. Patients who have a complete pathologic response to chemotherapy, as determined by second-look surgery, have up to a 50% risk of recurrence [4]. The use of chemotherapy drugs given either intravenously or intraperitoneally has only minimally changed survival over the past 15 to 20 years. Novel means of treating residual or recurrent disease in the peritoneal cavity may improve long-term survival.

One of the major issues facing investigators is the optimal treatment of patients with platinum- and paclitaxel-refractory ovarian cancer. We are investigating molecular mechanisms that may influence the growth and progression of epithelial ovarian cancers. Our goal is the development of therapeutic agents that are designed to correct defects at the molecular level and ultimately provide innovative treatment options for patients who do not respond to standard therapies.

The *p53* tumor suppressor gene is the most frequently mutated gene in human cancers, and *p53* abnormalities are found in approximately 30% to 79% of malignant ovarian tumors [5,6]. *p53* is a multifunctional protein that, among other functions, acts as a transcriptional activator and repressor, is induced by DNA damage and interacts with other proteins involved in DNA replication and repair [7,8]. *p53* has a vital role in sensing and initiating repair of DNA damage by inhibiting the cell cycle to allow DNA repair or inducing apoptosis to eliminate severely damaged cells [8].

Several reports have demonstrated that growth of human cancer cell lines, including cervical [9], colon [10], lung [11], squamous carcinomas of the head and neck [12], and ovarian [13–15], can be suppressed by reintroduction of the wild-type *p53* gene. This can be accomplished by DNA transfection or by retroviral- or adenoviral-mediated transfer of the wild-type *p53* gene. The adenovirus vector system was chosen for gene therapy because it can infect many cell types, both dividing and nondividing; it does not integrate into the host genome; it has high-level transgene expression; it supports high titer and large-scale manufacture; and the safety of adenovirus vaccines has been established [16–18]. The vector used in gene therapy is composed of the wild-type *p53* gene inserted into a first-generation adenoviral backbone.

Phase I and II clinical trials using an adenovirus vector to transfer *p53* were conducted in patients with lung and head and neck cancer. A phase I trial in ovarian cancer patients using a single dose of Adp53 has also been completed [19]. Our preclinical studies have suggested that multiple dosing of Adp53 may be necessary for maximal effectiveness [20]. The purpose of this study was to evaluate the safety and feasibility of multiple-dose Adp53 by intraperitoneal (IP) injections in patients with ovarian cancer that is resistant to platinum- and paclitaxel-based therapy.

Materials and methods

This study was reviewed and approved by the Institutional Review Board at The University of Texas M. D. Anderson Cancer Center, Houston, TX. Eligible patients were those with histologically confirmed metastatic epithelial ovarian cancer that was both platinum- and paclitaxel-resistant. Resistance was defined as: (1) progression of disease while on a first-line regimen containing a platinum drug or paclitaxel or (2) tumor progression within 6 months of completion of platinum- or paclitaxel-based therapy administered as either first- or second-line treatment. Patients could have failed an unlimited number of prior chemotherapy regimens. Patients with nonmeasurable disease were eligible if they had an elevated CA-125 level. All patients had to have adequate bone marrow, renal and liver function; a Zubrod performance status of 0, 1, or 2; and a life expectancy of more than 12 weeks. Patients with tumors of low malignant potential, previous abdominal or pelvic irradiation, or a positive HIV test were excluded from the study. Informed consent was obtained from all patients before entry onto the study.

Adp53 is a replication-defective adenovirus serotype 5 (Ad5) vector with a *p53* cDNA expression cassette that replaces the E1 region of the virus [21]. Adp53 (INGN 201; ADVEXIN®) was provided by Introgen Therapeutics (Houston, TX)/DCTDC (NCI-CTEP) and stored at −80°C in various concentrations in phosphate-buffered saline (PBS) supplemented with 10% glycerol in the M. D. Anderson Cancer Center pharmacy. Adp53 was thawed and diluted in PBS at 4°C within 2 h of use. Reconstituted Adp53 was then double bagged, packed in ice, and transported to the treatment area in an approved container marked with a biohazard label.

In this study, patients received Adp53 intraperitoneally (IP) for 5 consecutive days every 3 weeks until tumor progression was documented or toxicities precluded further therapy. Before beginning treatment, a history and physical examination, hematology, blood chemistries, coagulation profiles, electrolytes, CA-125 level, and performance status were done. Eligible patients then underwent a laparoscopy to place a Tenckhoff catheter (Lifemed, Rancho Dominquez, CA). During this procedure, an attempt was made to obtain tumor tissue for routine histopathologic examination and to determine *p53* status. Peritoneal adhesions were lysed if feasible. Patients were discharged the same day and were seen in clinic within 24 h to assess their overall condition, catheter patency, signs and/or symptoms of infection, and apply a waterproof dressing.

Patients could begin therapy within 10 days after laparoscopy and placement of the IP catheter. All treatment was given in a negative pressure room in the Gynecologic Oncology outpatient clinic. Only medical and nursing staff that had successfully completed biosafety training were allowed to administer Adp53. All injections were performed using reverse isolation procedures, including the use of a

HEPA-filtered mask during the injection of Adp53 and normal saline flush.

After aspirating any ascites, if present, the reconstituted solution was infused over 5 min in 50 ml of Dulbecco's PBS through the Tenckhoff catheter into the peritoneal cavity. In cycle one only, the first dose (Day 1) Adp53 was followed with 500 ml (or to patient tolerance) of 0.9% normal saline. For subsequent days and cycles, the amount of 0.9% normal saline used to flush the catheter was reduced to 50 ml. Following each dose, the patient was rotated 45° to the left, then to the right, then 30° in Trendelenberg, and then 30° in reverse Trendelenberg. Rotations occurred in 30-min intervals.

Laboratory work (hematology, blood chemistries, coagulation profiles, electrolytes, CA-125 level), physical examinations, Zubrod status, and assessment of toxicity preceded each course of therapy. Additionally, on days 8 and 15 of cycles 1 and 2, patients underwent a brief history and physical examination. Following each dose and before each new course, toxicity data were carefully reviewed and graded according to the National Cancer Institute Common Toxicity Criteria (NCI-CTC, Version 2.0) [22].

Three patients were enrolled at each dose level. Cohort 1 received 3×10^{10} vp daily for 5 days, cohort 2 received 3×10^{11} vp daily for 5 days, cohort 3 received 1×10^{12} vp daily for 5 days, and cohort 4 received 3×10^{12} vp daily for 5 days. Up to 3 additional patients could be added to a dose level if a dose-limiting toxicity (DLT) was observed. A DLT was defined as any grade 4 toxicity attributed to Adp53. The maximum tolerated dose (MTD) was defined as the dose before which no more than two out of six patients experience a dose limiting toxicity after the first treatment with Adp53. The maximum dose level chosen for this study was dependent on virus production capacity.

p53 mutation was not a criteria for entry into the study; however, *p53* sequencing was attempted on biopsies obtained at laparoscopy (sequencing performed by Introgen Therapeutics) or immunohistochemistry for *p53* staining was performed on tumor embedded in paraffin blocks obtained at a prior surgery. Eleven of 13 patients tested stained strongly for *p53* on immunohistochemistry analysis, suggesting *p53* mutations. The indirect immunofluorescence assay was used to detect anti-adenovirus antibodies in samples obtained before and after treatment. The assay is a general procedure for the rapid detection and measurement of antibodies to viral antigens. It employs a two-step procedure. In the first step, the primary serum is applied to the test smears. Antibodies bind to the homologous antigens present and any unbound antibodies are rinsed off. In the second step, the primary antibodies complexed to the antigen are detected with fluorescein-conjugated antiglobulin directed against the primary antibody globulin subclasses. The resultant fluoresceinated complexes can be observed under a fluorescence microscope [23]. In addition, urine, stool, sputum, and ascites or peritoneal washings were obtained on days 1–6, 8, 15, and 22 of the first two cycles and were assessed for viral cytopathic effect (CPE).

To measure disease, the longest diameter in its perpendicular of each lesion was measured in centimeters before beginning of cycle 2 and every third cycle thereafter. All patients were assessed using computed tomography. A complete response (CR) is defined as the disappearance of all evidence of tumor for at least one cycle of therapy. Patients must also have a normal CA-125 level and be free of all symptoms of cancer. A partial response (PR) is defined as a decrease in the products of diameters by 50% or more or a decrease in the CA-125 level of 50% or more compared with the pretreatment value. This response must persist for at least one cycle of therapy. A minor response (MR) is defined as a decrease in a measurable lesion that is too small or too brief to qualify as a partial response. Progressive disease (PD) is any increase of 25% or more in the sum of the products of diameters of measurable lesions or in the estimated size of non-measurable lesions. Any new lesion, or a 100% increase in the CA-125 level, represents progression in this study. Patients with no change (NC) in tumor size were continued on therapy. Response duration was measured from the time the response until progression of disease was documented.

Results

In this phase I study of Adp53, 17 patients were enrolled. The maximum tolerated dose (MTD) was not defined because no dose limiting toxicities (DLT) were observed. Six patients were treated at the 1×10^{12} vp dose level because one patient in that group was never treated and two other patients developed catheter infections during cycle 1 that resulted in their removal from the study.

Patients ranged in age from 32 to 67 years (mean age 51 years); 15 were white, 1 was Hispanic, and 1 was black. Other patient characteristics and their responses to therapy are listed in Table 1.

Of the 17 patients enrolled in the study, 15 were evaluable for toxicity. Two patients were not treated after study enrollment. One patient was found to have a second primary tumor in the urinary bladder before her scheduled laparoscopy and was removed from the study. Another patient was found to have extensive adhesions during surgery. Four intraoperative attempts were made to place the laparoscope. Because the surgeon could not enter the peritoneal cavity, the procedure was aborted.

The grade 2 and 3 toxicities observed in the study group are summarized in Table 2. There were no grade 4 toxicities observed. The grade 3 toxicities included fatigue (6 patients), abdominal pain (3 patients), nausea (2 patients), fever (2 patients), chills (1 patient), headache (1 patient), and sinus congestion (1 patient). One patient (patient 4) had grade 3 edema and headache and is described in more detail later in this report. All other toxic effects were grades 1 or

Table 1
Patient profile

Patient no.	Age	p53 Status	Prior failed therapies	Histology	Courses	Response	vp per injection	Status
1	38	IHC+	surgery, five chemotherapy regimens, hormonal therapy	HG mixed. carcinoma	3	NC	3×10^{10}	DOD
2	57	IHC−	surgery, three chemotherapy regimens, hormonal therapy	HG serous carcinoma	2	PD	3×10^{10}	DOD
3	56	IHC+	surgery, two chemotherapy regimens	HG serous.carcinoma	2	PD	3×10^{10}	DOD
4	51	P53 mutation	surgery, six chemotherapy regimens, hormonal therapy	HG serous carcinoma	3	?	3×10^{11}	DOD
5	54	IHC+	surgery, five chemotherapy regimens	HG serous carcinoma	1	INE	3×10^{11}	DOD
6	57	N/A	surgery, nine chemotherapy regimens	HG serous carcinoma	0	NT	Catheter could not placed	DOD
7	67	IHC+	surgery, four chemotherapy regimens, radiotherapy to ribs	HG serous and undifferentiated carcinoma	30	PR	3×10^{11}	AWD
8	55	N/A	surgery, six chemotherapy regimens, hormonal therapy	HG mixed carcinoma	0	NT	2nd primary found	DOD
9	50	IHC+	surgery, two chemotherapy regimens, hormonal therapy	HG serous carcinoma	1	INE	1×10^{12}	DOD
10	49	TNA	surgery, seven chemotherapy regimens	HG mixed carcinoma	1	PD	1×10^{12}	DOD
11	56	IHC+	surgery, five chemotherapy regimens, hormonal therapy	HG serous carcinoma	1	PD	1×10^{12}	DOD
12	50	IHC+	surgery, one chemotherapy regimen	HG serous carcinoma	3	NC	1×10^{12}	DOD
13	32	IHC+	surgery, five chemotherapy regimens	LG serous carcinoma	4	NC	1×10^{12}	DOD
14	41	IHC+	surgery, five chemotherapy regimens	HG serous carcinoma	4	NC	1×10^{12}	DOD
15	67	IHC+	surgery, one chemotherapy regimen	HG serous carcinoma	2	PD	3×10^{12}	DOD
16	42	IHC+	surgery, two chemotherapy regimens	HG serous carcinoma	1	INE	3×10^{12}	DOD
17	64	TNA	surgery, eight chemotherapy regimens	HG mixed carcinoma	2	PD	3×10^{12}	DOD

Abbreviations: DOD, dead of disease; AWD, alive with disease; vp, viral particles; IHC, immunohistochemistry; TNA, tissue not available for testing; HG, high grade; LG, low grade; N/A, not available, PD, progressive disease; INE, inevaluable; PR, partial response; NC, no change; NT, not treated.

2. There were no hematological toxicities. The flu-like symptoms experienced by some patients (fever, chills, headache, and fatigue) were mitigated with a pretreatment

Table 2
Toxic effects

Toxicity	No. of patients			Comments
	Grade 2	Grade 3	Grade 4	
Abdominal pain	2	3	0	
Allergic reaction	0	1	0	Patient removed from study
Anorexia	3	0	0	
Bone pain	1	0	0	
Chills	7	1	0	
Diaphoresis	2	0	0	
Drug fever	6	2	0	
Dyspnea	1	2	0	
Edema	0	1	0	
Fatigue	4	6	0	
Headache	4	1	0	
Catheter infections	2	2	0	Catheters removed; IV antibiotics given
Infection	1	0	0	Cellulitis around catheter
Myalgia	8	0	0	
Nausea alone	5	2	0	
Pain	1	0	0	
Pruritis	1	0	0	
Sinus congestion	0	1	0	
Sore throat	1	0	0	
Vomiting	2	0	0	

Abbreviations: IV, intravenous.

dose of acetaminophen or non-steroidal anti-inflammatory medication.

In spite of intraoperative antibiotic therapy, the absence of surgical complications and meticulous post-operative care of the catheter insertion site, infections occurred in five patients. Four patients developed catheter infections during the first course of therapy and subsequently were removed from the study. One patient (patient 7) developed a catheter infection after more than 1 year on therapy. In this case, the Tenckhoff catheter was removed and the patient was treated with intravenous antibiotics. After the infection resolved, another IP catheter was placed by interventional radiology and the patient was able to resume therapy. There were no further catheter complications during the remainder of her treatment and she ultimately received a total of 31 courses of therapy.

Tumor tissue was obtained in 13 patients for use in evaluating p53 status. One patient had a p53 mutation as determined by sequencing and 12 patients had p53 over-expression by immunohistochemistry. Tumor tissue was not available for two patients. Pre- and post-treatment anti-adenovirus antibody levels were determined in the 10 patients who received two or more cycles of therapy. All patients had evidence of prior adenovirus exposure, with pretreatment titers ranging from 1:128 to 1:1024. Post-treatment antibody levels taken on day 5 of cycle 1 increased by factors of 4 to 64 times baseline in all but one patient. In those patients with data at cycle 2, antibody

titers continued to increase. One patient whose titer had not increased at the end of cycle 1 demonstrated a 32-fold increase by the end of cycle 2. The patient (#7) on therapy for 31 cycles had a continued increase in antibody titer over the course of therapy. There was no evidence of vector based or CPE analysis of urine, stool, sputum, or ascites/ peritoneal washings collected at all time periods.

Although this was a Phase I study and response was not an endpoint, we did follow CA-125 levels on all patients. Of note, patient #7 who was on therapy for 31 cycles started with a CA125 of 338 U/ml, pre-cycle 2 it rose to 474 U/ml, and then decreased with the low level of 100 U/ml until she was off study when it increased to 329 U/ml. Although most patients had a continued elevation of CA125, there was no clear linear relationship of stability of disease or progression and CA125 levels. This could potentially be due to peritoneal inflammation causing an elevation in the CA125 secondary to the treatment itself.

Eleven patients received two or more cycles of Adp53 and are evaluable for response: six patients (55%) had stable disease after four courses of therapy and five patients (45%) progressed after two courses of therapy. Two patients in the stable disease category require further comment. Patient 7 had a greater than 50% reduction in the CA-125 level with stable retroperitoneal lymphadenopathy. Patient 4 had a 50% reduction in the measurable lesion in her pelvis, stable subcapsular and hepatic cystic areas in the liver, and stable right pleural effusion. Unfortunately, patient 4 developed angioedema just before her 3rd course of treatment and was withdrawn from the study. This condition eventually resolved with intravenous and oral corticosteroid therapy. Interestingly, this patient had a relatively low pretreatment anti-adenovirus titer (1:128) and the highest increase in titer level by the end of cycle 1 (64-fold, 1:8192). By the beginning of cycle 2, her titer level was 1:65,536.

Discussion

Ovarian cancer is the most lethal gynecologic malignancy among women in the United States. Despite high response rates to primary treatment most women eventually die of their disease. Innovative, effective therapies are needed to increase cure rates in this group of patients.

Gene therapy is an attractive modality for the treatment of ovarian cancer because ovarian cancer tends to remain localized in the peritoneal cavity, allowing for regional delivery of the gene of interest. In the laboratory, tumor suppressor genes have been successfully transferred into ovarian cancer cells resulting in the inhibition of cell growth [13–15]. In the present study, the feasibility and safety of giving multiple doses of Adp53 by IP administration to patients with chemo-resistant ovarian cancer was assessed.

No dose limiting toxicities were observed up to 3 × 10^{12} vp per injection. Fever was observed in 11 patients and was the most common toxic effect. Several patients

were withdrawn from the study because of catheter infections, which unfortunately remains a significant problem of IP therapy. The infection rate in this study (24%) is higher compared with other studies using intraperitoneal delivery of chemotherapy [24,25]. Infection rates may be due to the type of catheter used or the nature of the chemotherapy. In future studies, using an implantable intravenous port may decrease the incidence of this known complication. However, accessing these ports has proven to be difficult and sometimes painful in some patients. The inability to ascertain patency is another concern. Finally, separation of the septum from the catheter is a known complication of implanted ports [26,27].

Data concerning information on the p53 status of tumors from patients treated on this study confirm previous reports that suggest that the rate of p53 mutations in patients with advanced ovarian cancer is high. Also, as expected, all patients evaluated have evidence of previous exposure to adenovirus and respond to Adp53 with an increase in anti-adenovirus titers. It remains to be determined whether titer level will affect the ability to deliver p53 or any other gene therapy of interest to tumor cells. However, this is not completely addressed, as we did not do distribution studies in this trial. This phase I study does provide a hint of this type of activity, as two heavily pretreated patients had a mixed response to therapy.

One shortfall of this study is that although we found positive total anti adenovirus antibodies in the serum of all patients (which increased after therapy), we did not look for neutralizing antibodies in the serum or ascites.

Another shortfall of this study is that we did not evaluate for distribution of the virus throughout the peritoneal cavity. One potential problem therefore is that the therapy could be localized to one area of the abdomen and the virus only exposed to tumor in a limited area. Although we did not do a distribution study, we did do laparoscopy before installing any therapy and we were able to access adhesions, and in fact dissect away adhesions where possible in all of the patients who where treated. Distribution of therapy, I believe, is a problem of all intraperitoneal studies and the best way to manage this therapy is as yet unknown.

A third challenge in our study is that we were unable to study the adenovirus p53 to the maximum tolerated dose as we were limited by the viral production capacity. The dose chosen, however, corresponds to doses which were active in preclinical animal models. It is unclear and unknown if higher doses would be more active. Also, without evidence of gene transduction, it is unknown if higher doses are needed. This is another issue that should be addressed in future gene therapy studies.

Several early phase clinical trials of molecular or "gene" therapy for the treatment of ovarian cancer have been published (Table 3). These clinical trials used a replication deficient adenovirus, retrovirus, a conditionally replicative adenovirus or liposomes to deliver the gene of interest. As in this trial, therapy delivered with viral vectors commonly

Table 3
Gene therapy clinical trials for ovarian cancer

Study	Patients	Vector	Gene
Buller et al. [19]	43	adenovirus	p53
Vasey [28]	16	conditionally replicating adenovirus	Replicates only when p53 mutant
Alvarez et al. [29]	15	adenovirus	Single chain antibody to her-2/neu
Hortobagyi et al. [30]	6 ovary 6 breast	liposome	E1A targeting her-2/neu
Alvarez et al. [31]	14	adenovirus	Deliver HSV-TK gene with ganciclovir
Hasenburg et al.[32]	10	adenovirus	Deliver HSV-TK gene with ganciclovir and topotecan
Tait et al. [33]	12	retrovirus	BRCA-1
Tait et al. [34]	6	retrovirus	BRCA-1

caused viral syndrome symptoms, that is, fevers, chills, and myalgias. Abdominal pain was also common and was dose-limiting in the liposomal delivery of E1A.

All of the studies of intraperitoneal gene therapy for ovarian cancer have had difficulty with "proof of concept", that is, tissue acquisition to prove transduction of the gene of interest. In this study, we attempted to obtain cells from peritoneal washings after therapy with Adp53 to confirm transduction, however, cell counts were insufficient for evaluation. One potential reason for this is that we did not access the distribution of the therapy in this trial and may have only been able to sample limited areas of the peritoneal cavity. As mentioned above, we did not do distribution studies in this trial.

In the liposomal E1A study, which included both breast and ovarian cancer patients, both E1A expression in ascites or pleural effusion cells and a decrease in the expression of the targeted gene her-2/neu were demonstrated. Buller et al. [19], using a similar vector, was able to document transduction and expression of p53 in 85% (17/20) of samples after therapy. Although its not known what percentage of cells needs to be infected in order for this therapy to be effective in preclinical evaluations, it appears that with at least 50% tranfection efficiency, there is kill of tumor cells in the laboratory. Improving methods to detect gene transduction and gene expression will help establish the most effective transduction efficiency for therapeutic efficacy. This is one of several areas that need to be furthered investigated to improve gene therapy techniques for the future.

Adp53 is currently being evaluated in an international Phase III study of patients with head and neck cancer. In this trial, Adp53 is given by direct tumor injection allowing for better transduction and evaluation of delivery. As the present generation of gene therapy vectors proceeds clinically, continued improvement of available vectors, new delivery systems, and development of targeted therapies must continue.

A Phase III randomized trial of paclitaxel plus carboplatinum with or without intraperitoneal (IP) Adp53 for front line therapy was terminated early because the first interim analysis showed that the addition of p53 gene therapy did not improve therapeutic effectiveness and increased treatment morbidity. Several potential hypotheses to explain the failure of this study are put forth in an article by Zeimet and Marth [35]. These include, that correcting only one genetic change in the tumor may not inhibit tumor growth, p53 may not be the best target, the adenovirus may not be the best vector, host immunity may inhibit gene expression, and intraperitoneal delivery of the gene may not be the best delivery method.

These studies raise several important questions. What is the next appropriate step in evaluating the efficacy of Adp53 gene therapy specifically? What is the future of adenovirus-mediated molecular therapy in general? More broadly, what is the future direction of molecular therapy and can it be made more targeted and specific? With these concerns in mind, gene therapy for ovarian cancer is being re-evaluated in the laboratory, looking for more specific targets, better vectors, and better delivery systems.

References

[1] Jemal A, Thomas A, Murray T, Thun M. Cancer Statistics, 2002. CA Cancer J Clin 2002;52(1):23–47.

[2] Ozols RF, Young RC. Chemotherapy of ovarian cancer. Semin Oncol 1984;11(3):251–63.

[3] McGuire WP, Hoskins WJ, Brady MF, Kucera PR, Partridge EE, Look KY, et al. Cyclophosphamide and cisplatin compared with paclitaxel and cisplatin in patients with stage III and stage IV ovarian cancer. NEJM 1996;334(1):1–6.

[4] Hoskins WJ. The role of cytoreductive surgery in ovarian cancer. Update Princ Pract Oncol 1987;1:1–13.

[5] Kohler MF, Marks JR, Wiseman RW, Jacobs IJ, Davidoff AM, Clarke-Pearson DL, et al. Spectrum of mutation and frequency of allelic deletion of the p53 gene in ovarian cancer. J Natl Cancer Inst 1993;85(18):1513–9.

[6] Kupryjnczyk J, Thor AD, Beauchamp R, Merritt V, Edgerton SM, Bell DA, et al. p53 gene mutations and protein accumulation in human ovarian cancer. Proc Natl Acad Sci 1993;90(11):4961–5.

[7] Ko LJ, Prives C. p53: puzzle and paradigm. Genes Dev 1996;10(9):1054–72.

[8] Hansen R, Oren M. p53: from inductive signal to cellular effect. Curr Opin Genet Dev 1997;7:46–51.

[9] Hamada K, Zhang WW, Alemany R, Wolf J, Roth JA, Mitchell MF. Growth inhibition of human cervical cancer cells with the recombinant adenovirus p53 in vitro. Gynecol Oncol 1996;60:373–9.

[10] Baker SJ, et al. Suppression of human colorectal carcinoma cell growth by wild-type p53. Science 1990;249(4971):912–5.

[11] Cai DW, Mukhopadhyay T, Liu Y, Fujiwara T, Roth JA. Stable expression of the wild-type p53 gene in human lung cancer cells after retrovirus-mediated gene transfer. Hum Gene Ther 1993;4(5):617–24.

[12] Liu T-J, Zhang WW, Taylor DL, Roth JA, Goepfert H, Clayman GL. Growth suppression of human head and neck cancer cells by the introduction of a wild-type p53 gene via a recombinant adenovirus. Cancer Res 1994;54(14):3662–7.

[13] Wolf JK, Mills GB, Bazzet L, Bast Jr RC, Roth JA, Gershenson DM. Adenovirus-mediated p53 growth inhibition of ovarian cancer cells is

independent of endogenous p53 status. Gynecol Oncol 1999;75(2): 261–7.

[14] Santoso JT, Tang DC, Lane SB, Hung J, Reed DJ, Muller CY, et al. Adenovirus-based p53 gene therapy in ovarian cancer. Gynecol Oncol 1995;59(2):171–8.

[15] Mujoo K, Maneval DC, Anderson SC, Gutterman JU. Adenoviral-mediated p53 tumor suppressor gene therapy of human ovarian carcinoma. Oncogene 1996;12(8):1617–23.

[16] Berkner KL. Development of adenovirus vectors for the expression of heterologous genes. BioTechniques 1988;6(7):616–29.

[17] Horwitz MS. Adenoviruses. In: Fields BN, et al., editors. Field's virology. Third ed. Philadelphia (PA): Lippincott-Raven Publishers, 1996. pp. 2149–71.

[18] Korzarsky KF, Wilson JM. Gene therapy: adenovirus vectors. Curr Opin Genet Dev 1993;3(3):499–503.

[19] Buller RE, et al. A Phase I/II trial of recombinant adenoviral human p53 (SCH58500) intraperitoneal (IP) gene therapy in recurrent ovarian cancer. Gynecol Oncol 1999;72(3):452.

[20] Wolf K, Mills GB, Bast RC, Roth JA, Gershenson DM. Evaluation of efficacy and toxicity of Ad5CMV-p53 for ovarian cancer in a nude mouse model. Gynecol Oncol 1997;64(2):297.

[21] Zhang WW, Fang X, Branch CD, Mazur W, French BA, Roth JA. Generation and identification of recombinant adenovirus by liposome-mediated transfection and PCR analysis. BioTechniques 1993; 15(5):868–72.

[22] Ajani JA, Welch SR, Raber MN, Fields WS, Krakoff IH. Comprehensive criteria for assessing therapy-induced toxicity. Cancer Invest 1990;8(2):147–59.

[23] Herrmann KL, Erdman DD. Diagnosis by serologic assays. In: Lennette EH, et al., editors. Diagnostic Procedures for Viral, Rickettsial and Chlamydial Infections. Seventh ed. Washington (DC): APHA, 1995. pp. 121–38.

[24] Runowitz CD, Dottino PR, Shafir MK, Mark MA, Cohen CJ. Catheter complications associated with intraperitoneal chemotherapy. Gynecol Oncol 1986;24(1):41–50.

[25] Braly P, Doroshow J, Hoff S. Technical aspects of intraperitoneal chemotherapy in abdominal carcinomatosis. Gynecol Oncol 1986;25(3): 319–33.

[26] Rubin SC, Hoskins WJ, Markman M, Hakes T, Lewis Jr JL. Long-term access to the peritoneal cavity in ovarian cancer patients. Gynecol Oncol 1989;33(1):46–8.

[27] Davidson SA, Rubin SC, Markman M, Jones WB, Hakes TB, Reichman B, et al. Intraperitoneal chemotherapy: analysis of complications with an implanted subcutaneous port and catheter system. Gynecol Oncol 1991;41(2):101–6.

[28] Vasey PA. Resistance to chemotherapy in advanced ovarian cancer: mechanisms and current strategies. BJM 2003;89(Suppl. 3):S23–8.

[29] Alvarez RD, Barnes MN, Gomez-Navarro J, Wang M, Strong TV, Arafat W, et al. A cancer gene therapy approach utilizing an anti-erbB-2 single chain antibody-encoding adenovirus (AD21): a phase I trial. Clin Cancer Res 2000;6:3081–7.

[30] Hortobagyi GN, Ueno NT, Xia W, Zhang S, Wolf JK, Putnam JB, et al. Cationic liposome-mediated E1A gene transfer to human breast and ovarian cancer cells and its biologic effects: a phase I clinical trial. JCO 2001;19(14):3422–33.

[31] Alvarez RD, Gomez-Navarro J, Wang M, Barnes MN, Strong TV, Arani RB, et al. Adenoviral-mediated suicide gene therapy for ovarian cancer. Mol Ther 2000;2(5):524–30.

[32] Hasenburg A, Tong XW, Rojas-Martinez A, Nyberg-Hoffman C, Kieback CC, Kaplan A, et al. Thymidine kinase gene therapy with concomitant topotecan chemotherapy for recurrent ovarian cancer. Cancer Gene Ther 2000;7(6):839–44.

[33] Tait DL, Obermiller PS, Fraziier SR, Jensen RA, Welcsh P, Dann J, et al. A phase I trial of retroviral BRCA1 vs. gene therapy in ovarian cancer. Clin Cancer Res 1997;3:1959–68.

[34] Tait DL, Obermiller PS, Hatmaker RA, Frazier SR, Holt JT. Ovarian cancer BRCA1 gene. Phase I and II trial differences in immune response and vector stability. Clin Cancer Res 1999;5:1708–14.

[35] Zeimet AG, Marth C. Why did p53 gene therapy fail in ovarian cancer? Lancet Oncol 2003;4(7):415–22.

The cancer growth suppressor gene *mda*-7 selectively induces apoptosis in human breast cancer cells and inhibits tumor growth in nude mice

(melanoma differentiation associated gene 7/programmed cell death/recombinant adenovirus/selective antitumor activity)

ZAO-ZHONG SU*†, MALAVI T. MADIREDDI*†, JIAO JIAO LIN‡, CHARLES S. H. YOUNG§, SHINICHI KITADA¶, JOHN C. REED¶, NEIL I. GOLDSTEIN‖, AND PAUL B. FISHER*†**††

Departments of *Urology, ‡Pathology, §Microbiology, and **Neurosurgery, Herbert Irving Comprehensive Cancer Center, Columbia University, College of Physicians and Surgeons, New York, NY 10032; ¶Burnham Institute, La Jolla, CA 92037; and ‖GenQuest Incorporated, New York, NY 10032

ABSTRACT   A differentiation induction subtraction hybridization strategy is being used to identify and clone genes involved in growth control and terminal differentiation in human cancer cells. This scheme identified melanoma differentiation associated gene-7 (*mda*-7), whose expression is upregulated as a consequence of terminal differentiation in human melanoma cells. Forced expression of *mda*-7 is growth inhibitory toward diverse human tumor cells. The present studies elucidate the mechanism by which *mda*-7 selectively suppresses the growth of human breast cancer cells and the consequence of ectopic expression of *mda*-7 on human breast tumor formation *in vivo* in nude mice. Infection of wild-type, mutant, and null p53 human breast cancer cells with a recombinant type 5 adenovirus expressing *mda*-7, Ad.*mda*-7 S, inhibited growth and induced programmed cell death (apoptosis). Induction of apoptosis correlated with an increase in BAX protein, an established inducer of programmed cell death, and an increase in the ratio of BAX to BCL-2, an established inhibitor of apoptosis. Infection of breast carcinoma cells with Ad.*mda*-7 S before injection into nude mice inhibited tumor development. In contrast, ectopic expression of *mda*-7 did not significantly alter cell cycle kinetics, growth rate, or survival in normal human mammary epithelial cells. These data suggest that *mda*-7 induces its selective anticancer properties in human breast carcinoma cells by promoting apoptosis that occurs independent of p53 status. On the basis of its selective anticancer inhibitory activity and its direct antitumor effects, *mda*-7 may represent a new class of cancer suppressor genes that could prove useful for the targeted therapy of human cancer.

Abnormalities in cellular differentiation are common occurrences during cancer development and progression (1, 2). Correction of these defects resulting in the reversion of tumor cells to a more-normal differentiated phenotype represents a potentially useful therapeutic strategy (1, 2). Although the mechanism underlying cancer growth suppression and terminal differentiation is unknown, it is hypothesized that these changes result from the activation of genes negatively regulating cell growth and the suppression of genes promoting the cancer phenotype (1, 2). Induction of terminal differentiation can occur with and without the initiation of programmed cell death (2). Identification of the genes mediating these phenomena should provide mechanistic insights into these processes and also may elucidate potentially novel and selective targets for cancer therapy.

Induction of terminal differentiation combined with the molecular approach of subtraction hybridization, differentiation induction subtraction hybridization, is permitting the identification of critical gene changes associated with and controlling induction of terminal differentiation in human melanoma cells (1, 3, 4–6). The combination of recombinant human fibroblast interferon (interferon β) and the antileukemic compound mezerein elicits an irreversible loss of proliferation and induces terminal differentiation in human melanoma cells (7, 8). Several melanoma differentiation-associated (*mda*) genes have been isolated that either correlate with or directly influence human melanoma cell growth and differentiation (1, 3, 4–6). These include the cyclin-dependent kinase inhibitor p21, identified as *mda*-6, waf-1, cip-1, sdi-1 (4, 5, 9), and several novel genes, including *mda*-7 and *mda*-9 (10, 11).

Partial screening of a human melanoma temporally spaced differentiation inducer-treated cDNA (differentiation induction subtraction hybridization) library identified the *mda*-7 cDNA consisting of 1,718 bp that encode a novel protein of 206 amino acids with a predicted M_r of 23,800 (1, 3, 11). Induction of growth arrest and terminal differentiation in human melanoma cells results in elevated expression of *mda*-7 (1, 3). Moreover, the level of *mda*-7 expression inversely correlates with human melanoma progression, with highest levels found in actively proliferating normal melanocytes and lowest levels in metastatic melanoma (3). Ectopic expression of a transfected *mda*-7 gene in H0–1 human melanoma cells suppresses growth without inducing terminal differentiation, suggesting that this gene is involved in growth control and indirectly contributes to the terminal differentiation process (3). Additionally, ectopic expression of a transfected *mda*-7 gene induces growth suppression and a reduction in colony formation in cancer cell lines of diverse origin with multiple genetic defects (11). In contrast, no overt biological response is engendered in normal human epithelial or fibroblast cells by ectopic over-expression of *mda*-7 (11).

The present studies investigate the mechanism by which *mda*-7 selectively inhibits the proliferation of breast cancer cells and not normal mammary epithelial cells. Evidence is presented documenting a strong correlation between ectopic expression of *mda*-7 and induction of apoptosis in breast

---

Abbreviations: pfu, plaque-forming unit; TUNEL, terminal deoxynucleotidyltransferase-mediated UTP end labeling; HMEC, human mammary epithelial cells; HMC, high molecular weight.
‡Z.-Z.S. and M.T.M. contributed equally to this work.
††To whom reprint requests should be addressed at: Departments of Pathology and Urology, Columbia University, College of Physicians and Surgeons, 630 West 168th Street, New York, NY 10032. e-mail: pbf1@columbia.edu.

cancer cells. This process is characterized by an up-regulation of the proapoptotic effector Bax and an increase in the BAX/BCL-2 protein ratio (12, 13). A direct effect of *mda*-7 "gene therapy" on the growth of human tumor xenografts in nude mice also is demonstrated. On the basis of the selective breast cancer growth inhibitory properties of *mda*-7 and its apparent ability to distinguish and spare normal cells from growth inhibition and apoptosis, the *mda*-7 cDNA represents a potentially effective antitumor agent for breast cancer gene therapy.

MATERIALS AND METHODS

Cell Lines, Culture Conditions, and Growth and β-Galactosidase Assays. MCF-7, MDA-MB-157, MDA-MB-231, MDA-MB-453, and T47D human breast carcinoma cell lines were obtained from the American Type Culture Collection and were cultured as recommended. Normal human breast epithelial cells included immortal HBL-100 (American Type Culture Collection) and early passage mammary epithelial cells [human mammary epithelial cells (HMEC), passage nos. 9–12] (Clonetics, San Diego). HMEC cells were grown in serum-free defined medium supplied by Clonetics. To study the effect of *mda*-7 on monolayer colony formation or cell growth, cells were infected with 100 plaque-forming units (pfu)/cell of Ad.*mda*-7 S, Ad.Vec, or Ad.β-gal, and colony formation (3 to 4 weeks) or cell growth (daily over a 14-day period, with a medium change at days 4, 7, and 10) was determined (3, 11). To evaluate the effect of *mda*-7 coexpression with Bcl-2 or Ad E1B, MCF-7 or T47D cells were transfected with 10 μg of an *mda*-7 gene cloned in a pMAM-neo vector (3), alone or in combination with 10 μg of a Bcl-2 (pSFFV-Bcl-2) (14) or an Ad E1B (pCMV.E1B) (15) expression vector by using the lipofectin method (11). *In situ* β-galactosidase assays were performed by using standard protocols (16).

Construction and Assaying of Recombinant Adenoviruses. The recombinant replication-defective Ad.*mda*-7 S was created in two steps, as described for Ad.*mda*-7 antisense (11). Production of infectious virus in 293 cells, analysis of recombinant virus genomes to confirm the recombinant structure, plaque purification, and titration of virus were performed as described (17).

Cell Cycle Analysis. Fluorescence-activated cell sorter analysis was performed as described (18). The percentage of cells in the various phases of the cell cycle was estimated manually by gating the G_1/G_0, S, and G_2/M regions of the histograms. The percentage of cells to the left of the G_1/G_0 region (the A_0 region), representing apoptotic cells containing less than a diploid content of DNA, also was estimated by gating the appropriate region of the histograms.

DNA Extraction, Fragmentation Assay, and Terminal Deoxynucleotidyltransferase-Mediated UTP End Labeling (TUNEL) Assay. DNA was extracted, and fragmentation assays were performed as described (18) 2 and 4 days after infection of cells with 100 pfu/cell of Ad.*mda*-7 S or Ad.Vec. A modified TdT-mediated dUTP-digoxygenin nick end labeling (TUNEL) method (19) was used to evaluate apoptosis in cells treated for the fragmentation assay.

Immunohistochemistry, Immunoprecipitation, and Western Blotting. These assays were performed as described (3, 11, 20–22). However, immunoreactivity in Western blotting assays was detected by enhanced chemiluminescence (ECL) (Amersham).

Tumor Studies. MCF-7 cells were infected with 100 pfu/cell of Ad.*mda*-7 S or Ad.Vec, were incubated at 37°C for 96 hr, were resuspended at 2.5×10^6 cells/ml in PBS, and were mixed 1:1 with Matrigel (Collaborative Research), and 400 μl of this suspension (1×10^6 per animal) was injected s.c. into nude mice (Taconic Farms) (16, 23). Four weeks after injection,

animals were killed, and the tumors were removed, were snap frozen in liquid nitrogen, and were weighed. Data are presented as tumor weight. In addition, a tumor volume ratio was calculated. This is an index of tumor progression over the course of a study (23).

RESULTS

***mda*-7 Selectively Induces Apoptosis in Human Breast Cancer Cells with Different p53 Genotypes.** To define a potential mechanism by which *mda*-7 induces its selective effect on cancer versus normal cells and to define potential therapeutic applications for *mda*-7, we constructed replication-defective adenoviruses expressing *mda*-7 (Ad.*mda*-7 S) or, as a control, the β-galactosidase (Ad.β-gal) gene. Infection of human breast cancer cells, including MCF-7, MDA-MB-157, MDA-MB-231, MDA-MB-453, and T47D with 100 pfu/ cell of Ad.*mda*-7 S reduced growth and colony formation in comparison with untreated cells or cultures infected with a recombinant Ad lacking the *mda*-7 gene Ad.CMV null (Ad.*Vec*) (Figs. 1 and 2 and data not shown). Infection of the same cell types with 100 pfu/cell of Ad.β-gal resulted in β-galactosidase expression in the majority of treated cells and no significant change in growth properties (Figs. 1 and 2 and data not shown). Because the different breast cancer cell lines contain either wild-type p53 (MCF-7), mutant p53 (MDA-MB-231, MDA-MB-453, and T47D), or null p53 (MDA-MB-157), these results document that the growth-inhibitory activity of *mda*-7 occurs independently of the mode of action of this extensively studied tumor suppressor gene that is frequently altered in human cancers.

In contrast to malignant breast tumor cells, infection of immortal normal human breast epithelial cells, HBL-100, with 100 pfu/cell of Ad.*mda*-7 S resulted in a similar kinetics of growth and cloning efficiency in liquid medium as found after infection with Ad.*Vec* or Ad.β-gal (Fig. 1). Unaltered growth kinetics was also evident in early passage normal HMEC infected with the three viruses (Fig. 1). These results extend previous observations by using the less efficient approach of DNA transfection, indicating that ectopic expression of *mda*-7 selectively inhibits the growth of breast cancer cells *in vitro* (11).

A consistent observation with many tumor cells infected with Ad.mda-7 S is a change in cellular and nuclear morphology suggestive of programmed cell death. Fluorescence-activated cell sorter analyses of DNA content were performed to determine the effects of *mda*-7 on apoptosis-associated DNA degradation and to explore whether alterations in cell cycle progression occur. In all of the breast cancer cell lines, a hypodiploid (A_0) peak appeared or increased after infection with Ad.*mda*-7 S relative to infection with Ad.*Vec* (data not shown). This putative apoptotic response was not evident after infection of normal human breast cells, HBL-100 or HMEC, with 100 pfu/cell of Ad.*mda*-7 S.

Infection of MCF-7 and T47D cells with 10 or 100 pfu/cell of Ad.*mda*-7 S resulted in a temporal induction of growth suppression and apoptosis as indicated by the formation of cells with a hypodiploid DNA content, nucleosomal DNA ladders, positive TUNEL (TdT-mediated dTUP nick end labeling) reaction, and positive annexin V staining (Figs. 1, 3, and 4*C* and data not shown). When MCF-7 and T47D cells were analyzed for *MDA*-7 protein by using indirect immunofluorescence with *MDA*-7-specific mAbs 2 days after infection with 100 pfu/cell of Ad.*mda*-7 S, intense nuclear staining was visible (Fig. 4*A* and data not shown). In contrast, none of the parameters indicative of apoptosis occurred in HMEC or HBL-100 cells after infection with 100 pfu/cell of Ad.*mda*-7 S. The absence of an effect in normal breast cells did not result from a failure to infect these cell types and express genes controlled by the CMV promoter (as indicated by β-galacto-
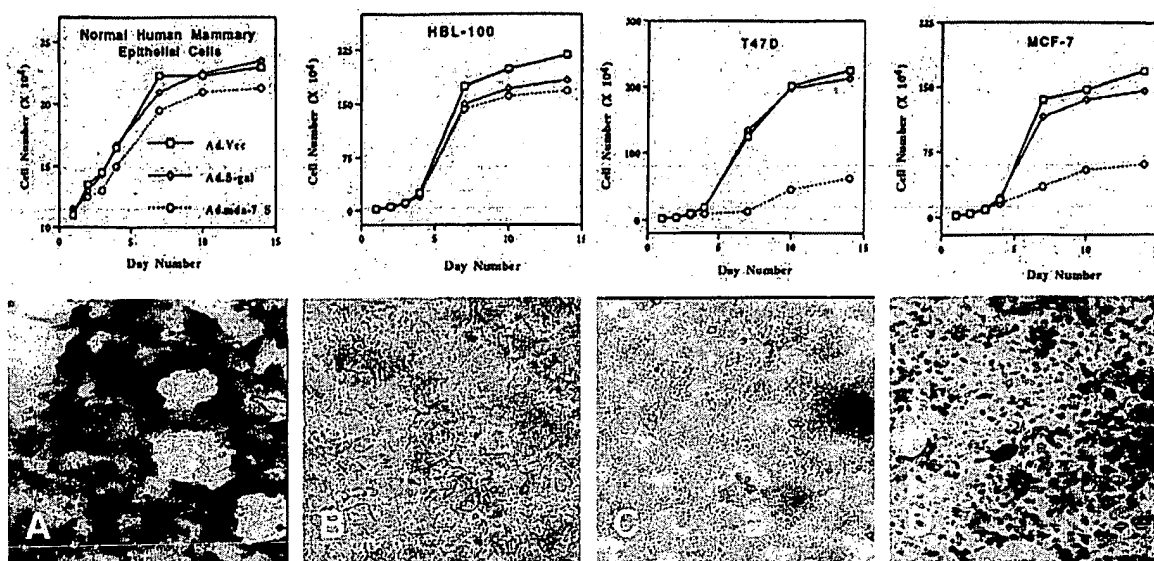
FIG. 1.   Effect of Ad. *Vec*, Ad.β-gal, and Ad.*mda*-7 S on the growth of normal breast and breast cancer cells. The indicated cell types were infected with 100 pfu/cell of Ad.*Vec*, Ad.β-gal, or Ad.*mda*-7 S, and cell growth was determined over a 14-day period. Triplicate samples varied by ≤10%. Similar results (±15%) were obtained in two additional replicate studies. In the lower panels, β-galactosidase activity was assayed in HMEC (*A*), HBL-100 (*B*), T47D (*C*), and MCF-7 (*D*) cells 48 hr after infection with the Ad.β-gal.

sidase staining after infection with Ad.β-gal) or to produce the *MDA*-7 protein (Figs. 1 and 5). Immunoprecipitation analysis of [^{35}S]methionine-labeled cell lysates from MCF-7, T47D, HBL-100, and HMEC cells with *MDA*-7 mAb indicated the presence of equivalent amounts of both the predicted *MDA*-7 protein (≈23.8 kDa) and a high molecular weight (HMC) interacting protein (≈90–110) in MCF-7, T47D, and HBL-100 cells and reduced levels of both proteins in HMEC cells (Fig. 5). These findings establish that *mda*-7 can induce apoptosis differentially in breast carcinomas but not in normal breast epithelial cells. Moreover, this selective apoptotic-inducing effect is not a direct consequence of differential levels of the *MDA*-7 protein or the HMC interacting protein in breast cancer versus normal breast epithelial cells.

Induction of Apoptosis in Human Breast Cancer Cell Lines Correlates with an Elevation in BAX Levels. Programmed cell death reflects a balance between signaling events and molecules that either promote or inhibit apoptosis (12, 13, 24, 25). Current data support the hypothesis that the ratio of death antagonists to agonists determines whether a cell will respond to apoptotic signals. Proteins such as Bcl-2, Bcl-X$_L$, Mcl-1, Bcl-w, and Ad E1B (19 and 55 kDa) protect cells from specific programs of apoptosis whereas BAX, Bad, Bak, and Bcl-X$_S$ proteins stimulate apoptosis in specific target cells (12, 13, 24, 25). We, therefore, determined by Western blotting if induction of *mda*-7-induced apoptosis in human breast carcinoma cells altered the expression of specific proteins associated with
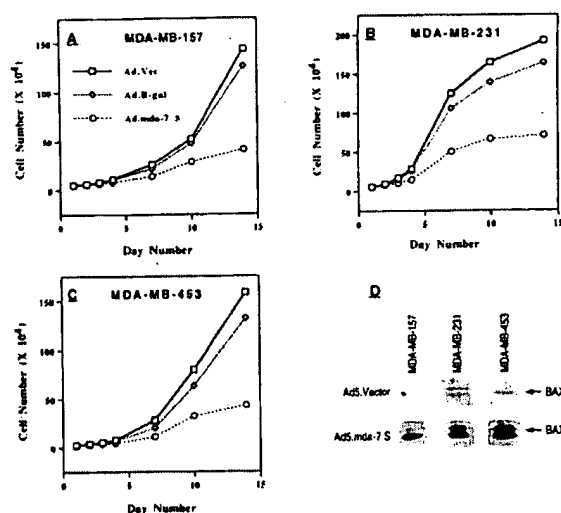

FIG. 2.   Effect of Ad. *mda*-7 S on growth and BAX protein levels in human breast cancer cells. The experimental growth protocol was as described in the legend to Fig. 1. The breast carcinoma cell lines analyzed include MDA-MB-157 (*A*), MDA-MB-231 (*B*), and MDA-MB-453 (*C*). *D* provides immunoblot analyses of BAX expression 2 days after infection of the indicated breast cancer cell line with 100 pfu/cell of Ad.*Vec* or Ad.*mda*-7 S. Coomassie blue staining of gels indicated equal protein loading.
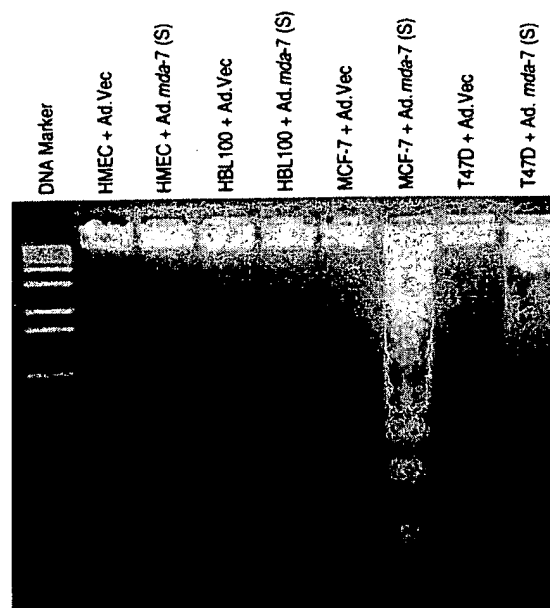

FIG. 3.   Induction of nucleosomal DNA degradation in human breast cancer cells, but not in normal breast epithelial cells, infected with Ad.*mda*-7 S. The indicated cell types were infected with 100 pfu/cell of Ad.*Vec* or Ad.*mda*-7 (S) and were analyzed for nucleosomal DNA degradation 4 days after infection.

Medical Sciences: Su et al.

Proc. Natl. Acad. Sci. USA 95 (1998)   14403

ANTI-MDA-7 / DAPI / TUNEL / PROPIDIUM IODIDE
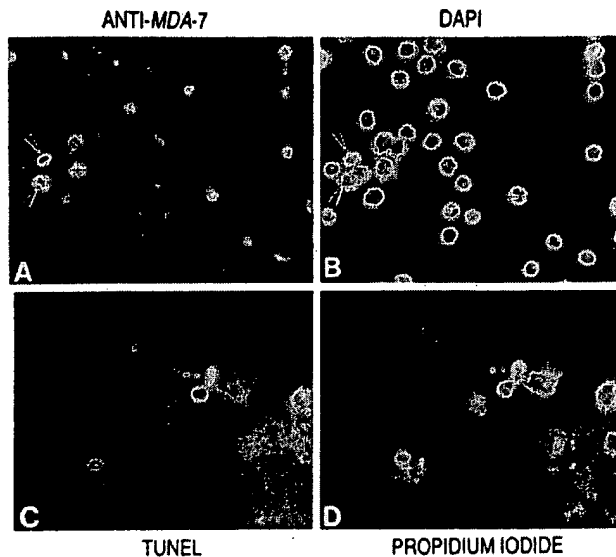

TUNEL   PROPIDIUM IODIDE

FIG. 4. Nuclear localization of mda-7 and induction of a positive TUNEL reaction in MCF-7 cells infected with Ad. mda-7 S. MCF-7 cells were doubly stained with Anti-MDA-7 antibody (A) and 4',6-diamidino-2-phenylindole (DAPI) (B) 2 days after infection with 100pfu/cell of Ad.mda-7 S. The position of two mitotic cells stained with Anti-mda-7 antibody are shown in A, and the corresponding 4',6-diamidino-2-phenylindole counterstain is indicated in B (arrows label metaphase chromosomes). MCF-7 cells 4 days after infection with 100 pfu/cell of Ad.mda-7 S were doubly stained by the TUNEL method (C) and propidium iodide (D).

apoptosis (Figs. 2D and 6). Western blotting of lysates prepared 2 and 4 days after infection of HMEC, HBL-100, MCF-7, and T47D cells with 100 pfu/cell of either Ad.mda-7 S or Ad.Vec demonstrated increased expression of BAX in both MCF-7 (p53 wild-type protein) and T47D (p53 mutant protein) cells after infection with Ad.mda-7 S but not with Ad.Vec (Fig. 6A). Ad.mda-7 S infection of MCF-7 and T47D cells also resulted in elevated levels of processed BAX protein of 18–21 kDa (25). Up-regulation of BAX after infection with Ad.mda-7 S was also evident in additional breast carcinoma cell lines containing mutant p53 (MDA-MB-231 and MDA-MB-453) or null p53 (MDA-MB-157) (Fig. 2D). Comparison of BAX to BCL-2 protein ratios revealed BAX/BCL-2 to be significantly higher in breast cancer cells (Fig. 6B and data not

A

B

Protein	Exptl. Condition*	HMEC+	HBL-100	MCF-7	T47D
BCL-2	Ad. Vec (4 D)	+	+++	-	-
BCL-2	Ad.mda-7 S (4 D)	+	++++	-	+/-
BAK	Ad. Vec (4 D)	+	++	+	+++
BAK	Ad.mda-7 S (4 D)	++	+++	+	+++

*Cells were infected with 100 pfu/cell of Ad.Vec or Ad.mda-7 S and cell lysates were prepared after 4 days and analyzed by Western blotting using antibodies to the indicated proteins.
+Relative expression levels indicated by + and - designations, with 4+ maximum and +/- minimum expression. A - designation indicates no detectable protein.

FIG. 6. Expression of Bcl-2, Bax, and Bak in normal breast epithelial and breast carcinoma cells infected with Ad. mda-7 S or Ad.Vec. (A) Immunoblot analyses of BAX protein in normal mammary epithelial and cancer cells. Equal amounts of whole cell protein (verified by Coomassie blue staining) from 2- and 4-day cell cultures infected with 100 pfu/cell of Ad.Vec or Ad.mda-7 S were resolved by SDS/PAGE (4–20%), were immunoblotted, and were probed with Anti-BAX mAb. Note that both intact BAX and processed BAX proteins are visible in the breast cancer cell lines 2 days after Ad.mda-7 infection. Low levels of BAX in 4-day MCF-7 is caused by proteolytic degradation because the cells in this study were 70% apoptotic by 4 days after infection with Ad.mda-7 S. (B) Tabular compilation of protein levels of the Bcl-2 gene family members, BCL-2 and BAK, 4 days after infection with 100 pfu/cell of Ad.mda-7 S or Ad.Vec in normal breast epithelial cells and breast carcinoma cell lines.

shown), implicating BAX as a potential component in mda-7-induced programmed cell death. Ectopic expression of mda-7 in HBL-100 cells variably modified BAX expression, which is generally quantitatively less than that observed in breast cancer cells. Moreover, the ratio of BAX/BCL-2 was consistently lower in HBL-100 cells after infection with Ad.mda-7 S than in the breast cancer cells. In contrast, in early passage HMEC, representing the best approximation of normal breast epithelial cells, Ad.mda-7 S failed to induce the BAX protein. No consistent changes were seen in other apoptosis-modifying proteins, including BAK, BAD, BAG-1, and BCL-X, after infection of breast carcinoma or normal breast epithelial cells with Ad.mda-7 S (Fig. 6B and data not shown). On the basis of these observations, it appears that BAX may be a crucial regulator of apoptosis induced selectively in breast cancer versus normal mammary epithelial cells after ectopic overexpression of mda-7.

Overexpression of Bcl-2 and Ad E1B proteins protects cells from apoptosis induced by diverse stimuli (13, 24, 25). This effect may be mediated by the formation of a stable complex between BAX and BCL-2 or BAX and Ad E1B proteins by heterodimerization, thereby nullifying the apoptotic-inducing effect of BAX (26–29). Because high levels of the antiapoptosis proteins BCL-2 or Ad E1B can counteract the proapoptotic signaling of BAX, studies were performed to determine whether overexpression of Bcl-2 or Ad E1B would protect breast carcinoma cells from mda-7-induced growth suppression and apoptosis. Cotransfection of MCF-7 and T47D cells with a pMAMneo-mda-7 expression construct (permitting controlled expression of mda-7 by dexamethasone and containing a neomycin resistance gene permitting colony selection in G418) (3) and a pSFFV-bcl-2 expression construct (express-

T47D   MCF-7   HBL-100   HMEC
Vec mda-7 Vec mda-7 Vec mda-7 Vec mda-7

←HMC

←mda-7

FIG. 5. Immunoprecipitation of MDA-7 and an HMC protein with an MDA-7 mAb. The indicated cell lines were infected with 100 pfu/cell of Ad.Vec or Ad.mda-7 for 4 days and were labeled with [35S]methionine, and the levels of the MDA-7 and HMC proteins were determined by immunoprecipitation analysis. Coomassie blue staining of gels indicated equal protein loading.
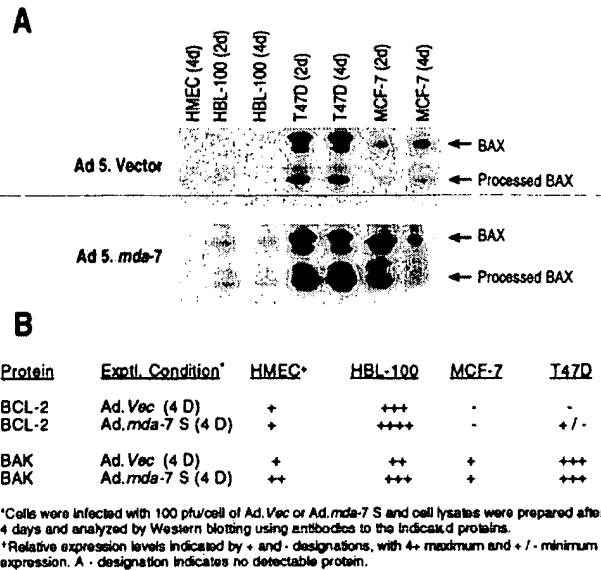
ing Bcl-2 and containing a neomycin resistance gene permitting colony selection in G418) (14) or pCMV.E1B expression vector (expressing both Ad E1B proteins and containing a neomycin resistance gene permitting colony selection in G418) (15) rescued cells from the growth-inhibitory effect of *mda-7* (Fig. 7). Moreover, MCF-7 cells, engineered to stably overexpress Bcl-2, were refractory to *mda-7*-induced (100 pfu/cell) growth suppression and apoptosis (data not shown). These results provide additional evidence that *mda-7* induces growth suppression and apoptosis in breast cancer cells by inducing a programmed cell death pathway that can be modified directly by overexpressing the antiapoptotic proteins BCL-2 or Ad E1B.

Ectopic Expression of *mda-7* in Human Breast Carcinoma Cells Inhibits Tumor Development in Nude Mice.

On the basis of *in vitro* studies indicating selective growth-inhibitory and apoptosis-inducing effects of *mda-7* when overexpressed in cancer cells, we investigated the effect of ectopic expression of *mda-7* on tumor formation by breast cancer cells *in vivo* in nude mice. The breast carcinoma cell line MCF-7 was infected with 100 pfu/cell of either Ad.*mda-7* S or Ad.*Vec* 96 hr before implantation in nude mice. In the control Ad.*Vec*-infected cells, tumors developed in all groups within 7 days and grew progressively during the course of the experiment (4 weeks). In contrast, the group of animals injected with tumor cells infected with Ad.*mda-7* S exhibited a statistically significant ($P < 0.01$) suppression of tumor development, as defined by tumor volume and tumor weight (Fig. 8 and data not shown). Moreover, Ad.*mda-7* S also inhibited the growth of MCF-7 tumors initiated in nude mice (100–150 mm³) before a 3-week Ad.*mda-7* S therapy protocol (three weekly intratumoral injections of 1×10^8 pfu/injection in 100 μl over four sites) (data not shown). These experimental findings document that
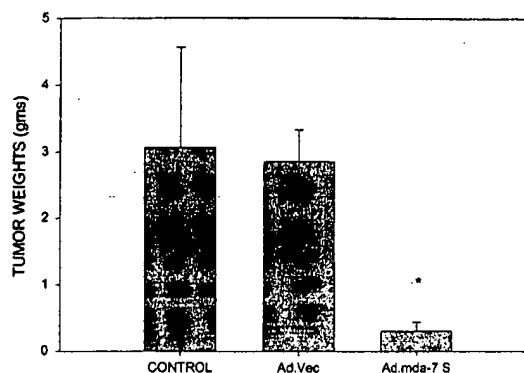

FIG. 8. Effect of *mda-7* on the growth of MCF-7 cells in nude mice. MCF-7 cells were uninfected (CONTROL) or infected with 100 pfu/cell of Ad.*Vec* or Ad.*mda-7* S and were incubated for 4 days at 37°C. Cells were removed with trypsin, were mixed with Matrigel (1:1), and were injected into nude mice (10^6 cells/animal). Results are shown as tumor weight in grams ± SD. Statistical significance was determined with a Student's *t* test using the computer program SIGMA STAT (Jandel, San Rafael, CA), and a *P* value of <0.05 is indicated by an asterisk. Two additional tumorigenicity studies have been performed with qualitatively similar results (data not shown).

Ad.*mda-7* S can inhibit tumor formation and progression directly *in vivo*.

DISCUSSION

In the present studies, we describe the antibreast carcinoma and apoptosis-promoting properties of a cancer growth suppressor gene, *mda-7*. On the basis of the previously confirmed genetic defects in the human tumor cell lines analyzed, including mutations in p53 and/or RB, it is evident that the biological activity of *mda-7* does not depend on the action of these tumor suppressor genes (11). The capacity of a cancer suppressor gene, such as *mda-7*, to efficiently inhibit the growth of wild-type, mutant, and null p53 breast carcinoma cells, as well as cancer cells with additional defects (11), supports the intriguing possibility, confirmed by *in vivo* studies, that *mda-7* may prove efficacious in the gene-based therapy of human breast and other cancers. Moreover, because elevated expression of *mda-7* in normal cells does not elicit a deleterious effect, a problem often encountered when using conventional gene therapy approaches should be avoided.

The mechanism by which *mda-7* differentially inhibits growth and induces apoptosis in breast cancer versus normal mammary epithelial cells remains to be determined. Preliminary studies using mAbs specific for *mda-7* demonstrate an association of this protein with chromatin in cells undergoing mitosis (data not shown). Moreover, in human melanoma cells, induction of terminal differentiation by treatment with interferon β plus mezerein results in translocation of *mda-7* from the cytosol into the nucleus of differentiated cells. These two observations suggest that *mda-7* may be associated with chromatin remodeling, which is apparent during both mitosis and differentiation. On the basis of primary protein sequence analysis, *mda-7* does not appear to possess any nuclear localization signals, suggesting that the *MDA*-7 protein requires an association with a cytosolic chaperone to translocate into the nucleus (3, 11). In this context, identification of proteins that interact with *mda-7* (such as the HMC) (3, 11) and that facilitate migration into the nucleus may provide insights into the mechanism by which *mda-7* selectively suppresses malignant but not normal mammary epithelial cell growth.

The Bcl-2 gene family members are important genetic elements in maintaining homeostasis between cell survival and death. The present study demonstrates that *mda-7*-induced


FIG. 7. Effect of inducible *mda-7* expression alone and in combination with Bcl-2 or Ad E1B expression on colony formation in MCF-7 and T47D cells. Cells were transfected with a pMAMneo-*mda-7* and a pSFFV-bcl-2 [MCF-7 (*A*) or T47D (*B*)] or a pCMVE1B [MCF-7 (*C*) and T47D (*D*)] expression plasmid, alone and in combination, and were grown in medium containing 300 μg of G418 per milliliter and in the presence or absence of 1×10^{-6} M dexamethasone (DEX). Colonies were enumerated after ≈3–4 weeks of growth ± SD for five replicate plates. Similar results have been obtained ±15% in a replicate study (data not shown).

Medical Sciences: Su *et al.*

Proc. Natl. Acad. Sci. USA 95 (1998)   14405

apoptosis in breast cancer cells is associated with the up-regulation of the proapoptotic protein BAX whereas levels of BCL-2, BCL-X$_L$, BAK, BAD, and BAG-1 were unchanged. The observation that the cell death signal induced by *MDA-7* can be counteracted by overexpression of Bcl-2 or its viral homologue adenovirus E1B (12, 27, 28) is consistent with a prominent role for *MDA-7*-induced up-regulation of BAX in the apoptotic mechanism used by this tumor suppressor. In this regard, recent studies suggest that BAX also may function as a tumor suppressor (29–31).

Although BAX expression is regulated positively by wild-type p53 (27), the ability of *mda-7* to induce BAX is clearly p53-independent, suggesting that alternative pathways can be involved in BAX up-regulation after ectopic overexpression of *mda-7*. At present, it is unknown whether *mda-7* directly or indirectly induces BAX expression in cancer cells. However, given the lack of similarity of *mda-7* to any known transcription factors, we suspect that it at least requires other cofactors. The lack of a significant biological effect of *mda-7* in normal cells may involve a failure of *MDA-7* protein to accumulate in the nucleus and induce the appropriate gene expression changes, such as Bax, that are necessary to inhibit cell growth and/or induce apoptosis or a combination of these effects. These possibilities are amenable to experimental testing. Defining the molecular basis of action of *mda-7* is merited and should provide important insights into the role of this cancer growth suppressor gene in tumor development and progression. This information also should assist in exploiting *mda-7* for cancer therapy.

Ectopic expression of *mda-7* by using a recombinant adenovirus delivery approach induces growth suppression and apoptosis in human breast cancer cell lines *in vitro* and inhibits human breast tumor growth *in vivo* in nude mice. In contrast, normal breast epithelial cells do not exhibit analogous changes in cell growth or survival after ectopic overexpression of *mda-7*. These findings indicate that *mda-7* represents a class of cancer-specific growth-arresting and apoptosis-inducing genes that may prove efficacious for the targeted therapy of breast cancer.

1. Jiang, H., Lin, J. & Fisher, P. B. (1994) *Mol. Cell. Differ.* 2, 221–239.

2. Waxman, S., Ed. (1995) *Differentiation Therapy* (Ares Serono Symposia Publications, Rome), Vol. 10, pp. 1–531.
3. Jiang, H., Lin, J. J., Su, Z.-z., Goldstein, N. I. & Fisher P. B. (1995) *Oncogene* 11, 2477–2486.
4. Jiang, H. & Fisher, P. B. (1993) *Mol. Cell. Differ.* 1, 285–299.
5. Jiang, H., Lin, J., Su, Z.-z., Kerbel, R. S., Herlyn, M., Weissman, R. B., Welch, D. & Fisher, P. B. (1995) *Oncogene* 10, 1855–1864.
6. Lin, J. J., Jiang, H. & Fisher, P. B. (1998) *Gene* 207, 105–110.
7. Fisher, P. B., Prignoli, D. R., Hermo, H., Jr., Weinstein, I. B. & Pestka, S. (1985) *J. Interferon Res.* 5, 11–22.
8. Jiang, H., Su, Z.-z., Boyd, J. & Fisher, P. B. (1993) *Mol. Cell. Differ.* 1, 41–66.
9. Chellappan, S. P., Giordano, A. & Fisher, P. B. (1998) *Curr. Top. Microbiol. Immunol.* 227, 57–103.
10. Lin, J. J., Jiang, H. & Fisher, P. B. (1996) *Mol. Cell. Differ.* 4, 317–333.
11. Jiang, H., Su, Z.-z., Lin, J. J., Goldstein, N. I., Young, C. S. H. & Fisher, P. B. (1996) *Proc. Natl. Acad. Sci. USA* 93, 9160–9165.
12. Sedlak T. W. Oltvai, Z. N., Yang, E., Wang, K., Boise, L. H., Thompson, C. B. & Korsmeyer S. J. (1995) *Proc. Natl. Acad. Sci. USA* 92, 7834–7838.
13. Reed, J. C., Zha, H., Aime-Sempe, C., Takayama, S. & Wang, H. G. (1996) *Adv. Exp. Med. Biol.* 406, 99–112.
14. Walton M. I., Whysong, S., O'Connor, P. M., Hockenbery, D., Korsmeyer, S. J. & Kohn, K. W. (1993) *Cancer Res.* 53, 1853–1861.
15. White, E. & Cipriani, R. (1990) *Mol. Cell. Biol.* 10, 120–130.
16. Bischoff, J. R., Kirn, D. H., Williams, A., Heise, C., Horn, S., Muna, M., Ng, L., Nye, J. A., Sampson-Johannes, A., Fattaey, A., et al. (1996) *Science* 274, 373–376.
17. Volkert, F. C. & Young, C. S. H. (1983) *Virology* 125, 175–193.
18. Su, Z.-z., Lin, J., Prewett, M., Goldstein, N. I. & Fisher, P. B. (1995) *Anticancer Res.* 15, 1841–1848.
19. Gravieli, Y., Sherman, Y. & Ben-Sasson, S. A. (1992) *J. Cell Biol.* 119, 493–501.
20. Wenkert, D. & Allis, C. D. (1984) *J. Cell Biol.* 78, 2107–2117.
21. Madireddi, M. T., Davis, M. C. & Alis, C. D. (1994) *Dev. Biol.* 165, 418–431.
22. Su, Z.-z., Yemul, S., Estabrook, A., Zimmer, S. G., Friedman, R. M. & Fisher, P. B. (1995) *Int. J. Oncol.* 7, 1279–1284.
23. Goldstein, N. I., Prewett, M., Zuklys, K., Rockwell, P. & Mendelsohn, J. (1995) *Clin. Cancer Res.* 1, 1311–1318.
24. White, E. (1996) *Genes Dev.* 10, 1–15.
25. Reed, J. C. (1997) *Nature (London)* 387, 773–776.
26. Cory, S. & Strasser, A. (1997) *Oncogene* 14, 405–414.
27. Han, J., Sabbatini, P., Perez, D., Rao, L., Modha, D. & White, E. (1996) *Genes Dev.* 10, 461–477.
28. Chen, G., Branton, P. E., Yang, E., Korsmeyer, S. J. & Shore, G. C. (1996) *J. Biol. Chem.* 271, 24221–24225.
29. Bargou, R. C., Wagener, C., Bommert, K., Mapara, M. Y., Daniel, P. T., Arnold, W., Dietel, M., Guski, H., Feller, A., Royer, H. D., et al. (1996) *J. Clin. Invest.* 97, 2651–2659.
30. Yin, C., Knudson, C. M., Korsmeyer, S. J. & Van Dyke, T. (1997) *Nature (London)* 385, 637–640.
31. Rampino, N., Yamamoto, H., Ionov, Y., Li, Y., Sawai, H., Reed, J. C. & Perucho, M. (1997) *Science* 275, 967–969.
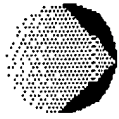
lalign output for Human long vs. Mouse

LALIGN finds the best local alignments between two sequences version 2.0u66 September 1998 Please cite: X. Huang and W. Miller (1991) Adv. Appl. Math. 12:373-381

```
Comparison of:
(A) ./wwwtmp/lalign/.5262.1.seq Human long
(B) ./wwwtmp/lalign/.5262.2.seq Mouse
 using matrix file: BL50, gap penalties: -14/-4

 68.6% identity in 175 aa overlap; score:   831 E(10,000): 1.2e-67

            40         50         60         70         80         90
Human   VLPCLGFTLLLWSQVSGAQGQEFHFGPCQVKGVVPQKLWEAFWAVKDTMQAQDNITSARL
        .:::!.. !:::!.:! : .:::!. : !:: !::  .::::::!.:!.:.!.:!.:!: ::
Mouse   ILPCLSLILLLWNQVPGLEGQEFRSGSCQVTGVVLPELWEAFWTVKNTVQTQDDITSIRL
          10         20         30         40         50         60

           100        110        120        130        140        150
Human   LQQEVLQNVSDAESCYLVHTLLEFYLKTVFKNYHNRTVEVRTLKSFSTLANNFVLIVSQL
        :. .:!.::! :!::::!:.:::.::!.:!:::.. .. .:.:.::!!.:!.:.!.:!::
Mouse   LKPQVLRNVSGAESCYLAHSLLKFYLNTVFKNYHSKIAKFKVLRSFSTLANNFIVIMSQL
          70         80         90        100        110        120

           160        170        180       .190        200
Human   QPSQENEMFSIRDSAHRRFLLFRRAFKQLDVEAALTKALGEVDILLTWMQKFYKL
        :::!..: !. : .:!::.:::::::::::::.:.:!.::.:!:::::::::::::.:
Mouse   QPSKDNSMLPISESAHQRFLLFRRAFKQLDTEVALVKAFGEVDILLTWMQKFYHL
          130        140        150        160        170        180
```

```
 71.4% identity in 7 aa overlap; score:    34 E(10,000): 6.5e+03

            . 200
Human   ILLTWMQ
        ::: : :
Mouse   ILLLWNQ
            20
```

```
 33.3% identity in 27 aa overlap; score:    32 E(10,000): 7.9e+03

            30         40         50
Human   QMQMVVLPCLGFTLLLWSQVSGAQGQE
        :.  :::: :  ..  :.  . :! :.
Mouse   QVTGVVLPELWEAF--WTVKNTVQTQD
            40         50
```

Back to ISREC bioinformatics group home page

Conversion of a β-Ketoacyl Synthase to a Malonyl Decarboxylase by Replacement of the Active-Site Cysteine with Glutamine[†]

Andrzej Witkowski,[‡] Anil K. Joshi,[‡] Ylva Lindqvist,[§] and Stuart Smith*,[‡]

Children's Hospital Oakland Research Institute, Oakland, California 94609, and Department of
Medical Biochemistry and Biophysics, Karolinska Institutet, Stockholm, Sweden

ABSTRACT: β-Ketoacyl synthases involved in the biosynthesis of fatty acids and polyketides exhibit extensive sequence similarity and share a common reaction mechanism, in which the carbanion participating in the condensation reaction is generated by decarboxylation of a malonyl or methylmalonyl moiety; normally, the decarboxylation step does not take place readily unless an acyl moiety is positioned on the active-site cysteine residue in readiness for the ensuing condensation reaction. Replacement of the cysteine nucleophile (Cys-161) with glutamine, in the β-ketoacyl synthase domain of the multifunctional animal fatty acid synthase, completely inhibits the condensation reaction but increases the uncoupled rate of malonyl decarboxylation by more than 2 orders of magnitude. On the other hand, replacement with Ser, Ala, Asn, Gly, and Thr compromises the condensation reaction without having any marked effect on the decarboxylation reaction. The affinity of the β-ketoacyl synthase for malonyl moieties, in the absence of acetyl moieties, is significantly increased in the Cys161Gln mutant compared to that in the wild type and is similar to that exhibited by the wild-type β-ketoacyl synthase in the presence of an acetyl primer. These results, together with modeling studies of the Cys → Gln mutant from the crystal structure of the Escherichia coli β-ketoacyl synthase II enzyme, suggest that the side chain carbonyl group of the Gln-161 can mimic the carbonyl of the acyl moiety in the acyl−enzyme intermediate so that the mutant adopts a conformation analogous to that of the acyl−enzyme intermediate. Catalysis of the decarboxylation of malonyl-CoA requires the dimeric form of the Cys161Gln fatty acid synthase and involves prior transfer of the malonyl moiety from the CoA ester to the acyl carrier protein domain and subsequent release of the acetyl product by transfer back to a CoA acceptor. These results suggest that the role of the Cys → Gln β-ketoacyl synthases found in the loading domains of some modular polyketide synthases likely is to act as malonyl, or methylmalonyl, decarboxylases that provide a source of primer for the chain extension reactions catalyzed by associated modules containing fully competent β-ketoacyl synthases.

β-Ketoacyl synthases play critical roles in the biosynthesis of a variety of natural products, including fatty acids, the polyketide precursors of commercially important pharmacological agents, and the mycolic acid precursors for the cell wall of disease-causing mycobacteria. These enzymes have been identified as targets for the development of new drugs for fighting cancer (1−4) and tuberculosis (5) and for the engineering of transgenic plants that could produce seed oils with unique compositions (6). The β-ketoacyl synthases catalyze the formation of new carbon−carbon bonds by condensation of a variety of acyl chain precursors with an elongating carbon source, usually malonyl or methylmalonyl moieties, that is covalently attached via a thioester linkage to an ACP.[1] The β-ketoacyl synthases exist in two different molecular forms. In plants and the majority of prokaryotes,

the enzymes consist of approximately 400 residues and typically form homodimers and are called monofunctional polypeptide, or type II, systems (7, 8). On the other hand, in the fatty acid-synthesizing systems of animals and the structurally related modular polyketide systems of prokaryotes, the β-ketoacyl synthases constitute one of the catalytic domains of large molecular complexes, called multifunctional polypeptide, or type I, systems (9−11). In the type II FAS systems of plants and microorganisms, multiple forms of β-ketoacyl synthases have been described that have different substrate specificities. Thus, β-ketoacyl synthases I and II can effectively elongate short-chain precursors to the 14-carbon stage, but further elongation, in particular the elongation of C16:1-ACP to C18:1-ACP, is more efficiently catalyzed by β-ketoacyl synthases II (8, 12−14). Type II β-ketoacyl synthases recently identified in Mycobacterium tuberculosis, named β-ketoacyl synthases A and B, apparently specialize in elongating acyl-ACPs containing more than 26 carbon atoms and play important roles in the production of mycolic acids by this organism (5). In the

---

* To whom correspondence should be addressed: Children's Hospital Oakland Research Institute, 747 52nd St., Oakland, CA 94609. Telephone: (510)428-3523. Fax: (510)428-3608. E-mail: ssmith@mail.cho.org.
‡ Children's Hospital Oakland Research Institute.
§ Karolinska Institutet.

[1] Abbreviations: ACP, acyl carrier protein; FAS, fatty acid synthase; KS[Q], β-ketoacyl synthase domain in which the usual active-site cysteine residue is replaced with glutamine.

Scheme 1: Reactions Catalyzed by the β-Ketoacyl Synthase Domain of (a) Wild-Type FAS and (b) the C161Q FAS Mutant

(a)

(b)
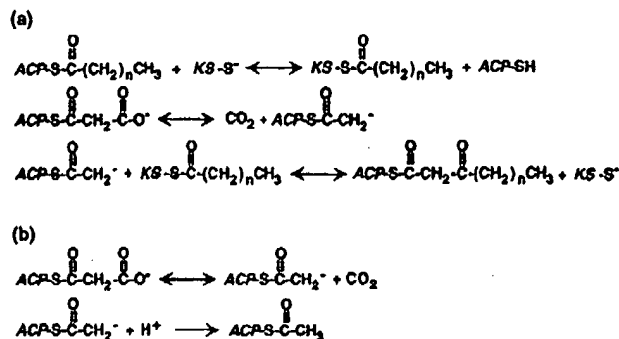
animal type I FAS, a single β-ketoacyl synthase catalyzes all of the condensation reactions that are necessary for elongation of a two-carbon precursor to palmitic acid (15–17). The type I modular polyketide synthases utilize a different β-ketoacyl synthase for each of the elongation steps, leading to the production of complex polyketides, whereas their type II counterparts utilize the same β-ketoacyl synthases for each condensation reaction that is required for the production of aromatic polyketides.

All of the various members of the β-ketoacyl synthase family of enzymes likely utilize the same basic reaction mechanism involving, successively, transfer of the first substrate from the ACP phosphopantetheine to a cysteine nucleophile, decarboxylation of the second substrate, either malonyl- or methylmalonyl-ACP, to yield the carbanion, and finally a nucleophilic attack of the carbanion on the carbonyl of the cysteine-bound acyl substrate, resulting in the formation of a new carbon–carbon bond (Scheme 1). Although the identity of the cysteine nucleophile is well-established, other residues that have been implicated in the reaction mechanism have not been unambiguously identified, this despite the recent determination of the crystal structure of one of the *Escherichia coli* β-ketoacyl synthases II (18).

The residues promoting decarboxylation of malonyl (or methylmalonyl)-ACP are particularly difficult to pinpoint since, in the absence of the first substrate, decarboxylation of malonyl moieties takes place at a rate that is far slower than when accompanied by a condensation reaction. Presumably, this phenomenon reflects the importance to the enzyme of generating the reactive carbanion species only when a recipient acyl chain is positioned on the active-site cysteine, thus avoiding the loss of malonyl moieties and establishing a futile cycle. In seeking a means of uncoupling the decarboxylation and condensation reactions, while maintaining the full capacity of the former, we were intrigued by the discovery that several modular polyketide synthases possess a β-ketoacyl synthase domain in which the active-site cysteine residue is replaced with glutamine. These unusual β-ketoacyl synthases, termed KS^Q domains, are found at the N-terminus of a loading module, the role of which is to provide the starter substrate for the first condensation reaction catalyzed by the adjacent fully competent module (19–21). In other modular polyketide synthases, loading modules are specialized either to facilitate the transfer of unusual primers, for example, a dihydrocyclohexylcarbonyl moiety in the FK506 (22) and rapamycin (23) polyketide synthases, or to contain only an acyltransferase and ACP domain, for

example, in the 6-deoxyerythronolide B polyketide synthase (11), or are lacking entirely, as in the pyoluteorin polyketide synthase (24).

A role for the KS^Q enzymes has yet to be proposed. Since replacement of the cysteine nucleophile with glutamine would preclude catalysis of the condensation reaction, we reasoned that the role of a KS^Q domain might be to increase the efficiency of primer delivery by the loading module. Modification of the active-site cysteine residue of β-ketoacyl synthases by iodoacetamide is known to increase the rate of uncoupled malonyl decarboxylase activity in yeast and fungal type I FASs (25, 26). Therefore, on the basis of the structural similarity between the Gln side chain ($CH_2CH_2CONH_2$) and that of the iodoacetamide-modified cysteine side chain (CH_2-SCH_2CONH_2), we hypothesized that KS^Q domains might provide the primer substrate for polyketide synthesis by promoting decarboxylation of malonyl, or methylmalonyl, moieties. The objective of this study, then, was to test the hypothesis that replacement of the cysteine nucleophile in a β-ketoacyl synthase would convert the condensing enzyme into a potent malonyl decarboxylating enzyme.

EXPERIMENTAL PROCEDURES

Construction of cDNAs Encoding His6- and FLAG-Tagged FASs and Expression of the Proteins in Sf9 Cells. The strategies for construction of cDNAs encoding the wild-type FAS, single domain-specific mutants and for introduction of His_6 or FLAG tags have been described in detail previously (27–30). The Cys161 mutant FASs were constructed by first generating mutated partial cDNA fragments by polymerase chain reaction amplification, using pFAS 74.20 (partial FAS cDNA in pUCBM20) as the template together with the appropriate primers (27). Oligonucleotide FAS1152B (5′-cac tag aat tcT TCA GGG TTG GGG TTG TGG AAA TGC; uppercase letters correspond to bp 1152–1176 of the rat FAS cDNA, and lowercase letters correspond to nucleotides added for the introduction of restriction sites) was used as the antisense primer. The sequence of the sense primers was 5′-TCA AAG GAC CCA GCA TTG CCC TGG ACA CAG CCN NNT CCT CTA GCC T (bp 530–575 of rat FAS cDNA), NNN being GBA for Cys161Ala/Gly (B denotes C, G, or T), ASC for Cys161Ser/Thr (S denotes C or G), AAT for Cys161Asn, and CAA for the Cys161Gln mutant.

The authenticity of the amplification products was confirmed by DNA sequencing, and the appropriate fragments were moved stepwise into the full-length, wild-type construct (27, 32). The final constructs for Cys161Ser/Gln/Asn mutants also encoded a C-terminal His_6 affinity tag, and those for the Cys161Ala/Gly mutants encoded a C-terminal FLAG tag, although the presence of the tags was not exploited in these studies. These FAS cDNA constructs, in the context of the pFASTBAC 1 vector, were used to generate recombinant baculovirus stocks by the transposition method employing the BAC-to-BAC baculovirus expression system according to the manufacturer's instructions. Sf9 cells were then infected with the purified recombinant viruses and cultured for 48 h at 27 °C. The tagged FAS proteins were partially purified from the cytosols as described previously (27) and then subjected to final purification by affinity chromatography (30); glycerol (10%, v/v) was included in all the buffers that were used for chromatography.
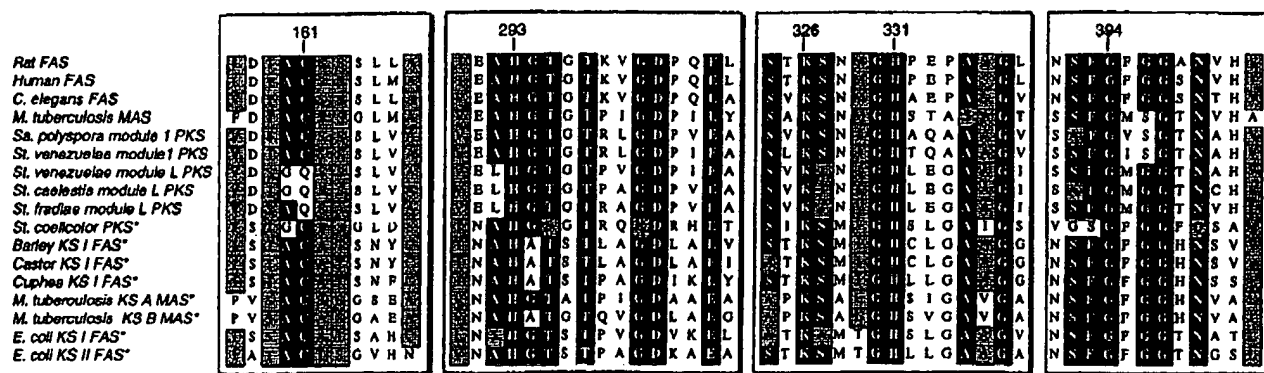
FIGURE 1: Alignment of the amino acid sequences from four regions of β-ketoacyl synthases. Those β-ketoacyl synthases associated with multifunctional (type I) and monofunctional (type II) polypeptides are distinguished by asterisks. MAS, mycolic acid synthesis; PKS, polyketide synthesis; *C., Caenorhabditis; M., Mycobacterium; Sa., Saccharopolyspora; St., Streptomyces; E., Escherichia.* The numbering system is that for the rat FAS. Consensus residues, defined by 75% compliance, are denoted by black shading and conservative replacements by gray shading. The GenBank protein ID numbers for the sequences, in the order in which they are listed, are (1) 66561, (2) 2117715, (3) 3876624, (4) 547900, (5) 416965, (6 and 7) 3800834, (8) 2558838, (9) 2317860, (10) 729876, (11) 119784, (12) 294666, (13) 3800749, (14) 1261947, (15) 1261948, (16) 119783, and (17) 729460.

Estimation of the Proportion of Monomers and Dimers in FAS Preparations. Proteins were chromatographed on a SigmaChrom GFC-1300 column (0.75 cm × 30 cm) in 0.25 M potassium phosphate (pH 7) and 1 mM EDTA, employing a flow rate of 0.5 mL/min at 20 °C, and were detected by monitoring the absorbance of the effluent at 280 nm. Blue dextran, FAS dimers, and FAS monomers were eluted with retention times of 9.0, 10.5, and 11.5 min, respectively.

Dissociation and Reassociation of FAS Subunits. FASs [in 50 mM potassium phosphate buffer (pH 7.0), 1 mM DTT, 1 mM EDTA, and ~1% glycerol] were aged at 4 °C for 7—9 days to promote dissociation into their component subunits (*31*). Spontaneous reassociation of the subunits was induced by adjustment of the solvent to approximately 0.2 M potassium phosphate (pH 7.0) and 10% glycerol and incubation at 30 °C for 75 min.

Assay for Decarboxylation of Malonyl Moieties. Decarboxylase activity was assayed by quantification of acetyl-CoA, β-ketobutyryl-CoA, and triacetic acid lactone formed from malonyl-CoA. Enzymes were incubated at 37 or 10 °C for 1—2 min with 110 μM [2-^{14}C]malonyl-CoA and 50 μM CoASH in 0.2 M potassium phosphate buffer (pH 6.6); CoASH was omitted from the reaction mixture when the activity of the wild-type FAS was assayed. Reactions were quenched with perchloric acid (*28*), and the products were identified by reversed-phase HPLC (*32*). Triacetic acid lactone (retention time of 9.3 min) was identified in the eluate by comparison with the elution position of a chemically synthesized standard. The overall decarboxylase activity was calculated on the basis of the total amount of acetyl units formed from malonyl-CoA, and includes those released from the enzyme by transfer to CoASH as well as those utilized as primers for condensation and subsequently released as either β-ketobutyryl-CoA or triacetic acid lactone. A unit of activity is equivalent to 1 μmol of malonyl moieties decarboxylated per minute at the specified temperature.

Overall Fatty Acid Synthesizing Activity. Activity was measured spectrophotometrically at 37 or 10 °C (*33*). A unit of activity is equivalent to 1 μmol of NADPH oxidized per minute at the specified temperature.

Modification of FAS by Iodoacetamide. The FAS storage buffer was replaced with 0.25 M potassium phosphate (pH

5.8) containing 1 mM EDTA and 0.5 mM tris(2-carboxy-ethyl)phosphine (Calbiochem-Novabiochem Corp., San Diego, CA) by centrifugation through a BioGel P-30 (Bio-Rad, Hercules, CA) gel filtration column (*34*). The modification reaction was carried out at 20 °C using 0.73 mM iodoacet-amide; to protect the phosphopantetheine thiol from modification, 0.96 mM malonyl-CoA was included in the reaction mixture. The reaction was quenched by addition of mercapto-ethanol to a final concentration of 10 mM, and the reaction buffer was replaced with storage buffer by repeated dilution and concentration in a Centricon-100 device (Amicon, Inc., Beverly, MA).

Modeling of Mutant Structures. Crude models of the various β-ketoacyl synthase mutants were generated from the crystal structure of β-ketoacyl synthase II from *E. coli* (*18, 35*), using the mutate option in the graphics program O (*36*) and manual optimization using the torsion command.

RESULTS AND DISCUSSION

Effect of Replacement of the β-Ketoacyl Synthase Active-Site Cysteine Residue upon Catalysis of the Malonyl Decarboxylation Reaction. Recently, it has become apparent that, with the possible exception of the β-ketoacyl synthase type III enzymes, all of the β-ketoacyl synthases involved in the biosynthesis of fatty acids, polyketides, and mycolic acid precursors share appreciable sequence similarity and are clearly related both structurally and evolutionarily (*37*). Thus, multiple sequence alignments provided the first clues about the possible identities of residues that play critical roles in catalysis (*37*). In addition to the cysteine nucleophile (Cys-161 in the rat FAS), three basic residues are universally conserved (corresponding to His-293, Lys-326, and His-331 in the rat FAS) that likely play important roles either catalytically or structurally (Figure 1). A conserved glycine-rich region near the C-terminus has also been implicated as facilitating the entry of substrates into the active-site pocket (*18*). With the exception of the cysteine nucleophile, all of these regions are also well-conserved in the KS^Q domains that are associated with the loading modules of the modular polyketide synthases responsible for the synthesis of the macrolides 10-deoxymethynolide and narbonolide (*Streptomyces venezu-elae*), tylactone (*Streptomyces fradiae*), and the macrolide

portion of niddamycin (*Streptomyces caelestis*). If the role of the KS^Q domains were to increase the efficiency of primer delivery, we surmised that replacement of the cysteine nucleophile alone might be sufficient to induce malonyl decarboxylase activity in the β-ketoacyl synthases. Several different amino acid replacements, including glutamine, were engineered into position 161 of the rat FAS and the recombinant proteins purified.

As anticipated, the Cys161Gln mutant is inactive in the spectrophotometric assay for fatty acid synthesis (Figure 2a). In this assay, the activity of the wild-type FAS is dependent on the presence of the cosubstrate, acetyl-CoA, as well as malonyl-CoA and NADPH (Figure 2, compare traces b and f). However, when the Cys161Gln mutant FAS is included in the same assay together with the wild-type FAS, the dependency on added acetyl-CoA is eliminated (Figure 2, compare trace b with traces c−e). In reaction mixtures containing the highest levels of the Cys161Gln mutant, the initial rate of reaction is similar to that observed in the presence of added acetyl-CoA but drops to zero after about 8 min (Figure 2e); the addition of more malonyl-CoA at this time sparks the reaction back to the original rate (denoted by arrow). These results are consistent with the Cys161Gln mutant having catalyzed the decarboxylation of malonyl-CoA, thus providing a supply of acetyl moieties required by the wild-type FAS. In the presence of high levels of the mutant, the availability of malonyl-CoA eventually becomes rate-limiting for the wild-type FAS (Figure 2e). These conclusions were confirmed by subsequent characterization of the Cys161Gln mutant and comparison of its properties with those of the other Cys-161 mutants.

Replacement of the cysteine nucleophile with Gln, Ser, Ala, Asn, Gly, or Thr completely eliminates the ability to catalyze the condensation reaction and consequently eliminates overall FAS activity (Table 1). Only replacement of Cys-161 with Ser produces a β-ketoacyl synthase with residual catalytic activity, as described previously (*38*). Introduction of the Cys161Gln mutation increases malonyl decarboxylase activity 150-fold compared to that of the wild-type FAS, whereas replacement of Cys-161 with other residues either reduces, or only slightly increases, malonyl decarboxylase activity. In the case of the wild-type FAS, most of the acetyl moieties produced by decarboxylation of malonyl moieties are condensed with either one or two malonyl moieties, resulting ultimately in the release of either β-ketobutyryl-CoA or triacetic acid lactone from the enzyme. However, in the case of the Cys161Gln mutant, since no condensation can take place, all of the acetyl moieties produced are released as acetyl-CoA (Table 1).

Decarboxylation of Malonyl Moieties Requires Prior Translocation from CoA to ACP Thioester. The malonyl decarboxylase activity associated with the Cys161Gln mutant is stimulated approximately 2-fold by the addition of 20−50 μM CoASH (data not shown), indicating that the malonyl moieties likely are decarboxylated following transfer to the FAS, so that release of the acetyl product requires the addition of CoASH as an acceptor. In the case of the wild-type FAS, where the rate of decarboxylation is relatively slow, most of the product is released as triacetic acid lactone and β-ketobutyryl-CoA. For each equivalent of triacetic acid lactone that is formed, 3 equiv of CoASH is released, and for each equivalent of β-ketobutyryl-CoA that is formed, 2
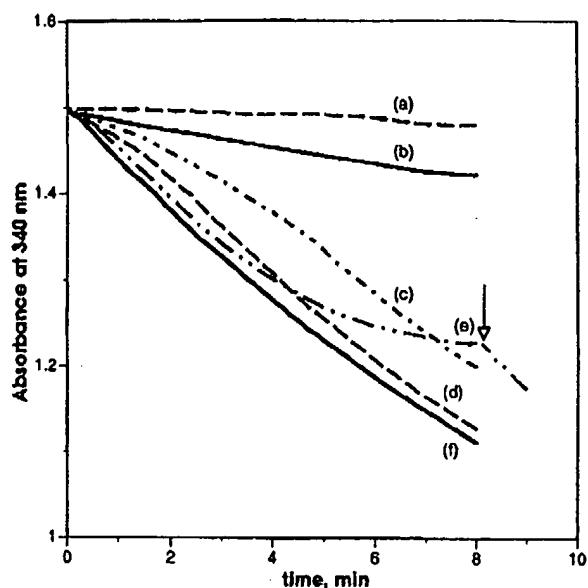

FIGURE 2: Elimination of the requirement for acetyl-CoA by the wild-type FAS in the presence of the Cys161Gln FAS mutant. Spectrophotometric assays were performed at 37 °C. All reaction mixtures contained, in a volume of 0.2 mL, 0.1 M potassium phosphate (pH 6.6), 0.25 mM NADPH, 135 μM malonyl-CoA, and 50 μM CoASH. In addition, individual assays contained (a) 10 μg of Cys161Gln FAS and 65 μM acetyl CoA, (b) 1.5 μg of wild-type FAS (no acetyl-CoA added), (c) wild-type and Cys161Gln FASs, 1.5 μg each (no acetyl-CoA added), (d) 1.5 μg of wild-type and 4.5 μg of Cys161Gln FASs (no acetyl-CoA added), (e) 1.5 μg of wild-type and 10 μg of Cys161Gln FASs (no acetyl-CoA added), with additional malonyl-CoA (200 μM) added at the time marked by the arrow, and (f) 1.5 μg of wild-type FAS and 65 μM acetyl-CoA.

equiv of CoASH is released and only 1 equiv is utilized. Presumably, this net overproduction of CoASH, together with the slow rate of decarboxylation, ensures that CoA availability does not become rate-limiting for product release by the wild-type FAS. The fact that the decarboxylation of malonyl moieties requires the initial loading of malonyl moieties onto the phosphopantetheine thiol attached to Ser-2151, via the active-site serine residue of the malonyl/acetyltransferase, Ser-581, is also supported by the observation that mutation of either of these serine residues to alanine eliminates decarboxylase activity (Table 1).

Since no condensation products are produced by the Cys161Ala, Cys161Asn, and Cys161Gly mutants, which lack an appropriate nucleophile at position 161, only acetyl-CoA is recovered as a product, although in these cases the rate of formation of acetyl-CoA is much slower than for the Cys161Gln mutant (Table 1). For comparison, the properties of the iodoacetamide-treated FAS were also studied. As has been reported for the yeast FAS (*25*), both the β-ketoacyl synthase and overall fatty acid synthesizing activity of the rat FAS are markedly lowered by the modification, whereas the malonyl decarboxylase activity is increased; most of the acetyl moieties that are produced are released by transfer to a CoA acceptor. However, the increment in decarboxylase activity is modest when compared to that produced by the Cys161Gln mutation.

To determine whether the dimeric form of the Cys161Gln FAS is required for catalysis of the decarboxylation reaction, we again utilized the spectrophotometric assay, in which the presence of an active malonyl decarboxylase activity obviates

Table 1: Characterization of FASs Mutated or Chemically Modified at Cys-161[a]

| FAS | FAS synthesis (milliunits/mg) | β-ketobutyryl-CoA synthesis (milliunits/mg) | malonyl decarboxylation | | | |
			activity (milliunits/mg)	TAL[b] (%)	β-ketobutyryl-CoA (%)	acetyl-CoA (%)
wild-type	2029 ± 43	130 ± 10	3.3 ± 0.2	49	49	2
Cys161Gln	0	0	495 ± 16	0	0	100
iodoacetamide-treated wild-type	53 ± 10	2.8 ± 0.1	6.4 ± 0.3	0	15	85
Cys161Ser	13 ± 1	5.8 ± 0.7	1.3 ± 0.2	7	42	51
Cys161Ala	0	0	7.0 ± 0.1	0	0	100
Cys161Asn	0	0	1.5 ± 0.1	0	0	100
Cys161Gly	0	0	0.2 ± 0.0	0	0	100
Cys161Thr	0	0	0			
Ser215Ala (ACP-)	0	0	0.0 ± 0.0			
Ser581Ala (MAT-)	0	0	0.0 ± 0.1			

[a] All assays were performed at 37 °C. [b] TAL is triacetic acid lactone.

the need for added acetyl-CoA in the synthesis of fatty acids by the wild-type FAS. In these experiments, the spectrophotometric assays were performed at 10 °C so that monomers added to the incubation system would not undergo reassociation during the course of the assay (*31*). Thus, in the absence of added acetyl-CoA, Cys161Gln FAS that had been dissociated into monomers, by aging in the cold, did not support fatty acid synthesis by the wild-type FAS (details not shown). Only when the subunits were reassociated prior to the assay did the Cys161Gln FAS support fatty acid synthesis by the wild-type FAS in the absence of added acetyl-CoA. The fact that the decarboxylation reaction is catalyzed only by the dimeric form of FAS was confirmed by direct assay. Thus, malonyl decarboxylase activities of Cys161Gln monomers and dimers, assayed directly at 10 °C, were 0.8 ± 0.1 and 64.5 ± 0.7 milliunits/mg, respectively, whereas activities of wild-type monomers and dimers were 0.03 ± 0.02 and 0.65 ± 0.01 milliunits/mg, respectively. These results are consistent with a mechanism that requires the proper juxtaposition of the malonyl/acetyltransferase, ACP, and β-ketoacyl synthase domains to allow transfer of the malonyl moiety to the ACP domain, interaction of the malonyl-S-ACP with the KS^Q domain, and release of the acetyl moiety by transfer back to a CoA acceptor. This critical juxtaposition of domains, existing only in the dimeric form of the enzyme, is also essential for catalysis of the condensation of acetyl and malonyl moieties by the wild-type FAS (*39*).

Mechanism of Induction of Malonyl Decarboxylase in the Cys161Gln Mutant. In the wild-type FAS, decarboxylation of an ACP-bound malonyl moiety normally takes place at an appreciable rate only when the cysteine nucleophile of the β-ketoacyl synthase domain, Cys-161, is occupied by an acyl moiety so that formation of the carbanion is tightly coupled to its reaction with the carbonyl group of the acyl moiety and little or no opportunity arises for reaction of the carbanion with a proton. It has not been demonstrated directly whether the decarboxylation reaction and addition of the carbanion to the carbonyl follow a concerted or stepwise pathway, although on the basis of theoretical considerations (*40*) and mechanistic similarities with other Claisen-type condensations (*41*), it has been inferred that the β-ketoacyl synthases also employ a stepwise path. In the Cys161Gln mutant, where acylation of residue 161 cannot take place, the only option for the carbanion is to react with a proton (Scheme 1). Since, in the Cys161Gln mutant, decarboxylation

of malonyl moieties can take place at a rate that is at least as great as that associated with the condensation reaction catalyzed by the wild-type FAS, it would appear that a proton is readily accessible.

We surmised that the elevated malonyl decarboxylase activity associated with the Cys161Gln mutant might result from an increase in the affinity of the β-ketoacyl synthase for malonyl moieties and devised an experimental system for examining the effect of the malonyl-S-ACP concentration on the rate of decarboxylation catalyzed by the wild type and the Cys161Gln mutant. Because the concentration of malonyl-S-ACP cannot be altered directly in the multifunctional form of FAS, we altered the level of saturation of the ACP with malonyl moieties by varying the concentration of malonyl-CoA in the presence of free CoASH; the latter compound influences the equilibrium between the enzyme-bound and CoA-bound forms of the substrate (*42*). The wild-type FAS and Cys161Gln mutant exhibited markedly different kinetics with respect to malonyl-CoA concentration. Whereas the rate of decarboxylation catalyzed by the Cys161Gln mutant almost reached saturation at 40 μM, the rate of decarboxylation catalyzed by the wild-type FAS was essentially a linear function of malonyl-CoA concentration over the range of 0−40 μM (Figure 3). Acetyl-CoA was the sole product formed by the Cys161Gln mutant, whereas the wild-type FAS produced a mixture of β-ketobutyryl-CoA (83%) and triacetic acid lactone (17%) under these conditions. Apparently, in the case of the wild-type FAS, acetyl moieties formed on the phosphopantetheine by decarboxylation of malonyl moieties are preferentially translocated to the Cys-161 thiol and utilized in the condensation reaction rather than being translocated back to the CoA acceptor, despite the high concentration of the latter used in these assays. At 40 μM malonyl-CoA, the rate of decarboxylation of malonyl moieties by the Cys161Gln mutant was 2 orders of magnitude higher than that catalyzed by the wild-type FAS. For comparison, we also examined the effect of malonyl-CoA concentration on the rate of β-ketobutyryl-CoA formation by the wild-type FAS in the presence of non-rate-limiting concentrations of acetyl-CoA (Figure 3). In contrast to the results obtained in the absence of added acetyl-CoA, 40 μM malonyl-CoA was sufficient to nearly saturate the system. The product, mainly β-ketobutyryl-CoA (triacetic acid lactone accounted for less than 3% of the products), was formed at a rate approaching that observed for the decarboxylation of malonyl moieties catalyzed by the
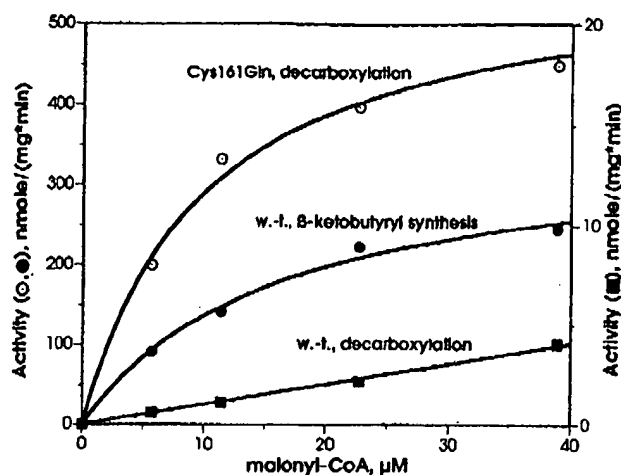
FIGURE 3: Kinetics of decarboxylation of malonyl-CoA by wild-type and Cys161Gln FAS. To assay decarboxylase activity, Cys161Gln (6.2 nM, O) and wild-type FASs (0.47 μM, ■) were incubated at 37 °C with radioactive malonyl-CoA in the presence of 50 μM CoASH for 1 min (see Experimental Procedures for more details). The β-ketobutyryl-CoA synthesizing activity of wild-type FAS (at 39 nM, ●) was assayed in the presence of 70 μM acetyl-CoA and 50 μM CoASH at 37 °C for 1 min. The reactions were stopped with perchloric acid and analyzed as described in Experimental Procedures. Cys161Gln and wild-type FASs were diluted with the storage buffer containing 0.75 mg/mL BSA, and as a consequence, these assays contained 37.5 μg/mL BSA. BSA by itself had no activity in either assay (data not shown). The V_{max} values calculated from the corresponding double-reciplocal plots were 360 (wild-type, β-ketobutyryl synthesis) and 580 nmol min^{-1} mg^{-1} (Cys161Gln, decarboxylation).

Cys161Gln mutant FAS. The malonyl-CoA concentration required to achieve a rate that equals half of the V_{max} value was similar for both reactions, indicating that the condensing wild-type FAS and the Cys161Gln FAS mutant interact similarly with the malonyl substrate. These results appear to be consistent with the hypothesis that the presence of a glutamine side chain at position 161 mimics the effect produced by the formation of an acyl-S-Cys-161 by the wild-type FAS. It may be significant that, of all the amino acid substitutions introduced at residue 161, only the glutamine side chain (CH$_2$CH$_2$CONH$_2$) introduces a carbonyl moiety at a position similar to that formed by the acyl-S-Cys intermediate (CH$_2$-S-COR).

More than 20 years ago, Lynen and co-workers (25) speculated that the β-ketoacyl synthase domain would exist in at least two distinct conformations, one favoring the acylation of the active-site cysteine and the other favoring the formation of the carbanion from malonyl-ACP; switching between conformations would be determined by the presence or absence of an acyl moiety on the cysteine nucleophile. Our results are consistent with this hypothesis since, in the absence of added acetyl-CoA, the β-ketoacyl synthase exhibits only weak affinity for malonyl moieties and decarboxylation occurs inefficiently. In contrast, in the presence of added acetyl-CoA, a relatively strong malonyl-binding site is created so that decarboxylation, coupled with condensation, takes place efficiently.

Structural Implications of the Cys → Gln Replacement. To probe possible structural effects of replacements of the active-site cysteine residue, the various mutants were modeled in the context of the structure of the β-ketoacyl synthase II of *E. coli* (18, 35). All mutations could easily be

accommodated in the substrate pocket with the exception of the Gln replacement (residue 163 in the *E. coli* enzyme, Figure 4). This substitution gives rise to close contacts with the side chain of a conserved phenylalanine (Phe-400 in the *E. coli* enzyme). However, it has been observed that this side chain changes conformation upon covalent attachment of cerulenin to the cysteine nucleophile, resulting in an opening of the substrate pocket both toward the surface and toward the dimer interface (35). This structural change might well influence the decarboxylase activity by facilitating access to the active-site pocket. The most striking feature of the Cys → Gln replacement, however, is that it is very homologous to an acyl intermediate in that the carbonyl groups occupy the same spatial position. When this intermediate is formed, it has to go through a tetrahedral transition state with a negative charge on the oxygen that has to be stabilized through protein interactions. From the crystal structure, one could surmise that this stabilization may be obtained through hydrogen bonds to the peptide NH group of the phenylalanine discussed above and perhaps by charge interactions with the second conserved histidine in the active site (18). Thus, this "oxy-anion binding pocket" would be open in the free enzyme, while in the acyl intermediate the acyl carbonyl oxygen would occupy this pocket. In the Cys → Gln mutant, the side chain could occupy this pocket in a similar way (Figure 4). It is very likely that in the case of the native free enzyme the negatively charged carboxyl group of the malonyl moiety would bind in this oxy-anion binding pocket in a fashion which is nonproductive for decarboxylation, while for the acyl intermediate or the Cys → Gln enzyme, the pocket is blocked and the malonyl moiety instead is bound in a productive way. Clearly, on the basis of our results to date, we cannot rule out unequivocally the possibility that decarboxylation of malonyl moieties by the Cys161Gln mutant occurs via a mechanism uniquely different from that which is operative in the wild-type enzyme when the reaction is coupled directly with condensation. Nevertheless, the predictions based on modeling of the Cys → Gln mutant in the context of the *E. coli* β-ketoacyl synthase II are entirely consistent with our observation that introduction of the glutamine side chain at position 161 creates a high-affinity binding site for malonyl moieties (Figure 3). Thus, identification of the Cys → Gln replacement as being particularly effective in uncoupling the decarboxylation and condensation steps of the β-ketoacyl synthase reaction may provide a unique model system that can be exploited to identify residues that are required for promotion of the decarboxylation step in the FAS reaction sequence.

The multifunctional FAS has proven to be a valuable paradigm for elucidation of the functional organization and programming rules that enable the modular polyketide synthases to synthesize a wide variety of macrolide products (11, 45). An immediate and important consequence of this study with a multifunctional FAS is the identification of a likely role for the KS^Q domains that are found characteristically at the N-termini of the loading modules of some multifunctional polyketide synthases. On the basis of the extensive sequence similarity of the β-ketoacyl synthases associated with polyketide and fatty acid synthesizing systems (Figure 1), it is reasonable to expect that these KS^Q domains also possess potent malonyl decarboxylase activity. Their location in the specialized loading modules represents
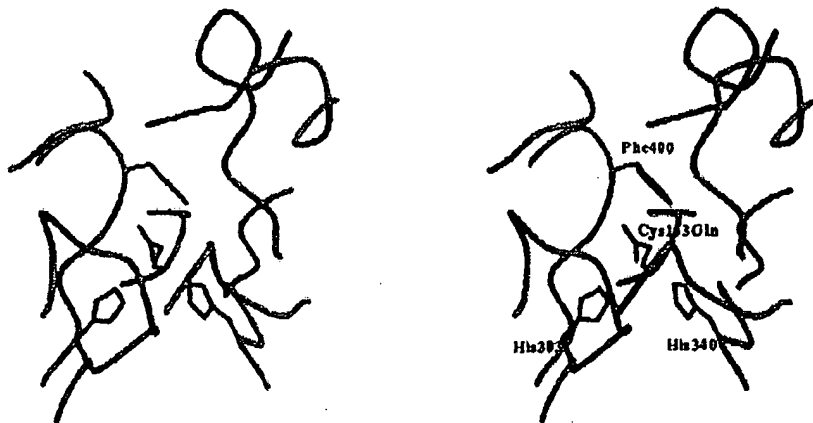
FIGURE 4: Stereoview of the active-site pocket in a model of the *E. coli* β-ketoacyl synthase II Cys163Gln mutant. Residues that are discussed are shown as ball-and-stick models and labeled according to the sequence numbering of the *E. coli* enzyme. The polypeptide chain of the surroundings is cyan, and part of the second subunit in the dimer is blue. This figure was prepared using Molscript (*43*) and Raster3d (*44*).

FIGURE 5: Comparison of conserved motifs within acyltransferase domains adjacent to KS^Q domains in the loading modules of several modular polyketide synthases. Consensus sequences for methyl-malonyl- and malonyl-specific acyltransferases were derived by sequence analysis of a large number of polyketide synthase domains (not including any KS^Q domains) that catalyze the transacylation of either methylmalonyl-CoA or malonyl-CoA onto ACP. Regions were identified in which the acyltransferase sequences diverged according to whether they were specific for malonyl-CoA or methylmalonyl-CoA (*46*). The locations of the conserved motifs are identified relative to the active-site serine within the GHSxG motif, which is designated position 1.

compelling circumstantial evidence indicating that this unique ability of the KS^Q domain to catalyze decarboxylation of the substrate normally used for chain extension has been exploited to optimize primer availability. Thus, the acetyl, or propionyl, moieties formed on the ACP domain by decarboxylation of malonyl, or methylmalonyl, moieties could be transferred directly to the ketoacyl synthase associated with the adjacent module responsible for performing the first elongation step. Further support for this hypothesis can be derived from an analysis of the amino acid sequences of the acyltransferase domains associated with loading modules that contain KS^Q domains (Figure 5). An earlier sequence analysis of acyltransferase domains associated with modular polyketide synthases revealed distinct differences in the sequences of those enzymes that exhibit specificity for malonyl and methylmalonyl moieties (*46*). Those acyltransferase domains that lie adjacent to the KS^Q domains of the modular polyketide synthases responsible for the synthesis of tylactone, in *S. fradiae*, and 10-deoxymethynolide and narbonolide, in *S. venezuelae*, contain the conserved sequence elements typical of the methylmalonyl-specific acyltransferases, whereas that associated with the niddamycin polyketide synthase, in *S. caelestis*, contains the sequence elements characteristic of the malonyl-specific class of acyltransferases. These specificities are exactly as anticipated if these acyltransferases were to supply the substrate for decarboxylation by the adjacent KS^Q domain. Thus, on the

basis of their chemical structures, it can be deduced that tylactone (*19*) and 10-deoxymethynolide and narbonolide (*21*) must be synthesized from a propionyl primer whereas niddamycin (*20*) is synthesized from an acetyl primer.

Conceivably, in the microenvironment surrounding the modular polyketide synthases, the substrate required for the multiple chain elongation steps may be present in excess over that required for the single priming step. The ability of the KS^Q domain to generate the primer substrate from the chain extender substrate moiety at precisely the right location could ensure that delivery of the priming substrate does not become rate-limiting for the overall reaction-sequence.

Discovery of the modular nature of the polyketide synthases responsible for production of complex macrolides has resulted in the emergence of novel strategies for the engineering of new pharmacological agents by genetic manipulation of the polyketide synthase modules. It is possible that the introduction of KS^Q domains into the loading modules of both engineered and natural polyketide synthases may offer an additional strategy for optimizing yields of macrolide products.

ACKNOWLEDGMENT

REFERENCES

1. Kuhajda, F. P., Jenner, K., Wood, F. D., Hennigar, R. A., Jacobs, L. B., Dick, J. D., and Pasternak, G. R. (1994) *Proc. Natl. Acad. Sci. U.S.A. 91*, 6379–6383.

2. Pizer, E. S., Wood, F. D., Pasternack, G. R., and Kuhajda, F. P. (1996) *Cancer Res. 56*, 745–751.

3. Pizer, E. S., Wood, F. D., Heine, H. S., Romantsev, F. E., Pasternack, G. R., and Kuhajda, F. P. (1996) *Cancer Res. 56*, 1189–1193.

4. Pizer, E. S., Jackisch, C., Wood, F. D., Davidson, N. E., Pasternack, G. R., and Kuhajda, F. P. (1996) *Cancer Res. 56*, 2745–2747.

5. Mdluli, K., Slayden, R. A., Zhu, Y., Ramaswamy, S., Pan, X., Mead, D., Crane, D. D., Musser, J. M., and Barry, C. E. 1. (1998) *Science 280*, 1607–1610.

6. Dehesh, K., Edwards, P., Fillatti, J., Slabaugh, M., and Byrne, J. (1998) *Plant J. 15*, 383–390.

7. Somerville, C., and Browse, J. (1991) *Science 252*, 80–87.

8. Magnuson, K., Jackowski, S., Rock, C. O., and Cronan, J. E. (1994) *Microbiol. Rev. 57*, 522−542.

9. Wakil, S. J. (1989) *Biochemistry 28*, 4523−4530.

10. Smith, S. (1994) *FASEB J. 8*, 1248−1259.

11. Donadio, S., Staver, M. J., McAlpine, J. B., Swanson, S. J., and Katz, L. (1991) *Science 252*, 675−679.

12. Clough, R. C., Matthis, A. L., Barnum, S. R., and Jaworski, J. G. (1992) *J. Biol. Chem. 267*, 20992−20998.

13. Tsay, J.-T., Oh, W., Larson, T. J., Jackowski, S., and Rock, C. O. (1992) *J. Biol. Chem. 267*, 6807−6814.

14. Edwards, P., Nelsen, J. S., Metz, J. G., and Dehesh, K. (1997) *FEBS Lett. 402* (1), 62−66.

15. Libertini, L. J., and Smith, S. (1979) *Arch. Biochem. Biophys. 192*, 47−60.

16. Anderson, V. E., and Hammes, G. G. (1985) *Biochemistry 24*, 2147−2154.

17. Witkowski, A., Joshi, K. A., and Smith, S. (1997) *Biochemistry 36* (51), 16338−16344.

18. Huang, W., Jia, J., Edwards, P., Dehesh, K., Schneider, G., and Lindqvist, Y. (1998) *EMBO J. 17*, 1183−1191.

19. Kuhstoss, S., Huber, M., Turner, J. R., Paschal, J. W., and Rao, R. N. (1996) *Gene 183* (1−2), 231−236.

20. Kakavas, S. J., Katz, L., and Stassi, D. (1997) *J. Bacteriol. 179* (23), 7515−7522.

21. Xue, Y., Zhao, L., Liu, H.-W., and Sherman, D. H. (1998) *Proc. Natl. Acad. Sci. U.S.A. 95*, 12111−12116.

22. Motamedi, H., and Shafiee, A. (1998) *Eur. J. Biochem. 256*, 528−534.

23. Schwecke, T., Aparicio, J. F., Molnar, I., König, A., Khaw, L. E., Haydock, S. F., Oliynyk, M., Caffrey, P., Cortes, J., Lester, J. B., Böhm, G. A., Staunton, J., and Leadlay, P. F. (1995) *Proc. Natl. Acad. Sci. U.S.A. 92*, 7839−7843.

24. Nowak-Thompson, B., Gould, S. J., and Loper, J. E. (1997) *Gene 204*, 17−24.

25. Kresze, E.-B., Steber, L., Oesterhelt, D., and Lynen, F. (1977) *Eur. J. Biochem. 79*, 191−199.

26. Tomoda, H., Kawaguchi, A., Omura, S., and Okuda, S. (1984) *J. Biochem. 95*, 1705−1712.

27. Joshi, A. K., and Smith, S. (1993) *Biochem. J. 296*, 143−149.

28. Witkowski, A., Joshi, A. K., and Smith, S. (1996) *Biochemistry 35*, 10569−10575.

29. Joshi, A. K., Witkowski, A., and Smith, S. (1998) *Biochemistry 37*, 2515−2523.

30. Joshi, A. K., Rangan, V. S., and Smith, S. (1998) *J. Biol. Chem. 273*, 4937−4943.

31. Smith, S., and Abraham, S. (1971) *J. Biol. Chem. 246*, 6428−6435.

32. Joshi, A. K., and Smith, S. (1993) *J. Biol. Chem. 268*, 22508−22513.

33. Smith, S., and Abraham, S. (1975) *Methods Enzymol. 35*, 65−74.

34. Penefsky, H. S. (1977) *J. Biol. Chem. 252*, 2891−2899.

35. Moche, M., Schneider, G., Edwards, P., Dehesh, K., and Lindqvist, Y. (1999) *J. Biol. Chem. 274*, 6031−6034.

36. Jones, T. A., Zou, J.-Y., Cowan, S., and Kjeldgaard, M. (1991) *Acta Crystallogr. A47*, 100−119.

37. Siggaard-Andersen, M. (1993) *Protein Sequences Data Anal. 5*, 325−335.

38. Joshi, A. K., Witkowski, A., and Smith, S. (1997) *Biochemistry 36*, 2316−2322.

39. Kumar, S., Dorsey, J. A., Muesing, R. A., and Porter, J. W. (1970) *J. Biol. Chem. 245*, 4732−4744.

40. Dewar, M. J. S., and Dieter, K. M. (1988) *Biochemistry 27*, 3302−3308.

41. Clark, J. D., O'Keefe, J. O., and Knowles, J. R. (1988) *Biochemistry 27*, 5961−5971.

42. Stern, A., Sedgwick, B., and Smith, S. (1982) *J. Biol. Chem. 257*, 799−803.

43. Kraulis, P. (1991) *J. Appl. Crystallogr. 24*, 946−950.

44. Merrit, E. A., and Murphy, M. E. P. (1994) *Acta Crystallogr. D50*, 869−873.

45. Donadio, S., and Katz, L. (1992) *Gene 111* (1), 51−60.

46. Haydock, S. F., Aparicio, J. F., Molnar, I., Schwecke, T., Khaw, L. E., Konig, A., Marsden, A. F., Galloway, I. S., Staunton, J., and Leadlay, P. F. (1995) *FEBS Lett 374*, 246−248.

Melamine Deaminase and Atrazine Chlorohydrolase: 98 Percent Identical but Functionally Different

JENNIFER L. SEFFERNICK,[1,2] MERVYN L. DE SOUZA,[1,2]† MICHAEL J. SADOWSKY,[1,2,3,4] AND
LAWRENCE P. WACKETT[1,2,3]*

Department of Biochemistry, Molecular Biology, and Biophysics,[1] Biological Process Technology Institute,[3]
Center for Microbial and Plant Genomics,[2] and Department of Soil, Water, and Climate,[4]
University of Minnesota, St. Paul, Minnesota 55108

The gene encoding melamine deaminase (TriA) from *Pseudomonas* sp. strain NRRL B-12227 was identified, cloned into *Escherichia coli*, sequenced, and expressed for in vitro study of enzyme activity. Melamine deaminase displaced two of the three amino groups from melamine, producing ammeline and ammelide as sequential products. The first deamination reaction occurred more than 10 times faster than the second. Ammelide did not inhibit the first or second deamination reaction, suggesting that the lower rate of ammeline hydrolysis was due to differential substrate turnover rather than product inhibition. Remarkably, melamine deaminase is 98% identical to the enzyme atrazine chlorohydrolase (AtzA) from *Pseudomonas* sp. strain ADP. Each enzyme consists of 475 amino acids and differs by only 9 amino acids. AtzA was shown to exclusively catalyze dehalogenation of halo-substituted triazine ring compounds and had no activity with melamine and ammeline. Similarly, melamine deaminase had no detectable activity with the halo-triazine substrates. Melamine deaminase was active in deamination of a substrate that was structurally identical to atrazine, except for the substitution of an amino group for the chlorine atom. Moreover, melamine deaminase and AtzA are found in bacteria that grow on melamine and atrazine compounds, respectively. These data strongly suggest that the 9 amino acid differences between melamine deaminase and AtzA represent a short evolutionary pathway connecting enzymes catalyzing physiologically relevant deamination and dehalogenation reactions, respectively.

Enzymes responsible for deamination reactions are widespread throughout intermediary metabolism and serve to incorporate and recycle nitrogen among key metabolites essential for DNA and protein synthesis. Some are members of an amidohydrolase protein superfamily, which catalyze at least 30% of the steps in four intermediary metabolic pathways (22). Recently, a new class of bacterial amidohydrolases has been identified; they catalyze the hydrolytic displacement of amino groups and chlorine substituents from *s*-triazine ring compounds (22, 32).

The *s*-triazine compounds have numerous applications throughout industry and agriculture (10, 19, 25, 30). Those containing *N*-alkyl substituents, like atrazine (2-chloro-4-*N*-ethylamino-6-*N*-isopropylamino-1,3,5-triazine), have been applied successfully as herbicides (3). Atrazine and analogous chlorinated *s*-triazines were initially considered to be incompletely metabolized by microorganisms (10, 19). However, 40 years after the initial introduction of atrazine into the environment, bacteria with the ability to completely mineralize this herbicide have been isolated (12, 26, 31, 40). Subsequently, bacteria were shown to initiate atrazine metabolism via dechlorination to yield hydroxyatrazine (2, 8, 12, 26, 31, 40). In 1996, the dechlorinating enzyme atrazine chlorohydrolase (AtzA) was purified and shown, via [18O]water experiments, to catalyze a hydrolytic displacement reaction (Fig. 1) (13).

The substrate specificity of AtzA from *Pseudomonas* sp. strain ADP was recently investigated (35). AtzA catalyzes the hydrolytic removal of a chlorine or fluorine substituent but does not remove cyano, azido, methoxy, thiomethyl, or amino substituents from compounds structurally analogous to atrazine. AtzA is also not active with any of the pyrimidine substrates tested (35).

Melamine (2,4,6-triamino-1,3,5-triazine), a related *s*-triazine that predates the use of atrazine (29), is also metabolized by soil bacteria. Worldwide production of melamine in 1994 was estimated to be 900 million lb (21). Melamine is most commonly used in the production of melamine-formaldehyde resins, which are used in laminates, adhesives, fire retardants, molding compounds, coatings, and concrete plasticizers (29). Prior to the identification of atrazine-mineralizing bacteria, Cook and Hutter isolated melamine-metabolizing pseudomonads (11). One of these, *Pseudomonas* sp. strain NRRL B-12227, catalyzes consecutive hydrolysis of the three amino substituents of melamine, producing the intermediates ammeline, ammelide, and cyanuric acid (Fig. 1). Another bacterium, *Pseudomonas* sp. strain NRRL B-12228, was unreactive with melamine but catalyzed deamination of ammeline to ammelide and of ammelide to cyanuric acid (11). Genes for ammeline and ammelide deamination, *trzB* and *trzC*, respectively, have been cloned from *Pseudomonas* sp. strain NRRL B-12228 (17). Detailed restriction site pattern analysis revealed conservation of *trzC* but not *trzB* in *Pseudomonas* sp. strain NRRL B-12227 (17). The genes encoding the enzyme for melamine or ammeline deamination in *Pseudomonas* sp. strain NRRL B-12227, however, were not reported. Furthermore, *Pseudomonas* sp.

* Corresponding author. Mailing address: Department of Biochemistry, Molecular Biology, and Biophysics, 1479 Gortner Ave., University of Minnesota, St. Paul, MN 55108. Phone: (612) 625-3785. Fax: (612) 625-1700. E-mail: wackett@biosci.cbs.umn.edu.
† Present address: Cargill, Inc., Minneapolis, MN 55440-5702.

A.

Melamine → TriA → Ammeline
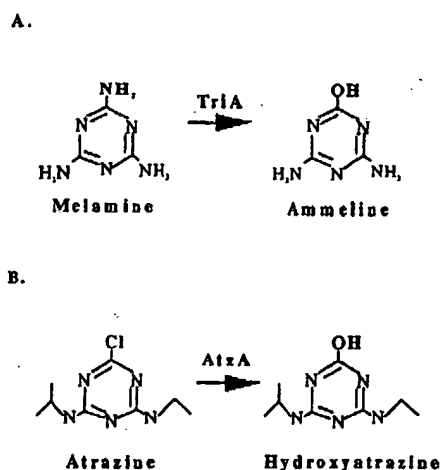
B.

Atrazine → AtzA → Hydroxyatrazine

FIG. 1. Comparison of the reactions catalyzed by melamine deaminase (TriA) from *Pseudomonas* sp. strain NRRL B-12227 (A) and AtzA from *Pseudomonas* sp. strain ADP (B).

strain NRRL B-12227 was shown not to metabolize atrazine (11).

Given the similarity in structure between melamine and atrazine and their similar hydrolytic metabolism, it was hypothesized here that AtzA gene probes and antibodies might be used to identify the melamine deaminase gene and protein, respectively, in *Pseudomonas* sp. strain NRRL B-12227. Using this strategy, the melamine deaminase gene, designated *triA*, was identified, cloned, and sequenced. The melamine deaminase gene from *Pseudomonas* sp. strain NRRL B-12227 was 99% identical to the *atzA* gene from *Pseudomonas* sp. strain ADP. The cloned melamine deaminase was expressed in *Escherichia coli* DH5α and shown to catalyze the deamination of melamine and ammeline. Melamine deaminase had no activity with any of the chlorotriazine substrates tested. Taken together with the known substrate specificity of AtzA, these studies identified two nearly identical proteins that catalyze clearly distinct biochemical reactions.

MATERIALS AND METHODS

Bacterial strains, plasmids, and growth conditions. *Pseudomonas* sp. strains NRRL B-12227 and NRRL B-12228 were provided by Richard Eaton (U.S. Environmental Protection Agency, Gulf Breeze, Fla.). *Pseudomonas* sp. strains NRRL B-12227 and NRRL B-12228 have similar restriction site patterns for the genes *trzC* and *trzD*, which convert ammelide to biuret (17). *Rhodococcus corallinus* NRRL B-15444R was obtained from the U.S. Department of Agriculture National Center for Agriculture Utilization Research (Peoria, Ill.). *Pseudomonas* or *Rhodococcus* strains were grown in R salt minimal medium (36) with either glucose or glycerol as the carbon source, respectively, and appropriate triazines as the sole nitrogen source. *Rhodococcus* strains were grown at 30°C, while *Pseudomonas* and *E. coli* strains were incubated at 37°C. *E. coli* DH5α transformants were grown on Luria-Bertani media (33) containing the appropriate antibiotic. The *atzA* clone *E. coli* DH5α(pMD4) was grown in media with chloramphenicol (30 μg/ml), while *E. coli* DH5α containing pUC18-derived clones was grown in media with ampicillin (100 μg/ml).

Chemicals and reagents. Atrazine, ammeline, and ammelide were generously provided by Syngenta Crop Protection (Greensboro, N.C.). Melamine was purchased from Sigma (St. Louis, Mo.), and cyanuric acid was from Fluka (Ronkonkoma, N.Y.). The other triazines used in this study, aminoatrazine, cyanoatrazine, and azidoatrazine, were synthesized in our laboratory by Gilbert Johnson as previously described (35).

DNA manipulation and Southern hybridizations. Total genomic DNA was isolated as previously described (33) and digested with *Eco*RI, *Hin*dIII, *Bam*HI,

and *Ava*I in four independent reactions. A double digestion using *Eco*RI and *Bam*HI was also performed. DNA was separated on a 0.7% agarose gel and transferred onto a nylon membrane. Southern hybridizations were performed under stringent conditions as previously described (33), using a 1.9-kb *Ava*I fragment from pMD4 containing the *atzA* gene as a probe (15).

Cloning of *triA*. The *triA* gene was isolated by using the PCR technique. Total genomic DNA from *Pseudomonas* sp. strain NRRL B-12227 was used as template for the PCR. Custom primers (Integrated DNA Technologies, Coralville, Iowa) were designed using the Primer Design package (version 2.01; Scientific and Educational Software, State Line, Pa.) and were based on regions external to and flanking the *atzA* gene from *Pseudomonas* sp. strain ADP. An *Eco*RI restriction site was added to the forward primer (atzA-87Eco, TGC GGG ATG ACC GAA TTC CGG TGC AGG TTT TTC GAT G), and a *Hin*dIII restriction site was added to the reverse primer (atzA1700Hindcomp, TTT CCT CAA GGG GCG GCG GAA GCT TCA ACG GCG TCA TTT C). A 1.5-kb PCR fragment was obtained using *Pfu* Turbo DNA polymerase (Stratagene, La Jolla, Calif.) as recommended by the manufacturer. The resulting PCR fragment was gel purified on a 0.8% agarose gel and was isolated using the Geneclean II system (Bio 101, Inc., Vista, Calif.). The *triA* gene was cloned into the *Eco*RI and *Hin*dIII sites of pUC18, and the resulting plasmid, pJS3, was transformed into Maximum Efficient *E. coli* DH5α (Gibco BRL, Gaithersburg, Md.). The melamine degradation phenotype of transformed cells was confirmed by incubating cell extracts with melamine, followed by analysis using high-pressure liquid chromatography (HPLC), as described below.

DNA sequencing. Plasmid DNA was isolated as previously described (33). The nucleotide sequence on both strands was determined in duplicate using a PRISM ready-reaction dideoxy terminator cycle sequencing kit (Perkin-Elmer Corp.) and an ABI model 373A DNA sequencer (Applied Biosystems, Foster City, Calif.). The Genetics Computer Group sequence analysis software package (Madison, Wis.) was used for all DNA and protein sequence comparisons and alignments.

Preparation of cell extracts. Overnight cultures were centrifuged at 14,000 × g for 2 min at 4°C. Cell pellets were resuspended in ice-cold 10 mM phosphate buffer (pH 7). Cell suspensions were subjected to sonication with a Biosonik sonicator (Bronwill Scientific, Rochester, N.Y.) at 80% intensity, followed by three freeze-thaw cycles. Lysed cell suspensions were centrifuged at 14,000 × g for 15 min at 4°C to obtain cell extracts.

Partial enzyme purification and Western hybridization. Overnight cultures were centrifuged at 10,000 × g for 10 min and resuspended in 25 mM morpholinepropanesulfonic acid (MOPS) (pH 7). Cell suspensions were passed through a French pressure cell as previously described (13). After three additional freeze-thaw cycles, cell debris was removed by centrifugation at 15,000 × g for 100 min at 4°C. A 0 to 20% ammonium sulfate precipitation of the supernatant was used as partially purified enzyme. AtzA was purified as previously described (13). The partially purified melamine deaminase and purified AtzA were dialyzed against 25 mM MOPS (pH 7) containing 0.5 g of iron sulfate per liter, followed by dialysis in metal-free 25 mM MOPS (pH 7) buffer.

Sodium dodecyl sulfate-polyacrylamide gel electrophoresis (SDS-PAGE) and Western hybridizations were performed as previously described (14, 32, 33). Cell extracts from DH5α(pMD4), containing AtzA, and *Pseudomonas* sp. strain ADP were used as positive controls for AtzA. *R. corallinus* NRRL B-15444R expresses an *s*-triazine hydrolase (TrzA) that is 43% identical to AtzA but does not cross-react with the AtzA antibody (J. L. Seffernick, unpublished). The *trzA* gene has been cloned but fails to be expressed in *E. coli* (38). This clone, DH5α(pSW1), and *Pseudomonas* sp. strain NRRL B-12228, a strain that fails to degrade melamine but mineralizes ammeline, were used as negative controls. Protein concentrations were determined with the Protein Bio-Rad Assay Dye Reagent in accordance with the manufacturer's instructions (Hercules, Calif.).

Ammelide competition studies. Enzymatic reactions were done using 100 μM melamine or ammeline in the presence or absence of ammelide (100 μM). Initial rates were determined at 22°C with crude extracts of *E. coli* DH5α(pJS3). Reaction mixtures with melamine as the substrate contained 12.4 μg of protein per ml, while reaction mixtures with ammeline required 124 μg of protein per ml to obtain 8 to 10% conversion of substrate to product within 30 min. Triazine degradation was monitored at 0, 5, 15, 20, and 30 min after substrate addition by HPLC analysis, as described below.

Determination of substrate range. Partially purified enzyme from *E. coli* DH5α(pJS3), isolated as described above, was incubated with the compounds listed in Table 1 at a final concentration of 8 μg of total protein per ml. Samples were assayed by HPLC at 16 and 24 h as described below. HPLC sensitivity limited detection of rates to those greater than 10 pmol/min/mg of protein. For those triazines that were substrates for melamine deaminase, initial rates of deamination and specific activities were determined from duplicate samples.

TABLE 1. Melamine deaminase substrate specificity[a]

Substrate	Sp act (nmol/min/mg)
Melamine (AAAT)	245 ± 2
CAAT	135 ± 1
Ammeline (AAOT)	17 ± 1
Aminoatrazine (IEAT)	17 ± 1
Ammelide (AOOT)	<0.01
Atrazine (CIET)	<0.01
Desethylatrazine (CIAT)	<0.01
Desisopropylatrazine (CEAT)	<0.01
Cyromazine	<0.01
Fluoroatrazine	<0.01
Azidoatrazine	<0.01
Atratone	<0.01
Cyanoatrazine	<0.01
2,4,6-Triaminopyrimidine	<0.01
2-Amino-4,6-dichloropyrimidine	<0.01
6-Chloro-2,4-diaminopyrimidine	<0.01

[a] Mean specific activities with partially purified melamine deaminase ($n = 2$).

Melamine deaminase and AtzA competition experiments. Initial rates of melamine deamination and atrazine dechlorination were determined in triplicate samples in the presence of equal molar concentrations of various triazines. Specific activities were calculated based upon partially purified protein and highly purified enzyme concentrations for melamine deaminase and AtzA, respectively.

Analytical procedures. HPLC analysis was performed on a Hewlett-Packard HP 1100 Series Chromatographic system equipped with a diode array detector and interfaced with an HP Chemstation (revision A.05.01). Melamine and its metabolites were separated either on an Alltech Inertsil 5μ (150 by 4.6 mm) phenyl column (Deerfield, Ill.) with an isocratic aqueous mobile phase consisting of 5 mM sodium octane sulfate in 0.05% H_3PO_4 (pH 2.8) and detected at 200 nm or on a Merck LiChrosorb RP-8 5μ (250 by 4 mm) column (Gibbstown, N.J.) with an acetonitrile (ACN)-water gradient as follows: 5 min, 3% ACN; 5-min linear gradient to 50% ACN; 5-min linear gradient to 100% ACN; 3-min linear gradient to 3% ACN; and 3% ACN for 2 min. An Alltech Adsorbosphere C_{18} 5μ (250 by 4.6 mm) column or a mixed-mode C_8-anion 5μ (250 by 4.6 mm) column was used to detect the alkylated triazines, including aminoatrazine, atrazine, and hydroxyatrazine, with an ACN-water linear gradient as previously described (7). Compounds with no detectable transformation after 24 h are listed below the detection limit of 0.01 nmol/min/mg.

Nucleotide sequence accession number. The *triA* sequence has been entered into GenBank under accession number AF312304.

RESULTS

Identification of an AtzA homolog in *Pseudomonas* sp. strain NRRL B-12227. Total genomic DNA from *Pseudomonas* sp. strain NRRL B-12227 was digested with *Bam*HI, *Eco*RI, *Hin*dIII, *Ava*I, and *Eco*RI-plus-*Bam*HI. The digested DNA was separated on a 0.7% agarose gel and subjected to Southern hybridization analysis. In each case, a single fragment of 14, 12, 10, 4, or 12 kb, respectively, hybridized to an *atzA* probe (data not shown).

Protein expression studies were performed to determine if an *atzA* homolog was expressed in *Pseudomonas* sp. strain NRRL B-12227. Cell extracts of *Pseudomonas* sp. strain NRRL B-12227 were separated by SDS-PAGE and subjected to Western blotting using an AtzA-specific antibody. This revealed the presence of a protein that cross-reacted with the antibodies for AtzA (Fig. 2). Therefore, both DNA and protein evidence supported the presence of an AtzA homolog in *Pseudomonas* sp. strain NRRL B-12227.
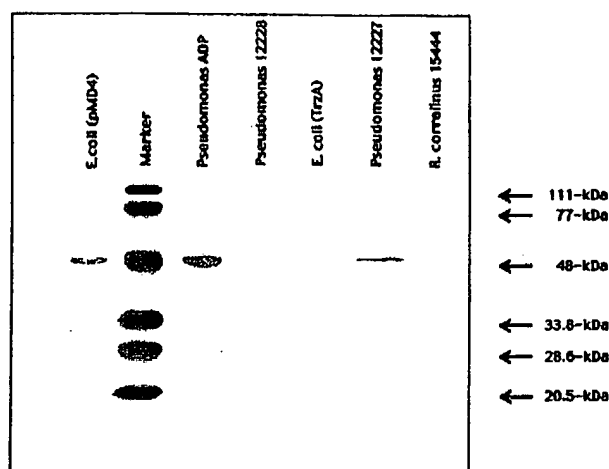

FIG. 2. Western blotting of an SDS-PAGE protein gel using antibodies against the AtzA protein. Lanes from left to right: 1, *E. coli* (pMD4) positive control for AtzA; 2, prestained protein standards; 3, *Pseudomonas* sp. strain ADP positive control for AtzA; 4, *Pseudomonas* sp. strain NRRL B-12228; 5, *E. coli* (TrzA) negative control; 6, *Pseudomonas* sp. strain NRRL B-12227; and 7, *R. corallinus* sp. strain NRRL B-15444R (TrzA).

Cloning of the *triA* gene. To determine whether the AtzA homolog was responsible for melamine degradation in *Pseudomonas* sp. strain NRRL B-12227, the gene was cloned by using the PCR technique and high-fidelity polymerase *Pfu* Turbo. A 1.5-kb PCR product was cloned into pUC18, and the resulting plasmid, pJS3, was transformed into *E. coli* DH5α cells. Cell extracts of the transformed *E. coli* cells showed melamine degradation activity by HPLC analysis. Control *E. coli* DH5α cell extracts failed to degrade melamine, suggesting that the cloned homolog in pJS3 was responsible for melamine degradation.

DNA sequence of *triA*. The cloned DNA in pJS3 was sequenced. Sequence analysis indicated a single open reading frame 1,425 nucleotides in length. The open reading frame was named *triA* (GenBank accession no. AF312304) and encodes melamine deaminase. Comparison of gene and protein sequences of *triA* and *atzA* revealed that these two genes were 99% and 98% identical at the nucleotide and amino acid levels, respectively. The 9 nucleotide differences between the two genes correspond to 9 amino acid changes in the protein sequences (Fig. 3). To establish that no additional mutations were introduced through PCR, three overlapping 0.6-kb fragments were also amplified directly from *Pseudomonas* sp. strain NRRL B-12227 genomic DNA and sequenced in duplicate in both directions. The smaller overlapping fragments were identical to the sequence obtained from pJS3.

Melamine deaminase-catalyzed melamine hydrolysis products. Cell extracts containing melamine deaminase were incubated with melamine (100 μM) for approximately 16 h. Formation of a white precipitate indicated production of less soluble products, which coeluted on HPLC with ammeline and ammelide. Mass spectral analysis of products confirmed that melamine deaminase catalyzes the hydrolysis of melamine to ammeline and ammelide (results not shown). To determine if melamine deaminase was also capable of deaminating amme-

TriA 1 MQTLSIQHGTLVTMDQYRRVLGDSWVHVQDGRIVALGVHAESVPPPADRV 50
AtzA 1 MQTLSIQHGTLVTMDQYRRVLGDSWVHVQDGRIVALGVHABSVPPPADRV 50

                        84   93
     51 IDARGKVVLPGFINAHTHVNQILLRGGPSHGRQLYDWLFNVLYPQOKAMR 100
     51 IDARGKVVLPGFINARTHVNQILLRGGPSHGRQYDWLPNVVYPGQKAMR 100

                        125
    101 PEDVAVAVRLYCABAVRSGITTINDNADSAIYPGNIBAAHAVYGBVGVRV 150
    101 PEDVAVAVRLYCAEAVRSGITTINENADSAIYPGNIBAAHAVYOBVOVRV 150

    151 VYARMFFDRMDGRIQGYVDALKARSPQVBLCSIMEBTAVAKDRITALSDQ 200
    151 VYARMFPDRMDGRIQGYVDALKARSPQVBLCSIMEBTAVAKDRITALSDQ 200

                        217 219
    201 YHGTAGGRISVWPAPAHHAVTVEGMRWAQAFARDRAVMWTLHHABSDHD 250
    201 YHGTAGGRISVWPAPAHHAVTVBGNRWAQAFARDRAVMWTLHHABSDHD 250

                        253 255
    251 BRHGHSPABYNBCYGLLDBRLOVAHCVYFDRKDVRLLHRBHVKVAEQVV 300
    251 BRHGHSPABYNECYGLLDBRLQVAHCVYFDRKDVRLLHRHHVKVASQVV 300

                        328 332
    301 SHAYLGSGVAPVPEHVBRGMAVGIOTHDHSNDSVNHIGDHKFHAHIHRA 350
    301 SHAYLGSGVAPVPBHVBROMAVGIOTHDHSNDSVNHIGDHKFHAHIHRA 350

    351 VHRDADVLTPBKILBMATIDGARSLGMDHEIGSIBTGKRADLILLDLRHP 400
    351 VHRDADVLTPBKILBMATIDGARSLGMDHBIGSIBTGKRADLILLDLRHP 400

    401 QTTPHHHLAATIVFQAYGNBVDTVLIDGNVVMBHRRLSFLPPERELAFLB 450
    401 QTTPHHHLAATIVFQAYGNBVDTVLIDGNVVMBHRRLSFLPPERELAFLB 450

    451 BAQSRATAILQRANHVASPAHRSL* 475
    451 EAQSRATAILQRANHVASPAHRSL* 475

FIG. 3. Amino acid sequences of AtzA and melamine deaminase (TriA) (GenBank accession no. AF312304). Boxes denote amino acid residues that differ between the two sequences.
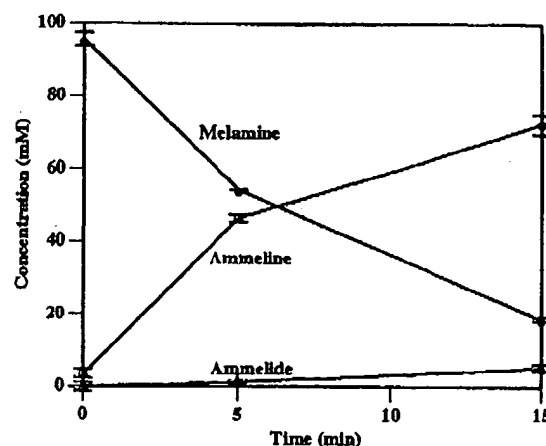

FIG. 4. Time course of melamine and ammeline deamination by cell extracts prepared from the TriA clone E. coli(pJS3). Error bars represent the standard error of the mean; n = 2.

line, cell extracts of E. coli(pJS3) were incubated with ammeline. HPLC analysis of enzymatic reactions revealed formation of ammelide. Incubation of ammelide with melamine deaminase failed to produce any detectable products, including cyanuric acid. These results indicated that melamine deaminase is capable of removing two of the three amino groups from melamine, producing ammelide as a final product (Fig. 4). Formation of ammelide was 15-fold slower than that of ammeline in cell extracts. Competition experiments, in which ammelide was added to reaction mixtures with melamine and ammeline, indicated that ammelide failed to influence melamine deamination activities.

Substrate specificity of melamine deaminase. In addition to melamine and ammeline, melamine deaminase catalyzed the deamination of other s-triazines. Partially purified melamine deaminase was used throughout these studies. Table 1 summarizes the specific activities for those compounds that were substrates for melamine deaminase. Deamination was confirmed in each case by detection of the corresponding hydroxylated product except in the case of 2-chloro-4,6-diamino-s-triazine (CAAT). The proposed product, 2-amino-4-chloro-6-hydroxy-s-triazine (CAOT), is unstable in water and hydrolyzes to ammelide. Mass spectometry confirmed the presence of ammelide as the final product of the reaction. An initial enzyme-catalyzed dechlorination reaction would produce ammeline, which was not detected.

Melamine deaminase displaced an amino group from CAAT and aminoatrazine (2-amino-4-N-ethyl-6-N-isopropyl-1,3,5-triazine) but not from ammelide, desisopropylatrazine (CEAT), desethylatrazine (CIAT), or cyromazine (2,4-diamino-6-N-cyclopropane). Individually, a chlorine or N-alkyl group on the triazine ring did not prevent catalysis. However, when both

were present simultaneously or if the alkyl group consisted of a strained ring structure like cyclopropane, no reaction occurred. Pyrimidines were also not substrates for melamine deaminase. This is significant since melamine deaminase is a member of the amidohydrolase superfamily, which contains many enzymes that catalyze reactions of intermediary metabolism, including enzymes that utilize pyrimidine and purine substrates. The three nitrogens in the ring were essential for catalysis. Melamine deaminase had no activity with atrazine and atrazine analogs containing the following halide and pseudohalide substituents: chloro, fluoro, azido, methoxy, and cyano.

Melamine deaminase competition experiments. The inhibition of melamine deamination activity (n = 3) by various triazines was determined, using partially purified enzyme. The percent inhibition of melamine deamination rates in the presence of equimolar concentrations of other triazine compounds differed. Aminoatrazine inhibited melamine turnover sixfold more than atrazine (71.0% ± 0.6% versus 12% ± 2%). This suggests that melamine deaminase may have active site determinants that bind an amino substituent of the triazine ring. Ammeline and CAAT both inhibited melamine deamination by approximately 50% (47% ± 3% and 49% ± 4%), suggesting that melamine, ammeline, and CAAT bind to similar extents. Therefore, the differences in the rates in Table 1 among these substrates are probably due to differences in turnover and not in substrate binding.

AtzA competition experiments. Inhibition of AtzA (n = 3) by aminotriazines was also investigated. Atrazine dechlorination rates were reduced (73% ± 6%) by aminoatrazine, but dechlorination was not inhibited by either melamine (0% ± 2%) or CAAT (0% ± 3%). This suggests that AtzA requires the N-alkyl group on the s-triazine ring for efficient substrate recognition. This differs from melamine deaminase, which was active with both N-alkylated and nonalkylated aminotriazines. The high degree of inhibition of melamine catalysis in the presence of aminoatrazine (71.0% ± 0.6%) suggests that melamine deaminase may bind the alkylated triazines better than it binds nonalkylated ones. However, the low degree of inhi-

bition observed in the presence of atrazine (12% ± 2%) suggests that the active site of melamine deaminase does not favor a chlorine substituent. These observations suggest the presence of a proton-donating group at the active site that might assist in binding the amino-leaving group of the substrate.

DISCUSSION

Homologous proteins catalyzing different reactions are being discovered at an increasing rate with genomic research focusing attention on the interplay between macromolecular sequence and function. As one part of functional genomics efforts, homologous proteins are being classified into superfamilies, some of which serve different biological functions by virtue of catalyzing a range of biochemical reactions (6, 9, 20, 22, 34, 45). For example, the amidohydrolase superfamily has members that catalyze ring deamination, amide bond hydrolysis, phosphotriester hydrolysis, and dechlorination reactions (22). AtzA had previously been shown to be a member of the amidohydrolase superfamily (32); in this study, melamine deaminase was added. In this superfamily and in others, members that catalyze different reactions are generally divergent to the extent that amino acid sequence identity is less than 50%. This underlies current genome annotation efforts where functional assignments based on >50% sequence identity are considered to be reasonably sound. The present finding that proteins with >98% sequence identity catalyze different reactions in different metabolic pathways is highly exceptional. Moreover, no vestigial reactivity could be detected with either enzyme. AtzA was previously shown to have no deaminase activity, even with a structural analog of atrazine containing an amino group in place of a chlorine substituent (35). In this study, melamine deaminase was observed not to catalyze dechlorination with chlorinated aminotriazine substrates. Moreover, data presented in this study are consistent with the presence of at least two areas of substrate recognition within the active site of melamine deaminase and one in AtzA. Both enzymes appear to contain a binding surface for an N-alkyl group, but melamine deaminase appears to contain an additional site for binding the amino leaving group.

While it is surprising that enzymes with such high sequence identity catalyze different reactions, it is well known that microbes adapt to metabolize new chemical compounds and that enzymes evolve in that context. This point is illustrated with the homologous enzymes enoyl-coenzyme A (CoA) hydratase and 4-chlorobenzoyl-CoA dehalogenase, which catalyze the addition of water to a double bond and hydrolytic dehalogenation of a chlorinated aromatic ring compound, respectively (34). These two enzymes show 56% amino acid sequence identity in pairwise comparison and have very similar three-dimensional structures (6, 45), yet neither member of the pair will catalyze the other's reaction. Similarly, plant fatty acyl desaturases and hydroxylases have been observed to share 81% sequence identity but catalyze different reactions (9). Each enzyme is thought to contain a binuclear iron cluster, which serves as the site of oxygen activation to catalyze either hydroxylation or electron abstraction, respectively (37). This commonality of structure and mechanism with a divergence during the latter part of the enzyme catalytic cycle is an emerging theme that will provide insight for studies in functional genomics and enzyme evolution.

The amidohydrolase superfamily fits this paradigm in that its best-characterized members are known to share a common $(\beta\alpha)_8$ barrel structure (22) and a common catalytic mechanism. For example, adenosine deaminase (39, 43, 44) and phosphotriesterase (4–5) catalyze their reactions via metal activation of water for nucleophilic attack on their substrates. AtzA and melamine deaminase are members of this superfamily and may share this common mechanism, although this remains to be established experimentally. The s-triazine hydrolase, TrzA, from R. corallinus NRRL B-15444R is also a member of the amidohydrolase superfamily (22). It catalyzes both deamination and dechlorination reactions with triazine ring substrates (27). The s-triazine hydrolase, which shares 44% and 43% sequence identity with melamine deaminase and AtzA, respectively, catalyzes melamine deamination but is not active in the dechlorination of atrazine (27).

Since the initial identification of AtzA in Pseudomonas sp. strain ADP, atrazine metabolism genes have been detected in other bacteria, including Rhizobium sp. strain PATR (8), Alcaligenes sp. strain SG1 (K. Boundy-Mills, unpublished), Agrobacterium radiobacter J14a (40), Ralstonia pickettii D (M. L. de Souza, N. R. Plechacek, L. P. Wackett, M. J. Sadowsky, and B. L. Hoyle, Abstr. 98th Gen. Meet. Am. Soc. Microbiol., abstr. Q-195, p. 453, 1998), Clavibacter michiganensis ATZ1 (2, 12), and Pseudaminobacter sp. strain C147 (41). Sequence analysis has indicated that the AtzA genes in various atrazine-degrading bacteria have greater than 99% sequence identity to AtzA from Pseudomonas sp. strain ADP within a 0.5-kb region (14). The identity of the atzA homologs present in diverse genera, the plasmid localization of atzA genes, and the identification of IS1071-like sequences flanking the atrazine degradation genes suggest that horizontal gene transfer and transposition may have contributed to the spread of the atrazine degradation genes among bacteria (16). The present study shows that the global distribution of highly identical genes extends beyond the catabolism of atrazine and includes a bacterium with a metabolic pathway to catabolize melamine. Since melamine has been used industrially for approximately 80 years and atrazine for 40 years (29), these observations are consistent with recent evolutionary adaption of the relevant genes.

Sequence comparison of triA and atzA indicates a lack of silent mutations, suggesting that strong selective pressure occurred relatively quickly (18, 42). Moreover, the 9 amino acid differences are positioned throughout the proteins, indicating that catalytic differences are most likely not due to an alteration in tertiary structure but rather due to localized changes. Under conditions of weak selection and due to genetic drift, silent mutations that do not lead to changes in the amino acid sequence evolve, resulting in a trend towards preferred codon usage (1, 24, 28). It has been estimated that only 10% of the amino acid differences between species are driven by positive selection (28) and that relatively few substitutions that lead to amino acid replacements are accepted and maintained (23). This suggests that the evolutionary divergence of melamine deaminase and AtzA occurred relatively recently and under conditions of strong selective pressure.

REFERENCES

1. Akashi, H. 1999. Within- and between-species DNA sequence variation and the 'footprint' of natural selection. Gene 238:39–51.
2. Alvey, S., and D. E. Crowley. 1995. Influence of organic amendments on biodegradation of atrazine as a nitrogen source. J. Environ. Qual. 24:1156–1162.
3. Belluck, D. A., S. L. Benjamin, and T. Dawson. 1991. Groundwater contamination by atrazine and its metabolites: risk assessment, policy and legal implications, p. 254–273. *In* L. Somasundaram and J. R. Coats (ed.), Pesticide transformation products: fate and significance in the environment. American Chemical Society, Washington, D.C.
4. Benning, M. M., J. M. Kuo, F. M. Raushel, and H. M. Holden. 1994. Three-dimensional structure of phosphotriesterase: an enzyme capable of detoxifying organophosphate nerve agents. Biochemistry 33:15001–15007.
5. Benning, M. M., J. M. Kuo, F. M. Raushel, and H. M. Holden. 1995. Three-dimensional structure of the binuclear metal center of phosphotriesterase. Biochemistry 34:7973–7978.
6. Benning, M. M., K. L. Taylor, R. Q. Liu, G. Yang, H. Xiang, G. Wesenberg, D. Dunaway-Mariano, and H. M. Holden. 1996. Structure of 4-chlorobenzoyl coenzyme A dehalogenase determined to 1.8 Å resolution: an enzyme catalyst generated via adaptive mutation. Biochemistry 35:8103–8109.
7. Boundy-K. Mills, M. L. de Souza, R. M. Mandelbaum, L. P. Wackett, and M. J. Sadowsky. 1997. The *atzB* gene of *Pseudomonas* sp. strain ADP encodes the second enzyme of a novel atrazine degradation pathway. Appl. Environ. Microbiol. 63:916–923.
8. Bouquard, C., J. Ouazzani, J.-C. Prome, Y. Michel-Briand, and P. Plesiat. 1997. Dechlorination of atrazine by a *Rhizobium* sp. isolate. Appl. Environ. Microbiol. 63:862–866.
9. Broun, P., J. Shanklin, E. Whittle, and C. Somerville. 1998. Catalytic plasticity of fatty acid modification enzymes underlying chemical diversity of plant lipids. Science 282:1315–1317.
10. Cook, A. M., and R. Hutter. 1981. Degradation of *s*-triazines: a critical view of biodegradation, p. 237–248. *In* T. Leisinger, A. M. Cook, R. Hutter, and J. Nuesch (ed.), FEMS symposium on microbial degradation of xenobiotics and recalcitrant compounds, vol. 12. Academic Press Inc., Zurich, Switzerland.
11. Cook, A. M., and R. Hutter. 1981. *s*-Triazines as nitrogen sources for bacteria. J. Agric. Food Chem. 29:1135–1143.
12. de Souza, L. M., D. Newcombe, S. Alvey, D. E. Crowley, A. Hay, M. J. Sadowsky, and L. P. Wackett. 1998. Molecular basis of a bacterial consortium: interspecies catabolism of atrazine. Appl. Environ. Microbiol. 64:178–184.
13. de Souza, L. M., M. J. Sadowsky, and L. P. Wackett. 1996. Atrazine chlorohydrolase from *Pseudomonas* sp. strain ADP: gene sequence, enzyme purification, and protein characterization. J. Bacteriol. 178:4894–4900.
14. de Souza, L. M., J. Seffernick, B. Martinez, S. J. Sadowsky, and L. P. Wackett. 1998. The atrazine catabolism genes *atzABC* are widespread and highly conserved. J. Bacteriol. 180:1951–1954.
15. de Souza, L. M., L. P. Wackett, K. L. Boundy-Mills, R. T. Mandelbaum, and M. J. Sadowsky. 1995. Cloning, characterization, and expression of a gene region from *Pseudomonas* sp. strain ADP involved in the dechlorination of atrazine. Appl. Environ. Microbiol. 61:3373–3378.
16. de Souza, L. M., L. P. Wackett, and M. J. Sadowsky. 1998. The *atzABC* genes encoding atrazine catabolism are located on a self-transmissible plasmid in *Pseudomonas* sp. strain ADP. Appl. Environ. Microbiol. 64:2323–2326.
17. Eaton, R. W., and J. S. Karns. 1991. Cloning and comparison of the DNA encoding ammelide aminohydrolase and cyanuric acid amidohydrolase from three *s*-triazine-degrading bacterial strains. J. Bacteriol. 173:1363–1366.
18. Endo, T., K. Ikeo, and T. Gojobori. 1996. Large-scale search for genes on

which positive selection may operate. Mol. Biol. Evol. 13:685–690.
19. Erickson, E. L., and K. H. Lee. 1989. Degradation of atrazine and related *s*-triazines. Crit. Rev. Environ. Contam. 19:1–13.
20. Gerlt, J. A., and P. C. Babbitt. 1998. Mechanistically diverse enzyme superfamilies: the importance of chemistry in the evolution of catalysis. Curr. Opin. Chem. Biol. 2:607–612.
21. Gorbaty, L., and S. Takahashi. 1996. Melamine, p. 673.3000–673.3049. Chemical economics handbook. SRI Consulting, Tokyo, Japan.
22. Holm, L., and C. Sander. 1997. An evolutionary treasure: unification of a broad set of amidohydrolases related to urease. Proteins 28:72–82.
23. Jones, C. W., and F. C. Kafatos. 1982. Accepted mutations in a gene family: evolutionary diversification of duplicated DNA. J. Mol. Evol. 19:87–103.
24. Jukes, T. H. 1980. Silent nucleotide substitutions and the molecular evolutionary clock. Science 210:973–978.
25. LeBaron, H. 1982. Herbicide resistance in plants. John Wiley & Sons, New York, N.Y.
26. Mandelbaum, R. T., D. L. Allan, and L. P. Wackett. 1995. Isolation and characterization of a *Pseudomonas* sp. that mineralizes the *s*-triazine herbicide atrazine. Appl. Environ. Microbiol. 61:1451–1457.
27. Mulbry, W. W. 1994. Purification and characterization of an inducible *s*-triazine hydrolase from *Rhodococcus corallinus* NRRL B-15444R. Appl. Environ. Microbiol. 60:613–618.
28. Ohta, T., and M. Kimura. 1971. On the constancy of the evolutionary rate of cistrons. J. Mol. Evol. 1:18–25.
29. Partington, J. R. 1961. A history of chemistry. Macmillan, London, England.
30. Quirke, J. M. E. 1984. 1,3,5-Triazines, p. 459–529. *In* A. R. Katritzky and C. W. Rees (ed.), Comprehensive heterocyclic chemistry. Pergamon Press, New York, N.Y.
31. Radosevich, M., S. J. Traina, Y. Hao, and O. H. Tuovinen. 1995. Degradation and mineralization of atrazine by a soil bacterial isolate. Appl. Environ. Microbiol. 61:297–302.
32. Sadowsky, J. M., Z. Tong, M. L. de Souza, and L. P. Wackett. 1998. AtzC is a new member of the amidohydrolase protein superfamily and is homologous to other atrazine-metabolizing enzymes. J. Bacteriol. 180:152–158.
33. Sambrook, J., E. F. Fritsch, and T. Maniatis. 1989. Molecular cloning: a laboratory manual, 2nd ed. Cold Spring Harbor Laboratory Press, Cold Spring Harbor, N.Y.
34. Scholten, J. D., K. H. Chang, P. C. Babbitt, H. Charest, M. Sylvestre, and D. Dunaway-Mariano. 1991. Novel enzymatic hydrolytic dehalogenation of a chlorinated aromatic. Science 253:182–185.
35. Seffernick, J. L., G. Johnson, M. J. Sadowsky, and L. P. Wackett. 2000. Substrate specificity of atrazine chlorohydrolase and atrazine-catabolizing bacteria. Appl. Environ. Microbiol. 66:4247–4252.
36. Selinofova, O., and T. Barkay. 1994. Role of Na$^+$ in transport of Hg$^+$ and induction of the Tn*21* mer operon. Appl. Environ. Microbiol. 60:3503–3507.
37. Shanklin, J., C. Achim, H. Schmidt, B. G. Fox, and E. Munck. 1997. Mossbauer studies of alkane ω-hydroxylase: evidence for a diiron cluster in an integral-membrane enzyme. Proc. Natl. Acad. Sci. USA 94:2981–2986.
38. Shao, Z. Q., W. Seffens, W. Mulbry, and R. M. Behki. 1995. Cloning and expression of the *s*-triazine hydrolase gene (*trzA*) from *Rhodococcus corallinus* and development of *Rhodococcus* recombinant strains capable of dealkylating and dechlorinating the herbicide atrazine. J. Bacteriol. 177:5748–5755.
39. Sharff, A. J., D. K. Wilson, Z. Chang, and F. A. Quiocho. 1992. Refined 2.5 Å structure of murine adenosine deaminase at pH 6.0. J. Mol. Biol. 226:917–921.
40. Struthers, J. K., K. Jayachandran, and T. B. Moorman. 1998. Biodegradation of atrazine by *Agrobacterium radiobacter* J14a and use of this strain in bioremediation of contaminated soil. Applied Environ. Microbiol. 64:3368–3375.
41. Topp, E., H. Zhu, S. M. Nour, S. Houot, M. Lewis, and D. Cuppels. 2000. Characterization of atrazine-degrading *Pseudaminobacter* sp. isolated from Canadian and French agricultural soils. Appl. Environ. Microbiol. 66:2773–2782.
42. Vacquier, V. D., and Y. H. Lee. 1993. Abalone sperm lysin: unusual model of evolution of a gamete recognition protein. Zygote 1:181–196.
43. Wilson, D. K., and F. A. Quiocho. 1993. A pre-transition-state mimic of an enzyme: X-ray structure of adenosine deaminase with bound 1-deazaadenosine and zinc-activated water. Biochemistry 32:1689–1694.
44. Wilson, D. K., F. B. Rudolph, M. L. Harrison, R. E. Kellems, and F. A. Quiocho. 1988. Preliminary X-ray analysis of crystals of murine adenosine deaminase. J. Mol. Biol. 200:613–614.
45. Xiang, H., L. Luo, K. L. Taylor, and D. Dunaway-Mariano. 1999. Interchange of catalytic activity within 2-enoyl-CoA hydratase/isomerase superfamily based on a common active site. Biochemistry 38:7638–7652.